Electrochemical sensors of environmental pollutants based on carbon electrodes modified by ordered mesoporous silica

Tauqir Nasir

University of Lorraine- Faculty of Sciences and Technology

Doctoral School SESAMES

Thesis

Presented for the title of

Doctor of Chemistry from the University of Lorraine

By

Tauqir Nasir

Electrochemical sensors of environmental pollutants based on carbon electrodes modified by ordered mesoporous silica

Public defence on 9th July 2018

Members of jury:

Reviewers:	**Dr. Florence Geneste**	Director of Research – CNRS, Université de Rennes 1
	Dr. Aoife Morrin	Associate professor – Dublin City University, Ireland
Examiners:	**Professor Jose-Paulo Pinheiro**	Professor – Université de Lorraine
	Dr. Florence Lagarde	Chargé de Recherche – CNRS, Université de Lyon
Supervisor:	**Dr. Alain Walcarius**	Director of Research – CNRS, Université de Lorraine
Co-Supervisor:	**Dr. Grégoire Herzog**	Chargé de Recherche – CNRS, Université de Lorraine

Laboratoire de Chimie Physique et Microbiologie pour les Matériaux et l'Environnement (LCPME)

UMR 7564, CNRS / Université de Lorraine 405, rue de Vandoeuvre 54600 Villers-lès-Nancy France

Université de Lorraine- Faculté des sciences et technologies

École doctorale SESAMES

Thèse

Présenté pour l'obtention du titre de

Docteur de l'Université de Lorraine en Chimie

Par

Tauqir Nasir

Capteurs électrochimiques de polluants environnementaux à base d'électrodes de carbone modifiées par de la silice mésoporeuse organisée

Electrochemical sensors of environmental pollutants based on carbon electrodes modified by ordered mesoporous silica

Soutenue publiquement le 9 juillet 2018

Membres du jury:

Rapporteurs:	**Dr. Florence Geneste**	Directeur de Recherche – CNRS, Université de Rennes 1
	Dr. Aoife Morrin	Professeur associé - Dublin City Université, Irlande
Examinateurs:	**Professeur Jose-Paulo Pinheiro**	Professeur – Université de Lorraine
	Dr. Florence Lagarde	Chargé de Recherche – CNRS, Université de Lyon
Directeur de thèse	**Dr. Alain Walcarius**	Directeur de Recherche – CNRS, Université de Lorraine
Co- Directeur de thèse	**Dr. Grégoire Herzog**	Chargé de Recherche – CNRS, Université de Lorraine

Laboratoire de Chimie Physique et Microbiologie pour les Matériaux et l'Environnement (LCPME)

UMR 7564, CNRS / Université de Lorraine 405, rue de Vandoeuvre 54600 Villers-lès-Nancy France

To my parents, siblings, wife and Shahwaiz

Acknowledgments

First and foremost, I would like to pay sincere gratitude to my thesis director **Alain WALCARIUS** for accepting me in his group, continuous support, patience, vast knowledge and guidance during my PhD thesis. Special thanks to co-director of my thesis, **Grégoire HERZOG** for having faith in me. Without his help; discussions, patience and ideas, this piece of work would not have been possible. His guidance helped me a lot throughout my research and stay in France, I express my deepest gratitude and appreciation for him to receive me on arrival in Nancy with a broad smile, helping me manage and settle in early days when I could not speak a single word of French.

I would also like to thank members of jury for the thesis defence **Professor Jose-Paulo Pinheiro, Dr. Florence Geneste, Dr. Aoife Morrin** and **Dr. Florence Lagarde** for taking time out of their busy schedules to evaluate my research work. Their suggestions and critical opinions will help me to improve quality of this work.

My sincere thanks to the other members of **ELAN team** including **Neus Vila**, **Christelle Despas**, **Marc Hébrant** and **Liang Liu** for discussions and help during research. To my office mate **Alonso Gamero-Quijano** for fruitful discussions and ideas during his stay in the lab. I am grateful to **Natalya A. Vodolazkaya, Mathieu Etienne** and **Thi Xuan Huong Le** for collaboration in our research.

I thank my lab fellows **Lukasz Poltorak, Cheryl Karman, Najwa Jajuli, Maciej Mierzwa,** and **Martha Collins** for making my stay memorable, fruitful discussions, time we spent and lunches we had together. More recently during my thesis writing, thanks to **Wahid Ullah** for always giving a reminder of tea time and humor we shared. I would also like to thank other people who helped me for instrumental measurements, **Jaafar Ghanbaja**, **Sylvie Migot** for **TEM**, and **Aurelien Renard** for **XPS. Jean-Paul Moulin, Gérard Paquot, Patrick Bombardier, Marie Rambeau, Pascal Kissienne** and **Claire Genois** for technical support. To **Christelle Charbaut, Jacqueline Druon, Marie Tercier and Séverine Bonenberger** for help in administrative tasks.

Special thanks are due to **Higher Education Commission (HEC) of Pakistan** for funding my PhD studies and **Campus France** for managing me during my stay in France.

Last but not the least, I would like to thank my (Late) grandmother, she contributed a lot to where I am today, My parents for their endless prayers and always supporting me through thick and thin, My wife **Samia** for unconditional affection, support and standing by my side through hard times and to my little stars **Samrah**, **Sidra** and **Toseef** for their love and support.

Tauqir Nasir

Nancy, France

Table of contents

Abstract

In this project we combined the wealth of surface modification by ordered mesoporous silica thin films with rich surface chemistry of carbon electrodes for electrochemical sensing of herbicides. Increasing population and demands of food safety has led to increased use of chemicals in agricultural practices and ultimately flow of these harmful chemicals to environmental systems. Electrochemical sensing has found its applicability over traditional detection methods in different fields ranging from health to environment due to favorable characteristics such as cost effectiveness, rapid, ease of application, possibility of need based surface modifications and considerably low detection limits.

Silica thin films generation by using electrochemically assisted self-assembly at electrode surfaces is well established process by our group at LCPME. The adhesion of silica thin films at glassy carbon electrodes (GCE) surface was an issue which required appropriate solution so that film modified carbon electrodes can be applied in the field of electroanalysis. Electrografting of the 3-aminopropyltriethoxysilane (APTES) on glassy carbon as a molecular glue for better adhesion of silica thin films at GCE is presented as a solution to above stated problem. APTES is a primary amine and by electrografting it forms a covalent bond with electrode surface by its amine group whereas the silanol groups forming stable interaction with silica molecules leading to formation of homogenous silica thin films without compromising their vertical orientation to electrode surface and porosity.

In the second part of this study we applied these modified GCE for the detection of paraquat, a well-known and world-wide used herbicide for weed control. Electrochemical sensing of paraquat was performed using square wave voltammetry (SWV). Paraquat is a cationic molecule and due to electrostatic interaction it has tendency to accumulate inside negatively charged silica film matrix and can give rise to higher electrochemical signal as compared to unmodified electrodes and ultimately enhancing the sensitivity. Effect of different experimental parameters such as solution pH, ionic strength and supporting electrolyte on sensitivity is also studied and finally applied for detection of paraquat in real samples. In the next part of thesis, we assess the effect of silica film thickness and electrode geometry on electrochemical sensing of paraquat. Film thickness can have obvious effect on sensitivity as thicker films can accommodate large amount of cationic molecules as compared to thinner films. Silica films thickness at electrode surface can be varied depending upon

deposition time and also by depositing multi-layered films, electrochemical and surface analysis studies of modified electrodes are performed. Microelectrode arrays can greatly enhance the sensitivity of electrochemical sensing due to higher mass transfer, large surface area and possibility of working at very low electrolyte concentrations. Microelectrode arrays at GCE substrates fabricated in clean room facility are also modified and paraquat sensing parameters at these arrays is carried out.

In the last part of this project the electrochemical Characterization and detection of isoproturon is performed. Isoproturon is a toxic compound used as herbicide and is commonly detected in rivers and streams at levels above than permissible limits of 0.1 µg / L^{-1}. Electrochemical behaviour of isoproturon at GCE and indium tin oxide (ITO) electrodes is studied in detail by cyclic voltammetry. Effect of different supporting electrolytes and solution pH ranging from acidic to neutral is also studied. Preconcentration by electrochemical polymerization coupled with SWV is applied for the detection of isoproturon at silica modified and unmodified GCE.

Keywords: Mesoporous silica films, Glassy carbon electrodes, APTES electrografting Electrochemical sensing, Paraquat, Isoproturon.

Résumé

Dans ce projet, nous avons combiné la richesse de la modification de surface par des films minces de silice mésoporeuse organisée avec la riche chimie de surface des électrodes de carbone pour la détection électrochimique de polluants environnementaux (herbicides). L'augmentation de la population et de la demande en matière de salubrité des aliments a entraîné une utilisation accrue des produits chimiques dans les pratiques agricoles et l'écoulement de ces produits chimiques nocifs dans les systèmes environnementaux. La détection électrochimique a trouvé son applicabilité par rapport aux méthodes traditionnelles de détection dans différents domaines allant de la santé à l'environnement en raison de caractéristiques favorables telles que la rentabilité, la rapidité, la facilité d'application, la possibilité de modifications de surface en fonction des besoins et des limites de détection basses.

La génération de couches minces de silice par auto-assemblage assisté électrochimiquement à la surface des électrodes est un processus bien établi par notre groupe au LCPME. L'adhérence des couches minces de silice à la surface des électrodes de carbone vitreux (GCE) était une question qui nécessitait une solution appropriée pour que les électrodes de carbone modifiées par film puissent être appliquées dans le domaine de l'électroanalyse. L'électrogreffage du 3-aminopropyltriéthoxysilane (APTES) sur du carbone vitreux comme colle moléculaire pour une meilleure adhérence des films minces de silice à la GCE est présentée comme une solution au problème mentionné ci-dessus. APTES est une amine primaire et par électrogreffage, elle forme une liaison covalente avec la surface de l'électrode par son groupe amine tandis que les groupes silanol forment une interaction stable avec les molécules de silice conduisant à la formation de films minces de silice homogènes sans compromettre leur orientation verticale par rapport à la surface de l'électrode et leur porosité.

Dans la deuxième partie de cette étude, nous avons appliqué ces CME modifiées pour la détection du paraquat, un herbicide bien connu et utilisé dans le monde entier pour la lutte contre les mauvaises herbes. La détection électrochimique du paraquat a été réalisée par voltampérométrie à ondes carrées (SWV). Le paraquat est une molécule cationique et, en raison de l'interaction électrostatique, il a tendance à s'accumuler à l'intérieur de la matrice de film de silice chargée négativement et peut donner lieu à un signal électrochimique plus élevé

par rapport aux électrodes non modifiées et, en fin de compte, augmenter la sensibilité. L'effet de différents paramètres expérimentaux tels que le pH de la solution, la force ionique et l'électrolyte de soutien sur la sensibilité est également étudié et finalement appliqué pour la détection du paraquat dans des échantillons réels. Dans la partie suivante de la thèse, nous évaluons l'effet de l'épaisseur du film de silice et de la géométrie de l'électrode sur la détection électrochimique du paraquat. L'épaisseur du film peut avoir un effet évident sur la sensibilité, car les films plus épais peuvent contenir une grande quantité de molécules cationiques comparativement aux films plus minces. L'épaisseur des films de silice à la surface de l'électrode peut varier en fonction du temps de dépôt et aussi en déposant des films multicouches, des études électrochimiques et d'analyse de surface des électrodes modifiées sont effectuées. Les réseaux de microélectrodes peuvent améliorer considérablement la sensibilité de la détection électrochimique en raison d'un transfert de masse plus élevé, d'une grande surface et de la possibilité de travailler à de très faibles concentrations d'électrolyte. Les réseaux de microélectrodes fabriqués en salle blanche sur les substrats GCE sont également modifiés et les paramètres de détection du paraquat sur ces réseaux sont réalisés.

Dans la dernière partie de ce projet, la caractérisation électrochimique et la détection de l'isoproturon sont effectuées. L'isoproturon est un composé toxique utilisé comme herbicide et est couramment détecté dans les rivières et les cours d'eau à des niveaux supérieurs aux limites permises de 0,1 µg / L^{-1}. Le comportement électrochimique de l'isoproturon aux électrodes GCE et d'oxyde d'indium-étain est étudié en détail par voltampérométrie cyclique. L'effet des différents électrolytes de soutien et le pH de la solution allant de l'acide au neutre est également étudié. La préconcentration par polymérisation électrochimique couplée à la SWV est appliquée pour la détection de l'isoproturon à la GCE modifiée et non modifiée par de silice mésoporeuse.

Mots-clés: Films de silice mésoporeuse, électrodes de carbone vitreux, électrogreffage APTES, détection électrochimique, Paraquat, Isoproturon.

Chapter I: Literature review

In this chapter, we have presented general introductory information about electrochemistry, electrochemical sensing, short literature review related to sol-gel based silica materials and their application in sensing. Types of electrochemical sensors, techniques, electrode materials and surface modifications for sensing or electroanalytical applications are discussed. Different types of herbicides, their production, detection methods, use and effects on environment as well as living organisms are also reviewed.

1.1 Electrochemistry and sensing

The word electrochemistry is derived from two words “electricity” and “chemistry”. It can be defined as, “the domain of science associated with studies of interactions between chemistry and electricity”. The more precise definition for electrochemistry would be "The science that analyses and describes the charge transfer reaction of matter at atomic level carried out by applying electric current or voltage with the help of electronic devices".[1] Electrochemical sensing is a broad analytical field, which is related to generating useful analytical information by the interaction of electroactive species with a conductive surface or a functional group. A typical chemical sensor is comprised of two fundamental units (i) a receptor and (ii) a transducer, depending on the nature of activity taking place at receptor it can be of physical, chemical or biochemical nature (Figure I-1). At the receptor, the information is generated as a result of above mentioned reactions; this information is transformed into a form of energy, which is changed to a useful analytical signal by the transducer. A transducer itself is non-selective, modifications are carried out at the receptor to improve the selectivity of a chemical sensor.[2]

An electrochemical sensor is a device that transforms electrochemical information into a useful analytical signal. An electrochemical sensor is normally comprised of a working electrode, reference electrode and a counter electrode connected to a potentiostat/galvanostat. The working electrode acts as receptor and is a component of the transducer as well. In a typical three electrode electrochemical sensor, a transducer is composed of working electrode, reference electrode, counter electrode and the other components of sensing device involved in the analysis. Electrochemical sensing is a promising analytical field and it has found its applicability in the fields of energy, health, environment, food and pharmaceutical industry.[3] Electrochemical sensing can be divided into chemical and biosensing. Chemical sensor provides the analytical information about a particular quantity of certain chemical species in the surrounding environment.[4] A biosensor is an integrated device that provides quantitative and semi-quantitative analytical information by using a biological recognition element which is in direct spatial contact with a transduction element.[5] Electrochemical sensors carry certain advantages which include their cost effectiveness, applicability to a vast range of chemicals, ease of use and functionalization, robust nature, high sensitivity and selectivity. In this study we will only focus on electrochemical sensors for chemical sensing.

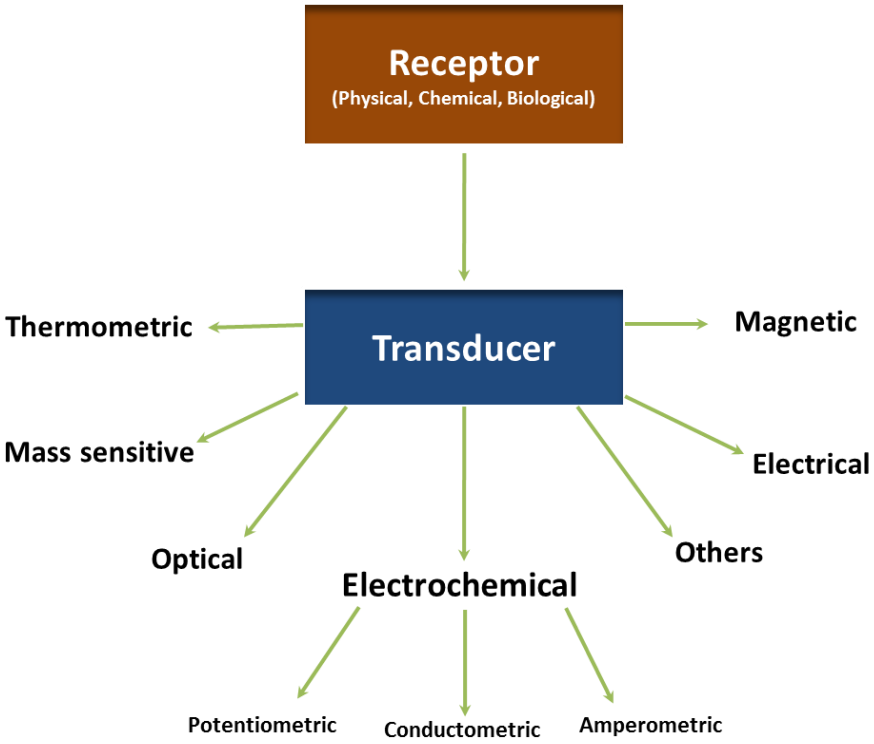

Figure I-1: Different classes of chemical sensors.

1.2 Types of electrochemical sensors

Electrochemical sensors can be divided into three types based on their nature and working principle, i.e. potentiometric, conductometric and amperometric/voltammetric sensors. Here we briefly discuss all types but will focus more on amperometric sensors as this study is related to the amperometric sensing of herbicides.

1.2.1 Potentiometric sensors

As the name suggests, potentiometric sensors measure the potential difference between a sample solution and a reference solution with the help of a reference electrode and an indicator electrode. The two solutions are separated by a membrane *m* which contains an ionophore that is selective to target ion. The Nernst equation provides the relationship between potential difference and target ion activity.

$$E = E_0 + \frac{RT}{zF} \ln \frac{a^s}{a^m} \qquad \textbf{Eq. 1.1}$$

Where E_0 is the standard potential of sensor electrode, F is Faraday's constant, T is absolute temperature, R is universal gas constant, s is sample, *z* is valency of ion and *a* is the target ion activity.[6] Potentiometric sensors have been widely used since 1930's due to their simplicity and ease of use. There are three main types of potentiometric devices used which include ion-selective electrodes (ISE), coated wire electrodes (CWES) and field effect transistors (FETS).[7]

The ion-selective electrode measures the activity of particular ionic species in the surrounding solution. The principle of ISE devices is based on permselective, ion conducting membrane which separates the electrode from outside solution. The composition of membrane is very important for producing the ISE for particular ionic species. In working principle of ISE, the reference electrode potential is kept constant while the potential of working electrode is determined by the surrounding environment. The change in working electrode potential or potential difference is considered as the concentration of the target ion.[8] pH electrode is the best and most widely used example of potentiometric sensor, the success of this electrode lays in its robust nature, easy handling, reproducibility, wide range of application and cost effectiveness.[7] Bakker and Pretsch discussed in detail the breakthrough developments in nanoscale potentiometry, limit of detection and sensor stability.[9]

1.2.2 Conductometric sensors

Conductometric sensors are based on the principle of providing sensory information as a result of changes in the electrical conductivity of material (used in construction of sensing device) which is in contact with the analyte. Conductometric sensors are basically non selective but as a result of more precise miniaturization and surface modification, selectivity can be improved. Conductometric sensors do not require reference electrode for functioning and hence reduce the cost as well as make these sensors simpler for use. Reports for different kind of thin films modifications are available in literature mainly for the detection of gases. Examples of these thin film modified conductometric sensors include, Copper doped oxides are used for the detection of H_2S,[10] CH_4 detection done by using Ga_2O_3 semiconductor films,[11] Modification by conductive polymers such as polypyrole for volatile amine detection,[12] CdS films modification for the detection of oxygen[13] and modification by $MnWO_4$ films to be used as humidity sensors.[14]

1.2.3 Amperometric sensors

In amperometric sensing, the current is measured as a result of an electron transfer reaction while the potential is controlled with a potentiostat. The potential can be kept constant (potentiostatic detection) or it can be scanned between two values (potentiodynamic detection). The principle is based on the electron transfer between the analyte and working electrode. The basic instrumentation for amperometric sensing includes a potentiostat and three electrodes (working, reference and counter) dipped in a suitable electrolyte to form an electrochemical cell. The auxiliary or counter electrode is made up of an inert conducting material such as graphite, platinum, stainless steel etc. In amperometric sensing the electron transfer reaction takes place at the surface of working electrode. The reference electrode provides a reference potential to working and counter electrode.[7] A typical amperometric sensing system and its principle is shown in Figure I-2.

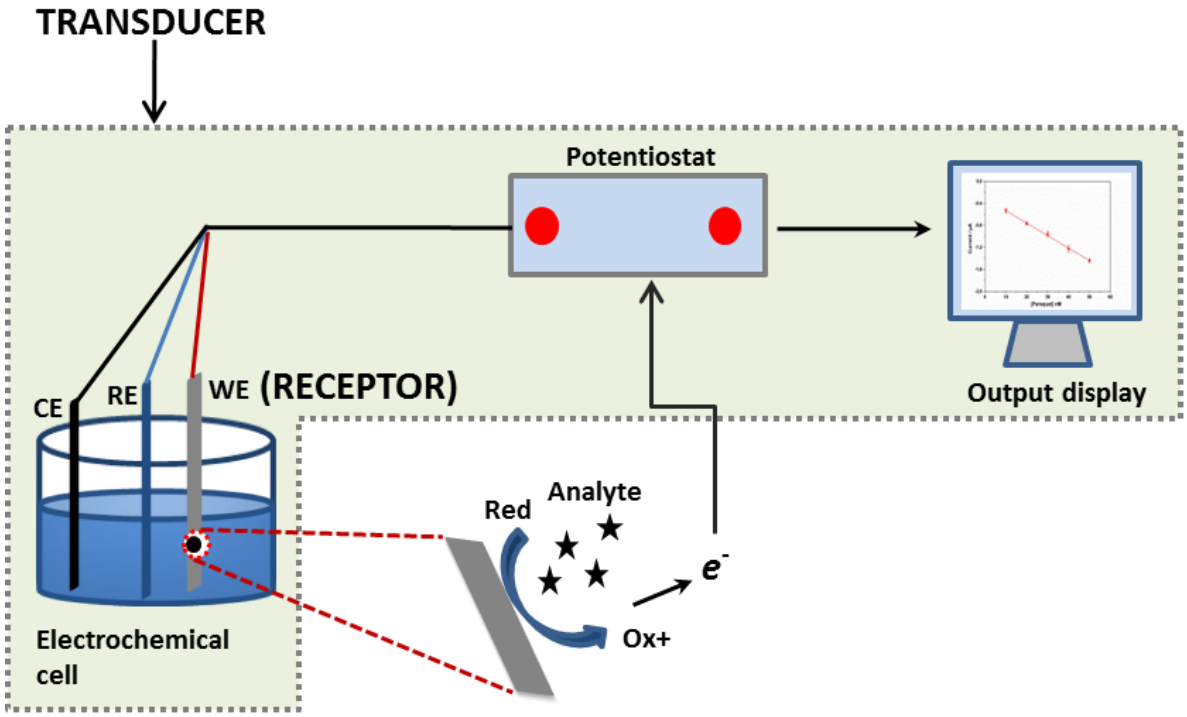

Figure I-2: Schematic representation of a typical amperometric sensing system.

Table I-1: Advantages and disadvantages of electrochemical sensors

Electrochemical sensors	Pros	Cons
Potentiometric or ion selective sensors (pH sensors, electrolyte and ion sensors, drug sensors)	✚ Simple ✚ Real time and on-site analysis ✚ No counter electrode required	✚ Reference electrode stability ✚ Low sensitivity ✚ Mostly used for ions detection ✚ Working electrode surface fouling ✚ Interference by non-target ions ✚ Frequent calibration is required
Conductometric sensors (Gas sensors, conductivity meters, humidity sensors)	✚ No reference electrode required ✚ Easy to use	✚ Limited applications ✚ Poor sensitivity and selectivity ✚ Limited shelf life
Amperometric sensors (Glucose sensors, screen printed sensors, modified and unmodified electrodes for sensing in health, environment and industry)	✚ Sensitivity ✚ Ease of modification for targeted analysis ✚ Real time and on-site analysis ✚ Redox active analytes can be detected	✚ pH dependence and need of supporting electrolyte ✚ Working electrode surface fouling ✚ Interference of non-target electro-active species ✚ Electrode surface modifications required for higher selectivity

In this study we have focused on the developments of amperometric sensors for the electrochemical detection of herbicides. Amperometric sensors were selected owing to their superior nature as compared to potentiostatic and conductometric sensors. Worth mentioning properties of amperometric sensors, which are favorable for sensing of pollutants include; wide variety of working electrode materials available, possibility of electrode surface modification, rapid and on-site analysis of analytes, ease of use and sensitivity.

1.3 Types of working electrodes

Working electrode is an important entity in electrochemical device, as the reaction of interest takes place on working electrode. As a general rule there are some characteristics which a working electrode should possess for its consideration as a suitable candidate in electrochemical analysis, these include inert nature, low background current over a wide potential window, cost and high rate of reproducibility. In addition to these properties composition and geometry of working electrode also play a major role in electroanalytical applications. There are many types of working electrodes available and this list is continuously increasing. Commonly used working electrodes are made from conducting materials such as platinum, silver, gold, carbon and mercury. Size and shape of working electrode also varies depending on application. Here we will discuss major types of electrodes which are or were important for environmental analysis by electroanalytical techniques.

1.3.1 Mercury electrodes

Mercury electrodes have attractive electrochemical properties which make them a good choice for use in electroanalytical applications (yielding low limits of detection and high selectivity). However the use of mercury electrodes has become obsolete due to many disadvantages attributed mainly to Hg toxicity. They are also unsuitable for on-site and flowing applications, for the study of oxidation of organic compounds.[15,16] There are three main types of mercury electrodes with wide spread use in previous years for electroanalytical applications which include dropping mercury electrode, hanging mercury drop electrode and mercury film electrodes. Dropping mercury electrode was the first mercury electrode developed for environmental and electroanalytical applications, in particular for reduction studies of organic compounds.

1.3.2 Solid electrodes

Concerns regarding the toxicity of mercury and limited anodic potential range led to increased use of solid electrodes for electroanalytical applications. Solid electrodes advantageous in different analytical applications which were not possible with mercury electrodes.[17] The most important is their non-toxic nature and ease of handling, on-site electroanalytical applications and possibility of surface modifications. The behaviour of voltammetric device is strongly influenced by the nature of working electrode.

1.3.2.1 Metal and metal oxides based electrodes

Metal based electrodes have widespread use in electroanalytical applications, such as gold, silver, platinum, palladium, copper and metal oxides films such as Indium tin oxide (ITO), Fluorine-doped tin oxide (FTO). Advantages associated with metal electrodes are their inert nature, good conductivity, fairly broad potential window, low background current, reproducibility and suitability for sensing applications. Few disadvantages include low overvoltage for hydrogen evolution, limited range in cathodic potential domain as compared to mercury and dissolution of metals to form metal oxide layers during aqueous reactions. The formation of oxide layers during an analysis can seriously hamper the validity of analysis, also it is difficult to explain how these electrode materials will interact with the analyte during preconcentration for stripping analysis.[18] ITO and FTO are made up of transparent metal oxide films and have applications in sensing and optical measurements. Platinum and gold are among the most widely used metal electrodes; both these electrodes provide fairly broad potential range, although in cathodic domain they are much inferior than mercury electrodes while at high anodic potential values they undergo oxide formation in aqueous solutions resulting in poor reproducibility as well as slow electron transfer reactions.[19]

1.3.2.2 Carbon based electrodes

Carbon based electrodes have been extensively used in electrochemical applications including sensing and electroanalysis. Characteristics such as inert nature, large potential window, rich surface chemistry and resistance to corrosion make carbon based electrodes a superior choice for electrochemists.[20] However a disadvantage which is usually associated to carbon based electrodes is slow electron transfer reactions as compared to the metallic counterparts. There are few basic electrochemical characteristics attributed to carbon based

electrodes, which depend on the composition of electrodes as well as procedure used to make them. These include background current, electron transfer rates, reproducibility and adsorption.[21,22] Adsorption can sometimes be beneficial or it can seriously hamper the output of analysis, for desired applications adsorption can greatly enhance the response of target analyte, whereas unwanted analytes can also adsorb on electrode leading to behaviour which is not in accordance with diffusion controlled processes and cause of electrode surface fouling as well.[15,17] On the basis of structure and composition, carbon based electrodes can be divided into two categories (i) Homogenous and (ii) Heterogeneous. Homogenous electrodes are composed of solely single carbon compound e.g. glassy carbon, carbon nanotubes, graphite while heterogeneous have another substance incorporated with carbon compound e.g. carbon paste and screen printed electrodes.[18]

Glassy carbon electrodes are popular among the carbon based electrodes, their success in the field of electrochemistry is attributed to properties i.e. wide potential window, low cost, highly inert nature, stability to chemical, mechanical and thermal aberrations, sensitivity and possibility of surface modifications.[20,22] Glassy carbon was first prepared in 1962 by Yamada and Soto by heating treatment of phenolic compound as a precursor.[23] Glassy carbon has a much smaller pore size and low oxidation rate at higher temperatures, which makes it more inert as well as more resistant to chemical attacks as compared to other carbon compounds. Heating process involved in the formation of glassy carbon is very important for its correct formation. Initially, the precursor is heated up to 300 °C and carbonization process starts. Oxygen and nitrogen removal takes place between 300-500 °C; temperature is increased slowly to allow complete diffusion of gases to the surface and also formation of a defect-free product. The hydrogen removal takes place gradually between 500-1200 °C and hence only carbon is left.[23,24] Jenkins and Kawamura studied in detail the structure formation of glassy carbon. They found out that glassy carbon is formed by the random tangling and orientation of ribbons of aromatic molecules. If the annealing process is performed above 1200 °C, local defects are eliminated and it leads to the formation of smooth ribbons which are stacked on each other to give rise to microfibrils. These microfibrils then give rise to final glassy carbon product by twisting, bending and convolutions.[25]

In this study we used GCE as working electrode due to its rich surface chemistry, inert nature and resistance to chemicals, hardness and compact nature, possibility of modifications, surface renewal, sensitivity and applicability for sensing applications as compared to other

electrode materials. Carbon paste electrodes (CPE), pyrolytic graphite and graphene, screen printed carbon electrodes, carbon nanotubes and boron doped diamond electrodes (BDD) are few other examples of carbon based electrodes used in electroanalytical applications.

1.4 Modified electrodes

Chemically modified electrodes (CMEs) found their applications in different electrochemical applications such as sensing, energy conversion, optical and electronics. Modification of electrode materials is carried out usually by adsorption or covalent attachment to form a layer of modifier which imparts properties of interest to the underlying electrode surface.[26] Different approaches used for chemical modification of electrode surfaces include:

Chemisorption: These modifications are based on adsorption process on the electrode surface. Self-assembled monolayers (SAMs) are formed by this method.

Covalent bonding: Organosilane are covalently attached to electrode surface to form a strong interaction, these modifications can also be performed by electrografting. In next step, these covalently bonded silane molecules can be used as linking agent for strong adhesion of modifier having properties of interest to form a thin film.

Composite: Chemical modifier is directly incorporated in electrode matrix to give it properties of interest, such as modified carbon paste electrodes in which a modifier is also used in addition to graphite and binder for formation of electrode.

Polymer films: Organic, organometallic or inorganic polymer films are deposited at electrode surface by having chemical interaction or physical attachment. Polymer films can be conductive or non-conductive in nature, these films deposited at electrode surface may have chemical modifier already incorporated inside them or may be introduced later by technique known as functionalization.[27] Polymer films can be formed by dip coating with film thickness of 0.1 - 10 µm, spin coating, electrochemical deposition and polymerization.[28]

Chemical modification of electrode surfaces for electroanalytical applications has been a topic of interest in recent years, opening new avenues in the field of sensing by providing the better control over the electrode surface behavior and by solving different electroanalytical problems related to unmodified surfaces. These modifications have helped

greatly in enhancing sensitivity, reproducibility, stability and selectivity of different electrochemical sensing applications. The selectivity and sensitivity is enhanced either by the process of preconcentration or by selecting the nature of modification in a way that the interaction between target analyte and modifier provides greater analytical response.[18] The purpose of electrode modification is to achieve few targets which include fast electron transfer, possibility of chemical reactions for enhanced electrochemical response, selective permeation and exclusion properties and managing mass transport of species to electrode surface.[22] Electrode modification for voltammetric sensing should be stable, easy to perform, provide reproducible and sensitive analytical response.[7] Important factors which can determine the efficiency of electrode modification in terms of sensitivity and selectivity are morphology, composition of modifier, and surface coverage by films. The chemical properties and nature of the modifiers can be used to enhance the sensitivity and selectivity of target analyte. Electrode modification is also carried out by organic ligands, micro particles, ion exchangers, clays, zeolites, and silica based materials.[29–33] Modification with mesoporous silica using sol-gel chemistry offers the possibility of improving the electrochemical properties of an electrode.[29]

1.4.1 The Sol-gel process

Sol-gel process is a well-established method and interest has grown in past three decades to produce materials with desired properties.[34] This process is usually used for production of coatings which have applications in surface protection, optical and electrocatalytic applications. The sol-gel process involves "bottom up" approach for forming a network structure by using molecular building blocks. A sol is a stable suspension of colloidal particles ranging in size from 0.001 – 1 µm in a suitable liquid solvent. A gel is a porous, three dimensional continuous solid network. Sol-gel process involves two steps (i) hydrolysis and (ii) condensation explained in Eq. 1.2 - 1.4.

$$\equiv Si - OR + H_2O \rightleftharpoons \equiv Si - OH + ROH \qquad \textbf{Hydrolysis} \qquad \textbf{Eq. 1.2}$$

$$\equiv Si - OH + \equiv Si - OR \rightleftharpoons \equiv Si - O - Si \equiv + ROH \qquad \textbf{Ethanol condensation} \qquad \textbf{Eq. 1.3}$$

$$\equiv Si - OH + \equiv Si - OH \rightleftharpoons \equiv Si - O - Si \equiv + H_2O \qquad \textbf{Water condensation} \qquad \textbf{Eq. 1.4}$$

In silicon alkoxides based systems, silanol groups (Si-OH) are produced in the hydrolysis step, silanol groups are necessary for condensation to start. Condensation process involves silanol groups reaction with (Si-OR) as well as other silanol groups to form siloxane groups (Si-O-Si) with production of alcohol and water. The most common precursors for silica based structures are alkoxysilanes, forming siloxane bonds to give rise to mesoporous materials. Maximum interaction of siloxane groups and presence of minimum number of silanol, alkoxo groups is essential for compact silica network formation.[29,35] Hydrolysis and condensation process is pH dependant, acidic solution (pH ~ 3) is essential for complete hydrolysis and alkaline solution favours the condensation.[36] Surfactants are used as soft templates for mesoporous materials with desired porosity and are added in the starting sol.

1.4.2 Mesoporous silica modified electrodes

In recent years, the emergence of electrodes modified with mesoporous materials as electrochemical sensors has gained much importance.[37] IUPAC classifies the porous materials into microporous < 2nm, mesoporous 2-50 nm and macroporous > 50nm.[38] Mesoporous silica materials generation by using surfactant molecules was pioneered by scientists at Mobil Oil Corporation in 1992.[39] These materials from M41S family have been classified into three classes namely (MCM = Mobil Composition of Matter) (i) MCM-41 (ii) MCM-48 and (iii) MCM-50 giving rise to hexagonal, cubic and lamellar shaped materials respectively (Figure I-3).[40] MCM-41 among other is the most commonly used mesoporous material in electrochemical applications due to its pore size, distribution and uniform distribution of hexagonal channels.[41]

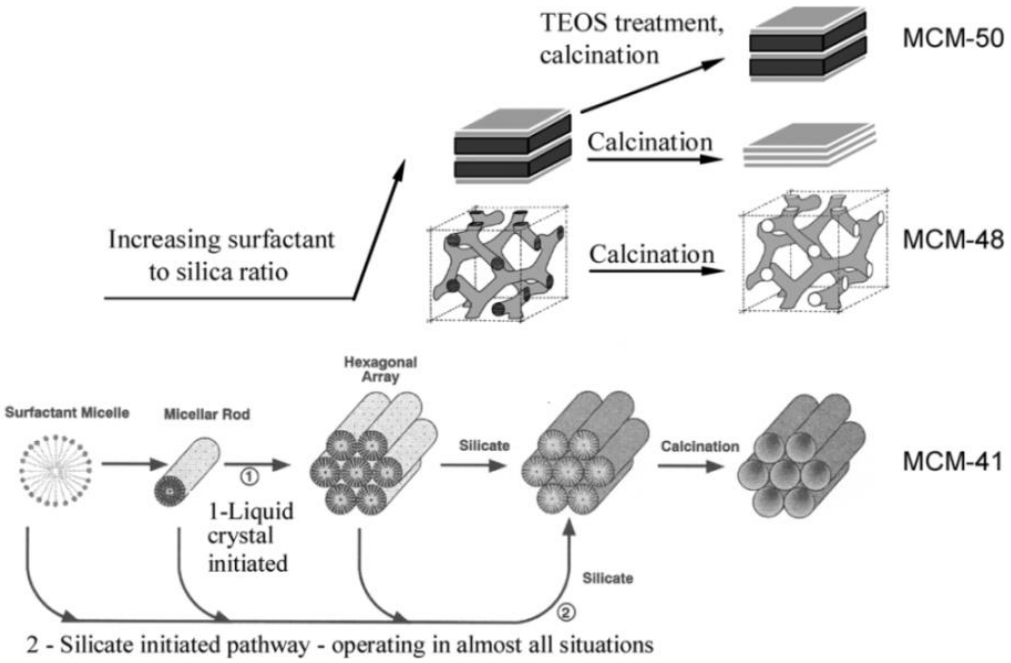

Figure I-3: Pathways for production of different mesoporous structures related to M41S family.[40]

Ordered mesoporous silica materials have unique characteristics which make them excellent choice to be used as electroanalytical applications. These characteristics include high surface area, possibility of composition amendment, ease of functionalization, hosting/support to absorbed species, isolating properties and orderness of pores which could help in mass transport and charge transfer.[42,43] Most mesoporous materials in the field of electrochemistry exist between 2-10 nm with uniform dispersion. Pore size can be tuned depending on the size of template used. The electrode modification involving production of ordered mesoporous materials are performed by using a template[44] to control the size, shape, properties and arrangement of resulting structures.[45] Most commonly used mesoporous silica materials in electrochemistry are MCM-41, MCM-48 (small pore size), SBA-15, SBA-16 (SBA = Santa Barbara Amorphous) (large pore size), HMS (Hexagonal Mesoporous Silica) and MSU (Michigan State University). MCM-41 and SBA-15 give rise to hexagonal arrangements whereas MCM-48 and SBA-16 produce structures with cubic arrangements.[42] Possibility of mesoporous silica materials functionalization with different organic compounds has also provided new dimensions to application of these materials in electrocatalysis, sensing and other electrochemical applications by providing better control over the chemical behavior of mesoporous structures.[46–48] Functionalization of mesoporous materials with organic compounds can be performed either by co-condensation or grafting these compounds in

mesoporous structure after its synthesis.[49,50] In co-condensation process, organic compound is added to the sol and hydrolysed together with silica precursor which results in incorporation of these compounds in mesoporous material matrix when condensed, whereas in post-synthesis grafting, suitable organic compounds are made to form strong interaction with silica structures.

1.4.3 Configurations of mesoporous silica modified electrodes

Configuration of mesoporous silica modified electrodes depends upon the nature of desired electrochemical application as well as nature of the material used for modification. In general, two common types of electrode configurations exists (i) Composite and (ii) Thin film modified electrodes.[42]

1.4.4 Composite electrodes

Composite electrodes are prepared by the mixing of mesoporous materials (mostly silica based and non-conducting) with a conducting compounds such as graphite powder. Carbon paste electrodes modified with silica compounds are the first examples of composite electrodes whereas modified screen printed electrodes (SPE) are the more recent ones.[51,52] There is a considerable interest in production of SPE with different organic and inorganic compounds incorporated in carbon inks which are used to make SPE. Composite electrodes are widely applied in the field of electroanalysis.[53] Composite electrodes have certain advantages such as close association of mesoporous materials and conducting matrix results in efficient electrochemical response and possibility of electrode modifications with compounds that usually does not form homogenous thin films.[42]

1.4.5 Silica coated electrodes

Deposition of powdered mesoporous materials present in a suspension can result in the formation of thin films of respective materials at electrode surfaces. These thin films can be prepared either by dipping the electrode inside suspension or putting it at the surface and letting solvent to evaporate. Major drawback of thin films prepared this way is their mechanical stability and poor homogeneity at electrode surface making them unfit for electrochemical applications.[42] To resolve these issues different approaches have been proposed including formation of strengthening layers of different organic polymers such as Nafion, Styrene and Poly (vinyl alcohol) over deposited mesoporous films and also mixing

mesoporous silica materials with these polymers to form polymer films containing encapsulated mesoporous silica materials.[54–58] However, these organic polymers are not very inert in nature and can interact with mesoporous silica materials in solution and hence can change its properties. Formation of thin films using template molecules result in homogenous and mechanically stable mesostructures at electrode surfaces. In addition to composite and thin films as electrodes modifiers, mesoporous silica based materials with different morphologies i.e. nanoparticles, monoliths, spheres and rods have found their applications in the field of drug delivery, catalysis, as a support, encapsulation and selective adsorption of biomolecules.[59–62] In this study we focused on deposition of surfactant-templated mesoporous silica thin films on glassy carbon electrodes. Various methods available for production of mesoporous silica thin films using template route are discussed.

1.5 Mesoporous silica thin films

The deposition of mesoporous silica thin at electrode surfaces is based on the local control of sol-gel chemistry. Mesoporous silica thin films are synthesized by surfactant templating. A general method for the synthesis of mesoporous silica thin films with parallel arrangement to electrode surface is evaporation induced self-assembly (EISA).[63] This process is used for depositing silica film by dip coating, spin coating and drop coating methods with the help of a sol prepared with surfactant and silica precursors in water and ethanol medium. In the next step, solvent evaporation results in the deposition of a homogenous film due to polycondensation of silica precursors and surfactant critical micelle concentration (CMC).[64] Mesoporous silica thin films formed by EISA process have parallel arrangement of pores to electrode; this can result in poor performance of silica films in electrochemical applications due to transport limitations. Schematic representation of mesoporous silica films deposition by EISA process is presented in Figure I-4.

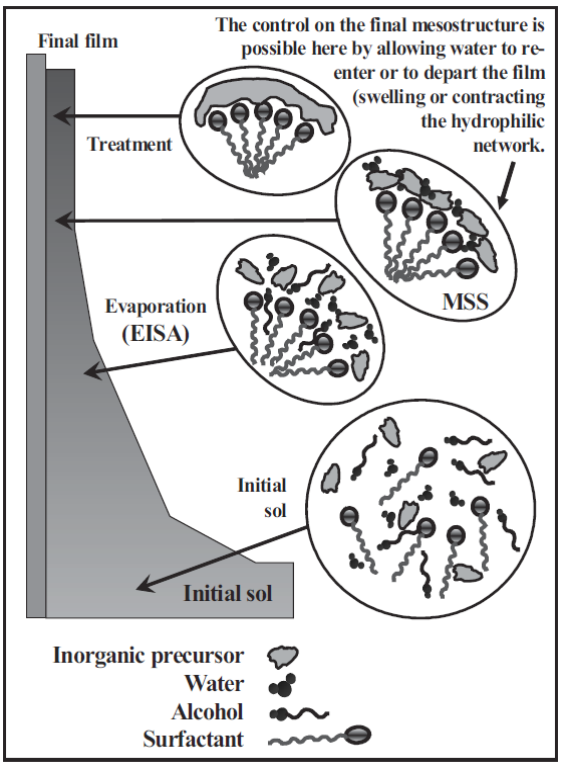

Figure I-4: Schematic representation of mesoporous silica thin films synthesis by evaporation induced self-assembly.[64]

1.5.1 Vertically oriented mesoporous silica thin films

Vertically oriented mesoporous silica thin films are advantageous in electroanalytical application as the can offer fast mass and electron transfer due to normal pore arrangement towards electrode surface. Various strategies have been proposed to generate mesoporous silica thin films with hexagonally packed mesochannels aligned vertically to electrode surface such as (i) dimensional confinement and self-assembly process in exotemplates (pre-assembled block copolymer films[65] or porous membranes[66] (ii) combination of photoaligning and micropatterning techniques or surface mediated alignment via π-π interactions;[67,68] (iii) epitaxial growth;[69] (iv) magnetically induced orientation;[70] (v) oil-induced co-assembly approach;[71] (vi) electrochemically assisted self-assembly (EASA);[72] and (vii) Stöber-solution growth method.[73] Among them, the most robust ones are certainly the last two methods, as they have been reproduced by independent groups (especially the EASA method).[74–83] These two methods lead to small-pore materials (2-3 nm in diameter) as a result of using cetyltrimethylammonium bromide (CTAB) as the surfactant template. The Stöber-solution growth method[73] involves a controlled kinetic interface nucleation and slow growth (1-3 days' time range, at 60-100°C) originating from the gradual transformation of silicate-CTAB

composites from spherical to cylindrical micelles with the assistance of ammonia hydrogen bonding and progressive silicate polymerization, such films can be manufactured in mono- or multi-layered structures.[73]

1.5.2 Electrochemically assisted self-assembly (EASA) process

The EASA method[72,84], like Stöber-solution growth method operates under kinetic control but is much faster (5-30s deposition time) and film formation is achieved at room temperature. It is based on the application of a reductive potential to an electrode immersed in a hydro-alcoholic sol containing a hydrolysed tetraalkoxysilane as silicate source and CTAB surfactant as template, inducing concomitant self-assembly of surfactant hemi-micelles at the electrode surface and polycondensation of the silica precursors driven by the electrochemically generated pH increase.[72] (under cathodic potentials, protons and water molecules are being reduced inducing a local increase of the pH at the electrode/solution interface and hence favouring the self-assembly condensation of silica around the surfactant template). Film growth occurs from the electrode surface, explaining the vertical arrangement of the hexagonally packed mesochannels. The mesoporosity is then revealed by the removal of surfactant molecules from the film. In this study, silica thin films were deposited at electrode surface by EASA technique which were subsequently Characterized by transmission electron microscopy (TEM). Figure I-5 is the schematic representation of mesoporous silica thin films formation at electrode surface with the help of EASA method.

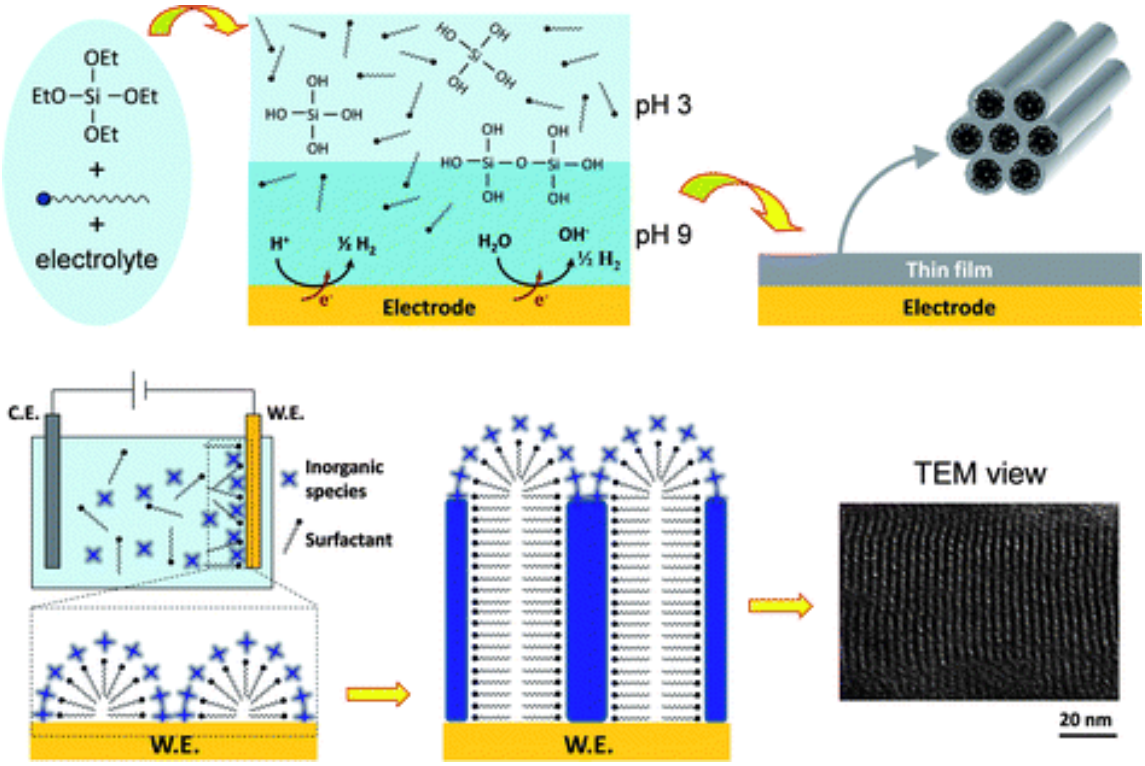

Figure I-5: Schematic representation of electrochemically assisted self-assembly method to generate ordered and vertically oriented mesoporous silica films onto an electrode surface.[85]

1.5.3 Mesoporous silica thin film applications

Mesoporous thin films prepared from the self-assembly of surfactant templates are attractive materials and several studies are available in literature, which describe their synthesis, properties and potential applications.[86–90] These systems exhibit the advantageous features of ordered mesoporous materials (large surface area, narrow pore size distribution, widely-open uniform pore structure). In addition, thin films show a high capability of device integration, thus opening up enormous opportunities for practical applications (Figure I-6). Mesoporous silica films constitute a sub-category of family of materials,[91] offering a wide palette of surface modification to generate nanostructured organic-inorganic hybrids with extended properties.[50,92,93] Highly ordered thin films offer significant advantages in electrochemical sensing.[43] Mesoporous silica films are very effective in the detection of small redox active molecules,[80,94,95] while keeping away larger molecules that could passivate the underlying electrode surface (anti-biofouling properties).[95] Oriented mesoporous silica films have proven to be a successful choice for sensing applications such as detection of drugs,[94] aromatic explosives and pesticides,[80] polyphenolic compounds,[96] and heavymetals.[97,98] Moreover, simple functionalization of the silica films generated by EASA process provide

extra advantage for their application in the field of sensing and electrocatalysis.[85,99] A challenging avenue is getting continuous nanoporous films with controlled orientation of the mesochannels and the vertical alignment of one-dimensional mesochannels (i.e., perpendicular to the underlying substrate) is highly desired as it ensures fast mass transport through the film and induces anisotropic properties in the materials.[86,100,101] Figure I-6 presents the detailed overview of vertically oriented mesoporous silica thin films applications.

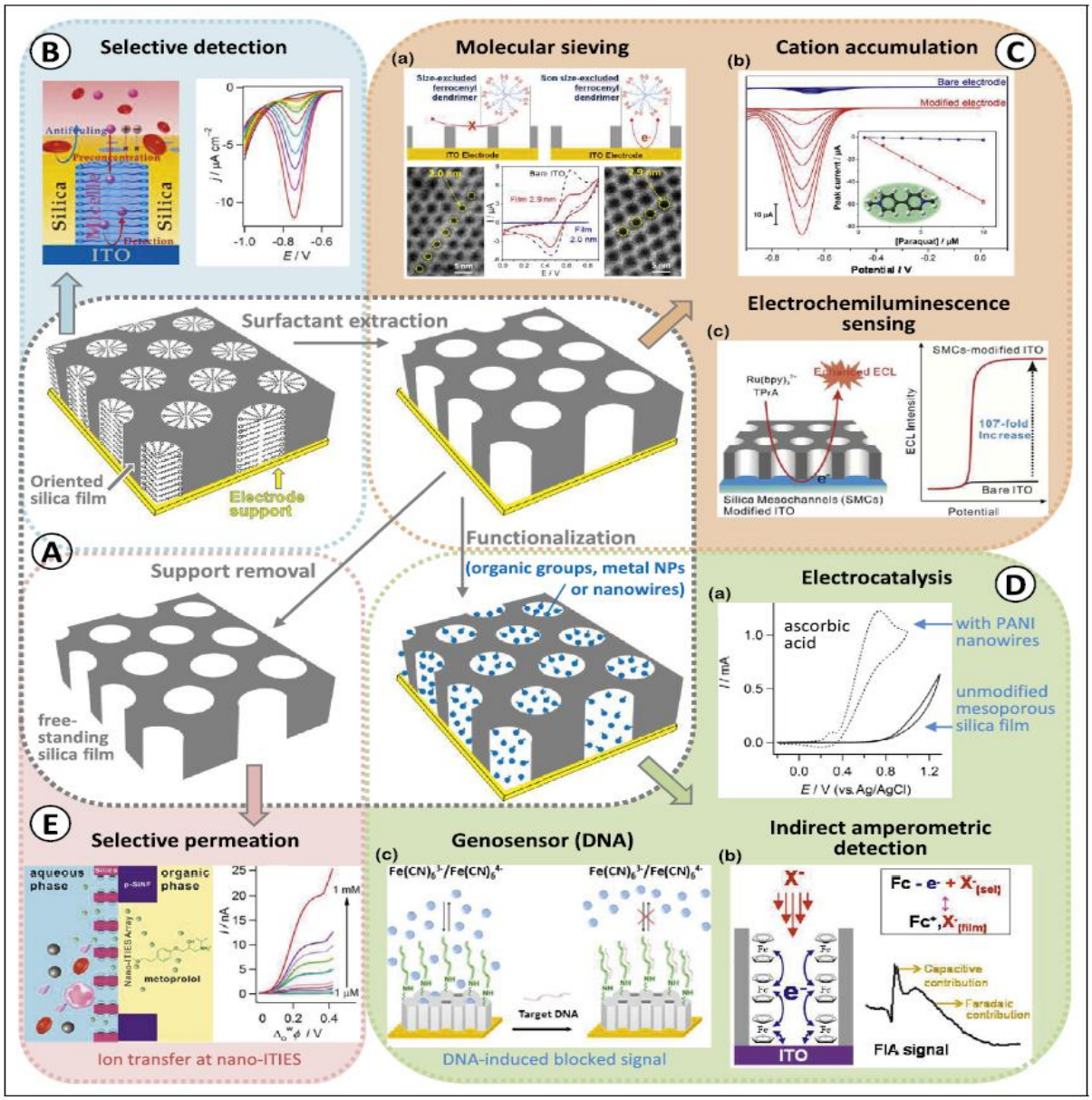

Figure I-6: Applications of mesoporous silica thin films in electrochemical application, from[102] and references therein.

In this thesis I have focused my research work on preparation of non-Functionalized tetraethoxysilane (TEOS) based mesoporous silica thin films by EASA method.

1.6 Use of pesticides in agriculture

Pesticide is a broad term for a number of chemical compounds in agricultural practices which include herbicides, fungicides etc. Herbicides are the organic compounds used to control the growth of unwanted plants or herbs in a crop. Herbicides are normally classified into two categories on the basis of mode of action (i) Contact (ii) Systematic. Contact herbicides act by destroying the parts of the plants in which they come in contact with and systematic herbicides destroy the herbs by transporting through the plant system. Agricultural practices changed dramatically after the World War II towards more automation and widespread use of chemical compounds for increased crop yield. As the global population kept increasing, the pressure on agriculture sector mounted for higher crop yield to meet the needs of more people which led to intense use of pesticides and herbicides.[103] The use of pesticides and herbicides undoubtedly increased the production of crops and ultimately increased the quality of human lifestyle but on the other hand these chemical compounds have serious implications on the health of living organisms (non-target) as well as on the environment which needs to be addressed.[104] The adverse effects of pesticides and herbicides include direct impact on human lives which include serious health problems, cancer, reproductive system complications and thousands of deaths per year.[105–107] Impact on the environment includes contamination of air, soil and water systems and hence affecting the living organisms and disturbing the natural balance.[108–110] Global sales of pesticides and herbicides is shown Figure I-7 which is constantly increasing every year.

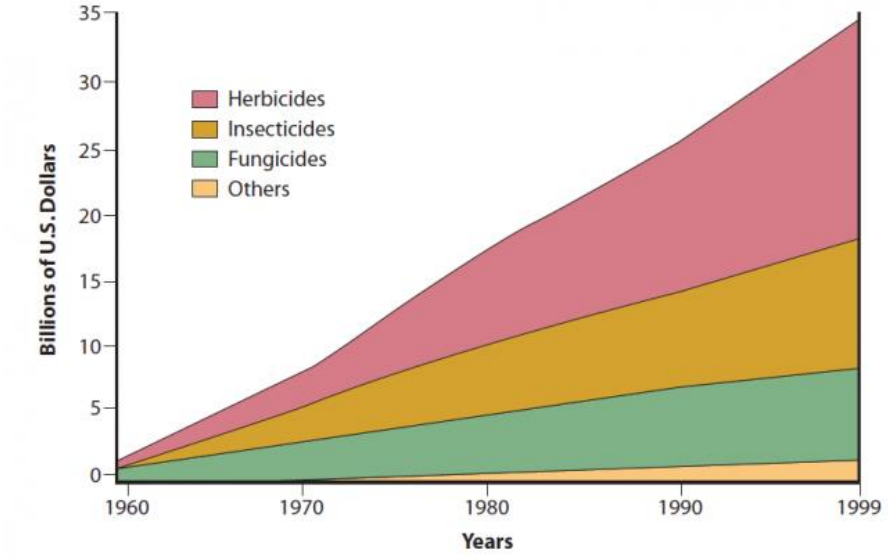

Figure I-7: Worldwide sale of pesticides 1960-1999.[111]

Herbicides constitute a major portion of total pesticides consumption worldwide, pesticide consumption over the past years have reached up to 3.5 million tons every year with market worth of 45 billion dollars.[112] Figure I-8 shows the consumption percentage of different chemicals being used in agriculture sector worldwide.

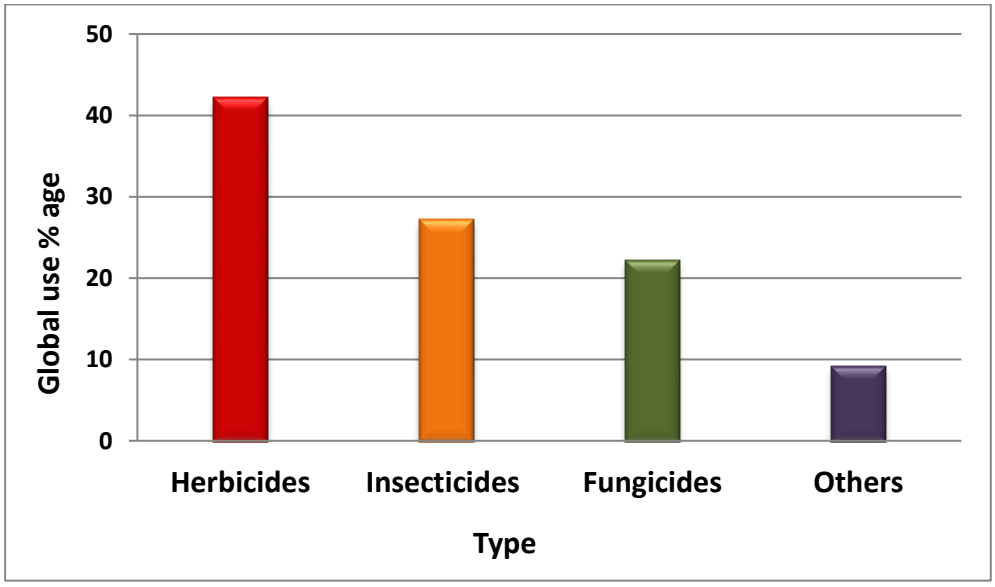

Figure I-8: Consumption of pesticide worldwide (2015).[112]

1.6.1 Paraquat and diquat

Paraquat (1, 1-dimethyl-4, 4-bipyridinium dichloride) is a yellowish solid with ammonia like odor and chemical formula $C1_2H_{14}Cl_2N_2$, whereas diquat (1, 1'-Ethylene-2, 2,-

bipyridyldiylium dibromide) is also a yellow crystalline solid with chemical formula $C1_2H_{12}Br_2N_2$. Both paraquat and diquat are highly soluble in water; paraquat is produced by pyridines coupling in the presence of sodium and ammonia followed by oxidation and finally methylation of the compound by chloromethane. Diquat synthesis include oxidation of pyridines in the presence of Raney nickel catalyst followed by formation of ethylene bridge as a result of chemical reaction with 1,2 dibromoethane.[113] Paraquat and diquat are both non-contact, selective and synthetic herbicides from the same class also termed as dipyridils. Paraquat products are commercially available with a range of 20-50 % active ingredient concentration, formulations used for on field applications range from 0.07-0.14% of concentrations. Diquat is prepared as dibromide monohydrate salt with commercially available in concentration range of 15-25% and formulations for on field applications are made upto 0.23%.[113] They are used to control the growth of unwanted broad leaved herbs for the seed crops, potatoes and sugarcane. Many countries have banned the use of paraquat including the European union but still is widely used in developing countries[114], it effects the vital organs due to ingestion or by absorbing through skin. Initial signs of paraquat poisoning include burning pain in chest, throat, abdomen and mouth due to corrosive effect of paraquat and damage to mucosal lining.[115] Diquat is less toxic as compared to paraquat, effects on the vital organs are less serious and reversible whereas neurotoxic effects of diquat are more severe as compared to paraquat.[116] Paraquat and diquat are from same family of herbicides and show very similar electrochemical behavior and therefore electrochemical sensor developed for paraquat can also be successfully applied for the detection of diquat.

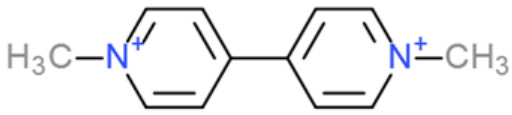

(A) Paraquat

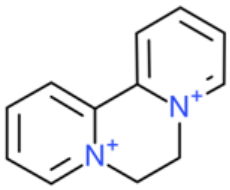

(B) Diquat

1.6.2 Isoproturon

Isoproturon (3-(4-isopropylphenyl)-1, 1-dimethylurea) is a colourless, odourless solid and soluble in water with chemical formula $C_{12}H_{18}N_2O$. Isoproturon is a phenylurea herbicide; it is used to control the seasonal grasses and broadleaf herbs in the grain crops. This

compound has gained increasing attention due to its widespread use and harmful effects on human life and environment. Isoproturon was the most used herbicide on wheat and barley in France and is banned in the European Union since 2016.[117] It is detected in ground and surface water as well as in soil in areas of use. Its hydrolysis is very slow and has a half-life of about 30 days in water while in soil its half-life is about 40 days, it can undergo some photochemical degradation to different metabolites.[118] Oral LD_{50} of isoproturon for rats varies in different studies from 1-2.9 g/kg of body weight.[119] Studies have shown that prolonged exposure to higher limits of isoproturon affects the kidneys, lungs and heart function. It is also proved that isoproturon exposure cause chromosomal aberrations and hence can cause mutations leading to disabilities in future generations.[120] Isoproturon exposures also effect the reproductive systems, it is neurotoxic and carcinogenic.[121]

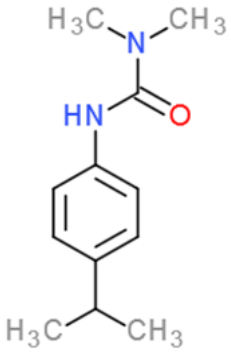

Isoproturon

1.6.3 Other herbicides

2-4-dichlorophenoxyacetic acid or 2-4-D is an organic compound and the first among herbicides to be used in agriculture starting from 1940's. It's a systematic herbicide and used in more than 1500 herbicides as active ingredient.[122] It is toxic for humans and living organisms and World Health Organisation (WHO) classifies it as possible carcinogenic.[123] Atrazine is another family of herbicides which was started to be used in 1950's. Atrazine is among the most used in US and Australia while it was banned in European union in 2003 due to ground water contamination.[124] In US and Australia it is also associated with the groundwater and is major herbicide found responsible for ground water contamination.[125] Glyphosate is another organic compound which is currently the most used herbicide

worldwide, more than 50% use of total herbicides is glyphosate. It is a broad spectrum herbicide and strongly absorbs in the soil, contaminate water and disturb aquatic life.[126]

1.7 Electrochemical detection of herbicides

Conventional methods for the detection of herbicides and pesticides in general include high performance liquid chromatography[127], spectroscopy[128], capillary electrophoresis[129], gas chromatography mass spectrometry (GC/MS)[130], radioimmunoassay[131], fluorescent probe titration[132], spectrophotometry[133], and more recently flow injection colorimetric assay[134] or surface-enhanced Raman spectroscopy.[135] These methods may provide quite low detection limits but suffer from the disadvantages of requiring cumbersome instrumentation, time consuming, highly trained personnel, inability to perform real time analysis and can be costly as well. There is need for systems which can provide rapid, cost effective, reliable and on-site detection of pollutants. Electrochemical sensing of pollutants in aqueous samples is rapidly growing technique these days with having the advantage of electrode surface modification, ease of handling, cost effectiveness and possibility of on-site applications for real time detection.[43,136,137] Electrochemical sensing with technological advancements can provide these detection systems for harmful compounds. This can lead to proper management of the risk for lowest possible damage to human health and environment. In table I-2 few examples related to electrochemical sensing of paraquat[139,140,141,142–148,149–158,159] and isoproturon[159–164] are presented.

Table I-2: Comparison of different electrochemical methods reported in literature for detection of paraquat and isoproturon

Herbicide	Electrode material	Modification	Method	Linear range (mol L^{-1})	LOD (mol L^{-1})	Preconcentration/s	Reference
Paraquat	Mercury	-	SWV	5×10^{-8}-1×10^{-5}	1.5×10^{-8}	No	138
-	BDD	-	SWV	8×10^{-7}-1.6×10^{-4}	7×10^{-8}	No	139
-	BDD	-	SWV	5×10^{-9}- 1×10^{-6}	1.5×10^{-9}	No	140
-	Au-µE	-	SWV	No data	1.76×10^{-8}	No	141
-	Au-µE	-	SWV	5×10^{-7}-1×10^{-5}	8.2×10^{-8}	No	142
-	Cu	Bismuth film	DPV	0.1×10^{-6}-4.2×10^{-6}	1.2×10^{-8}	No	143
-	Cu	Bismuth Film	DPV	6.6×10^{-7}-4.8×10^{-5}	9.3×10^{-8}	No data	144

Herbicide	Electrode material	Modification	Method	Linear range (mol L^{-1})	LOD (mol L^{-1})	Preconcentration/s	Reference
-	Au	Au NPs-DNA	SWV	5×10^{-6}-1×10^{-3}	1.9×10^{-6}	No data	145
-	CPE	Ag NP	SWV	1×10^{-7}-1×10^{-3}	2.01×10^{-8}	600	146
-	CPE	Sb NPs-Biochar	SWV	0.2-2.9 $\times10^{-6}$	3.4×10^{-8}	120	147
-	Au	Au NPs-DNA	DPV	7×10^{-9}-1.5×10^{-6}	2×10^{-10}	No data	148
-	Graphene	(Ppy-g-NGE)	DPV	5×10^{-8}-2×10^{-6}	4.1×10^{-8}	300	149
-	GCE	Carbon nanotubes - DHP	SWV	5×10^{-8}-1.5×10^{-6}	1×10^{-8}	No data	150
-	GCE	PVP-GNs/Cu_2O	DPV	1×10^{-6}-2×10^{-4}	2.7×10^{-7}	No data	151
-	PG	Metallophtahlocyanines	SWV	5×10^{-7}-2.9×10^{-5}	1.03×10^{-7}	600	152
-	CPE	Biochar	DPAdSV	3×10^{-8}-1×10^{-6}	7.5×10^{-9}	300	153
-	GCE	Nafion	CDPV	3.9×10^{-9}-3.9×10^{-7}	1.9×10^{-9}	180	154
-	GCE	Nafion - Clay	SWV	3.9×10^{-8}-2.7×10^{-7}	1.9×10^{-9}	240	155
-	CPE	Amberlite XAD-2 resin	CSV	4.2×10^{-6}	3.9×10^{-7}	180	156
-	CPE	Natural phosphate	SWV	2.3×10^{-8}-3×10^{-6}	7.8×10^{-10}	600	157
-	CPE	Hydroxyapatite	SWV	8×10^{-7}-2×10^{-5}	1.5×10^{-8}	1800	158
Isoproturon	GCE	MWCNT/P3MT	AdSV	3.9×10^{-7}-1.2×10^{-6}	3.9×10^{-7}	600	165
-	Wall-jet	-	Ad SWV	4.9×10^{-9}-7.3×10^{-5}	7.3×10^{-7}	300	166
-	Au	MIP	ECL	9×10^{-11}-5.1×10^{-9}	3.8×10^{-12}	900	167
-	SPE	Graphene	SWSV	9.7×10^{-7}-4.9×10^{-4}	9.7×10^{-7}	120	162
-	GCE	SM-Clay	DPSV	0.2×10^{-6}-6.2×10^{-5}	1.0×10^{-5}	20	163
-	GCE	Clay	SWSV	4.9×10^{-9}-1.5×10^{-6}	4.9×10^{-9}	5	164

BDD: Boron doped diamond; PG : Pyrolytic graphite; GCE: Glassy carbon electrode, CPE: Carbon paste electrode; AuNPs: Gold nanoparticles; PVP-GNs/Cu_2O: Polyvinyl pyrrolidone-graphene nanosheets/Cuprous oxide; Au-µE: Gold microelectrode; DHP: dihexadecylhydrogenphosphate; SM-Clay: Sodium montmorillonite-clay; DPAdSV: Differential pulse adsorptive stripping voltammetry; DPV: Differential pulse voltammetry; SWV: Square wave voltammetry; CDPV: Cathodic differential pulse voltammetry; CSV: Cathodic stripping voltammetry; SWSV: Square wave stripping voltammetry; DPSV: differential pulse stripping voltammetry; ECL: Electrochemical luminescence; MIP: Molecularly imprinted.

1.8 Brief introduction of research project

Glassy carbon electrodes were selected as working electrode materials based on the literature review. Electrode modification using electrochemically assisted self-assembly (EASA) is a well-established method by our group but poor adhesion of silica thin films at glassy carbon electrodes was an obstacle for successful surface modification. **Chapter III** is based on solving this issue of silica thin films adhesion at glassy carbon electrodes by electrografting 3-aminopropyltriethoxysilane (APTES) as a molecular glue prior to silica film deposition. **Chapter IV** is related to the application of successfully modified glassy carbon electrodes for electrochemical detection of paraquat. Paraquat is an intensively used herbicide in agricultural practices; it is extremely toxic and known to severely affect health of living organisms leading to death. Effect of different solution parameters on sensitivity was studied. **Chapter V** includes the study of electrode modification parameters and electrode geometry effect on sensitive detection paraquat. **Chapter VI** is related to the investigation of electrochemical behavior and detection of isoproturon at both bare and modified electrodes.

Chapter II: Experimental section

This chapter is aimed for providing the detailed overview of different chemicals and procedures which were used to carry out the present work. Experimental section is divided into different parts comprising of (i) detailed list of chemicals, (ii) electrodes and their preparation (iii) protocols for electrodes modification and electrochemical setup (iv) analytical techniques used in this study.

2.1 Chemicals

Chemicals used in this study are summarized in table II-1

Table II-1 List of chemicals

Electrolytes and surfactants				
Name	**Formula**	**MW ($g.mol^{-1}$)**	**Purity %**	**Supplier**
Cetyltrimethylammonium bromide (CTAB)	$C_{19}H_{42}BrN$	364.45	99	Acros
Tetrabutylammonium tetrafluoroborate (NBu_4BF_4)	$C_{16}H_{36}BF_4N$	329.275	99	Sigma-Aldrich
Sodium dihydrogen phosphate	$NaH_2PO_4. H_2O$	156.01	99.6	Prolabo
Sodium perchlorate monohydrate	$NaClO_4. H_2O$	140.46	99	Merck
Sodium chloride	NaCl	58.44	98	Prolabo
Sodium nitrate	$NaNO_3$	84.99	98	Prolabo
Sodium perchlorate	$NaClO_4$	122.44	99	Merck
Sodium sulfate	Na_2SO_4	142.04	98	Prolabo
Potassium chloride	KCl	74.55	99	Prolabo
Silica precursors				
Tetraethoxysilane (TEOS)	$Si(OC_2H_5)_4$	208.33	98	Alfa Aesar
3-Aminopropyltriethoxysilane (APTES)	$H_2N(CH_2)3Si(OC_2H_5)_3$	221.37	99	Sigma-Aldrich

(3-mercaptopropyl) trimethoxysilane (MPTMS)	$HS(CH_2)_3Si(OCH_3)_3$	196.34	>97	Fluka
Tetramethoxysilane (TMOS)	$Si(OCH_3)_4$	152.22	98	Sigma-Aldrich
Trimethoxyphenylsilane (PTMOS)	$C_6H_5Si(OCH_3)_3$	198.29	98	Sigma-Aldrich
Methyltrimethoxysilane (MTMOS)	$CH_3Si(OCH_3)_3$	136.23	97	Alfa Aesar
Solvents				
Acetonitrile (ACN)	CH_3CN	41.05	99.9	Sigma-Aldrich
Ethanol	C_2H_6O	46.07	>95	Carlo Erba
Redox probes				
Hexaammineruthenium(III) chloride	$[Ru(NH_3)_6]Cl_3$	309.61	98	Sigma-Aldrich
Ferrocene	$Fe(C_5H_5)_2$	186.03	98	Merck
1,1'-Ferrocene dimethanol	$C_{12}H_{14}FeO_2$	2460.8	97	Sigma-Aldrich
Potassium hexacyanoferrate	$K_3Fe(CN)_6$	329.24	>99	Fluka
Herbicides and pesticides				
Methylviologen (Paraquat)	$C_{12}H_{14}C_{l2}N_2.\ xH_2O$	257.16	98	Sigma-Aldrich
Isoproturon	$C_{12}H_{18}N_2O$	206.3	99.1	Chem Service

Catechol	$C_6H_6O_2$	110.11	99	Acros
Other chemicals				
Hydrochloric acid	HCl	36.46	37	Prolabo
Perchloric acid	$HClO_4$	100.46	60	Riedel de haen
Nitric acid	HNO_3	63.01	65	Sigma-Aldrich
Sulfuric acid	H_2SO_4	98.08	95	Sigma-Aldrich
Sodium hydroxide	NaOH	39.99	Pure pellets	Riedel de haen

2.2 Electrodes and electrochemical apparatus

Conventional three electrodes electrochemical system was used in this project comprised of working, reference and counter electrodes.

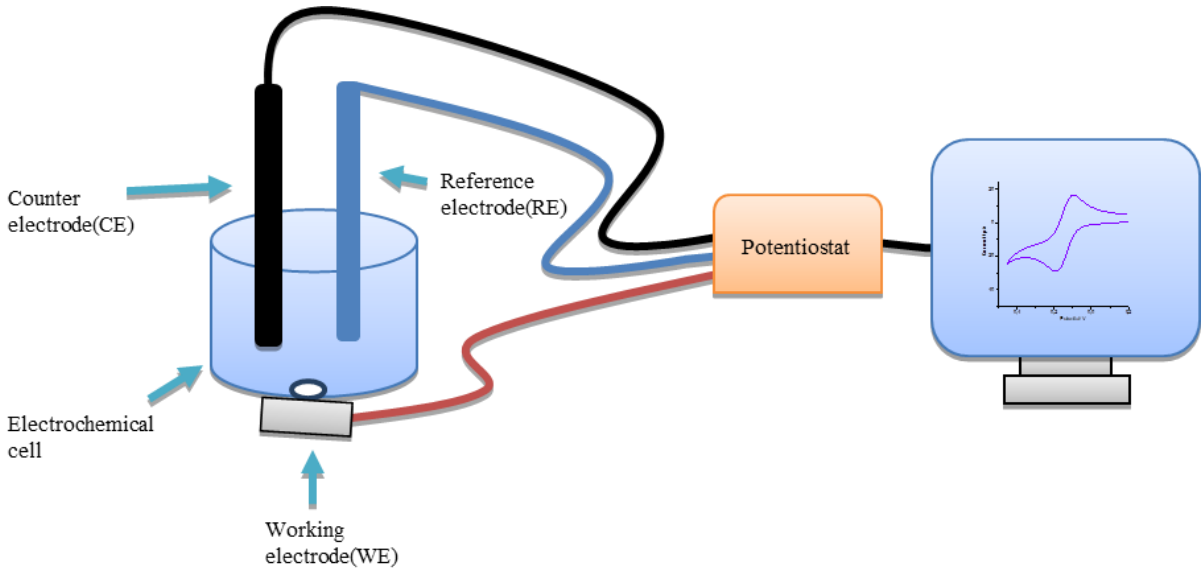

Figure II-1: Schematic representation of a typical three electrode system electrochemical setup.

2.2.1 Working electrodes

In an electrochemical setup the reaction of interest takes place at working electrode, Working electrodes used in this study were Glassy carbon plates (SIGRADUR G plates, 20 mm × 10mm × 1 mm) purchased from HTW (Germany), and indium tin oxide (ITO) plates with surface resistivity 8-12Ω (Delta technologies).

2.2.2 Reference electrodes

Reference electrode in an electrochemical setup has a stable and well known potential and is used as a point of reference for potential control and measurements. Current flowing through reference electrode is kept close to zero (ideally zero) which is achieved by closing the current circuit by counter electrode and by high input impedance on the electrometer.[168] Reference electrode provides control over the potential of working electrode. Ideally a reference electrode must have few characteristics e.g. (i) its potential should be governed by Nernst equation (should be chemically and electrochemically reversible) (ii) Potential should

remain constant when a small current is passed and back to original value after small current flow (iii) thermal coefficient of potential should be small.[169]

Most commonly used reference electrodes and their chemical equation with standard potential (E°) are as follows:

(i) Saturated Calomel Electrode (SCE)

$Hg_2Cl_2 + 2e^- \rightleftharpoons 2Hg + 2Cl^-$ (E° = 0.268V vs. NHE) **Eq. 2.1**

(ii) Silver/Silver chloride electrode (Ag/AgCl)

$AgCl + e^- \rightleftharpoons Ag + Cl^-$ (E° = 0.222V vs. NHE) **Eq. 2.2**

(iii) Normal hydrogen electrode (NHE)

$2H^+ + 2e^- \rightleftharpoons H_2$ (E° = 0.000V) **Eq. 2.3**

In this study reference electrode, Ag / AgCl / 1 M KCl (purchased from Metrohm, Switzerland) for aqueous solutions was used, for organic solutions and silica film electrogeneration a silver wire as pseudo reference electrode was used.

2.2.3 Counter electrode

Counter electrode is also known as auxiliary electrode (source and sink of electrons); it is used to close the current circuit in an electrochemical cell and usually does not participate in electrochemical reaction. Counter electrode is made up of an inert material (Au, Pt, graphite, glassy carbon, stainless steel etc.) As the current flows between working and counter electrode in an electrochemical reaction, total surface area of counter electrode should be higher than working electrode so that it does not limit the kinetics of reaction under investigation. Stainless steel rod and sheet was used as counter electrode for all experiments in present study.

2.2.4 Electrochemical cells

Four type of electrochemical cells were used in this project

(a) Open cell for electrochemical characterization with electrochemically active area (O ring diameter = 5 mm).

(b) Cell for electrochemical deposition of silica thin film with electrochemically active area (O ring diameter = 10 mm).

(c) Closed cell for APTES grafting and organic solutions (as organic solvents are evaporated if analysis is carried out in an open cell).

(d) Closed cell with electrochemically active area (O ring diameter = 5 mm) for electrochemical reaction which require to be done in the absence of oxygen (achieved by continuous nitrogen purging) as shown in (Figure II-2).

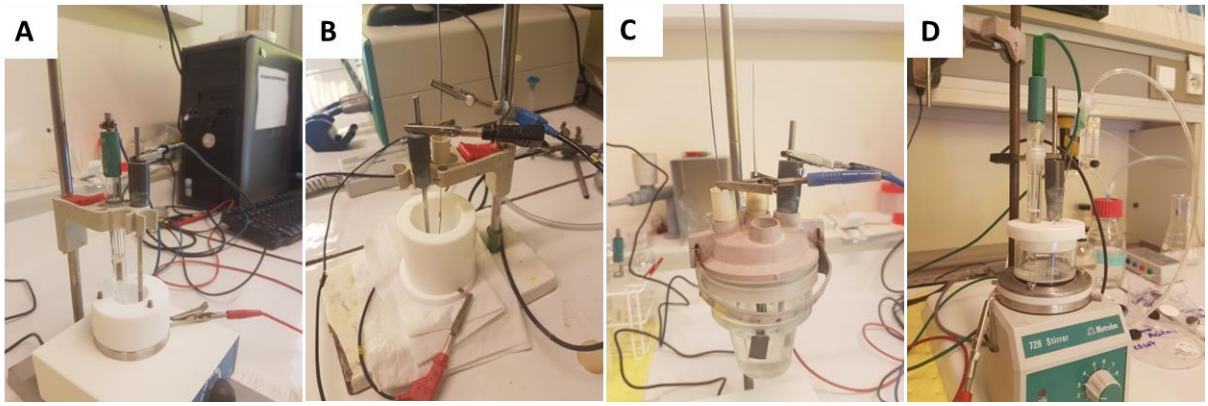

Figure II-2: Four types of electrochemical cells (a) for electrochemical characterization (b) for electrochemical silica thin film deposition (c) for APTES grafting (d) for analysis in the absence of oxygen.

2.2.5 Electrochemical apparatus

All galvanostatic experiments were carried out with a PGSTAT 100 apparatus from Ecochemie (Metrohm, Switzerland), and all cyclic voltammetry measurements were performed with an EMStat2 potentiostat (PalmSens, Netherlands). Square wave voltammetry measurements were performed with PalmSens potentiostat (PalmSens, Netherlands) by using a special electrochemical cell in the absence of oxygen (N_2 purging continuously and stopping while recording the scan).

Figure II-3: Electrochemical apparatus (A) EMStat2 potentiostat (B) PalmSens potentiostat (C) PGSTAT 100.

2.2.6 Electrodes preparation

The glassy carbon plates were polished with alumina (1, 0.3 and 0.05 μm) on a polishing cloth, rinsed thoroughly with ultrapure water and sonicated for 5 minutes before using for electrochemical analysis and modification. ITO plates were washed with ultrapure water before use.

2.3 Protocols for mesoporous silica film preparation

Protocols for preparation of solutions required for electrografting of primary amine, as a molecular glue and sol for preparations of silica thin films are discussed in this section.

2.3.1 3-Aminopropyltriethoxysilane (APTES) electrografting

APTES was electrografted on GCE surface (A = 3.4cm^2) by cyclic voltammetry (200 mV s^{-1}) using an EMStat2 potentiostat (Figure II-3 A) according to a procedure published for oxidation of aliphatic amines[170] by scanning potentials between +0.7 V and +2 V. Acetonitrile as a solvent while 0.1 M $Bu_4N^+BF_4^-$ as electrolyte and closed electrochemical cell for organic solvents (Figure II-2 C) was used. A concentration of APTES to be electrografted was optimized between 1 to 5 mM. Electrodes were rinsed with ethanol after electrografting to remove any remaining traces of electrolyte and non-grafted APTES molecules.

2.3.2 Sol gel preparation and thin film electrodeposition (monolayer films)

A typical sol solution was prepared by mixing ethanol and 0.1 M $NaNO_3$ in 1:1 v/v ratio, tetraethoxysilane (TEOS) and cetyltrimethylammonium bromide (CTAB) was added to this solution (100 mM and 32 mM respectively) according to previously optimized concentration.[84] The pH of sol solution was adjusted to 3 by adding 0.1 M HCl and hydrolysed by stirring for 2.5 hours at room temperature before using it for electrodeposition of silica film; Sol was prepared on daily basis. The area of the GCE to be modified with silica film was 0.5cm^2, electrochemical cell used for film deposition is shown in (Figure II-2 B). Film deposition was achieved through galvanostatic conditionsby using PGSTAT 100 apparatus (Figure II-3 C) from Ecochemie (Metrohm, Switzerland), Electrodes were immersed in hydrolysed sol and a current density, *j*, of -0.74 mA cm^{-2} was applied for 30 seconds, while in case of ITO electrodes silica thin films were deposited using potentiostatic conditions (-1.3 V for 30 seconds). Silver wire was used as pseudo reference and stainless

steel rod as counter electrode. Modified electrodes were treated overnight at 130 °C for proper cross linking of silica network. Template was removed from film matrix under moderate stirring conditions in 0.1 M HCl-ethanol solution for 1 hour as previously described.[97] Modification of electrodes was characterized at each step by hexaamine ruthenium as redox probe.

2.3.3 Sol preparation and thin film deposition (multi-layered films)

Sol for multi-layered films, different deposition time and microelectrode arrays modification was prepared according to the previously described procedure for chapter III and IV. For multi-layered and various deposition time GCE plates were used, microelectrode arrays at GC substrates were prepared in clean room followed by curing at high temperature in N_2 presence. GCE plates were cleaned as described previously and microelectrode array were thoroughly rinsed with ultrapure water before use. GCE and microelectrode array were electrografted with 1 mM APTES by cyclic voltammetry (1 cycle) prior to silica film deposition. Silica film was deposited by applying a current density, *j*, of -0.74 mA cm^{-2} for 5-30 seconds for various deposition time experiments while 8 and 16 seconds deposition was selected for multi-layered films. Microelectrode arrays were modified with silica films for deposition time ranging from 10-45 seconds and 20 seconds modification was found to be suitable. Electrodes were dried in oven at 130 °C overnight for better cross linking of silica films. Electrochemical characterization by 0.5 mM Ruthenium hexaamine III was done at each step of modification. Template extraction was carried out in 0.1 M HCl ethanol solution from 15 to 90 minutes depending on the silica film deposition time.

2.4 Electrochemical techniques for analysis

Different analytical techniques used in this study for analysis and characterization of electrode modifications are discussed briefly.

2.4.1 Cyclic voltammetry (CV)

Cyclic voltammetry (CV) is one of the basic techniques performed in electrochemical studies; CV provides qualitative information about electrochemical reactions. The important parameters in cyclic voltammogram are two peak potential (Ep_c, Ep_a) and two peak current (ip_c, ip_a), where *c* and *a* refer to cathodic and anodic peak respectively. Cyclic voltammetry

involves applying a potential to the working electrode and changing it with time at a certain rate. Subsequently the current (A) flowing through the working electrode is recorded as a function of applied potential (V), resulting plot which is constructed (current vs potential) is called cyclic voltammogram (Figure II-4). Typically a starting voltage (E1) is selected and then potential is swept in a linear manner to a voltage (E2) at that point the direction of scan is reversed back to original value. The potential value (E2) is selected so that potential interval (E2-E1) contains an oxidation or reduction process of interest, if the chemical reaction results in formation of new species in that case reverse scan can be extended beyond initial potential (E1) for the better understanding the nature and electrochemical characterization of species being studied.[22]

$$A \pm e^{-} \rightleftharpoons B \qquad \textbf{Eq. 2.4}$$

A and B are solution phase species.[171] In this work cyclic voltammetry was used to study the electrochemical behavior of different chemicals for initial electrochemical characterization and also at different stages of electrodes modification to analyze and electrochemical confirmation of the modification.

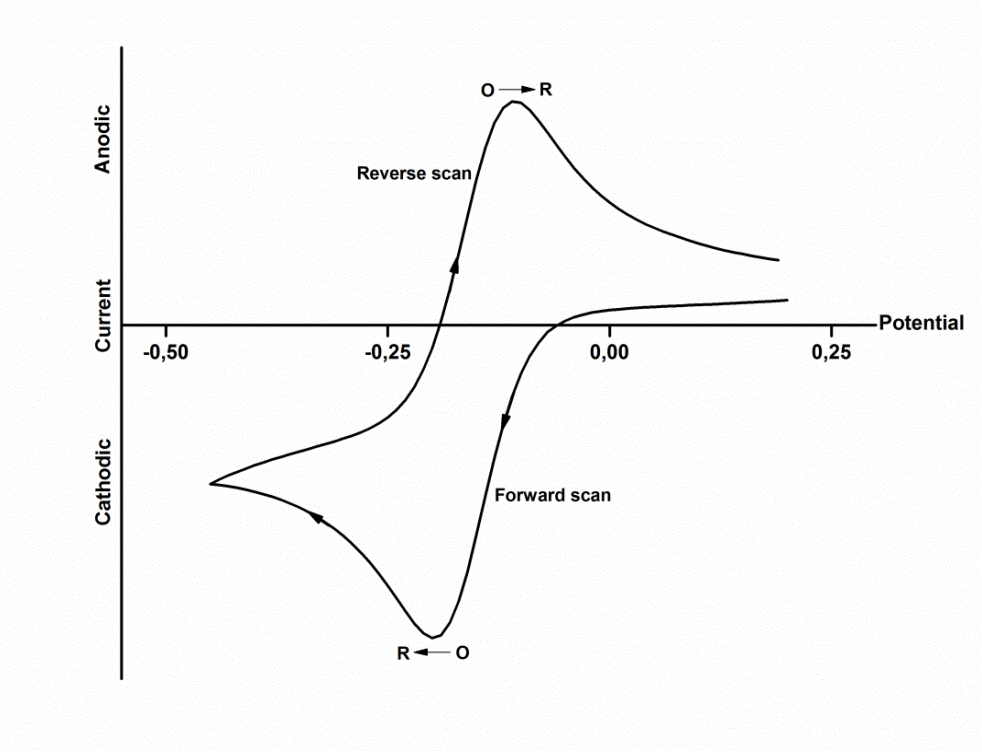

Figure II-4: Typical cyclic voltammogram of a reversible redox reaction.

2.4.2 Square wave voltammetry (SWV)

Square wave voltammetry (SWV) is a powerful electrochemical technique, more suited for quantitative applications and mechanistic study of electrode processes. It is one of the most rapid and advanced electrochemical technique that solely has the advantages of pulse voltammetry (high sensitivity) cyclic voltammetry (insight into electrode mechanisms) and impedance spectroscopy (kinetic information of electrode processes). Typical modulation in SWV consists of a staircase potential ramp modified with square shaped potential pulses. At each step of staircase ramp, two equal in height and opposite in direction potential pulse are imposed to give rise to a single potential cycle in SWV. This potential cycle in SWV is repeated at each step of the staircase ramp during the voltammetric experiment (Figure II-5).[172]

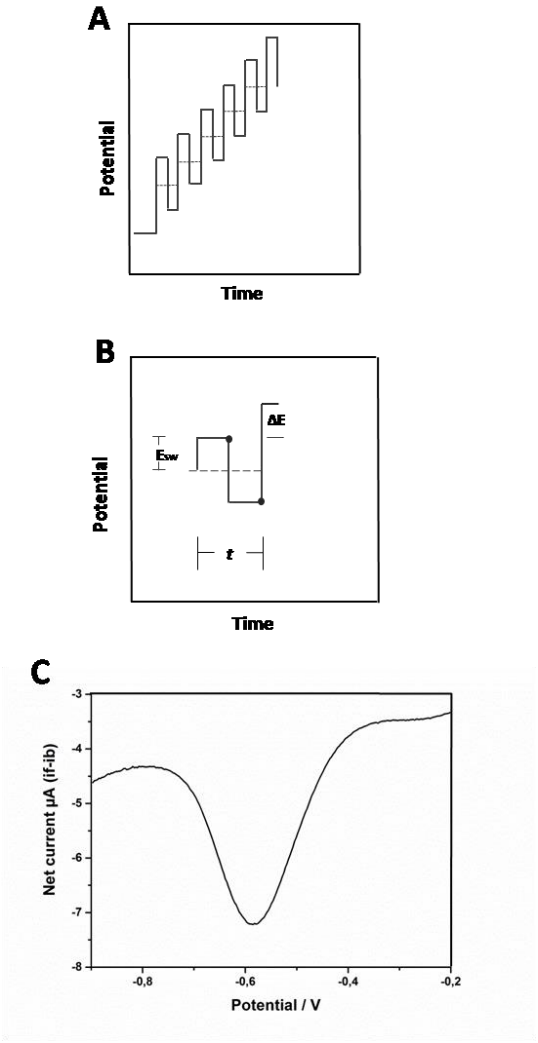

Figure II- 5: Square wave voltammetry (A) One potential cycle (B) Single potential cycle in SWV and (C) SWV scan of 10µM paraquat at GCE.

In this project, square wave voltammetry measurements were performed with PalmSens potentiostat (Figure II-3 B) by using a special electrochemical cell (Figure II-2 D) in the absence of oxygen (N_2 purging continuously and stopping while recording the scan). Optimized square wave voltammetry conditions used were; t_{eq} 5 s, E_{step} 3 mV, Amplitude 50 mV, and Frequency 10 Hz.

2.4.3 Stripping voltammetry

Stripping techniques were initially developed to be used with mercury electrodes but after the use of Hg electrodes is almost over; these methods are still very successfully used for the sensitive determination of many trace elements. Preconcentration and stripping analyses are widely used and very sensitive methods. Stripping techniques typically involve two processes (i) target analyte in the solution is concentrated for a certain period of time at the electrode surface or inside the modification performed at electrode surface, (ii) concentrated analyte is then stripped or removed from electrode surface by using a potential scan. Preconcentration technique can be used with anodic and cathodic stripping voltammetry. Important parameters for efficient analysis of analytes include using a constant electrode surface and surface area, rate of stirring and time of preconcentration.[173] Preconcentration with SWV was used in this study for detection of isoproturon (Chapter VI). Isoproturon was preconcentrated at electrode surface by applying a potential and followed by detection using SWV parameters mentioned above.

2.4.4 Electrochemical impedance spectroscopy (EIS)

Electrochemical impedance is the response of an electrochemical system to an applied AC potential or current, frequency dependence of the impedance can reveal underlying chemical processes. EIS or AC impedance was initially applied for the determination of double layer capacitance. It is carried out at different frequencies that's why its termed as impedance spectroscopy. Advantages of EIS include sensitivity, large amount of data, fine-tuning mechanisms and determination of kinetics of processes, resistance, capacitance and real surface areas in situ.

Applications of EIS include:

(i) Interfacial processes: Redox reactions at electrodes, adsorption, electrosorption and kinetics of homogenous reactions in solution combined with redox processes.

(ii) Geometric effects: linear, spherical, cylindrical mass transfer, limited volume electrodes, porous electrodes and determination of solution resistance.

(iii) Applications in power sources systems: (Batteries, fuel cells, membranes) corrosion studies, electrocatalytic reactions, self-assembly monolayers and sensors.

EIS generated data interpretation is carried out most frequently by complex plane (Nyquist) and Bode plot. Nyquist plots are most used in electrochemical literature as they provide easy prediction of circuit elements and allows easy relation to electrical model.[174]

In present study potentiostatic impedance was performed by PGSTAT 100 apparatus using (Frequency response analysis) FRA2 module. Measurements were carried out on both bare and mesoporous silica modified GCE, complex plane (Nyquist) and bode plots were constructed. Condition for impedance measurements were; Potential applied 0V, wait time 5 s, Highest frequency 100 kHz and lowest was 0.1 Hz, Amplitude 0.01 V_{RMS}, and current ranges highest 100 µA and lowest 10 µA. Fitting and simulation was carried out using analysis tool in the software of Nova 2.1.

2.5 Analytical techniques for chemical and structural analysis

2.5.1 Ion chromatography

Ion chromatography is one among the many chromatographic methods available these days, it can be used to determine all the ions carrying one or two charges in a solution. Ion exchange chromatography or Ion chromatography (IC) is based on stoichiometric chemical reaction between ions in a solution and normally a solid substance having functional groups which can fix the ions with the help of electrostatic interactions. In anion chromatography these functional groups are mostly quaternary ammonium groups whereas for cation chromatography they are sulfonic acid groups.[175]

The anionic composition of real samples from Meuse River, France (Chapter 4) was determined by ion chromatography using a Metrohm 882 Compact IC plus instrument equipped with a high pressure pump, sequential (Metrohm CO_2 suppressor MCS) and chemical (Metrohm suppressor MSM II for chemical) suppression modules and a conductivity detector. The separation was performed on a Metrosep A Supp 5-250 column packed with polyvinyl alcohol particles functionalized with quaternary ammonium group (5 µm particles

diameter) and preceded by a guard column (Metrosep A supp 4/5 guard) and an RP 2Guard column to remove traces of organic compounds. The mobile phase consisted of a solution of Na_2CO_3 (3.2 mmol L^{-1}) and $NaHCO_3$ (1 mmol L^{-1}) in ultrapure water (18.2 MΩ cm at 293 K). The flow rate was 0.7 mL min^{-1} and the sample loop volume was 20 µL. The MagIC Net™ 2.3 Professional chromatography software controlled the 882 Compact IC plus instrument and its peripherals.

2.5.2 Scanning electron microscopy (SEM)

Scanning electron microscopy combined with energy dispersive X-ray spectroscopy (EDS) is one of the most versatile techniques used for the analysis and examining the microstructure morphology and chemical composition characterization. The typical SEM instrument is made up of two main components (i) the electronic console and (ii) electron column. Electronic console comprise of control knobs and switches which allow adjustments of instrument such as filament current, accelerating voltage, focus magnification, brightness and contrast. Electron column is where electron beam is generated under vacuum, focused to a small diameter and scanned across the surface of specimen by electromagnetic deflection coils. Lower portion of electron column is called electron chamber, the secondary electron detector is situated above the sample stage (Figure II-6). Specimen are mounted and secured onto the stage, manual controls outside the specimen chamber allow the movement of specimen stage during analysis.[176,177]

Components of electron chamber are:

(i) **Electron gun** produces free electrons using tungsten filament.

(ii) **Condenser lens** converge electronic beam and it pass through a focal point

(iii) **Aperture** reduce and exclude extraneous electrons in the lens

(iv) **Scanning system** form images by rastering electron beam across the specimen using deflection coils. Astigmatism corrector located in objective lens reduces aberrations of electronic beam using magnetic field.

(v) **Specimen chamber** is comprised of specimen stage, secondary electrons detector and manual controls located outside the chamber.

Scanning electron microscopy (SEM) micrographs were obtained using a JEOL JCM-6000 (acceleration voltage of 15 kV).

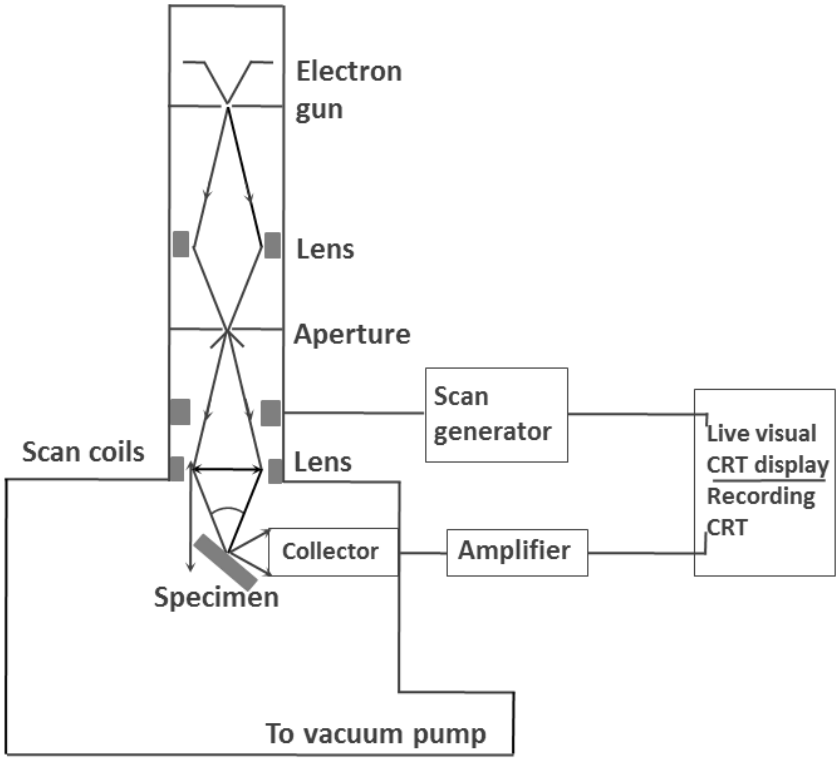

Figure II-6: Schematic diagram of a typical scanning electron microscope.

2.5.3 Transmission electron microscopy (TEM)

In transmission electron microscopy (TEM) a very thin specimen (less than 100 nm thickness) is irradiated by high energy beam of electrons (from few tens of keV to 1 M eV). Crystallographic information can be obtained in TEM either from selected area or by convergent beam diffraction modes, elemental characterization is done either by EDS or electron energy-loss spectroscopy (EELS).[178]Although SEM and TEM both operate at high vacuum and use electron source for radiation, there are few differences between both techniques:

- In TEM electron beam passes through the sample and provide details about structure its components and internal composition, images are based on the electrons passed through the sample or primary electrons. While in case of SEM it is used to study the surface morphology and images are based on the scattered electrons from sample surface or secondary electrons.
- High resolution and magnifying power as compared to SEM.
- Produces two dimensional images while SEM produces three dimensional images.

- High skill level is required to operate TEM and sample preparation as compared to SEM.

Transmission electron microscopy (TEM) micrographs were recorded with a Philips CM20 microscope at an acceleration voltage of 200kV. The silica thin films were scratched off the glassy carbon electrode and transferred to a TEM grid for analysis.

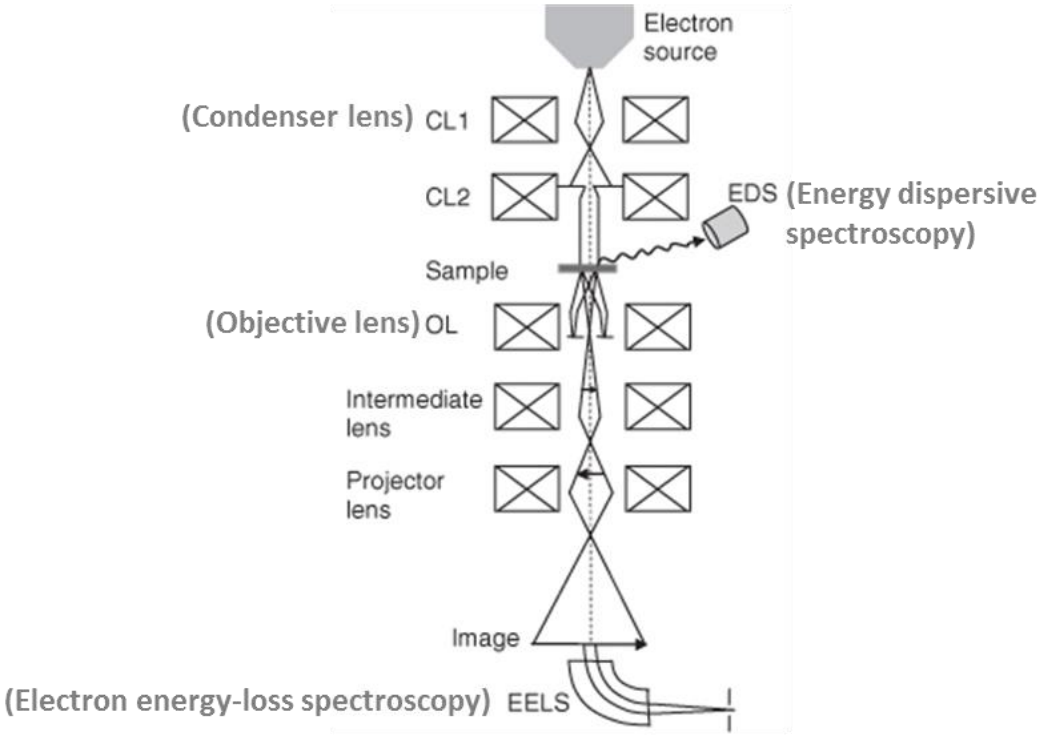

Figure II-7: Schematic diagram of Transmission electron microscope (TEM).[178]

2.5.5 Silica thin film Characterization by profilometry

Profilometry studies were carried out using Bruker's DektakXT® Stylus Profiler for silica film modified electrodes to measure the film thickness. Glassy carbon electrodes due to its roughness and uneven surface are not a good substrate to study film thickness by profilometry specially for very thin films. Silica thin films deposited at ITO electrodes (to counter the problem of uneven surface and roughness faced in case of GCE) for same deposition time as GCE were also Characterized by profilometry.

2.5.6 X-ray photoelectron spectroscopy (XPS)

X-ray photoelectron spectroscopy (XPS) also known as electron spectroscopy for chemical analysis (ESCA) is most widely used among electron spectroscopies as surface

analytical techniques for defining the elemental composition and/or speciation of outer 1-10 nm of a solid substrate. XPS is mainly based on photoelectric effect which was first observed by Heinrich Hertz in 1887 and later explained with simple mathematical description by Albert Einstein in 1905 which led to Nobel Prize in 1912. The popularity of XPS is due to its ability of identification and quantification of almost all elements except H and He in the outer surface of a solid sample, reveal the chemical environment where the respective element exist and it provides all this information with relative ease and minimal sample preparation. An XPS instrument primarily consists of an X-ray source, extraction optics, energy filters and a detection system (Figure II-8). XPS works in Ultra high vacuum (UHV) condition around 10^{-9}-10^{-11} torr.[179] UHV conditions provide advantages such as:

- Maintain sample surface integrity
- Minimize scattering of photoelectrons
- Remove absorbed gases and other contaminants from sample.

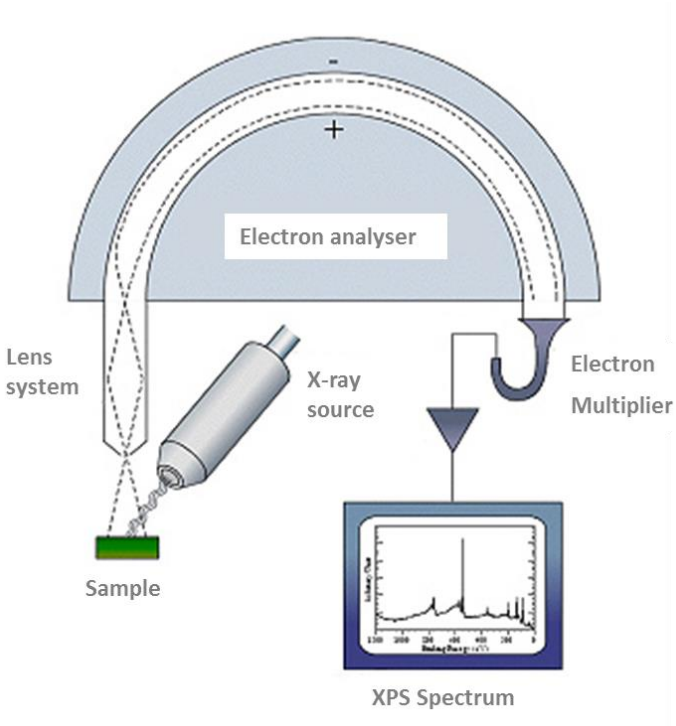

Figure II-8: Schematic diagram of X-ray photoelectron spectroscopy (XPS) instrumentation.[180]

X-Ray Photoelectron Spectroscopy (XPS) analyses were performed using a KRATOS Axis Ultra X-ray photoelectron spectrometer (Kratos Analytical, Manchester, UK) equipped with a monochromatic Al Kα X-ray source ($h\nu$= 1486.6 eV) operated at 150 W.

Chapter III: Improved adhesion of mesoporous silica thin films on glassy carbon electrodes by electrografting of 3-aminopropyltriethoxysilane

In this chapter, we modified the surface of glassy carbon electrodes electrochemically for better adhesion of mesoporous silica thin films. Glassy carbon is widely used as an electrode material, but the adherence of mesoporous silica films on these electrodes is rather poor and mechanically unstable. A solution to improve the adhesion of silica films onto glassy carbon electrodes without compromising the vertical orientation and the order of the mesopores will greatly contribute to spread the use of glassy carbon electrodes modified with mesoporous silica. Here, we electrografted 3-aminopropyltriethoxysilane on glassy carbon to be used as molecular glue. Its presence at the electrode surface improves the mechanical stability of the silica film without disturbing the vertical orientation and the order of the mesoporous silica obtained by electrochemically assisted self-assembly. These findings were supported by a series of surface chemistry techniques such as X-Ray photoelectron spectroscopy, scanning and transmission electron microscopies and cyclic voltammetry. The results presented in this chapter were published in ***Langmuir*, 2016,** 32 4323-4332.

3.1 Introduction

Oriented mesoporous silica films on electrodes have proven to be of interest for electrochemical sensing, biosensing, electrochemiluminescence, energy, growth of polymer nanowires, and separation/permselective membranes.[75,76,80,81,83,95181–186] The EASA (Electrochemically assisted self-assembly) approach developed in our group[72] is applicable to the generation of functionalized thin films, in one step by self-assembly co-condensation using organosilane reagents,[85,97,187–189] including a method applicable to any kind of organo-functional groups via 'click chemistry' for mono or multi-functionalized materials.[190]

Previous electrochemical investigations with vertically-aligned mesoporous silica films were mainly based on indium-tin oxide (ITO) electrodes, due to fact that the surface hydroxyl groups on the ITO surface contribute to ensure a good mechanical stability to the silica material via covalent bonding of the film to the electrode surface. If EASA is applied to generate oriented mesoporous silica films onto a variety of conducting substrates classically used as electrode material (other than ITO, such as carbon, gold, copper, platinum), the resulting thin films suffer from poor adhesion to the underlying support. Unfortunately, the easy electrochemical reduction of ITO restricts the potential window and forbids strong cathodic conditions[191]. An attempt to overcome this limitation was reported by Robertson *et al.*,[78] who proposed the use of a titanium nitride substrate, usable over extended cathodic potentials and containing surface hydroxyl groups for ensuring durable attachment of the mesoporous silica film to the electrode, but this remains a rather unusual electrode material.

Adhesion of silica films on gold electrode was improved by the use of a mercaptosilane acting as a molecular glue between gold and silica.[192,193] This approach is restricted mostly to gold electrodes and the negative end of the potential window is limited by the electrochemical reductive desorption of thiols from the gold surface.[194] Carbon presents a wide interest as an electrode substrate; modification of carbon electrodes with mesoporous silica thin films would combine the wealth of carbon electrochemistry with the versatility of oriented silica materials, provided that the adhesion of silica on carbon substrates can be approved without affecting the quality and orientation of the mesostructures. Covalent modification of carbon surfaces can be achieved by electrografting as previously reported.[195–197] In particular, the electrochemical oxidation of aliphatic amines has proven to be an effective way to attach amine-bearing moieties to carbon surfaces,[170] such covalent

modification is exploitable for fabricating three-dimensional multilayer films (*e.g.*, polyoxometalates on glassy carbon[198]), but this has not been applied to silica materials yet.

Here, we have thus investigated the electrografting of 3-aminopropyltriethoxysilane (APTES) onto glassy carbon and its use as an adhesive layer to anchor mesoporous silica thin films onto the electrode surface. The modified electrodes were characterized by electrochemistry, scanning and transmission electron microscopies (SEM and TEM) and X-Ray Photoelectron Spectroscopy (XPS), at various stages of their modification.

3.2 Electrochemical modification and characterization of glassy carbon electrodes

APTES was selected as a potential candidate to improve the adhesion of mesoporous silica thin films onto the surface of glassy carbon electrodes. APTES is likely to be electrografted onto the carbon surface via the oxidation of its amine function, while its three silane functional groups are available to anchor the mesoporous silica thin films.[199] Two key questions have to be answered in this respect. First, the bonding of APTES to the glassy carbon surface by electrografting has to be checked and how the presence of electrografted APTES affects the electrochemical properties of the modified carbon electrode. Second, when attempting to deposit mesoporous silica thin films by EASA, we must have to evaluate the eventual deleterious effect of the APTES layer on the electrochemically assisted self-assembly process and check if a good level of mesostructural order and the vertical alignment of mesochannels can be maintained. The effectiveness of the APTES electrografting process and its effect on the electrode behaviour were first assessed. A glassy carbon substrate was immersed in a solution of 5 mM APTES dissolved in acetonitrile (+0.1 M $Bu_4N^+BF_4^-$ as electrolyte), and analysed by cyclic voltammetry (CV). From CV curves (Figure III-1 A), a first ill-defined anodic process was observed between + 0.9 V and +1.2 V, followed by a well-defined anodic peak at +1.75 V. On the reverse scan, no reduction peak was observed, indicating the irreversible nature of the oxidation signals. The anodic peak, which corresponds to the electron transfer between the amine and the electrode, was found to decrease in intensity with the number of cycles (Figure III-1 D) and the peak potential shifted gradually towards more positive values (a behaviour consistent with previous observations made for electro oxidation of aliphatic primary amines.[198]

1, 3 and 5 mM concentration of APTES were used to optimise the concentration and number of cycles and 1mM concentration for 1 cycle electrografting was selected as the best condition. The oxidation of primary amines on carbon consisted of the transfer of one electron and the loss of one proton from the amine radical cation[200] and a C-N covalent bond was formed. The glassy carbon substrate was thoroughly washed with ethanol to remove unreacted APTES and electrolyte salt after electrografting.

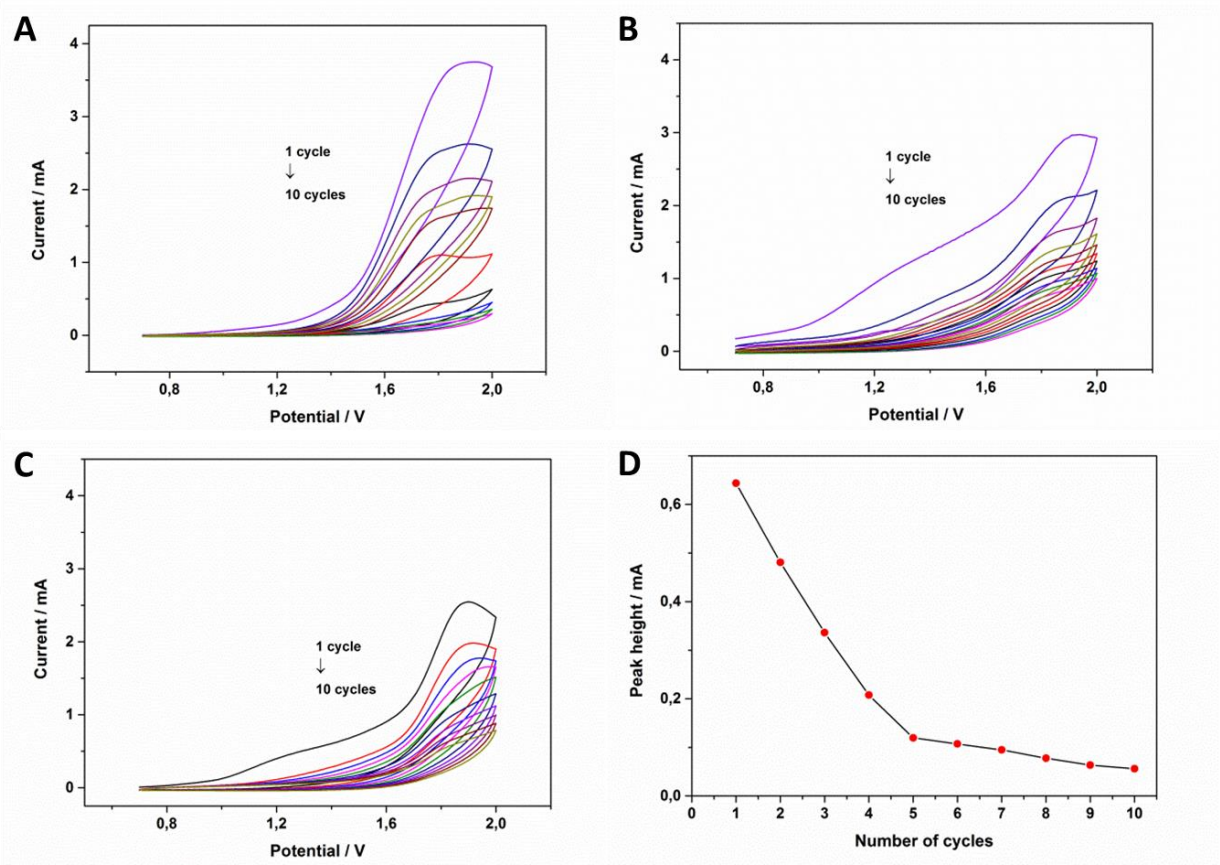

Figure III-1: Cyclic voltammograms of GCE modification (10 cycles) by electrografting APTES; dissolved in Acetonitrile and 0.1M NBu_4BF_4 as electrolyte. (A) 5 mM APTES, (B) 3 mM APTES (C) 1 mM APTES, (D) 1mM APTES electrografting peak height as a function of number of electrografting cycles, Scan rate = 200 mV s^{-1}.

3.2.1 Electrochemical Characterization of APTES electrografting

Glassy carbon electrodes modified with APTES for 1 cycle or 10 cycles were Characterized by cyclic voltammetry of $Ru(NH_3)_6^{3+}$ (Figure III-2 A). After 1 cycle, the current intensity for $Ru(NH_3)_6^{3+}$ was *ca.* 70 % (1 mM APTES) of the one obtained at a bare electrode, confirming the presence of APTES at the electrode surface. Furthermore, the reduction peak was merged with the background current and the oxidation peak was shifted to slightly more positive potentials. Nevertheless, the electrode surface remained easily, yet partially accessible to the redox probe. After 10 cycles, no redox signal was recorded suggesting that the electrode surface was totally blocked by the presence of APTES. Similar observations were made for the cyclic voltammetry of ferrocene in acetonitrile (Figure III-2 B), suggesting that immobilised APTES molecules are indeed blocking the surface and that the drop in the current for $Ru(NH_3)_6^{3+}$ was not due to solvation effects. Graph in (Figure III-2 C) represents the peak height of 0.5 mM Ruthenium and ferrocene at bare, after 1 and 10 cycles of APTES electrografting. For future experiments, 1 mM APTES layer was formed by cycling the potential window once. Previously published study showed that amines are oxidized on the surface of different electrode surfaces including glassy carbon by forming a covalent bond.[170] APTES electrografting at GCE in this study is presented in the form of Scheme III-1.

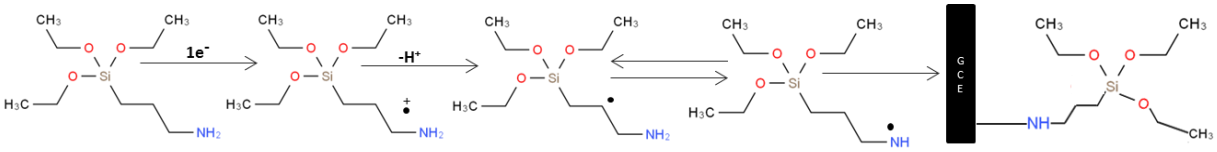

Scheme III-1: Schematic representation of APTES electrografting at the GCE surface by cyclic voltammetry.

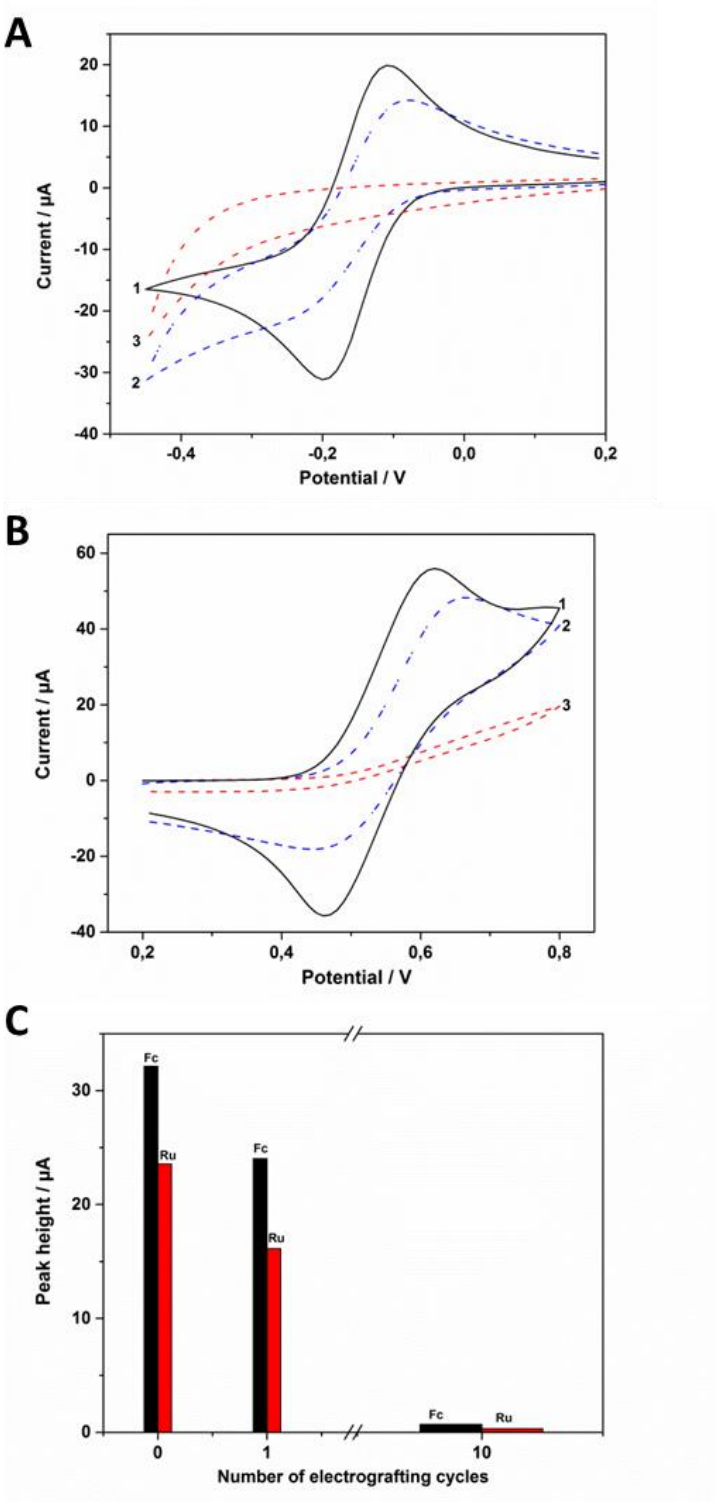

Figure III-2: Cyclic voltammograms of (A) 0.5 mM $Ru(NH_3)_6^{3+}$dissolved in 0.1 M KCl. (1) Bare, (2) 1 mM APTES 1 cycle, (3) 1 mM APTES 10 cycles modified GCE, (B) 0.5 mM Ferrocene in 0.1 M NBu_4BF_4 dissolved in acetonitrile. (1) Bare, (2) APTES modified 1 cycle, (3) APTES modified 10 cycles modified GCE. (C) Graph representing peak height for 0.5 mM Ru and Fc at bare, after 1 and 10 cycles APTES modification of GCE. Scan rate =100 mV s^{-1}.

In order to further test the chemical stability of the electrografted layer (formed by one CV scan), the electrode was treated in a 0.1 M HCl in ethanol solution for 30 minutes (i.e., a treatment which was applied later to remove the surfactant template from mesoporous silica films prepared onto such modified electrodes). Comparing the CV curves recorded for $Ru(NH_3)_6^{3+}$ before and after this treatment (Figure III-3 A) reveals a very small increase in the redox signals after this step but far from full recovery of the signal observed at the bare electrode. While in case of the GCE onto which APTES was electrografted for 10 cycles and $Ru(NH_3)_6^{3+}$ was almost completely blocked after the grafting, there is no observable change in signal even after it is treated under the same conditions as stated above for 1 hour. These treatments suggested that, even if some adsorbed APTES molecules are removed from the electrode surface (in case of 1 cycle treatment), most electrografted moieties remained anchored to the glassy carbon surface and if the electrografting is carried out for extended number of cycles the electrode surface is blocked irreversibly.

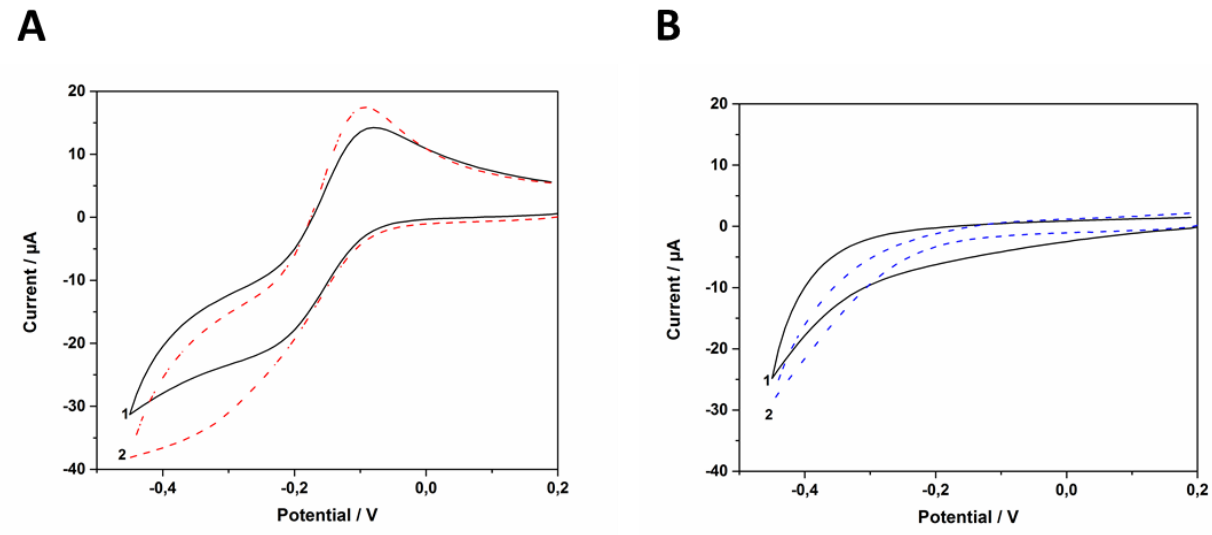

Figure III-3: Cyclic voltammograms of 0.5 mM $Ru(NH_3)_6^{3+}$dissolved in 0.1 M KCl, (1) after APTES modification, (2) After extraction with 0.1 M HCl in ethanol of modified GCE (A) 1 cycle APTES electrografting, (B) 10 cycles APTES electrografting. Scan rate = 100 mV s^{-1}.

3.2.2 Electrogeneration and Characterization of the mesoporous silica films

Glassy carbon electrodes (with and without APTES electrografting) were modified with mesoporous silica deposits generated by the EASA method, which is likely to induce the vertical orientation of mesopores channels onto the electrode surface.[72] The purpose of the APTES layer is to anchor the silica thin film onto the glassy carbon electrode and improve its adhesion by acting as molecular glue. With EASA, the cathodic bias of the electrode served

two purposes: (i) it caused a pH increase in the vicinity of the electrode and hence the condensation of hydrolysed TEOS; (ii) it favoured the formation of hemispherical micelles of CTA^+ on the electrode surface around which the silica was condensed and the mesoporous film expected to grow. A typical sol for electrogeneration of silica film was prepared as explained in chapter II. Briefly, ethanol and aqueous $NaNO_3$ (0.1 M) were mixed in 1:1 v/v ratio, TEOS and CTAB were added to this solution. The surface area of glassy carbon modified with a film was 0.5 cm^2. Previously optimized TEOS and CTAB concentrations (respectively 100 mM and 32 mM) were used.[84] The pH of the sol was adjusted to 3 by addition of HCl and the sol was hydrolysed under stirring at room temperature for 2.5 hours prior to use as electrodeposition medium. Film deposition was achieved under galvanostatic conditions, by immersing the electrodes in the hydrolysed sol and applying a current density, *j*, of -0.74 mA cm^{-2} for 30 s (using a silver wire as a pseudo-reference electrode and stainless steel rod as a counter electrode). After film formation, the electrodes were treated overnight at 130 °C (to ensure good cross-linking of the silica network). Template removal was achieved using 0.1 M HCl in ethanol, as previously described.[97]

Mass transport of redox species from a solution to the electrode surface can be greatly affected by the presence of a porous silica thin film. Its mesostructural type, pore orientation and diameter, level of mesostructural order, or thickness can have dramatic impact on its permeability properties (as shown by cyclic voltammetry using model redox probes[19,31,85,187]). Figure III-4 shows the cyclic voltammograms recorded in 0.5 mM of $Ru(NH_3)_6^{3+}$, as obtained using glassy carbon electrodes at the different stages of their modification. As aforementioned, the reversible signal observed on bare GC electrode (curve 1, solid line on Figure III-4) was less intense and slightly less reversible after APTES electrografting (curve 2, dotted curve), in agreement with the data depicted in Figure III-2 (A). After generation of the surfactant-templated silica thin film, the voltammetric response was totally suppressed (curve 3, solid line), suggesting that the silica film was uniformly deposited over the whole electrode surface area and defect-free. In the presence of the surfactant in the mesopores the hydrophilic $Ru(NH_3)_6^{3+}$ cannot reach the electrode surface. The same behaviour was observed for the electrochemistry of $Ru(NH_3)_6^{3+}$ at mesoporous silica thin films of good quality on ITO electrodes.[72] After removal of CTA^+ cations from the mesopore channels, the electrochemical signal of $Ru(NH_3)_6^{3+}$ was recovered (curve 4, solid line), with current intensities of the same order of magnitude as the signal obtained at the bare electrode.

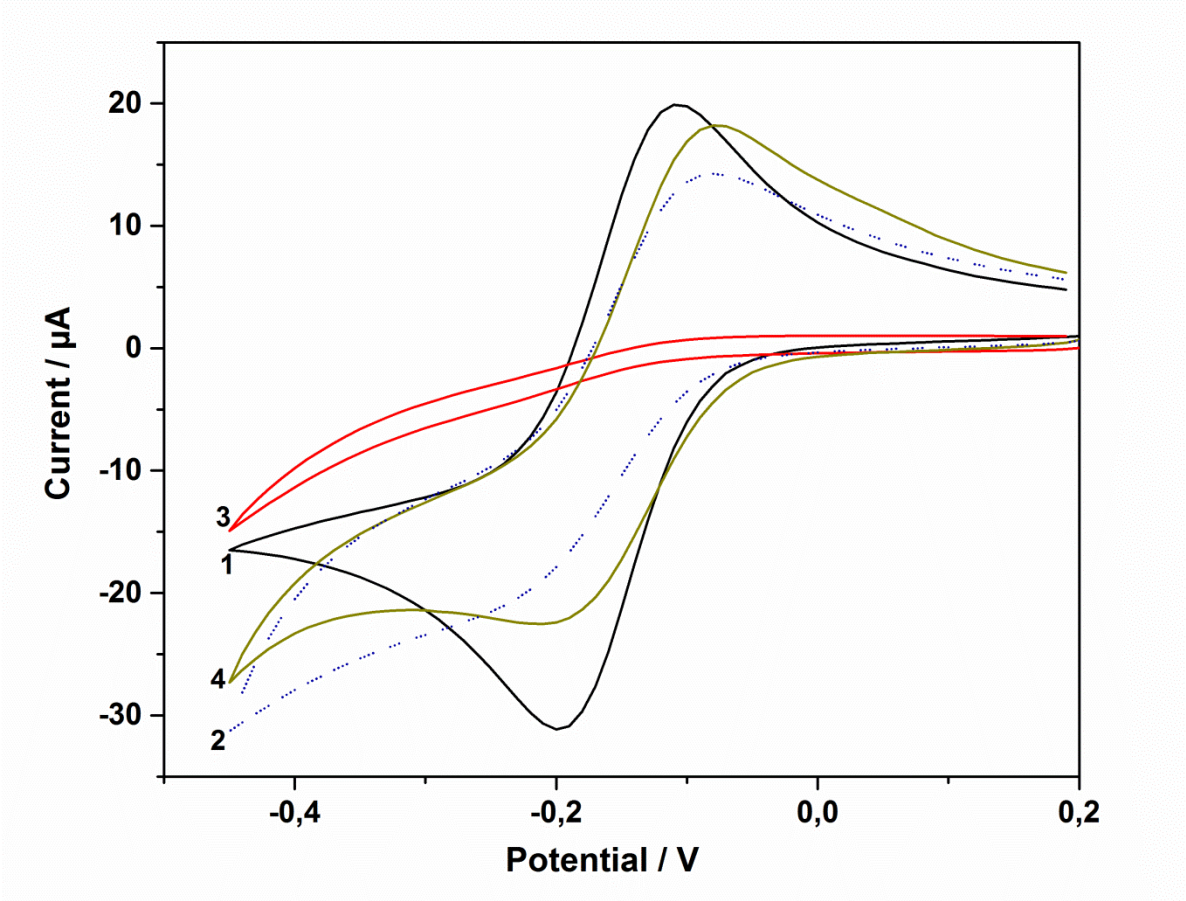

Figure III-4: Cyclic voltammograms of 0.5 mM $Ru(NH_3)_6^{3+}$ dissolved in 0.1 M KCl at (1) Bare GCE, (2) APTES electrografted GCE, (3) Surfactant-templated silica film, (4) After removal of template from mesopores. Scan rate = 100 mV s^{-1}.

3.2.3 Characterization of modified GCE by neutral and anionic redox species

Modified glassy carbon electrodes were also characterized by anionic (hexacyanoferrate) and neutral (ferrocene dimethanol) redox species (Figure III-5). A similar electrochemical behaviour was observed regardless of the charge of the redox probe (cationic, neutral or anionic), in good agreement with previous results obtained at ITO electrodes.[19] Similarly good electrochemical performance can be also achieved with redox-active mesoporous silica films generated on APTES electrografted GC electrodes.

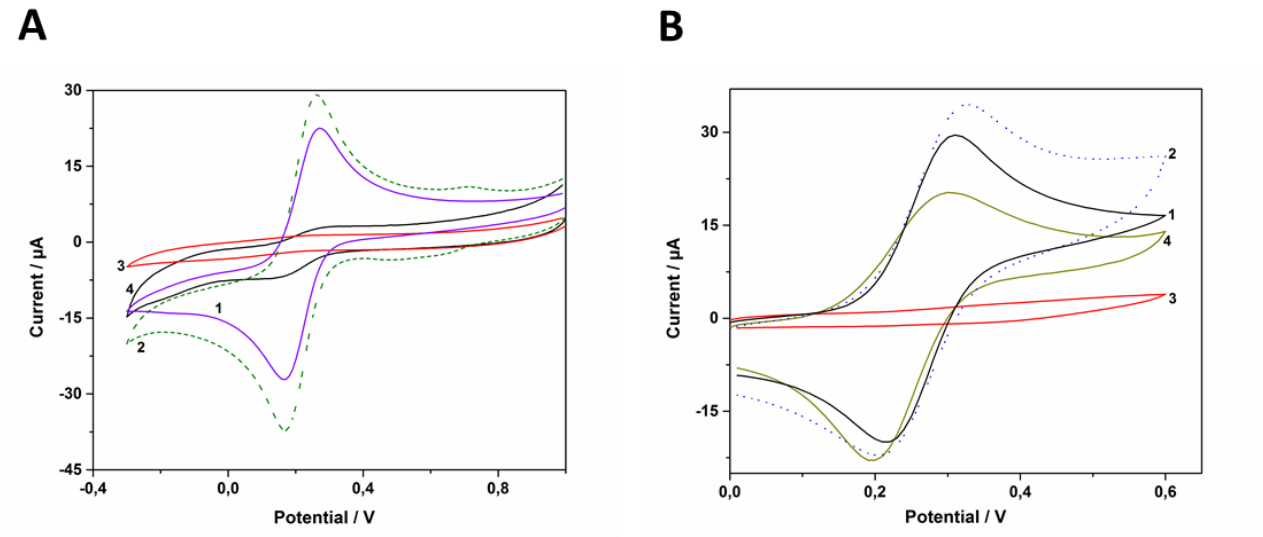

Figure III-5: Cyclic voltammograms of 0.5 mM (A) Hexacyanoferrate and (B) Ferrocene dimethanol dissolved in 0.1 M KCl at (1) Bare GCE, (2) APTES electrografted GCE, (3) surfactant-templated silica film, (4) After removal of template from mesopores. Scan rate = 100 mV s^{-1}.

In this figure we can observe the response of anionic and neutral probe at each step of modification, after electrografting the APTES on GCE surface we see increased response in case of both anionic and neutral probe (Figure III-5 A, B dotted lines). After the formation of mesoporous silica thin film no response is observed for both of the probes (Figure III-5 A, B solid curve 3) which is in accordance to the previously observed phenomenon with $Ru(NH_3)_6^{3+}$, it also confirms that the silica film is uniform and well deposited. Finally after extraction of surfactant from the film matrix we do not see any response in case of anionic probe (Figure III-5 A solid line curve 4), this is due to the presence of negative charge on both silica film and anionic probe which prevents the diffusion of hexacyanoferrate through mesochannels. Neutral probe can easily diffuse through the mesochannels of films after extraction (Figure III-5 B solid line curve 4), and hence we see a similar response of ferrocene dimethanol after extraction and on bare GCE.

3.2.4 Characterization of modified electrodes by scanning electron microscopy (SEM)

We can wonder if the grafted APTES layer would not disrupt the growth of highly ordered and perpendicularly oriented mesoporous silica, and if it would really contribute to strengthen its adhesion to the electrode surface. These observations were confirmed by CV characterization of the modified electrodes before and after the scotch tape test using

$Ru(NH_3)_6^{3+}$ as redox probe in solution (Figure III-6 C,D). The scotch tape test is performed to assess the mechanical stability of silica films onto electrodes surface, it involves placement of scotch tape piece on the film and then removal after gently pressing it with the thumb. These experiments were performed before template extraction (*i.e.*, with mesopores filled with CTAB surfactant, blocking the access to the electrode surface in case of a defect-free mesoporous silica film covering uniformly the whole electrode surface[84]). As shown (Figure III-6 C), with the APTES electrografted electrode, the access for $Ru(NH_3)_6^{3+}$ to the electrode surface was completely blocked by the presence of the silica thin film whether it is before or after the scotch tape test. This demonstrates the prevalent role of APTES pre-coating in ensuring good adhesion properties to the film and its integrity under moderate mechanical stress. On the contrary, the film modified electrode without APTES electrografting showed electron transfer for $Ru(NH_3)_6^{3+}$ which was blocked before the scotch tape test (curve 2 on Figure III-6 D), an important electrochemical signal was observed afterwards (almost the same as the one obtained at a bare electrode), confirming the dramatic damages revealed by SEM (Figure III-6 B). In the absence of APTES electrografting, the silica thin film, yet covering the whole electrode surface area upon synthesis, did not adhere well to the GC support.

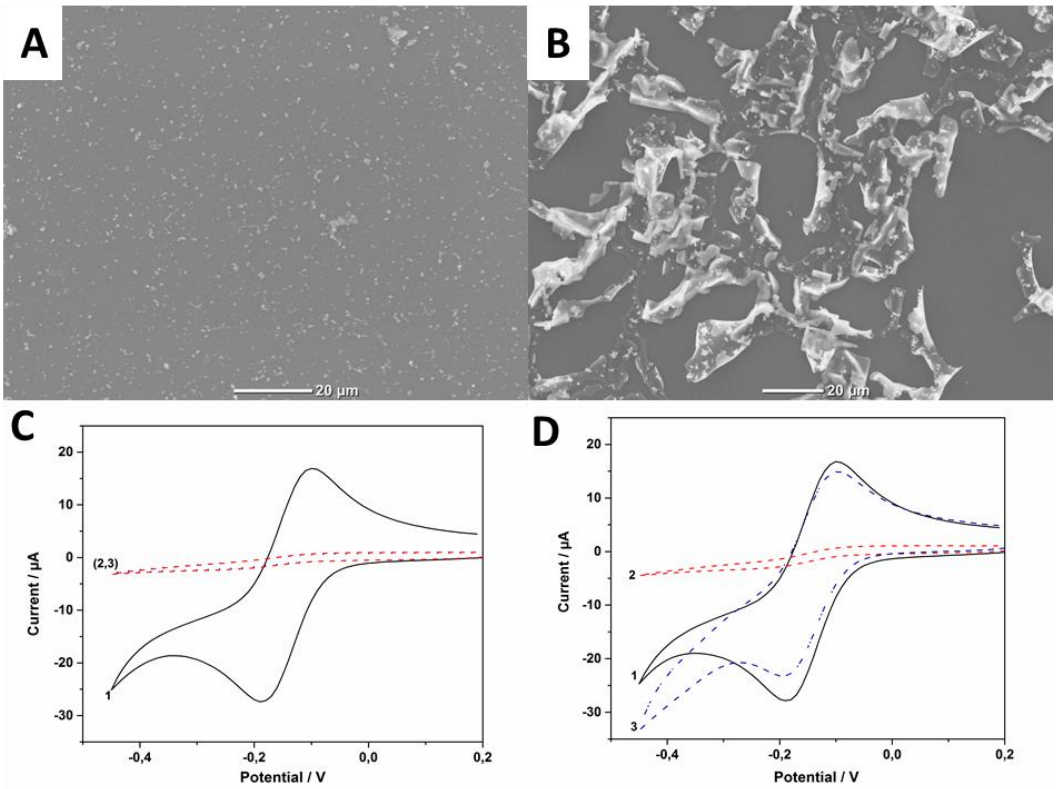

Figure III-6: Scanning electron microscope images after scotch tape test of silica film on GCE (A) with APTES modified, (B) without APTES modified. (C, D) Cyclic voltammograms of 0.5 mM $Ru(NH_3)_6^{3+}$dissolved in 0.1 M KCl at (1) Bare GCE, (2) surfactant-templated silica film, (3) After scotch tape test at GCE with and without APTES modification. Scan rate = 100 mV s^{-1}.

3.2.5 Silica film characterization by transmission electron microscopy (TEM)

TEM micrographs sampled from portions of the mesoporous silica films collected from the electrode surface (see top and cross-sectional views in Figure III-7), demonstrated that the presence of the APTES pre-coating did not disturb the quality of the mesoporous silica thin films formed by EASA on such engineered GC surface. Indeed, both long-range order of the hexagonal packing of mesopores and their orientation perpendicular to the electrode surface is maintained in the presence of electrografted APTES as it was on electrodes modified without APTES electrografting.[72] The top-view (Figure III-7 A) reveals the hexagonal compact arrangement of mesopores (ø = 2.3 nm), forming a uniform thin film with a high degree of organization over wide areas, yet with grain boundaries between hexagonal regions (as common for mesoporous silica films generated by EASA[84]).

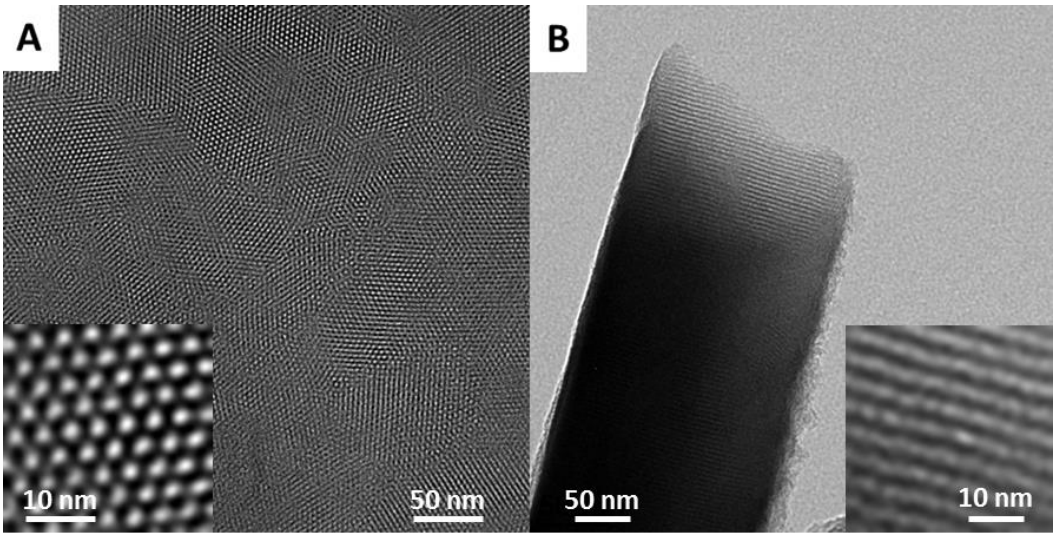

Figure III-7: Transmission electron microscopy image of silica thin film deposited on APTES modified GCE (A) Top view, (B) Cross sectional view.

The cross-section (Figure III-7 B) demonstrates that mesopores channels are all oriented perpendicular to the membrane plane. The thickness of the film was around 150 nm, this value being adjustable by tuning the experimental conditions of the EASA process (deposition time and potential, sol composition).[84]

3.2.6 X-ray photoelectron spectroscopy analysis of GCE modification

The elemental surface composition of the modified glassy carbon electrodes was analyzed by XPS. In addition to full spectra (Figure III-8), high-resolution O_{1s}, N_{1s}, C_{1s} and Si_{2p} core level spectra are shown in Figure (III-9) respectively before (part a) and after APTES electrografting (part b). At the bare GC electrode, the classical response of a slightly oxidized GC surface was observed, with main contributions of O_{1s} (at 532.3 eV for C=O and 533.6 eV for C-O bonds) and C_{1s} (at 284.2 eV C-C, 284.7 eV for C=C and 285.9 eV for C-O bonds, and a weak component at 288.0 eV which could be the signature of COOH function), as well as a weak N_{1s} contribution presumably to traces of N originating from some contamination of the GC surface. After APTES electrografting, O_{1s} and N_{1s} signal intensities increased significantly as a result of the presence of single nitrogen and three oxygen atoms of in each APTES molecule, confirming the electrode surface modification. A closer look to the N_{1s} core level spectrum revealed two main contributions (one centered at 400.3 eV and the other located at 402.2 eV), in agreement with previous reports on anodic electrografting of aliphatic amines on carbon.[170,196] The peak at 400.3 eV was attributed to amine groups and would correspond to APTES molecules attached to the surface by a C-N covalent bond.

The contribution at 402.2 eV was relative to amines protonated by the release of protons during the electrochemical oxidation.[170] The origin of the very small N_{1s} contribution appearing at 407 eV is unclear but might be due to residual nitrate species.[202] The C_{1s} contribution was less intense after electrografting, as expected from the presence of the APTES layer acting as a barrier for the underlying GC surface. It was also broader and asymmetric with a shoulder appearing at higher binding energy values (286.1 eV) and even smaller signal at 288.7 eV. As in the case of the bare glassy carbon, the two first components were attributed to the C-C and C=C contributions. The peak at 286.1 eV was resulting in this case from the contribution of the C-O and C-N bonds. The overlap of both contributions led to a full width at half maximum of 1.64 eV which was slightly larger compared to the analog component observed on a bare glassy carbon electrode (285.7 eV) with a value of 1.23 eV. Moreover, the ratio of the components corresponding to the C-C and C=C and C-O and C-N increased from 0.3 to 0.5 after electrografting of the APTES suggesting the contribution of the C-N bonds to the component located at 286.1 eV. Another possibility for the grafting of APTES on the carbon surface was the formation of an amide bond as suggested by the peak observed at 288.7 eV. These observations are consistent with previously reported data for amines covalently grafted to GC.[203] The presence of APTES on the electrode surface was further confirmed by the rise of N/C ratio from 1.0×10^{-2} at a bare glassy carbon electrode to 9.9×10^{-2} after electrografting. These values are slightly higher than the ones reported by Porter's group for the electrografting of alkylamines.[204] The presence of Si was confirmed by the high resolution peak at 102.7 eV. The Si/N ratio of 0.48 is lower than the expected one at unity, as explained by the presence of residual N present on the bare GC surface. Attachment of APTES could occur through the reaction of the ethoxysilane groups with the O-H groups available from the electrode surface.

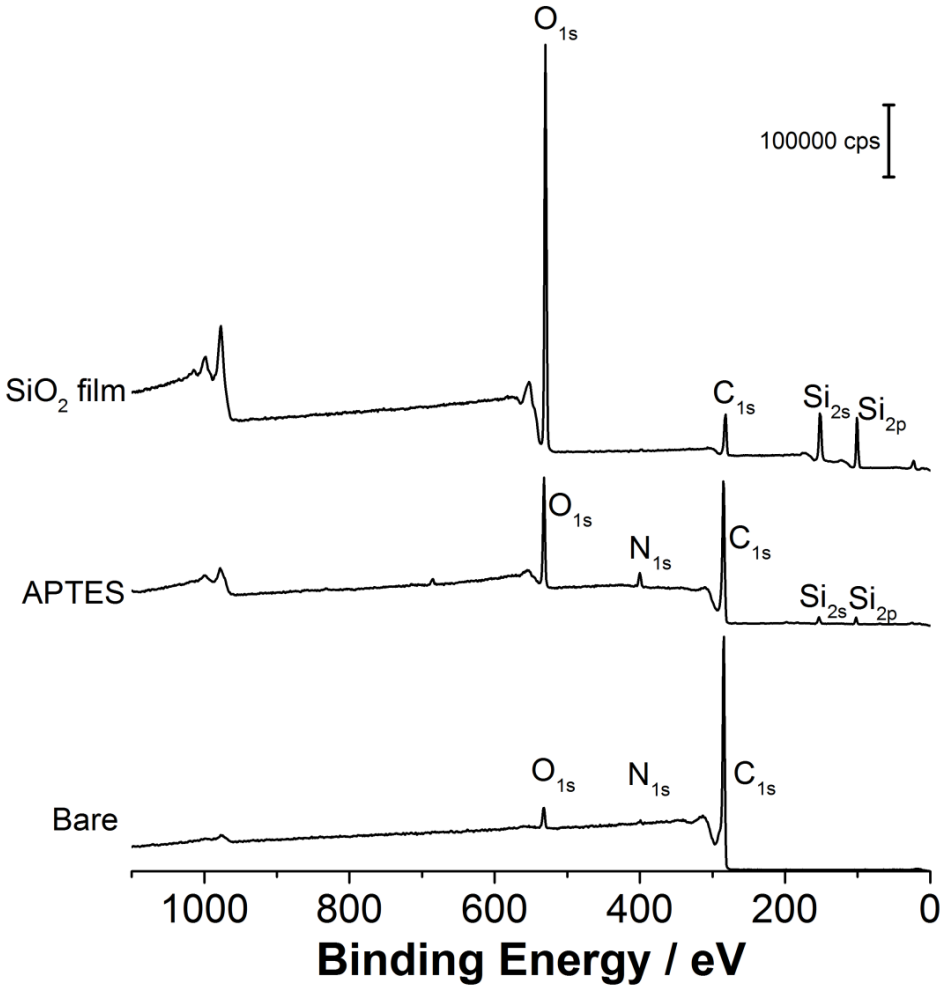

Figure III-8: Full spectra of XPS analysis of bare, APTES modified and silica film deposited after APTES modification at GCE.

APTES electrografting via the amine oxidation confirmation was done by performing the following experiment: a glassy carbon substrate was immersed in a solution of APTES in acetonitrile for the same duration as a single CV. The substrate was then rinsed with ethanol and analysed by XPS. The relative abundance of silicon measured was then 0.3 % whereas it was of 3.4% in the case of electrografting. This confirmed that the majority of silicon present on the glassy carbon substrates is grafted via the amine group. Both electrochemical and XPS experiments demonstrate the successful grafting of APTES onto the GC electrode.

The surface of mesoporous silica modified electrodes was also analysed by XPS (O1s, N_{1s}, C_{1s} and Si_{2p} core level spectra in Figure III-9), before (part c) and after surfactant removal (part d). The presence of SiO_2 is clearly shown through the intense O_{1s}, and Si_{2p} signals, respectively located at 532 eV and 103 eV. Both peaks were visible before and after

surfactant extraction and, as expected, more intense after removal of the organic template. Before surfactant removal, an important N_{1s} contribution was observed at 402.5 eV, confirming the presence of quaternary ammonium originating from the CTA^+ cations filling the mesopores. This signal disappeared almost completely after surfactant extraction. The intensity of the C_{1s} signal was also found to drop dramatically upon surfactant removal and a small additional contribution appeared at 288.7 eV due to the amide bond of the electrografted APTES moieties located in the bottom of the mesopores channels, which became visible after having emptied the space occupied by the surfactant molecules.

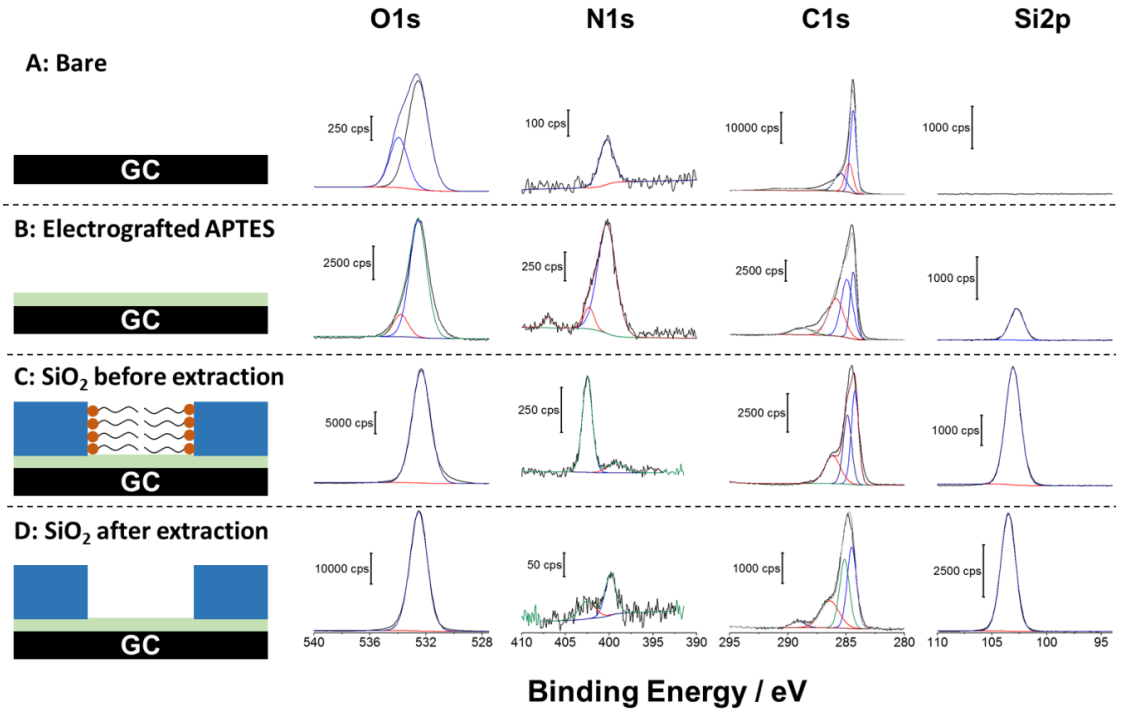

Figure III-9: High resolution spectra of XPS analysis of GCE modification (A) Bare (B) After APTES electrografting (C) After silica film deposition (D) After extraction of template from silica film.

3.3 Functionalization of the mesoporous silica with click chemistry

Ferrocene-functionalized mesoporous silica thin film production is already established from a combination of self-assembly co-condensation of TEOS with an azide organosilane and subsequent click coupling of the azide functions with propargyl ferrocene (Scheme III-2), according to a published procedure for ITO electrodes.[99] This technique has been developed to get ferrocene-functionalized highly ordered and vertically-aligned mesoporous silica films,[99] and was applied here to generate such thin films onto an APTES-modified glassy

carbon electrode. Again, a good quality of mesoporous film was achieved and the electrochemical response of ferrocene moieties attached to the internal walls of the silica mesochannels gave rise to a well-defined voltammogram (Figure III-10), with a shape similar to voltammograms for densely-packed monolayers of ferrocene on electrodes.[205] The generation of a similar film on GC in the absence of the APTES pre-coating was impossible as the azide-functionalized deposits did not remain onto the electrode surface during the click chemistry step due to lack of mechanical stability. This illustrates once more the interest of electrografting APTES on glassy carbon for improving the adhesion of oriented mesoporous silica thin films.

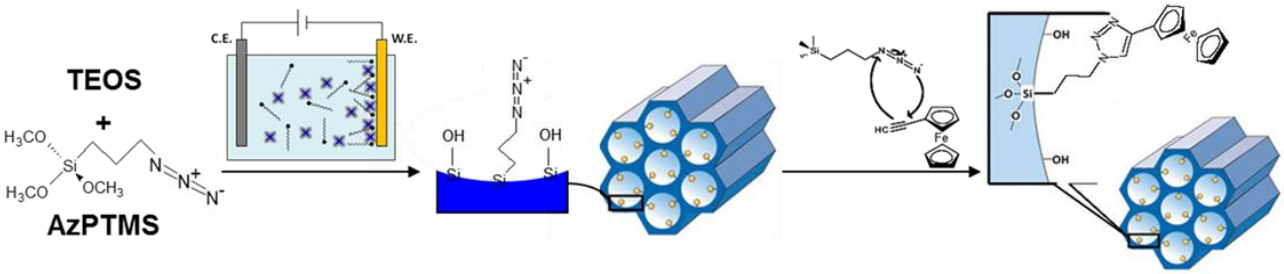

Scheme III-2: Schematic representation of combining the 'click chemistry azide/alkyne' and electro-assisted self-assembly approaches.

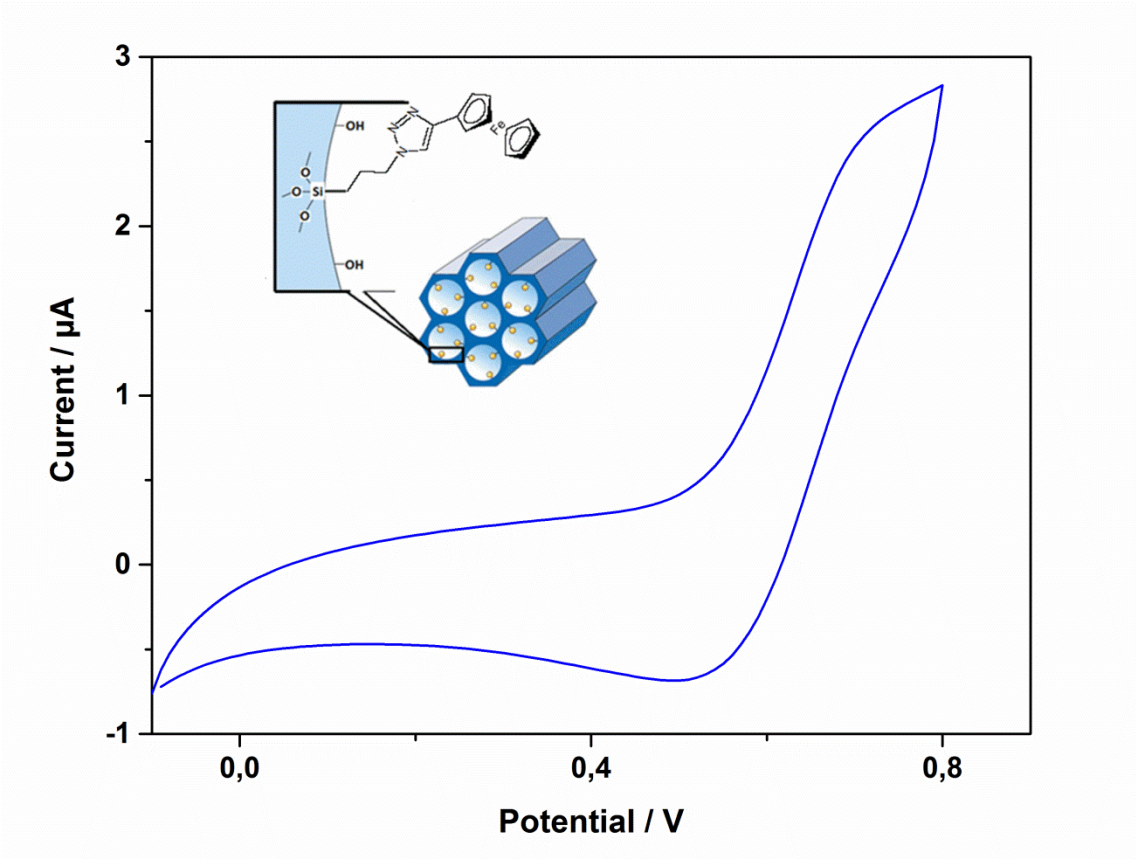

Figure III-10: Cyclic voltammogram of a glassy carbon electrode modified with a ferrocene-functionalized mesoporous silica thin film. The CV curve was recorded in 0.1 M NBu_4BF_4 in acetonitrile. Scan rate = 20 mV s^{-1}.

3.4 Conclusions

XPS spectra and electrochemical Characterization have demonstrated that APTES is grafted by oxidation onto GC electrodes, where it fulfilled its anchoring role by improving the adhesion of silica films. Furthermore, TEM micrographs showed that the presence of electrografted APTES on the electrode surface did not prevent the formation of a mesoporous silica thin film by electrochemically assisted self-assembly (EASA). The mesopores remained vertically aligned with a long-range order of hexagonal packing, proving that the attractiveness of the EASA process is maintained after modification of the electrode surface with an organic monolayer. Both these features, improved adhesion on GC and vertically oriented and ordered silica, open up an avenue for electroanalytical applications. Indeed, most of the electroanalytical applications reported in the literature are using ITO substrates as electrodes, which are limited at potentials lower than -1.2 V (vs. Ag/AgCl/1 M KCl). GC electrodes do not suffer from such a restriction of cathodic potentials. GC electrodes modified with mesoporous silica offer new possibility in the reduction range.

Chapter IV: Electrochemical detection of paraquat at mesoporous silica thin films modified glassy carbon electrodes

This chapter summarizes the electrochemical detection of herbicide paraquat also known as methylviologen, extensively used in agricultural practices worldwide and cause serious health hazards to living organisms. We modified glassy carbon electrodes with mesoporous silica thin films with improved adhesion to carbon electrode thanks to 3-aminopropyltriethoxysilane (APTES) electrografting which was achieved in the previous chapter. Electrochemical behavior was studied at bare and mesoporous silica modified electrodes by cyclic voltammetry (CV) and square wave voltammetry (SWV). Effect of various parameters (solution pH, ionic strength and nature of electrolyte) on sensitivity and electrochemical signal was also studied. Electrochemical impedance spectroscopy (EIS) measurements were performed to calculate the resistance of solutions with different ionic strengths. Square wave voltammetry was used to detect the paraquat at mesoporous silica modified and unmodified GCE. SWV is a very sensitive and powerful electrochemical technique which is widely used for sensing applications. Calibration curves were also constructed for paraquat in real aqueous samples. The results presented in this chapter were published in ***ACS Sens.* 2018, 3, 484−493.**

4.1 Introduction

Recent years have seen the emergence of electrodes modified with mesoporous and nanostructured materials, with promising applications in the fields of electroanalysis.[42] Silica-based mesoporous materials have unique characteristics which make them excellent choice to be used for electrochemical sensing[43] or biosensing.[206] These characteristics include (i) open and ordered mesopores structure exhibiting high surface area which can be fully accessible to external reagents; (ii) ease of derivatization with various organo-functional groups; (iii) hosting and support to different compounds into the mesostructures such as absorbed species, catalysts and biomolecules.[42,43,206] Vertically oriented mesoporous thin films on electrodes are of particular interest as they enable fast transport features from the solution to the underlying electrode surface,[206] leading to efficient electroanalytical performance.[207]

Highly ordered thin films have advantage in electrochemical sensing as they transport the molecules to electrode surface very effectively[208] have thermal and mechanical stability, controllable pore size and provide rapid mass transfer.[207] Mesoporous silica thin films are very effective in electrochemical sensing of small redox active molecules such as pesticides, herbicides, pollutants, drugs and antibiotics[94] as mesoporous films allow selective permeability to these small redox molecules and keeps away the larger molecules which can passivate the underlying electrode surface and resulting in poor sensitivity and reproducibility of a sensor.[95] Mesoporous thin films can also be used against electrode surface fouling (challenge for longer life of sensors) as molecular sieve to control the movement of molecules on the basis of their size.[95] Oriented mesoporous silica films have proven to be a successful choice for sensing applications such as detection of aromatic explosives and pesticides[80], drugs[94], polyphenolic compounds[96], heavy metals.[97,98] Moreover, ease of functionalization of the silica films generated by EASA process provide extra advantage for their application in the field of sensing and electrocatalysis.[85,209]

The use of pesticides and herbicides is increasing in agricultural practices to meet the global demand of food security; as a consequence these chemical compounds are a major cause of pollution to the environment mainly to aquatic systems. Paraquat (1, 1-dimethyl-4, 4-bipyridinium dichloride) also known as methylviologen is non-selective, contact herbicide being used in agricultural practices to control broad leaf weeds since 1962.[210] Paraquat is highly toxic for humans and animals, it causes serious damage to liver, lungs, heart, kidneys[211] and is involved in development of Parkinson's disease[212] with thousands of deaths

reported in last few decades.[114,212] Paraquat is soluble in water with LD_{50} for humans 40-60 mg/kg, It is banned in European Union but still widely used in more than 100 countries. China being the biggest producer produces more than 100 k tons of paraquat every year and its production is increasing every year worldwide.[114] Standard detection methods for paraquat such as gas chromatography mass spectrometry (GC/MS)[130], radioimmunoassay[131] and spectrophotometry[133] have certain disadvantages as they require complex and expensive equipment and are time consuming, moreover they are not suitable for in situ measurements. In contrast electrochemical techniques and instruments are easier to handle, less expensive and robust for sensing applications. Maximum permissible levels for paraquat residues in drinking water varies in different countries from 10-100 µg / L,[213] limit of detection up to 0.1 µg/ L by electrochemical analysis can be considered sensitive detection of paraquat.

4.2 Electrode modification

The general scheme of glassy carbon electrode modification to be used in this chapter is shown in figure IV-1, electrodes were modified with APTES and silica films and subsequently Characterized by redox probe as described in chapter 3.

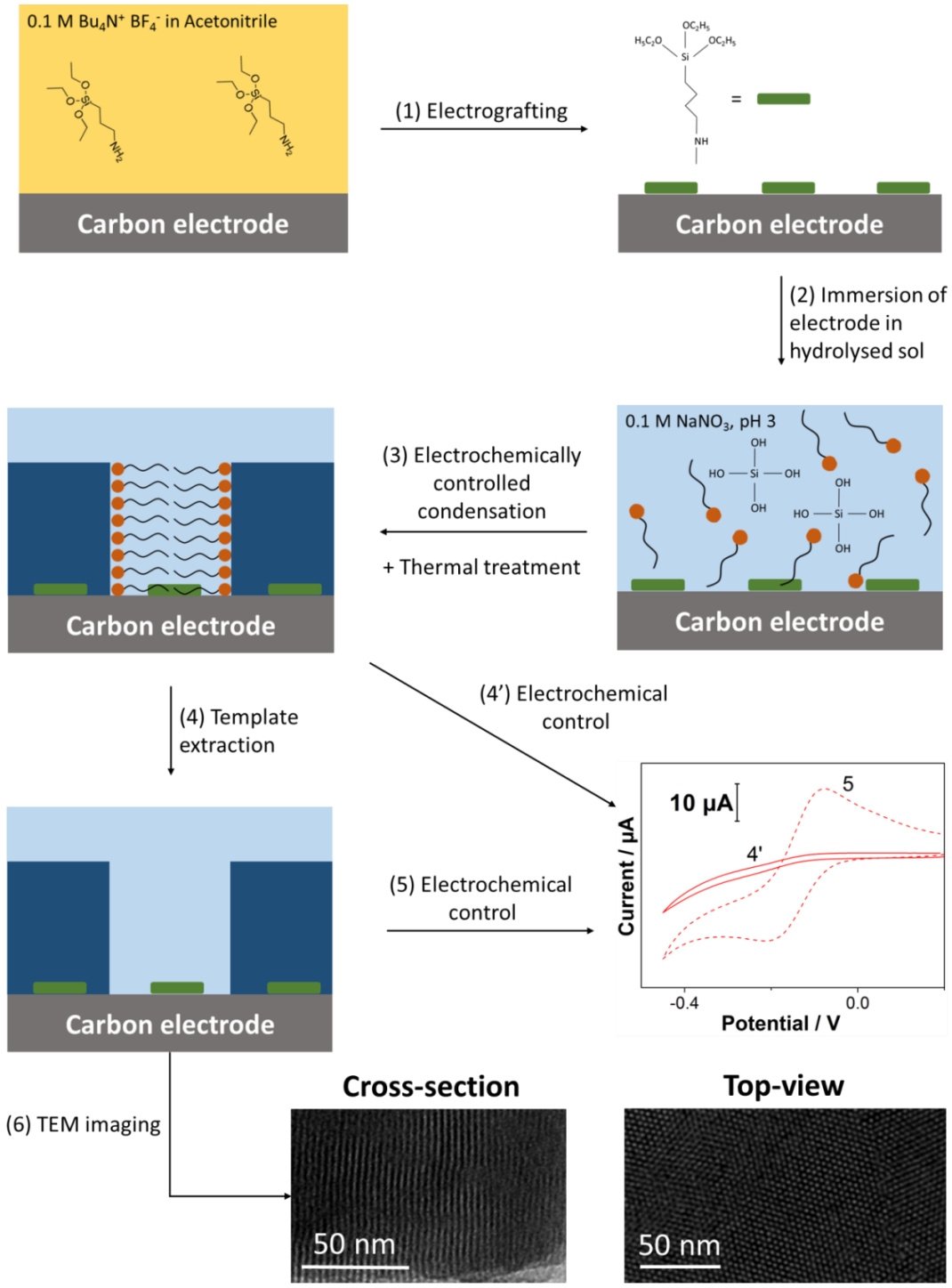

Figure IV-1: Experimental protocol for the electrode preparation and characterization: APTES is electrografted onto a carbon electrode (1) The modified carbon substrate is then immersed into the sol (2) And mesoporous silica thin film is formed by electrochemically assisted self-assembly (3) Cross-linking of the silica matrix is ensured by heat treatment and the template is extracted (4) The quality of the silica thin film (4') And the efficiency of the extraction is checked electrochemically (5) Orientation and order of the mesoporous silica was verified by transmission electron microscopy (6) Modified electrodes were Characterized by cyclic voltammetry of 0.5 mM $Ru(NH_3)_6^{3+}$ in 0.1 M KCl; Scan rate = 100 mV s^{-1}.

4.3 Electrochemistry of paraquat

To further illustrate the interest of depositing mechanically stable mesoporous silica films on carbon substrates rather than only on ITO electrodes, here we compare the electrochemical response of paraquat which is active in the cathodic domain. Paraquat is a cation of the viologen family, which can be reduced in two successive one electron transfer reactions.[214] The first one was reversible on both APTES electrografted GCE and ITO electrodes modified with a mesoporous silica thin film (Figure IV-2 A), with $E^{1/2}$ = -0.694 V (for GCE) and $E^{1/2}$ = -0.7 V (for ITO), in good agreement with the values reported in the literature for the corresponding bare electrodes.[214]

The second reduction signal, observed at $E^{1/2}$ = -1.06 V at the modified glassy carbon electrode (compared to the values of -1.072 V reported in the literature[214]), was as well-defined as the first one (dashed curve and inset in Figure IV-2 B). However, this was not the case for the ITO electrode (plain curve in Figure IV-2 B) when the potential is scanned down to -1.5 V. The application of such cathodic potentials did not allow the observation of the second redox reaction (it was disturbed by the intrinsic response of the ITO, as also occurring at the bare electrode in the absence of paraquat (Figure IV-2 C). When applying highly cathodic potentials to ITO, an anodic peak appeared at -1.0 V on scan reversal, which can be attributed to the oxidation of metallic indium.[191] Photographs of the state of a bare ITO electrode surface before and after a series of voltammograms are presented as an inset of Figure IV-2 (C). The brownish disc shown in the figure corresponds to the area that was exposed to the solution when the potential was scanned down to -1.5 V. This colour change is due to the irreversible reduction of ITO in the presence of chloride ions, generating metallic InSn particles on the electrode surface.[191] Such transformation of the electrode surface results in a loss of both conductivity and transparency of ITO electrodes, making them inoperative. These experiments demonstrate that glassy carbon electrodes modified with mesoporous silica thin films offer a good alternative to similar films on ITO for being used at cathodic potentials below -1.2 V where ITO electrodes suffer from lack of stability.

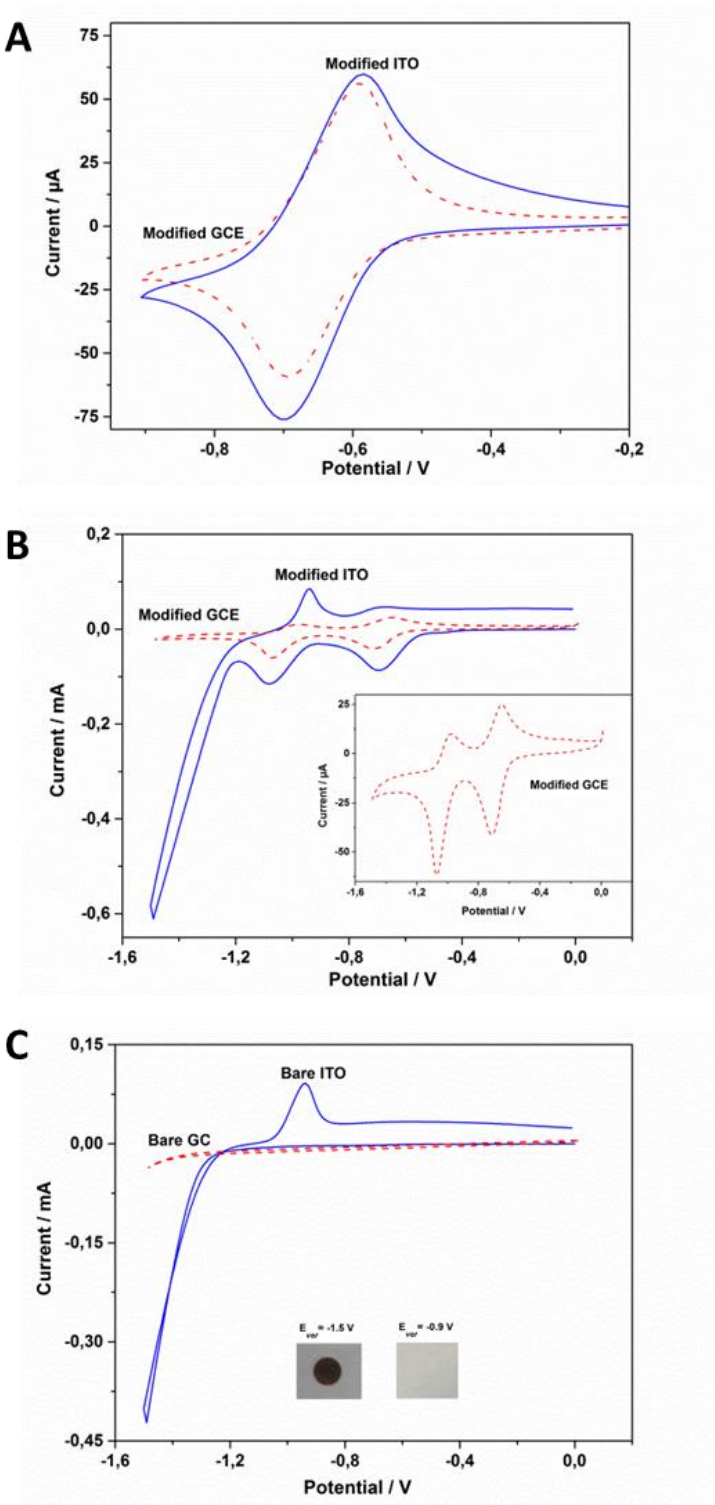

Figure IV-2: CV of 500 µM paraquat in 0.1 M KCl, at ITO and APTES-modified GC electrodes covered with a mesoporous silica thin film: (A) In the -0.2 to -0.9 V potential range; (B) In the 0 to -1.5 V potential range. Inset of (B) shows the CV of paraquat at a modified glassy carbon electrode. (C) Blank CVs in 0.1 M KCl, in the 0 to -1.5 V potential ranges at bare ITO and glassy carbon electrodes. The solid lines are for the CVs at the ITO electrodes and the dashed lines for the CVs at the GC electrodes. Inset of (C) shows the picture of bare ITO after cycling down to -1.5 V and -0.9 V, Scan rate = 100 mVs^{-1}.

4.3.1 Effect of charge on redox analytes at their electrochemical behaviour

Mesoporous silica thin films as the ones prepared according to the protocol shown in Figure 1, present a high number of mesochannels per unit area with a diameter of 2.3 nm and a length of 150 nm (corresponding also to the film thickness) as it was determined by TEM (Figure IV-1). The mesochannels are densely packed in a regular hexagonal arrangement (approximately 10^{13} mesochannels per cm^2) and all oriented perpendicular to the electrode surface, as it was reported in previous reports by our group.[215,216] Prior to surfactant extraction, the films are impermeable to a cationic probe such as $Ru(NH_3)_6^{3+}$ (curve 4' in Figure IV-1). After template removal, the film becomes highly porous and the vertical orientation of mesopore channels ensures fast mass transport of chemical species toward the electrode surface (see well-defined voltammetric signal for $Ru(NH_3)_6^{3+}$ on curve 5 in Figure IV-1).The narrow diameter of the mesochannels and the anionic nature of the silica walls (originating from surface silanolate groups) at pH higher than 2 strongly influence the electrochemical behaviour of target analytes according to their charge. We investigated the cyclic voltammetry of three organic species: paraquat (cationic), catechol (neutral) and diclofenac (anionic) before and after modification of the electrode surface with a mesoporous silica thin film (Figure IV-3). Although paraquat can be reduced in two successive one-electron transfers at -0.7 and -1.025 V,[214] we used here the first electron transfer reaction as the analytical signal (Figure IV-3 A), which is sufficient to obtain adequate quantification of analyte in the solution.[155] The reduction peak current at a bare glassy carbon electrode was measured at 26 µA (blue curve on Figure IV-3 A), while the peak current increased to 55 µA in the presence of a mesoporous silica thin film on the electrode surface (red curve on Figure IV-3 A). In the case of neutral catechol, the peak current recorded at the modified electrode is 70 % of the peak current obtained at the bare electrode (Figure IV-3 B). Finally, the irreversible oxidation of anionic diclofenac is not observed at a modified electrode while it is clearly visible at a bare electrode (Figure IV-3 C).

Electrostatic interactions between the anionic walls of the mesochannels and the charge of the species studied play an important role on the electrochemical response. While the voltammetric signal of the cationic analyte doubles at the modified electrode, the one corresponding to the anionic species is suppressed, due to charge selectivity (cation accumulation and anion rejection at such mesoporous silica film modified electrodes were already described in the literature,[80,181,215,217,218] but the permselective effects observed with

the quite large organic ions used here are really dramatic). The optimized structure of diclofenac, determined by X-ray diffraction, showed that the molecule larger dimension is around 1.1 nm.[219] Although the size of diclofenac molecules may vary slightly when dissolved, we can assume that they are small enough to penetrate the mesochannels, which have a diameter of 2.3 nm. The absence of signal is not due to size exclusion effect and can then be attributed to electrostatic repulsions (i.e. charge exclusion). The presence of anionic silica mesochannels on the electrode surface did not influence the electrochemistry of the neutral catechol species. Note that catechol signal can be also seen before surfactant extraction as a result of its solubilisation into the liquid crystalline phase (as previously observed for other neutral species[80,181,215,217,218]), showing however a shift of peak potentials explained the excess of energy required for charge compensation to maintain the electric charge balance after catechol oxidation. Only a small decrease in peak currents is observed due to some resistance to mass transport (compare blue and red curves in Figure IV-3 B). In the following we will exploit the charge selectivity properties for sensitive detection of cationic paraquat species.

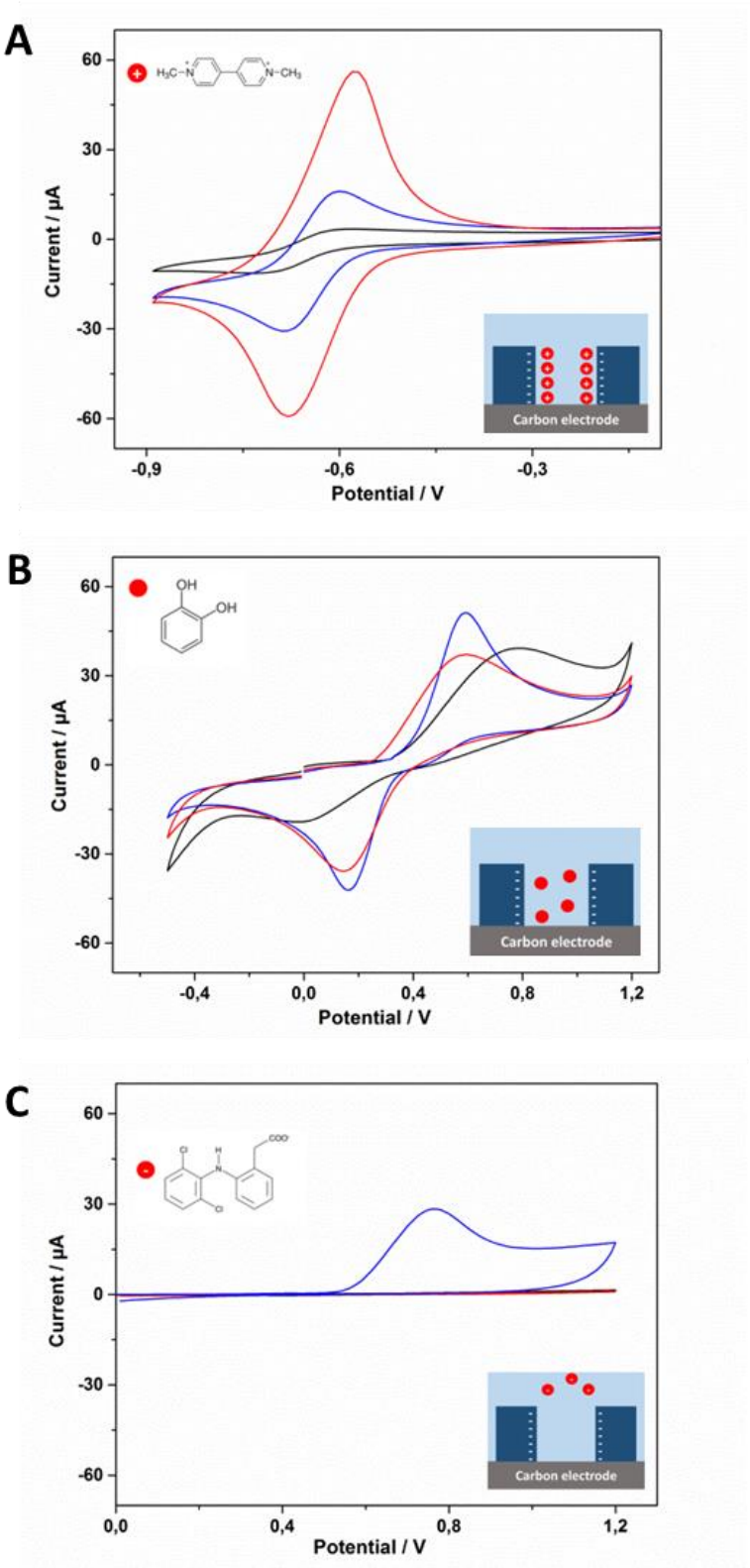

Figure IV-3: Cyclic voltammograms of 500 µM of (A) Paraquat, (B) Catechol and (C) Diclofenac at a bare glassy carbon electrode (blue), at a modified electrode before (black) and after (red) template extraction. Background electrolyte: 0.1 M NaCl, Scan rate = 100 mV s^{-1}.

4.3.2 Electrochemical behavior of paraquat at mesoporous silica modified GCE

The electrochemical behaviour of paraquat at mesoporous silica thin film modified glassy carbon electrodes was studied at low concentrations (2 and 5 µM), with the help of cyclic voltammetry (repetitive cycling 100 cycles). The electrostatic interactions between the paraquat cations and the negatively-charged silica surface (due to the deprotonated silanol groups on the mesopore walls) contributed even to the accumulation of the paraquat in the film upon repetitive cycling, with site saturation being more rapidly reached for the more concentrated medium, as expected (Figure IV-4).

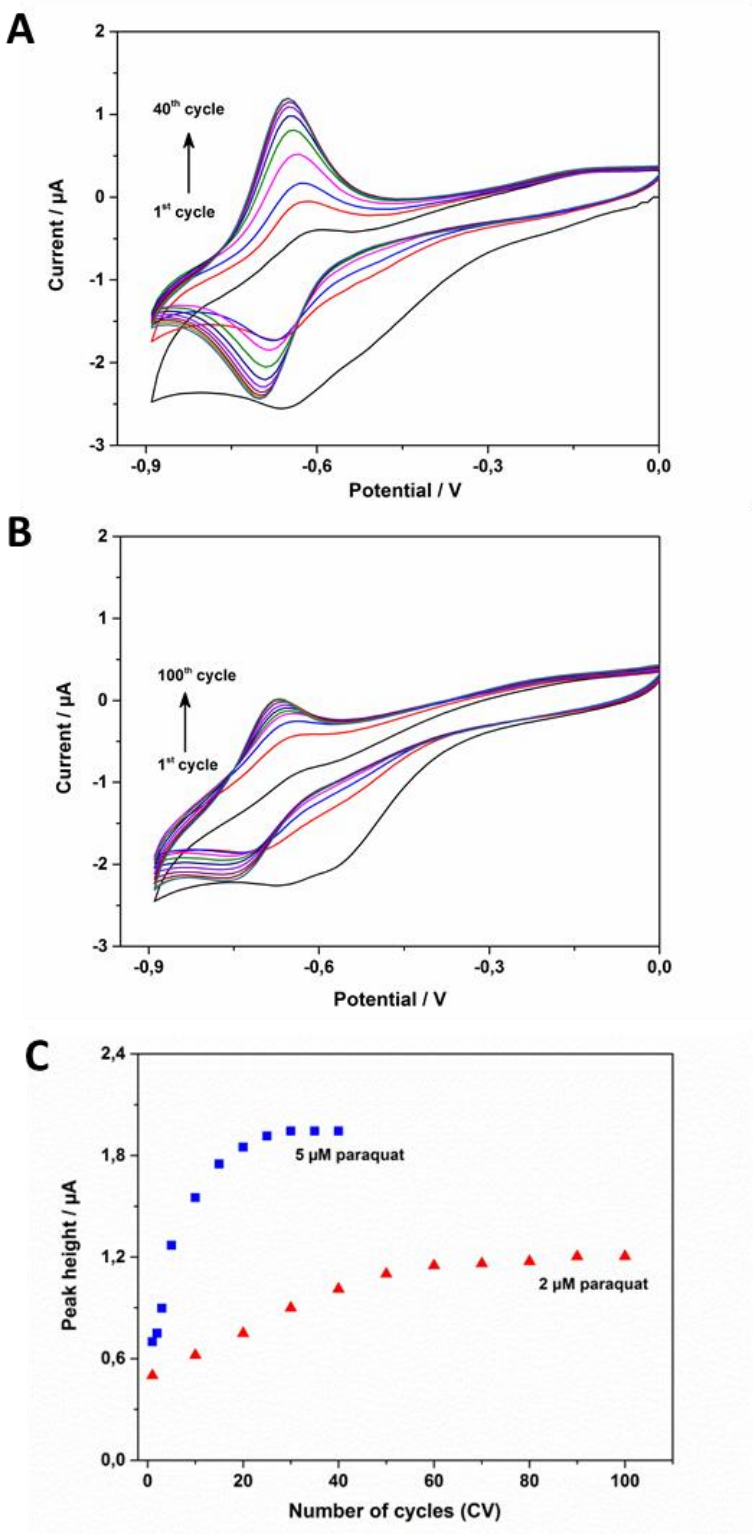

Figure IV-4: Repetitive CVs of (A) 5 µM and (B) 2 µM paraquat in 0.1 M KCl at a glassy carbon electrode modified with mesoporous silica thin film anchored with an APTES layer. (A) The CVs shown are the 1st, 2nd, 3rd, 5th, 10th, 15th, 20th, 25th, 30th, 35th and 40th. (B) The CVs shown are the 1st, 10th, 20th, 30th, 40th, 50th, 60th, 70th, 80th, 90th and 100th. (C) Reverse peak current as a function of the number of cycles for 5 µM (■) and 2 µM (▲) paraquat. Scan rate = 20 mV s^{-1}.

4.3.3 Investigation of paraquat electrochemical behavior by square wave voltammetry

Paraquat reduction was investigated by square wave voltammetry for concentrations ranging from 0.5 to 10 µM (Figure IV-5). The cathodic peak currents measured at an electrode modified with a silica thin film were higher by more than one order of magnitude compared to the ones obtained at a bare GCE, due to favourable electrostatic interactions between the cationic analyte and the anionic silica walls, as discussed above. In both cases, the peak currents increase linearly with the concentration showing a sensitivity of (-7.79 ± 0.27) A M^{-1} for the modified electrode against a sensitivity of (-0.32 ± 0.01) A M^{-1} for the bare electrode. The gain in sensitivity achieved with the modified electrode should allow us to push further the limits of the electrochemical detection of paraquat in water, but experimental factors likely to affect the detection process (such as ionic strength, pH, and nature of anions) should be considered beforehand.

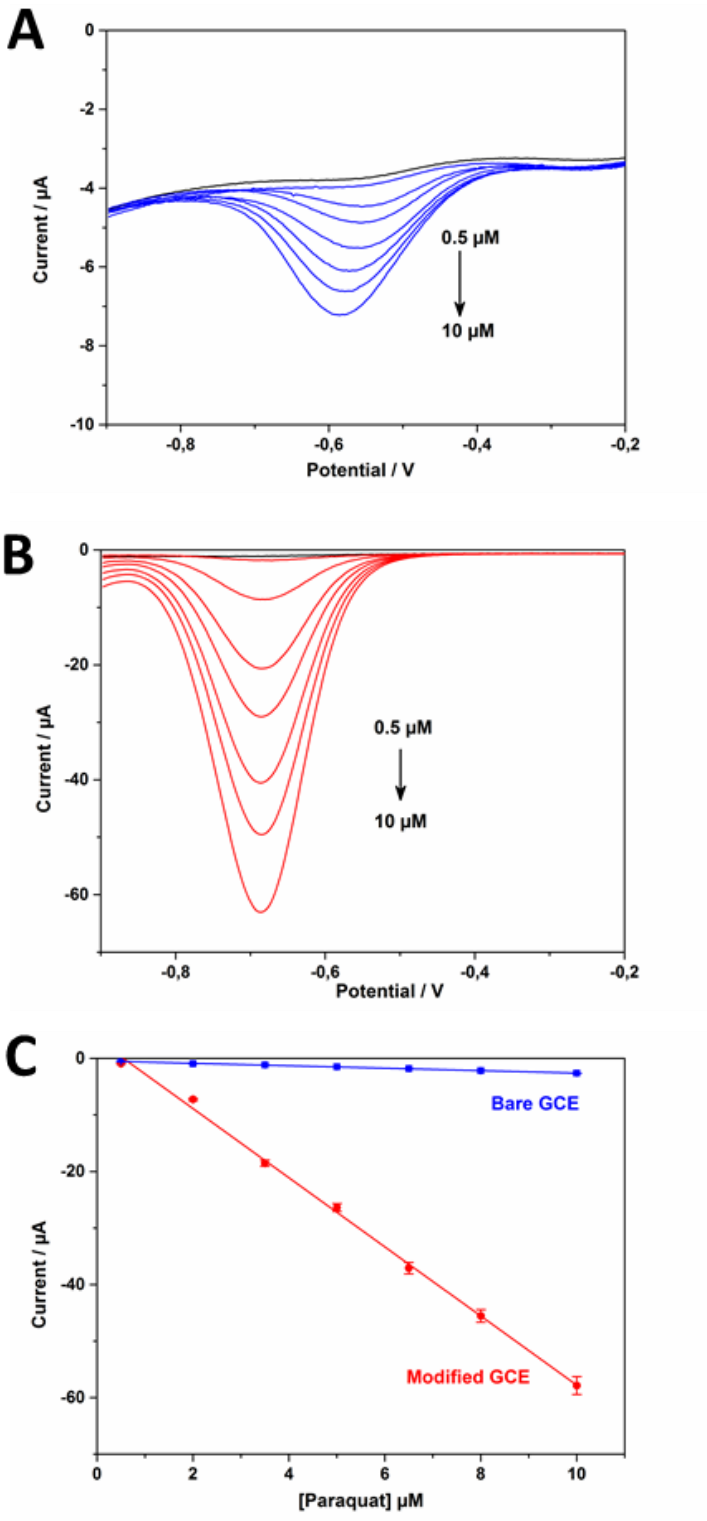

Figure IV-5: Square wave voltammograms of 0.5 – 10 µM paraquat (A) at bare (blue curves) and (B) modified (red) electrodes, (C) calibration curves. Background electrolyte: 0.1 M NaCl, pH 6.

4.3.4 Influence of ionic strength on SWV signal intensity

The influence of the solution ionic strength (between 10 and 500 mM) on the SWV response is investigated at both bare and modified electrodes (Figure IV-6 A). At the modified electrode, as the ionic strength decreases from 500 to 70 mM, the reduction peak current for paraquat increases. After reaching a maximum at 70 mM of supporting electrolyte, the peak current decreases continuously with the ionic strength at lower values. The particular V shape observed (Figure IV-6 B) should be explained by two antagonistic effects of the ionic strength. In the presence of large amounts of electrolyte, the accumulation of paraquat might undergo competition with the electrolyte cation (but this is not necessarily the main reason); at I < 70 mM, the paraquat response drop is even less obvious. A first hypothesis could be the increase in solution resistance. We have investigated the solution at different ionic strengths by electrochemical impedance spectroscopy at both bare and modified electrodes (Figure IV-8). As no variation in the reduction peak current with ionic strength is observed at bare GCE, for which the peak current remains almost constant throughout the ionic strength range (suggesting that the solution resistance does not impact paraquat reduction), the variation with ionic strength observed at the modified electrode can be related to the presence of the mesoporous silica film on the electrode surface.

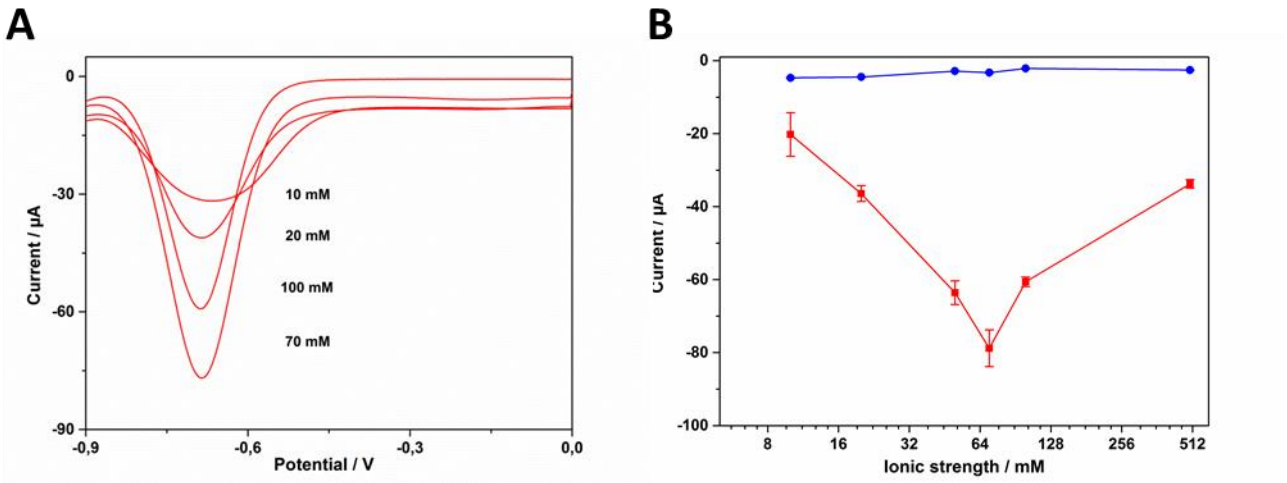

Figure IV-6: Square wave voltammograms of 10 µM paraquat at different NaCl concentrations. Inset shows the peak current values obtained for different electrolyte concentrations at bare (blue dots) and modified (red squares) electrodes for paraquat concentration = 10 µM. pH 6.

4.3.5 Effect of electrolytes nature on SWV response

In an electrochemical system if the movement of anions is hindered to maintain the electroneutrality, this results in drop of electrochemical signal. Paraquat reduction is investigated (Figure IV-7) for a series of background electrolyte anions (Cl^-, NO_3^-, SO_4^{2-}, $H_2PO_4^-$ and BF_4^-). Chloride, nitrate, sulfate and dihydrogen phosphate are selected for their occurrence in environmental samples while BF_4^- is selected for its solvated ionic radius (r_i = 11.5 Å)[220] close to the radius of the mesochannels (r = 1.15 nm). Ionic radius of Cl^-, ClO_4^- SO_4^{2-}, NO_3^-, and $H_2PO_4^-$ are 1.81, 2.5, 2.3, 1.79, 2.38 Å respectively.[221] The reduction peak currents varies greatly with the different anions of the background electrolyte although the ionic strength is maintained constant (I = 70 mM, except for $Na^+BF_4^-$, where I = 50 mM due to solubility constraints). Even when counter anions such as Cl^-, NO_3^-, SO_4^{2-}, $H_2PO_4^-$, are partially excluded by the thickness of the Debye layer, the electrochemical signal remains greater at a modified than at a bare electrode. For BF_4^-, the electrochemical signal is totally blocked as BF_4^- do not penetrate in the mesochannels, regardless of the ionic strength.[222] The intensity of reduction peak currents followed this order: $NO_3^- > ClO_4^- > Cl^- > SO_4^{2-} > H_2PO_4^- > BF_4^-$. It should be noted that no correlation is found between the ionic radius or the ionic conductivity of the anions and the reduction peak current observed.

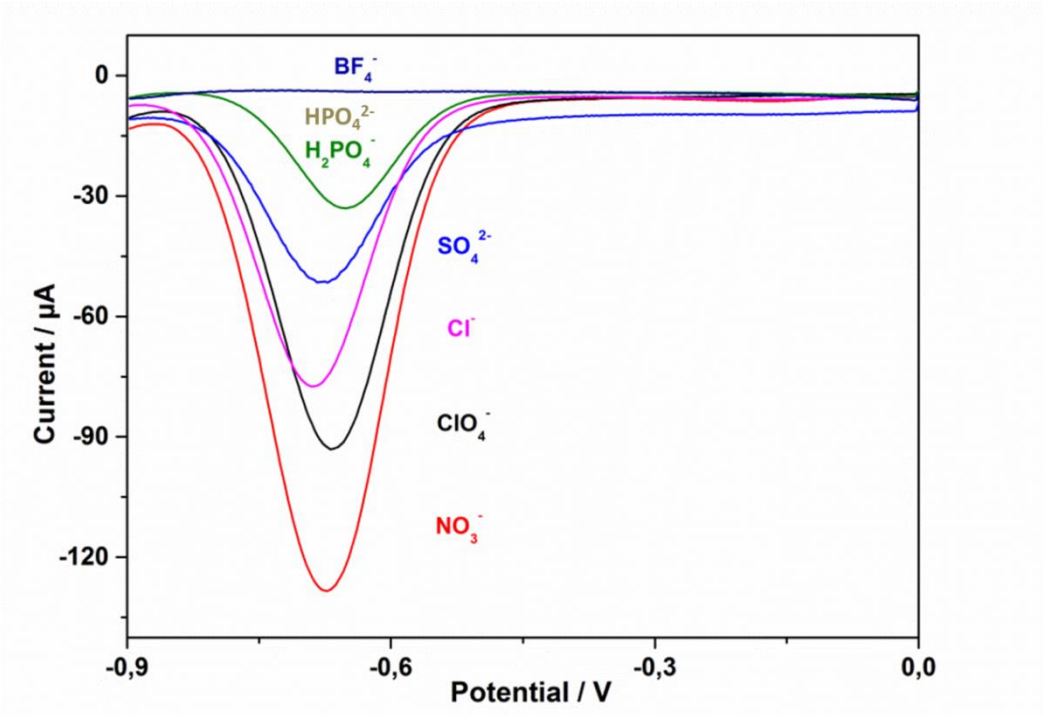

Figure IV-7: Square wave voltammograms of 10 µM paraquat at a modified electrode using different background electrolyte anions. Ionic strength was 70 mM for all anions except BF_4^- for which the ionic strength was 50 mM; pH 6.

4.3.6 Electrochemical impedance spectroscopic (EIS) analysis of electrolyte solutions

Potentiostatic impedance studies were performed using (Frequency response analysis) FRA2 module (PGSTAT 100 apparatus) for the supporting electrolyte concentrations 10-500 mM $NaNO_3$, real sample and 65 mM $NaNO_3$ added to real sample on both bare and silica modified electrodes. Nyquist plots for the impedance measured for bare GCE are presented in Figure IV-8; the plots for modified GCE were similar to that of bare GCE. Meuse River (real samples) sample showed the highest resistance which confirmed presence of very low electrolyte concentration (measured to be around 3.3 mM by ion chromatography), whereas after addition of 65 mM $NaNO_3$ these samples exhibited similar values as that of 70 mM $NaNO_3$ (Figure IV-8 B). The solution resistance extracted from the impedance data, ranges between 64 (for I = 500 mM) to 2344 Ohms (for I = 10 mM) and does not differ much whether the bare electrode or the modified one (Table IV-1). Resistance of the solution was measured by using R (Q) R circuit.

Table IV-1: electrolyte solution resistance measured by Impedance studies

I / mM	R_S / Ω[a](Bare)	R_S / Ω[a] (Modified)
10	2344	2528
20	1392	1516
50	573	608
70	422	412
100	295	319
500	64	75
Real sample	4335	4751
Real sample + 65 mM $NaNO_3$	460	500

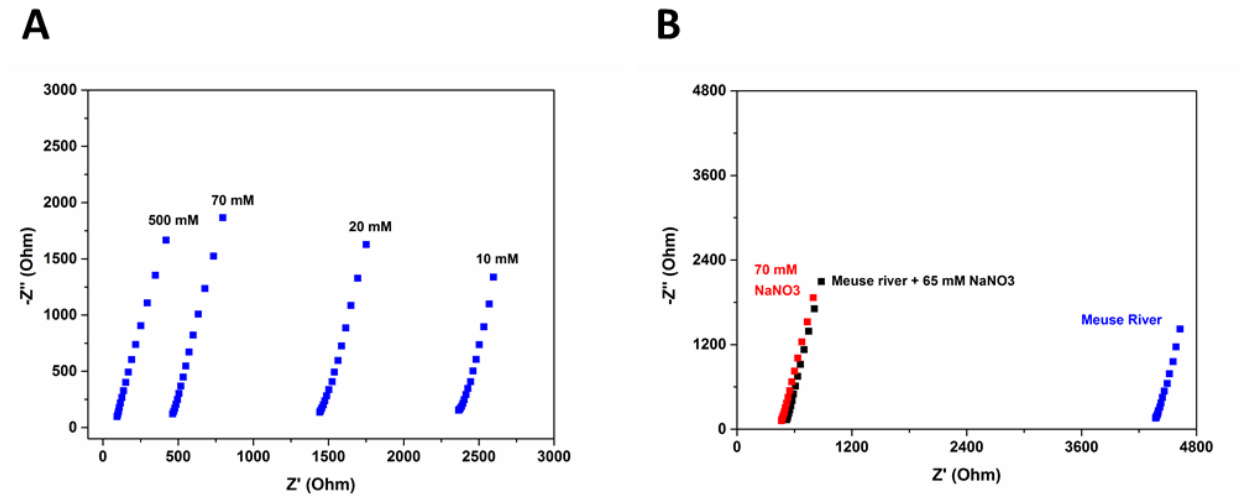

Figure IV-8: Nyquist plot for the impedance measured (A) at bare GC electrodes in solutions of different $NaNO_3$ concentrations (B) in a laboratory solution of 70 mM $NaNO_3$ (red squares), in Meuse River sample before (blue squares) and after the additions of 65 mM $NaNO_3$ at a modified electrode. Frequencies were between 60 and 2000 Hz. pH = 6.

4.3.7 Effect of solution pH on SWV response

In order to further investigate electrochemical behaviour of paraquat, the reduction peak current for paraquat is measured as a function of pH (in the range 1.2-10), while the ionic strength is maintained constant at 70 mM (Figure IV-9). At pH < 4, silica walls are either neutral or cationic and hence do not favour adsorption of cationic paraquat. For pH > 4, cationic paraquat can interact with the anionic walls of silica and an increase of the reduction peak current is observed. Maximum peak height is recorded at pH 6, whereas the reduction peak currents decay beyond this optimal pH value. As for ionic strength studies, the voltammetric signal of paraquat at the bare electrode does not vary noticeably in the pH range studied. We could therefore attribute the strong variation of peak current intensity at the modified electrode (Figures IV-6 & 9) to a dramatic influence of both pH and ionic strength on the state of mesochannels (surface charge density),[223,224] and hence the ability of cationic species to adsorb onto the silica walls of the mesoporous film. In addition, nanoscale dimensions of the channels allow the occurrence of cationic enrichment, which does not happen in channels of greater dimensions.[225] Under certain conditions of ionic strength and pH, nanochannels with negatively-charged walls lead to the further enrichment of cationic species and to the exclusion of their counter anions as it has been described earlier by Plecis et al.[226]

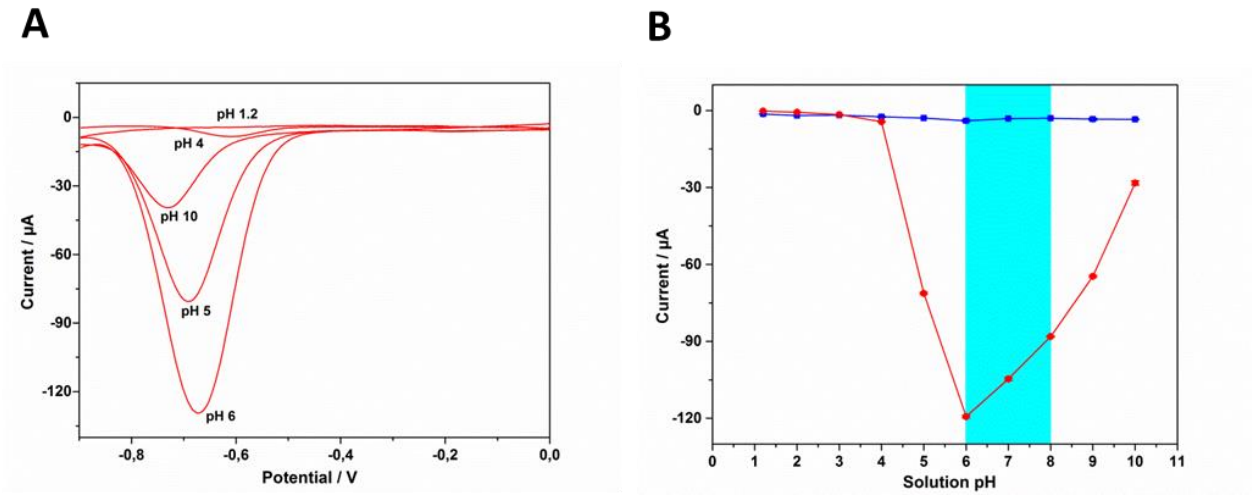

Figure IV-9: (A) Square wave voltammograms of 10 µM paraquat at a modified electrode for pH values of 1.2, 6 and 10. HNO_3, $NaNO_3$ and NaOH stock solutions were used to prepare the background electrolyte solutions for which the ionic strength was kept constant at 70 mM. (B) Peak current as a function of pH for modified electrodes (red) and bare electrode (blue). The pale blue zone represents the pH range generally encountered for real samples. When not visible, error bars are smaller than the symbols.

4.3.8 Effect of Debye length and mesochannels Interaction on sensitivity

When considering the accumulation (and detection) of paraquat, charge compensating anions should also be taken into account. In meso and nanochannels, the level of exclusion of counter anions and the degree of enrichment with cationic species are dependent on the Debye length, λ_D, which can be calculated according to equation (4.1), where ϵ_0 is the permittivity of free space (8.85×10^{-12} F m^{-1}), ϵ_r is the permittivity of water (6.95×10^{-10} F m^{-1} at 20°C), k_B is the Boltzmann constant (1.38×10^{-23} J K^{-1}), T is the temperature (293 K), N_A is the Avogadro's number (6.02×10^{23} mol^{-1}), e is the elementary charge (1.60×10^{-19} C) and I the ionic strength (expressed in mol m^{-3}).

$$\lambda_D = \sqrt{\frac{\epsilon_0 \epsilon_r k_B T}{2 N_A e^2 I}} \qquad \textbf{Eq. 4.1}$$

Under the experimental conditions for the formation of the mesoporous silica thin film, the pore radius, r, is measured at 1.15 nm, which is between the Debye lengths calculated for the highest and the lowest ionic strengths (Figure IV-10). When the ionic strength I >70 mM, then $r > \lambda_D$, we can divide the channel in two zones: (i) a Debye layer in contact with the silica walls and (ii) a 'free' space in the centre of the mesochannel. As the ionic strength decreases, the Debye layer is increasing, reducing the 'free' space until it fully

disappears when $r < \lambda_D$ *(i.e.* $I < 70$ mM), leading to an overlap of the electrical double layers. We consider here the second case (i.e. when $r < \lambda_D$); the potential distribution across the mesochannel width is not homogeneous. It varies according to the *z* position (*z* direction is defined here as the width of the mesochannel) in the mesochannel, Ψ (z), and it is calculated according to the following equation:[226]

$$\psi(z) = \frac{\zeta \cos h((r-z)/\lambda_D)}{\cos h(r/\lambda_D)} \qquad \textbf{Eq.4.2}$$

Where ζ is the zeta potential of the silica walls, The absolute potential value is the highest close to the charged silica walls and is equal to the zeta potential. It drops to reach a minimum in the centre of the mesochannel (when $z = r$) (Figure IV-11).

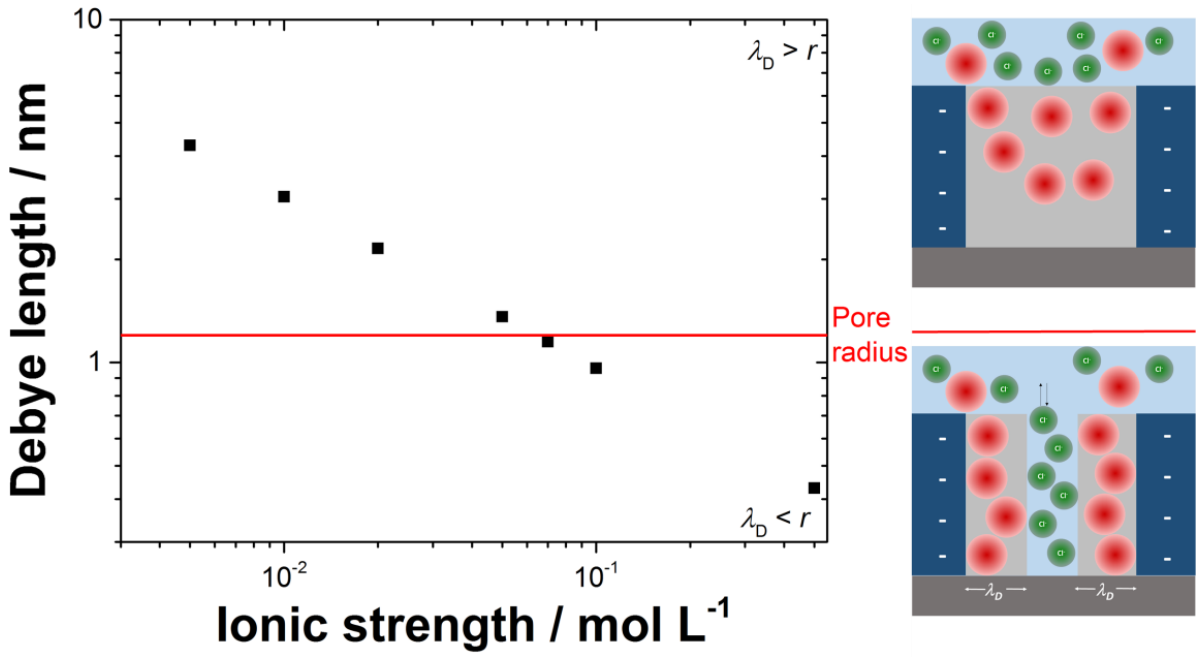

Figure IV-10: Debye length as a function of the ionic strengths used in the SWV experiments. The red line symbolizes the value of the mesochannel radius. On the right, two schemes represent anion exclusion of the mesochannels (top) and the 'free' anion zone.

Based on such a potential distribution, the mesochannel is enriched in cationic species as the concentration *C (z)* can be calculated from the bulk concentration C_0 according to the Poisson-Boltzmann equation (4.3):[226]

$$C(z) = C_0 exp\left(-\frac{e\psi(z)}{k_B T}\right) \qquad \textbf{Eq. 4.3}$$

Equations (4.2) and (4.3) show that the zeta potential at the diffuse layer of the mesochannel determines the overall enrichment in cationic species, hence the improved electrochemical signal is obtained. When Ψ is negative, paraquat is accumulating within the mesochannel and thus leading to a higher voltammetric signal than at bare electrodes. Zeta potential values for silica surface depend on the pH and ionic strength.[223,224,227] As the solution pH increases, silica surfaces become more negatively charged and the absolute zeta potential increases, leading therefore in an increase of the paraquat concentration within the mesochannels. However, we observed a drop in the reduction peak current for pH > 6 (Figure IV-9), which can be related to some degradation of the film mesostructure due to partial dissolution of the silica.[228] Similarly, the drop of reduction peak current for I < 70 mM can be linked to the overlap of the double layers, leading to the exclusion of anions from the mesochannels.[224] Equations (4.2) and (4.3) show that paraquat concentration is higher in the Debye layer than in the centre of the mesochannel. As the ionic strength decreases from 500 mM to 70 mM, the Debye layer thickens, allowing the paraquat concentration within the mesochannels to rise, contributing to higher peak current for I = 70 mM than for I = 500 mM. As the ionic strength decreases, the zone from which anions are excluded (marked in grey in Figure IV-11) increases until they are excluded when $r < \lambda_D$ *(i.e.* I < 70 mM).

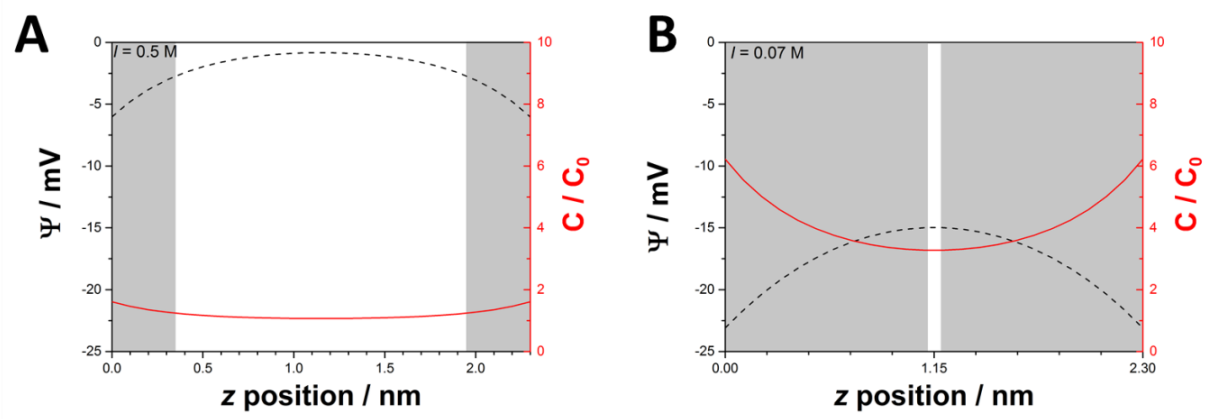

Figure IV-11: Distribution of the potential Ψ (dashed black lines) and the paraquat concentration ratio (C/C_0) (solid red lines) along the mesochannel width, z, for an ionic strength, I, of (A) 0.5 and (B) 0.07 M. The grey area represents the Debye layer; Ψ and C/C_0 are calculated based on equations (2) and (3). (A) ζ = -6 mV;[224,227] λ_D = 0.35 nm for I = 0.5 M and (B) ζ= -23.1 mV;[224,227] 1.13 nm for I = 0.07 M; r = 1.15 nm in all cases.

The above results, can explain that the best electroanalytical response of paraquat at mesoporous silica modified GCE is recorded with 70 mM $NaNO_3$ as supporting electrolyte and when the pH is 6.

4.4 Square wave voltammetric analysis with low concentration of paraquat

With above optimized conditions, paraquat reduction peak current showed linear response at concentrations range between10–50 nM with a detection limit of 4 nM (Figure IV-12 C). For comparison purposes, the voltammograms obtained for a bare GCE (Figure IV-12 A) and an electrode modified with a non-mesoporous silica thin film (i.e. electrogenerated in the absence of surfactant) (Figure IV-12 B) does not show any reduction peak, confirming that the mesochannels are responsible for the improved detection of paraquat. The limit of detection is within the same concentration range of the best methods reported in Table I-3 in chapter I, and is achieved with a preconcentration time of 3 minutes, which remains lower than most of methods reported (Table I-2).

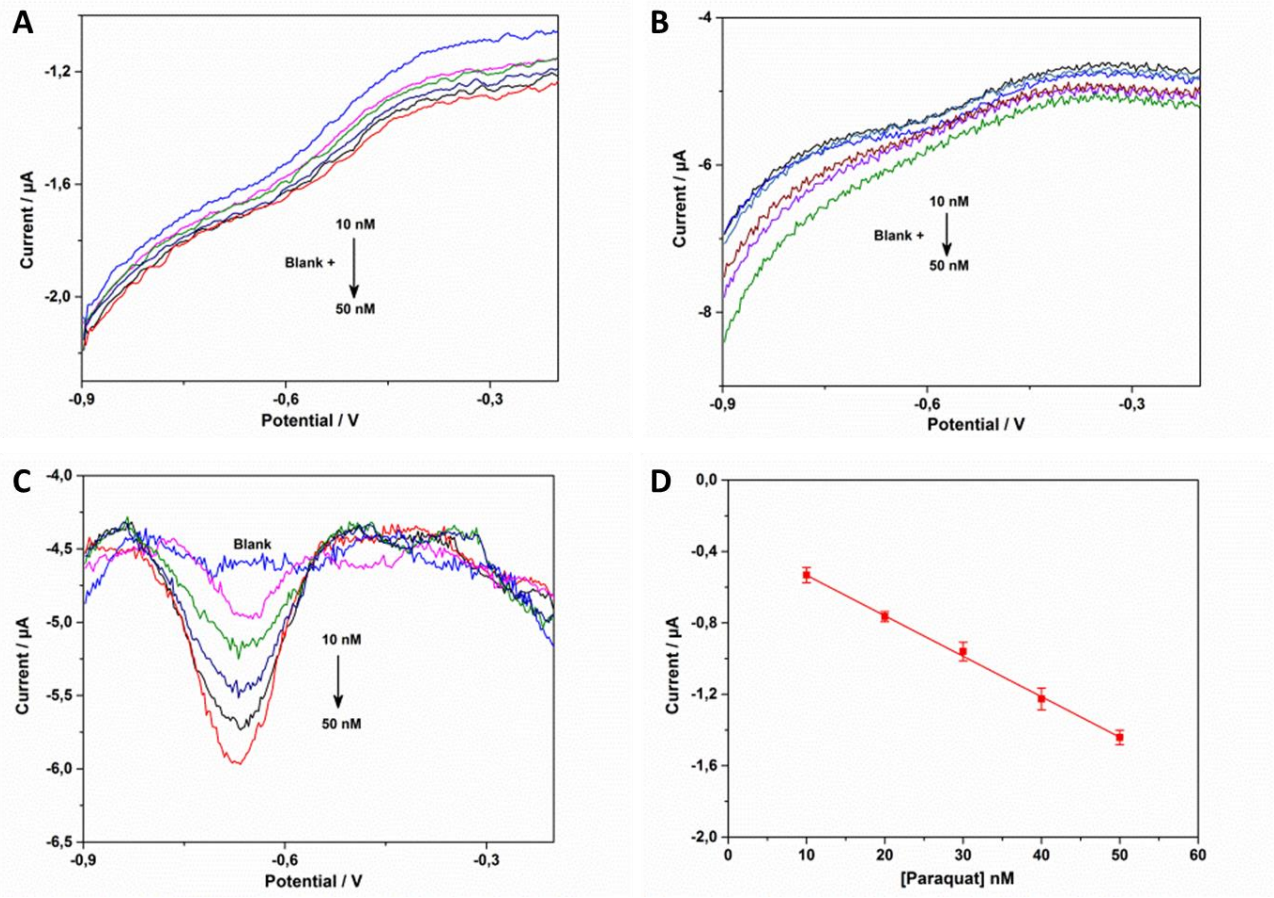

Figure IV 12: Square wave voltammograms of 10 – 50 nM paraquat (A) at bare electrode (B) at non-porous silica modified electrode and (C) at mesoporous silica modified electrode obtained in the optimal experimental conditions (i.e.70 mM $NaNO_3$ and pH 6). (D) Calibration curve for 10 – 50 nM paraquat at a mesoporous silica modified electrode.

4.4.1 Analysis of real samples spiked with paraquat

River samples from the Meuse River (France) were spiked with Paraquat and analysed by square wave voltammetry at both bare and modified electrodes (Figure IV-13). Electrochemical impedance spectroscopy (Table IV-1) shows that the solution resistance (R_s = 4300 Ω) is relatively high, Ion chromatography analysis shows that chloride, nitrate, sulfate and phosphate anions are present in the river water samples for a total concentration of 3.34 mM. These two values suggest an ionic strength in the same order of magnitude. A calibration curve for paraquat is built at the modified electrode between 10 and 40 nM with a sensitivity of 0.021 µA nM^{-1} (R^2 = 0.946; N = 4). At the bare electrode, paraquat reduction is not observed for any of the four paraquat concentrations tested (10, 20, 30 and 40 nM). These results demonstrate that the presence of the mesoporous silica thin film improves the sensitivity reaching concentration levels in real samples that cannot be detected at a bare electrode. The limit of detection of paraquat at an electrode modified with a mesoporous silica thin film is estimated at 12 nM (in a spiked real sample solution), which is much lower than the maximum concentration of paraquat in drinking water recommended in guidelines and regulatory limits by different countries.[229] Limit of detection was calculated by using following eq.

$$\mathrm{LOD} = \frac{3.3 \times \text{Standard deviation of y-intercept}}{\text{Slope of calibration curve}} \qquad \textbf{Eq. 4.4}$$

This example shows that electrochemical analysis with mesoporous silica modified GCE can also be used for analyzing real water samples with low detection limit. The quantification may be further improved by fixing the type and concentration of anions in the solution.

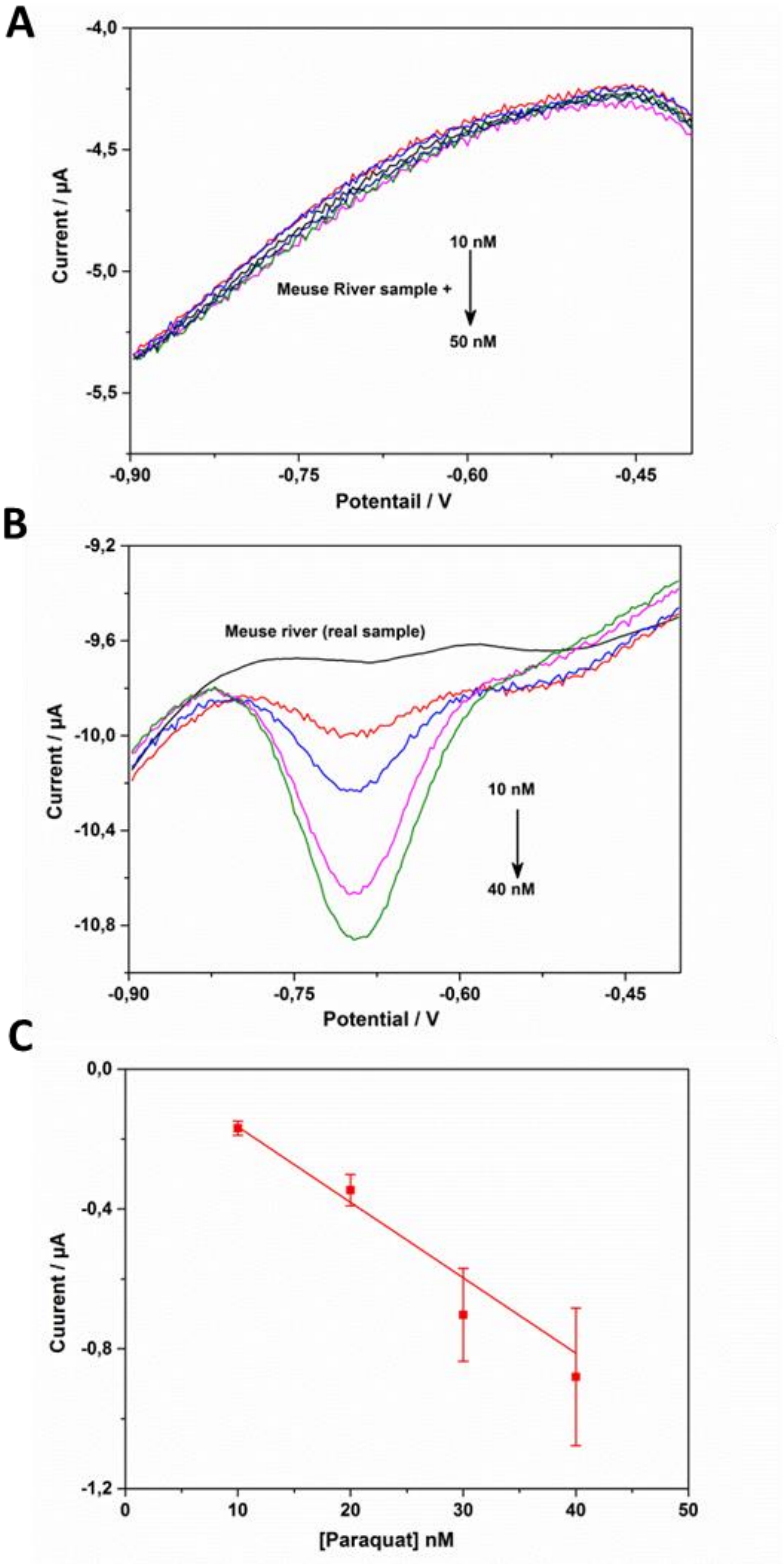

Figure IV-13: (A) Square wave voltammograms of 0, 10, 20, 30, 40 and 50 nM paraquat in Meuse River water samples at bare (B) 0, 10, 20, 30 and 40 nM paraquat in a Meuse River water at mesoporous silica modified electrode (C) Standard addition of paraquat to river samples at mesoporous silica modified electrode. Electrolyte concentration ~ 4 mM, pH 7.6

4.5 Conclusions

Mesoporous silica thin films favour the electrochemical detection of cationic paraquat in aqueous samples. The nanoscale dimension of the oriented and organised channels contributes to concentration enrichment within the mesochannels, which varies with experimental conditions such as ionic strength, pH and nature of the supporting electrolyte anion due to local potential variations. Limit of detection (LOD) in real samples spiked with paraquat by this method is 12 nM which is more than 3 times below the strictest permissible limit of 40 nM established for paraquat in drinking water. Electrochemical detection of paraquat at mesoporus silica thin films modified electrodes and results showed that response of paraquat is greatly enhanced at modified electrodes as compared to unmodified ones. The reason for increased signal is the interaction of cationic paraquat with anionic silica films. We discussed in detail the effect of solution parameters such as pH, ionic strength and nature of supporting electrolyte.

Chapter V: Studies of electrode modification and electrode geometry effect on paraquat sensing

In the previous chapter we described the electrochemical detection of paraquat at silica thin film modified glassy carbon electrodes (GCE). Presence of silica film on electrode surface is beneficial for sensitive detection of paraquat, herein we explored the effect of silica film thickness and electrode geometry on paraquat detection by adopting protocols established in previous chapter. Silica films were electrogenerated for various deposition times with the help of EASA method. Multi-layered silica thin films were also deposited on GCE. Electrochemical and microscopic Characterizations of film thickness were performed. Microelectrode arrays at GCE substrate were also fabricated, modified with silica films and Characterized. Electrochemical detection of paraquat at these modified electrodes was performed by square wave voltammetry and calibration curves were established.

5.1 Introduction

Electrode modification is a powerful tool which provides the control over electrode surface manipulation for electrochemical sensing applications. Electrode modifications with suitable chemical compounds can provide the high levels of selectivity for target analytes. These delibrate modifications impart the characterstics of the coating substance to underlying electrode surface and hence can help in achieving specific requirements for electrochemical sensing. Modified electrodes are more useful for environmental sensing as compared to bare electrodes as they provide beneficial properties which enhance sensitivity and selectivity, these properties include faster electron transfer, selective accumulation and controlled transport.[33,230] In present work GCE were modified with silica thin films by electrochemically assisted self-assembly (EASA) method for different deposition times to vary the film thickness and subsequently study the effect of film thickness on paraquat sensing. Multi-layered mesoporous silica thin films were also deposited on GCE by procedure established already.[231] Earlier studies have shown that it is possible to deposit multilayer of silica thin films by EASA method.[232] The motivation behind multilayer deposition is to produce thicker films without compromising the mesoporosity and film structure which is affected in case of long deposition times where growth of mesoporous films reaches to a maximum thickness and beyond it results in generation of higher number of silica beads at film surface which can effect the reproducibilty of electroanalytical applications.

Microelectrode arrays have become important in the field of electrochemical sensing as they offer certain beneficial properties such as high signal to noise ratios,[233] operating in dilute supporting electrolyte,[234] steady state diffusion of electroactive analyte species towards electrode,[235] lower capacitance of electrical double layer,[236] suitability for realtime and trace elements analysis.[237,238] All these characterstics contribute to high sensitivity and selectivity of the electrochemical sensor. The disadvantage associated with microelectrodes is lower current due to their smaller size which can be solved by using microelectrode arrays instead of single microelectrode.[239] Microelectrode arrays are fabricated in a way where individual microelectrodes are placed close to each other at a certain distance which allows the overlapping of diffusion layer, hence solving the problem of lower current as well as providing extra benefits in electroanalysis. In microelectrode arrays each microelectrode can be polarized by the same potential and also with different potentials by using multipotentistat system.[240]

This chapter is divided into three parts (i) First section is dealing with silica thin films deposition for different time 5-30 seconds to control film thickness, (ii) second section is about the multilayer silica thin films deposited by electro-assisted self assembly process and (iii) last part includes modification and characterization of inhouse fabricated microelectrode arrays on GCE substrate. Modified electrodes were characterized electrochemically with the help of a redox probe whereas scanning electron microscopy was used for surface Characterization of modification. Accumulation behaviour of paraquat inside silica thin film matrix was studied by cyclic voltammetry (CV) and square wave voltammetry (SWV) was used to detect paraquat.

5.2 Electrochemical deposition and characterization of monolayer films

Mesoporous silica thin films were formed by the EASA method at glassy carbon electrodes for various deposition times ranging from 5-30 seconds according to previously optimized parametrs[216] and electrochemical characterization of modification was carried out with the help of CV using redox probe $Ru(NH_3)_6^{3+}$. Figure V-1 (A) shows the electrochemical characterization of bare and silica modified GCE before template extraction. One can observe with lower time of deposition thinner film is deposited resulting in ruthenium hexaamine signal. As the deposition time is increased the signal of redox probe tends to decrease suggesting the development of thicker silica film and gradually blocking the access of redox probe to electrode surface. The extraction of template by acid-ethanol solution resulted in gain of electrochemical signal.

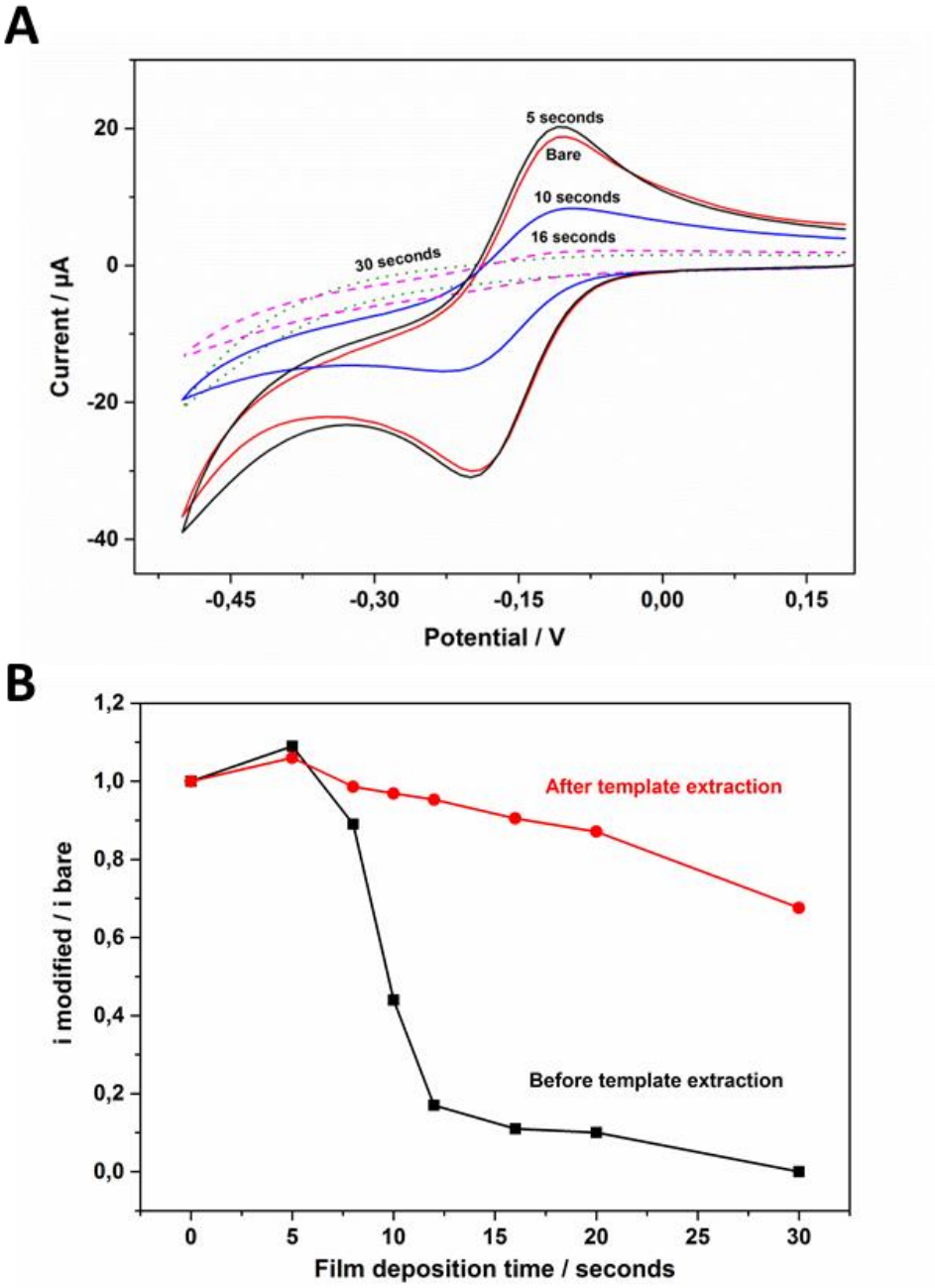

Figure V-1: Cyclic voltammetry of 0.5 mM $Ru(NH_3)_6Cl_3$ in 0.1 M KCl (A) at bare and after silica film deposition on GCE for various deposition time (5-30 seconds). Scan rate =100 mV s^{-1}, Silica film deposition current density = 3.71×10^{-4} A / cm^{-2} (B) Maximum peak current height for 0.5 mM $Ru(NH_3)_6Cl_3$ in 0.1 M KCl at silica modified GCE before and after template extraction divided by I peak at bare GCE.

Two possible explanations can be presented for the redox probe signal behavior observed above, (i) Heterogeneous and non-uniform film growth (ii) homogenous and uniform film growth. In the first option, as explained by Liang and Walcarius,[241] the film

starts to grow by EASA method, it is heterogeneous and non-uniform but as the time of deposition increases the oligomers of silanol moieties are condensed to form polymeric groups which results in thicker and homogenous silica films[241]. This explains well the higher signal of redox probe at small deposition time and complete loss of signal at longer deposition time. Also the higher signal observed for 5 seconds deposition than bare electrode could be due to accumulation of cationic redox probe in relatively less uniformly deposited film as time is insufficient for the silane molecules to condensate around template molecules and form uniform film. In the second option, it is supposed that silica film grows uniformly but as at shorter deposition time the film is considerably thinner so redox probe can manage to pass through it and give rise to electrochemical signal. The first hypothesis is stronger as it is supported by already published literature.[241] Silica film deposition for 30 seconds results in complete loss of redox signal confirming the film is uniformly deposited and there is no space (due to densely packed mesopores with template molecules of CTAB) for the redox probe to pass through the film and reach electrode surface to exhibit electron transfer reaction.[72,85,216,] Figure V-1 B shows the response of redox probe at modified GCE for different film deposition time. Current intensity recorded for oxidation peak of redox probe after silica film modification (before and after template extraction) is divided by the maximum oxidation peak at bare GCE and resulting values are plotted as a function of film deposition time. As the time of film deposition is increased more thicker film is deposited and signal at modified GCE as compared to bare is decreased and ultimately at 30 seconds film there is no signal for redox probe unless the CTAB is extracted and mesopores are open to facilitate the electron transfer reaction between underlying electrode surface and redox probe.[215]

5.2.1 Microscopic characterization of electrode modification

Scanning electron microscopy (SEM) was performed to Characterize the modification of electrodes carried out at varying deposition time. SEM images confirmed the presence of silica film at GCE modified for 8-30 seconds deposition time; while for 5 seconds film deposition, film visualization was not possible and electrochemical Characterization also confirmed the same so it can be said there is very thin or almost no silica film deposited. 8 seconds modified electrode showed better deposition as compared to 5 seconds and film deposition can be clearly seen. 10, 16, 20 and 30 seconds deposited films were more easy to visualize and as the the deposition time increased the quality of film and amount of silica beads also increased. Amount of silica beads present at thin film surface increase by

increasing deposition time. From microscopic images it can be observed that the silica films are homogenously deposited with good adhesion to electrode surface and ther are no visible cracks in the films thanks to APTES electrografting carried out in chapter III.

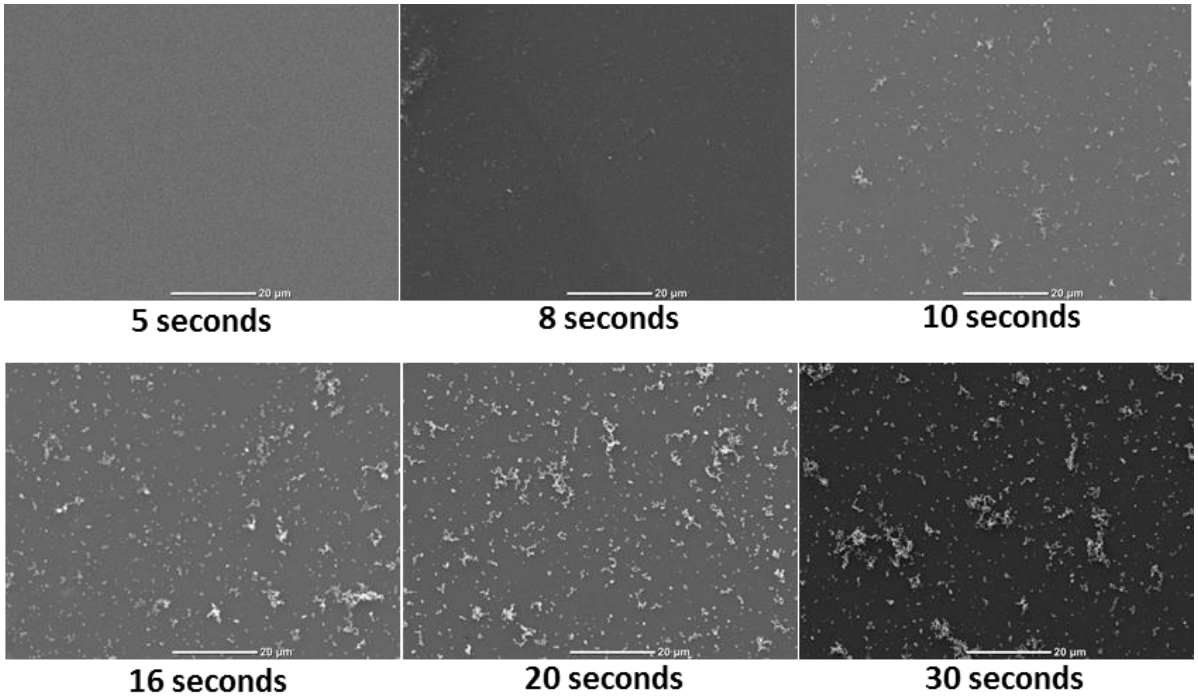

Figure V-2: Scanning electron microscopy images of monolayer silica thin films formed for various deposition time. Scale bar is 20 µm.

5.2.2 Film thickness measurements by profilometry

Profilometry is a useful technique for the thickness measurements especially for thin films. Stylus profilometry is contact based measurement , it involves movement of stylus over the grove which is made mechanically accross the fim. As a result this technique can provide accurate thickness measurements up to few nm scale. Roughness of the substrate at which film is deposited is very important factor for accurate measurements.[242] Figure V-3 shows the film thickness measured by profilometry technique at GCE and ITO respectively, film thickness is plotted as a function of deposition charge. Film thickness determination at GCE is difficult due to surface roughness as compared to ITO as seen in (Figure V-3 B,C). In case of very thin films (5, 8, 10 and 12 seconds) it was not possible to measure the thickness by this technique at GCE. Silica films were also deposited at ITO which has smoother surface compared to GCE but here also due to very thin films (5 and 8 seconds) measurement of film thickness was not possible.

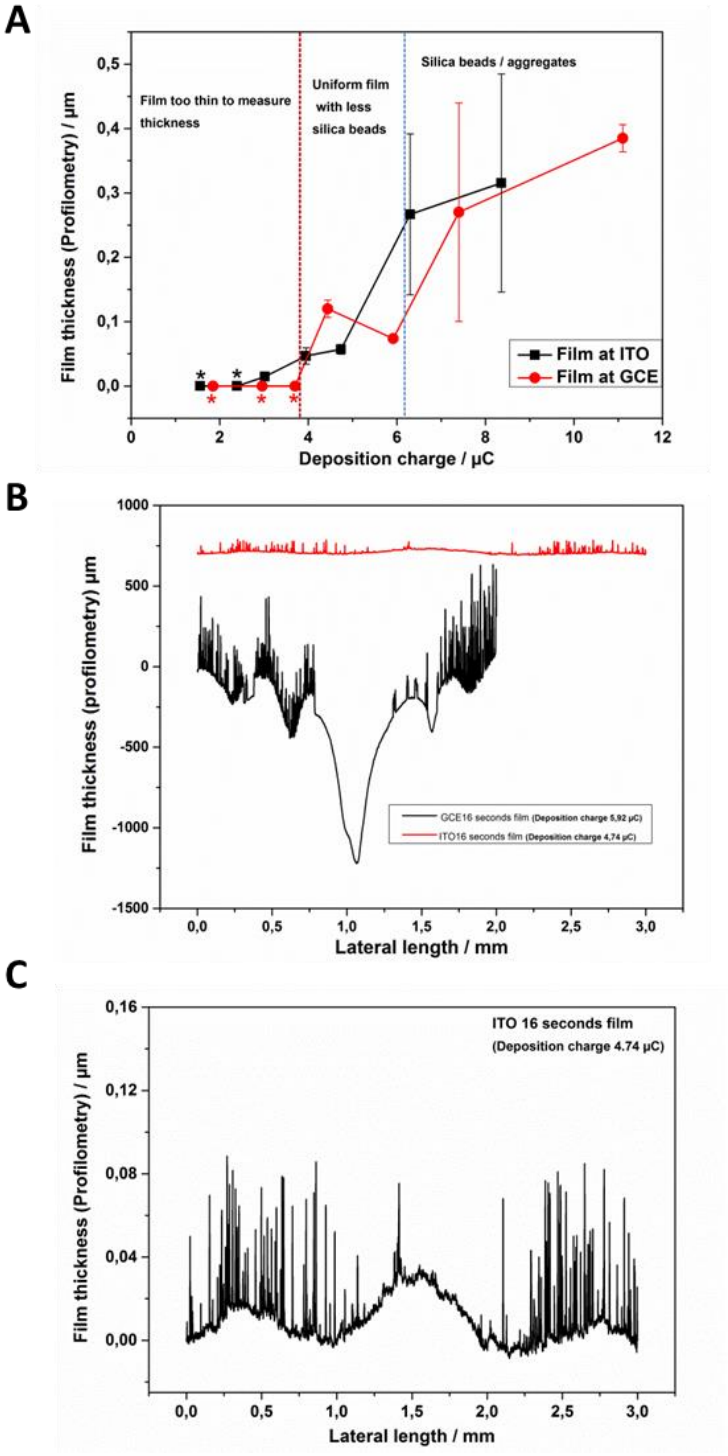

Figure V-3: Film thicknesses measured for different deposition time as a function of deposition charge at (A) GCE and ITO (charge corresponds to deposition time 5-30 seconds), 16 second deposited film profilometry graph at (B) GCE and ITO at same scale (C) ITO **Film thickness could not be measured by profilometry technique. Silica film deposition current density for GCE= 3.71×10^{-4} A / cm^{-2}, Potential for silica film deposition at ITO = -1.3 V.

5.2.3 Paraquat accumulation by CV at modified electrodes

Repetitive cyclic voltammetry was used to study the accumulation behavior of paraquat at modified electrodes for various deposition times with silica thin film after template extraction. Figure V-4 (A) shows the accumulation of paraquat in silica film matrix due to its cationic nature, previous results have shown that when high concentration of paraquat is used silica film is saturated with paraquat much earlier as compared to low concentration which can result in lower signal as described in chapter IV. Film thickness is very critical and has direct effect on the amount of paraquat to be accumulated in silica thin films and ultimately on the signal intensity. Thicker films can accommodate large amount of paraquat as compared to thinner films. Accumulation behavior of paraquat is shown with 30 seconds film in Figure V-4 (B), signal intensity was increasing with each scan.

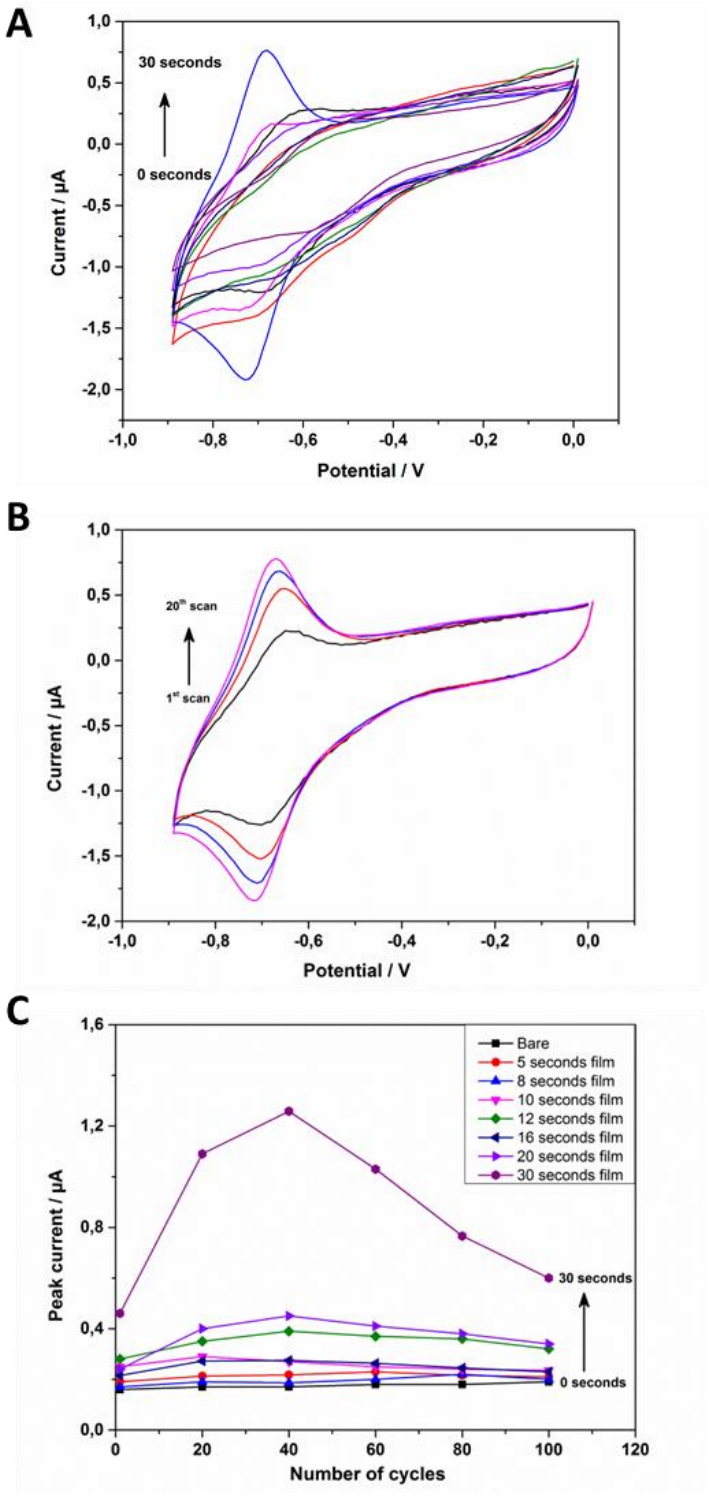

Figure V-4: Cyclic voltammograms of 5 µM paraquat in 70 mM $NaNO_3$ (A) by cyclic voltammetry multiple cycling (100th scan) at GCE modified with silica thin films for deposition time 0, 5, 8, 10, 12, 16, 20 and 30 seconds, (B) Paraquat accumulation behavior in silica film (30 seconds) for same concentration as above, (C) Current intensity as a function of number of CV cycles (Accumulation of paraquat in mesoporous silica film) at modified GCE for different deposition time. Scan rate= 20 mV s^{-1}.

Peak current as function of number of CV scans plots (figure V-4 C) are constructed for 5 µM paraquat at bare and modified GCE with silica film formed for deposition time ranging from 5 seconds to 30 seconds. Maximum response by cyclic voltammetry is observed for the film deposited for 30 seconds. Cyclic voltammetry scans show an increasing signal with every cycle up to a certain limit and then signal starts to decrease again, this shows the film is saturated and it cannot accumulate paraquat anymore. This increasing response is at highest normally up to 40 cycles and after that signal starts to decay, the decay in signal can be attributed to loss of silica mesostructure as these repetitive scans are carried for longer period of time at low scan rate.

5.2.4 SWV analysis of paraquat on monolayer thin films

Square wave voltammetric detection at mesoporous silica film modified glassy carbon electrode is very effective as described in previous chapter. In this part, we used modified electrodes on which silica thin films were deposited for time period ranging from 5 to 30 seconds to study the effect and influence of film thickness on its ability to detect paraquat. Square wave voltammetry parameters as optimized previously were used for analysis of 0.5-10 µM paraquat at bare and silica film modified GCE.[243] Results showed continuously increasing response with increasing concentration of analyte. The signal at silica modified GCE at optimal conditions is much higher (30 times) as compared to bare GCE and also increase in linear manner as the silica film thickness is increased. The highest response is recorded at GCE modified for 30 seconds by silica thin film. Square wave voltammograms of 0.5-10 µM paraquat at bare and silica modified electrodes are shown in Figure V-5, each scan was repeated thrice, mean and standard deviation values were used to draw calibration curves with standard error. At bare GCE the reductive potential of paraquat is observed around -0.58 V and is shifted to reduction potential of paraquat (-0.7 V) at silica modified GCE as reported.[214]

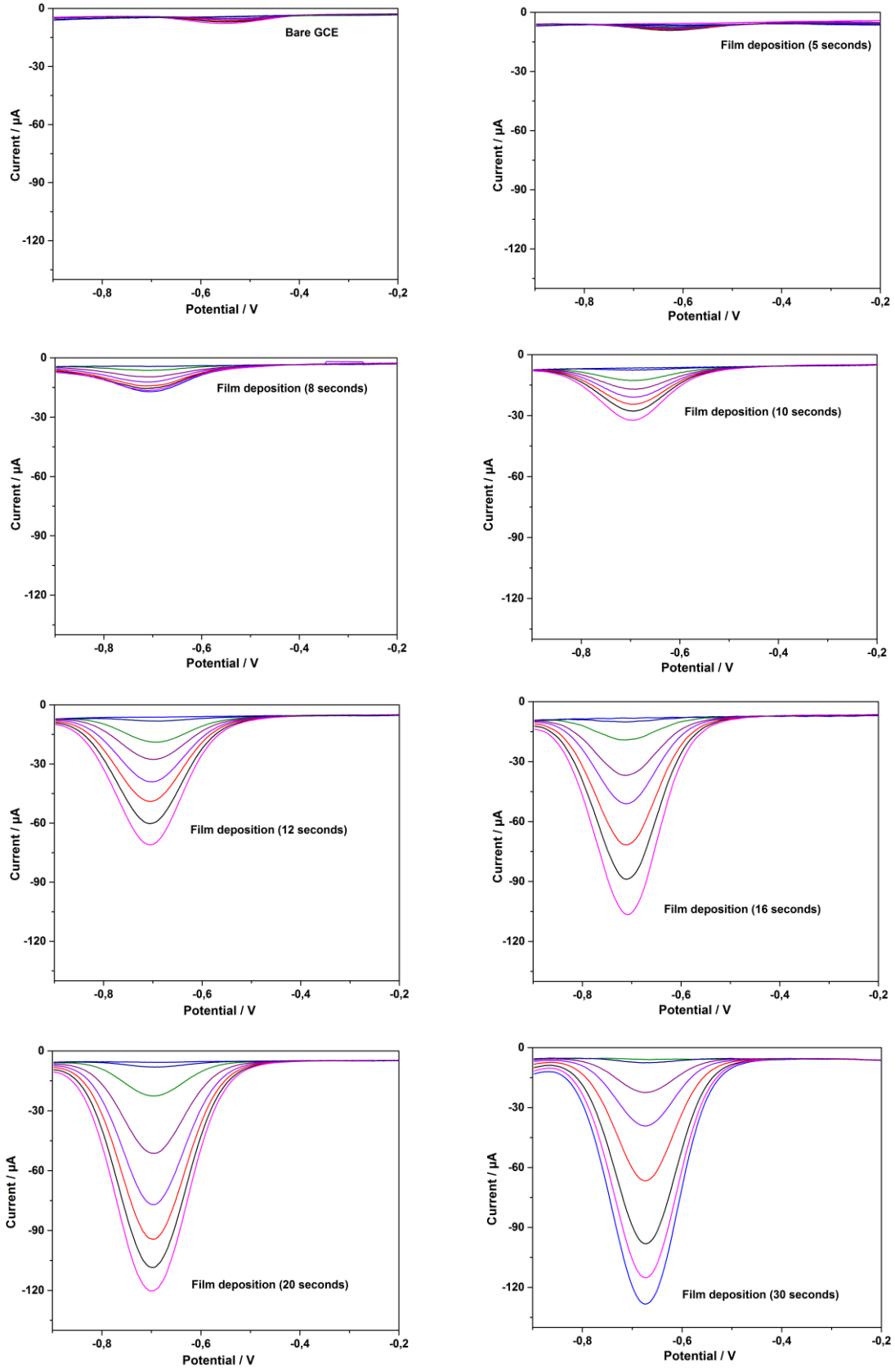

Figure V-5: Square wave voltammograms of 0.5, 2, 3.5, 5, 6.5, 8 and10 µM of paraquat in 70 mM $NaNO_3$ (pH 6) on bare and 5-30 seconds film modified GCE.

Calibration curves for 0.5-10 µM (N = 7) paraquat in 70 mM $NaNO_3$ (pH 6) at silica film modified GCE for 0-12 seconds showed linear response to increasing concentration whereas for 16, 20 and 30 seconds films, calibration curves are linear for middle concentrations and tend to level off at high concentration which can be attributed to limited diffusion of paraquat by SWV in thick films, during the initial concentrations paraquat accumulate slowly at film surface and behavior is similar in almost all deposition times. In the middle part thicker film showed higher response as compared to thinner ones, as there is more space for paraquat accumulation. For higher concentrations there is limited space for paraquat to accumulate as the films get saturated in the middle part so we can observe the leveling off behavior in last points. All the calibration curves (figure V-6) exhibited good R^2 values (Table V-1).

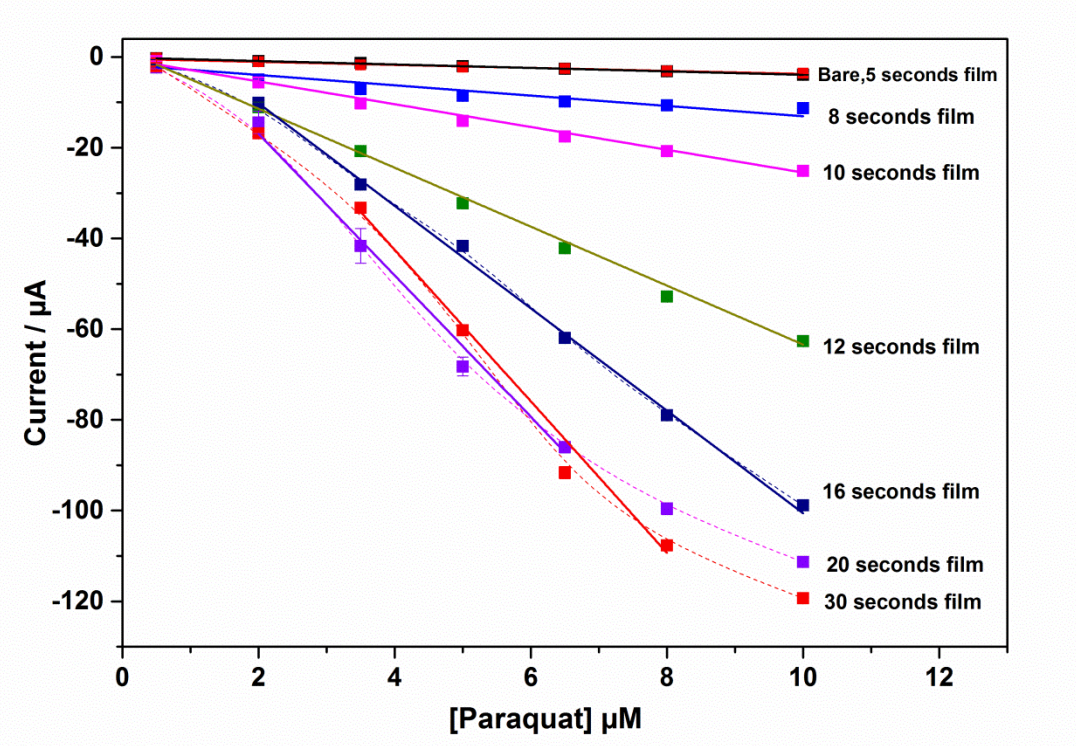

Figure V-6: Calibration curves by square wave voltammetry of bare and 5-30 seconds silica film modified glassy carbon electrodes, where not visible, error bars are smaller than points.

Table V-1: Slope, Intercept and R^2 values for monolayer silica film deposited for different deposition time at glassy carbon electrodes

Film deposition time	Slope	Intercept	R^2
0 seconds	-0,379	-0,130	0,998
5 seconds	-0,334	-0,396	0,984
8 seconds	-1,136	-1,694	0,978
10 seconds	-2,510	-0,374	0,994
12 seconds	-6,495	1,568	0,999
16 seconds	-11.294	12.376	0,996
20 seconds	-15.601	14.287	0,986
30 seconds	-16.710	24.356	0,994

Graph (Figure V-7) shows the maximum peak height of 3.5, 5 and 10 µM paraquat at silica film modified GCE for 0-30 seconds. Initially the difference between unmodified and modified electrodes is not very evident but as the film deposition time is increased the response increase linearly and comes to point of saturation at 20 and 30 seconds.

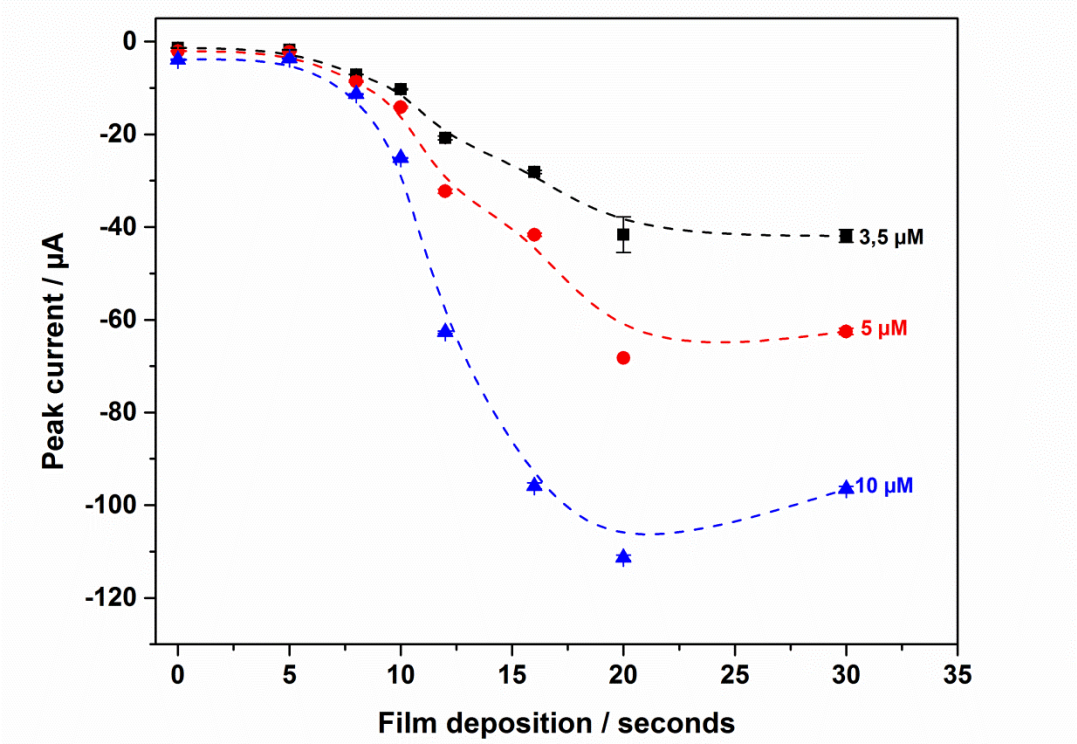

Figure V-7: Peak current by square wave voltammetry of paraquat in 70 mM $NaNO_3$ (pH 6) for concentrations of 3.5, 5 and 10 µM paraquat at bare and 5, 8, 10, 12, 16, 20, and 30 seconds film modified GCE.

5.2.5 Conclusions

From the above results it can be concluded that mesoporous silica film thickness has direct effect on the sensitivity due to cationic and anionic interaction of paraquat and silica films respectively. Sensitivity is increased with thicker film but also as seen in SEM images amount of silica beads at film surface increases for higher time of film deposition, which in turn can hamper the reproducibility of analytical results.

As a prospect, if the silica film thickness is increased by multi-layered deposition rather than increased deposition time for monolayer, can we achieve thicker films without having silica beads at film surface which can increase sensitivity as well as reproducibility of the system? In the next section we will discuss the multilayer silica film deposition at glassy carbon electrode, their characterization and paraquat detection.

5.3 Multi-layered silica thin films

This section deals with multi-layered silica film deposition, their electrochemical and microscopic characterization and subsequently paraquat detection using these modified GCEs. Multi-layered silica thin films at glassy carbon electrodes were deposited by adopting a previously published procedure.[244] As stated in previous section monolayer deposition of silica thin film may give rise to formation of unwanted silica beads, to address this problem we hypothesized that the multilayer deposition of silica films by using short deposition time can provide thicker films as well as less amount of silica beads which in turn can enhance sensitivity and reproducibility. We selected 8 and 16 seconds deposition time for multi-layered film formation as larger deposition time will again pose the same problem of silica beads formation as faced in case of monolayer films.

5.3.1 Characterization of multi-layered silica films

Cyclic voltammetric characterization of silica films deposited for 8, 16 seconds monolayer and 8 seconds bilayer was performed with the help of redox probe. As seen in Figure V-8 (A) 8 seconds monolayer deposition was not enough to form a uniform film and hence redox probe response is observed even in the presence of template inside the pores, while this response is lowered when the deposition is done for 8 seconds bilayer and also 16 seconds monolayer suggesting uniform deposition of silica film. In other experiments silica film deposited for 16 seconds bilayer and 16 seconds trilayer were also characterized in the similar manner. Small redox activity is seen in case of 16 seconds monolayer, suggesting that large deposition time is required for monolayer deposition to completely cover the electrode surface for an intact and uniform silica film. Whereas in case of 16 seconds bilayer and trilayer redox signal is completely absent confirming silica film is uniform and homogeneous (figure V-8 B). Electrochemical signal of redox probe was appeared after the extraction of surfactant template.

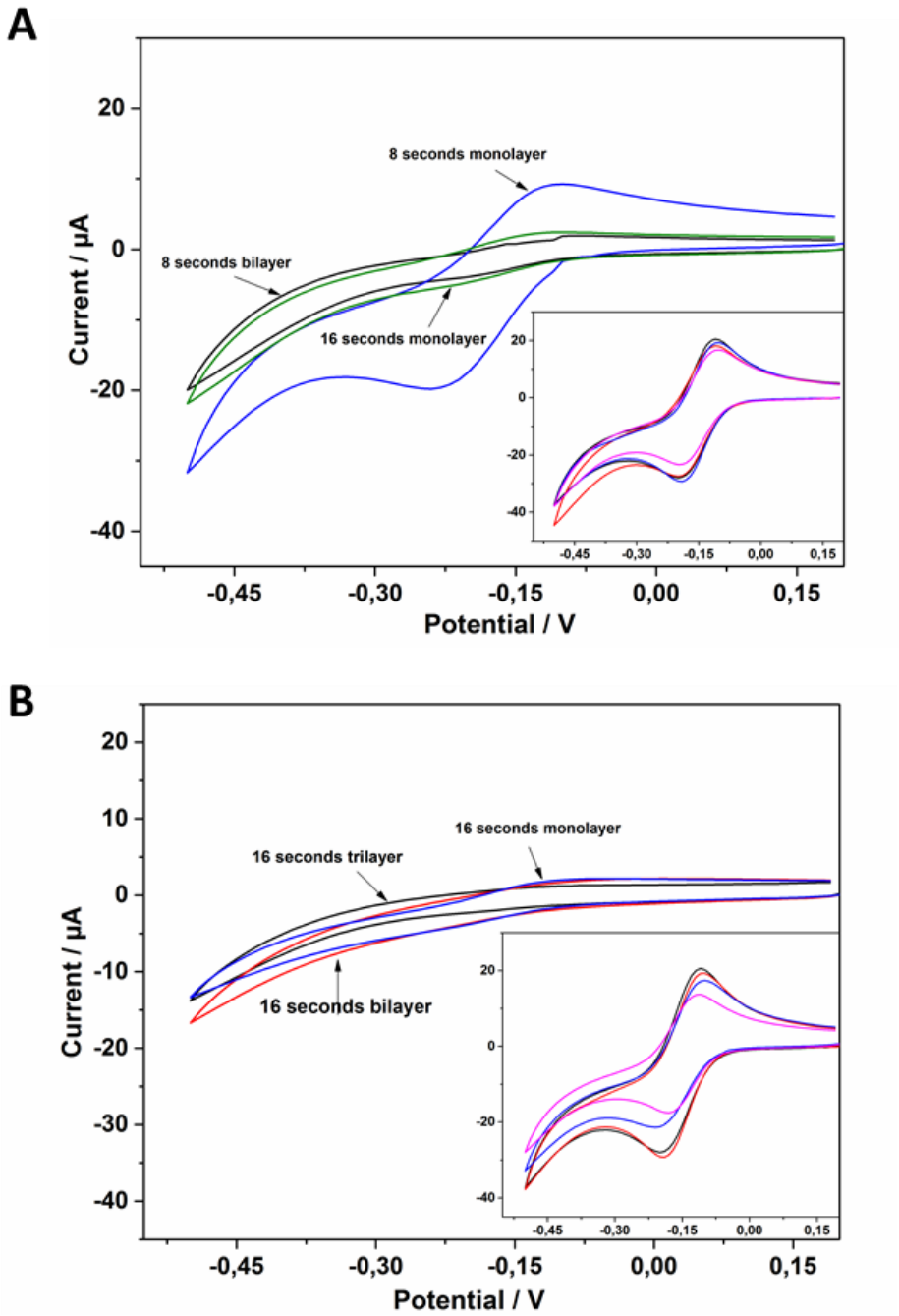

Figure V-8: Cyclic voltammetry of 0.5 mM $Ru(NH_3)_6Cl_3$ in 0.1 M KCl at (A) 8 seconds monolayer, 16 seconds monolayer and 8 seconds bilayer (B) 16 seconds monolayer, 16 seconds bilayer and 16 seconds trilayer film modified GCE before template extraction. Inset shows redox signal of 0.5 mM $Ru(NH_3)_6Cl_3$ at modified electrodes after template extraction. Scan rate = 100 mV s^{-1}.

5.3.2 Microscopic characterization of multi-layered silica film modification

Scanning electron micrscopic (SEM) Characterization of multi-layered silica thin films deposited at GCE was performed. SEM images (Figure V-9) were similar to the images

recorded in case of monolayer silica films. 8 seconds bilayer films were homogeneously deposited with minimal number of silica beads, 16 seconds bilayer films also showed unifom nature with slightly more silica beads as compared to 8 seconds bilayer, 16 seconds trilayer deposited film were thicker and had large amount of silica aggregates as compared to 16 seconds bilayer and 8 seconds bilayer films as well as 30 seconds monolayer. Large aggregates of silica at 16 seconds trilayer make these films unfit to use for electroanalytical applications as the motivation for depositing multi-layered films was to have films with lesser amount of silica beads.

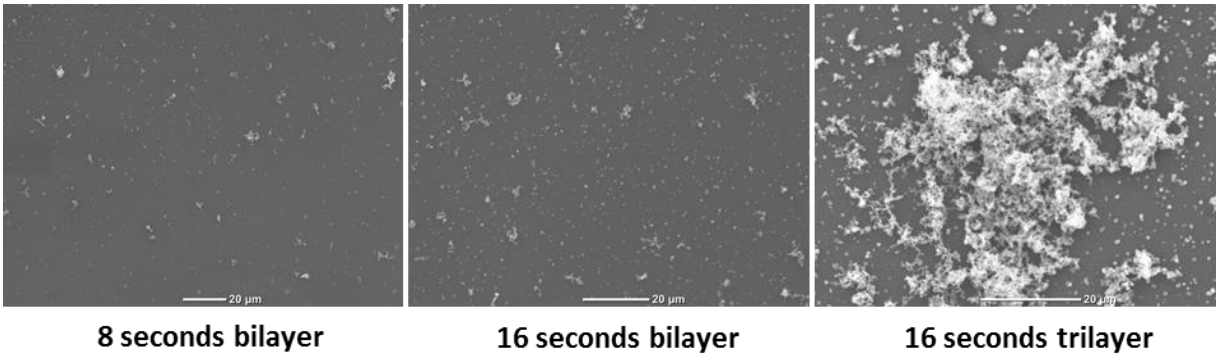

Figure V-9: Scanning electron micrscopic images of multilayer silica film for different deposition time.

5.3.3 Paraquat electrochemistry at multilayer silica thin films

Paraquat accumulation in silica films deposited for 8, 16 seconds monolayer, bilayer and 16 seconds trilayer was studied with the help of repetitive cyclic voltammetry for 100 scans. Accumulation of paraquat in these films by cyclic voltammetry is not very distinctive in case of 8, 16 seconds monolayer and 8 seconds bilayer (Figure V-10 A). Signal intensity was drastically increased in case of 16 seconds bilayer and trilayer film as compared to 16 seconds monolayer (Figure V-10 B). This behavior can be attributed to film thickness as thicker film can accommodate large amount of paraquat by cyclic voltammetry as compared to thinner film. Accumulation of paraquat in mono and bilayer films by cyclic voltammetry was lower though response with square wave voltammetry was quite high, whereas trilayer films showed greater response with cyclic voltammetry. In addition to film thickness presence of large number of silica beads can also contribute to higher signal by accumulating paraquat. As cyclic voltammetry is not a very sensitive technique for electroanalysis and hence it is not ideal for lower concentration detection and electrochemical sensing of pollutants in environmental samples. On the other hand square wave voltammetry is thought to be one the

most sensitive techniques available currently for electrochemical sensing of pollutants.[140,158,245,246]

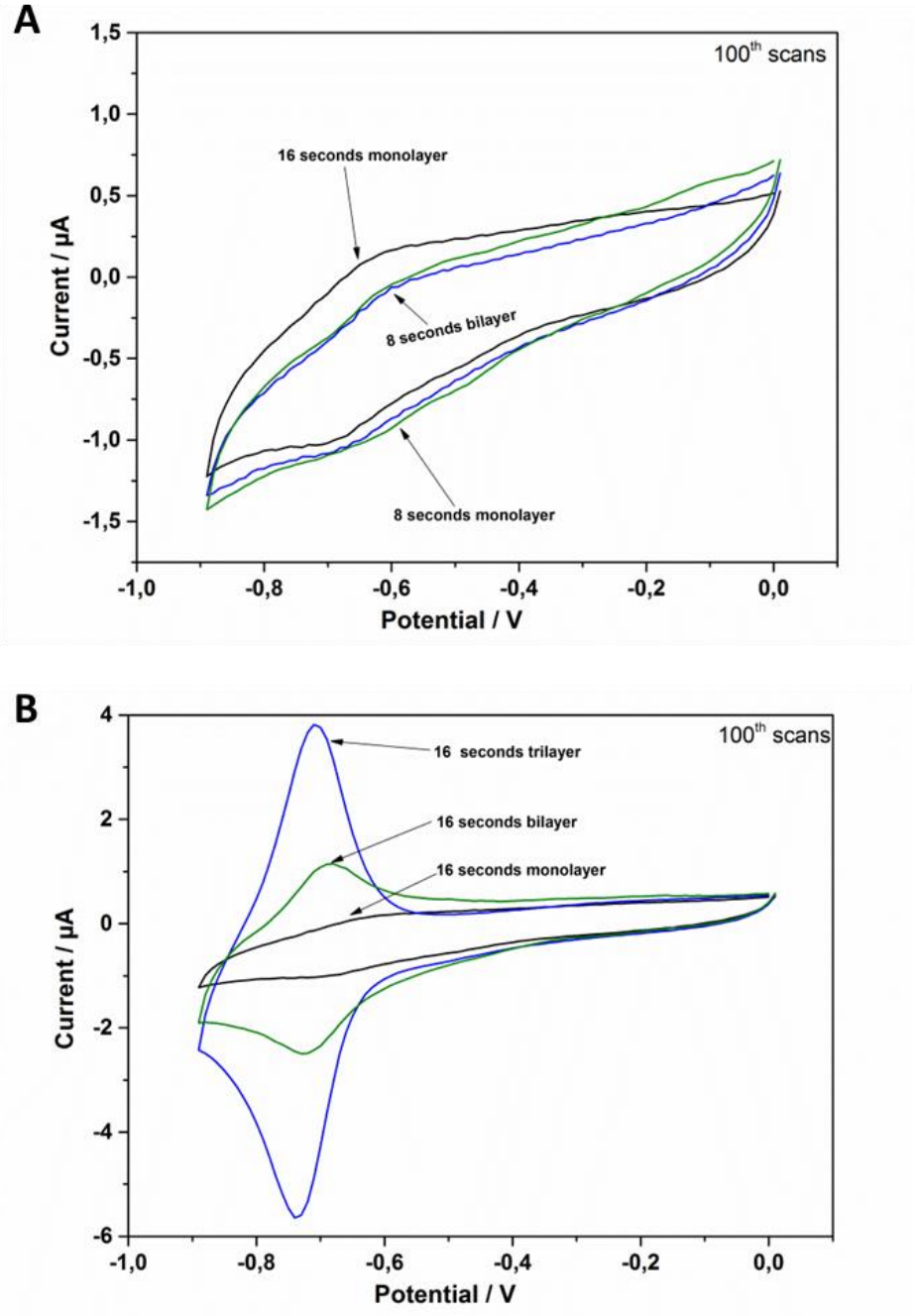

Figure V-10: Cyclic voltammograms of 5 µM paraquat in 70 mM $NaNO_3$ by repetitive cycling (100th scans) at GCE modified by silica thin film for deposition time (A) 8, 16 seconds monolayer and 8 seconds bilayer, (B) 16 seconds monolayer, 16 seconds bilayer and trilayer. Scan rate = 20 mV s^{-1}.

5.3.4 Paraquat detection on multilayer silica thin films

Square wave voltammetric response of 0.5-10 µM was studied on 8, 16 seconds monolayer and 8 seconds (Figure V-11) bilayer film deposited at GCEs. 8 seconds monolayer and 8 seconds bilayer modified GCE showed almost similar response and signal intensity (bilayer slightly higher). Higher response was recorded for 16 seconds monolayer although theoretically the 8 seconds bilayer deposition time is equal to 16 seconds monolayer but the response was not similar, suggesting that depositing multilayer films for shorter deposition time is not very effective for accumulation of paraquat in silica film. The idea to use 8 seconds multilayer was abandoned because to obtain suitable films for higher sensitivity we have to increase the number of layers more than or equal to 4 which may not be a suitable condition for vertical orientation of mesopores as vertical orientation of mesopores is very critical for efficient diffusion of analyte through film towards electrode surface. For this reason we decided to use 16 seconds multilayer films up to 3 layers to study the cyclic and square wave voltammetric response of paraquat.

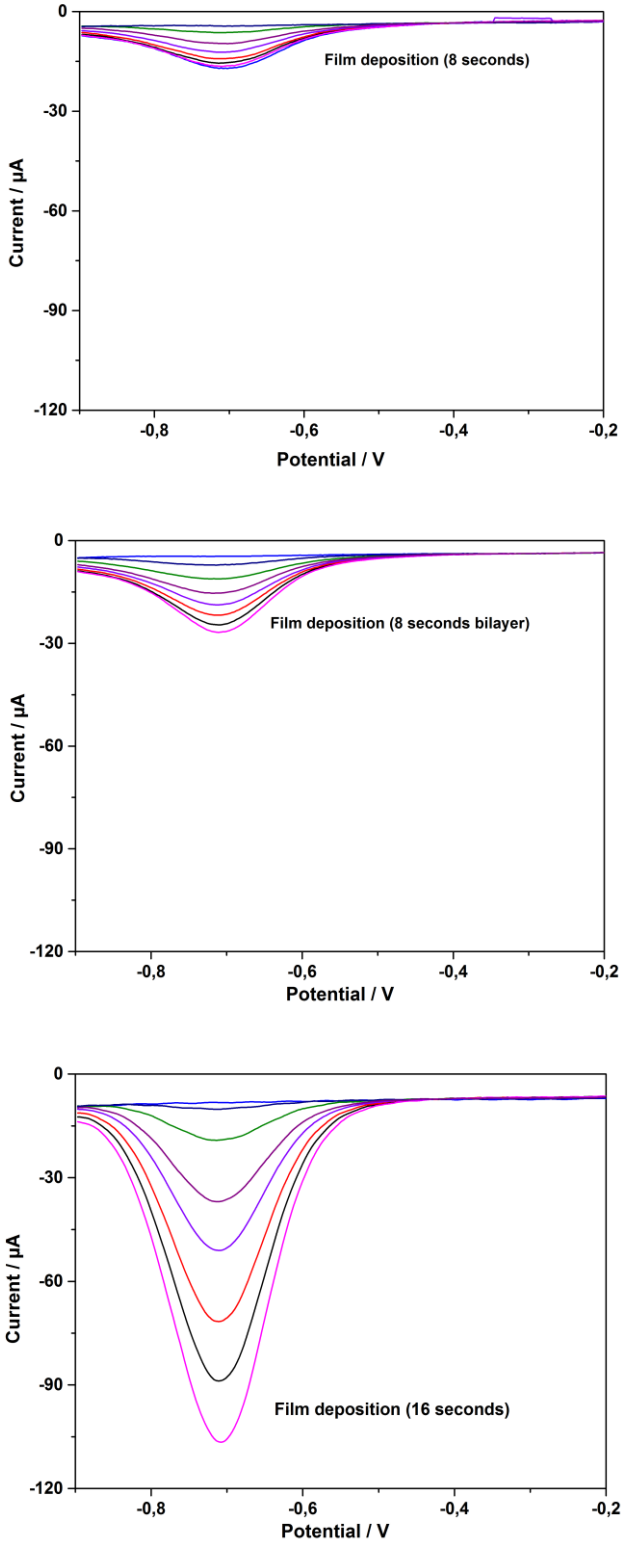

Figure V-11: Square wave voltammograms of 0.5-10 µM of paraquat in 70 mM $NaNO_3$ (pH 6) on 8, 16 seconds monolayer and 8 seconds bilayer film deposition.

Calibration curves obtained for 8, 16 seconds monolayer and 8 seconds (Figure V-12) bilayer are linear for increasing concentration of paraquat from 0.5-10 µM (N = 7) with R^2 values shown in table V-1 & 2.

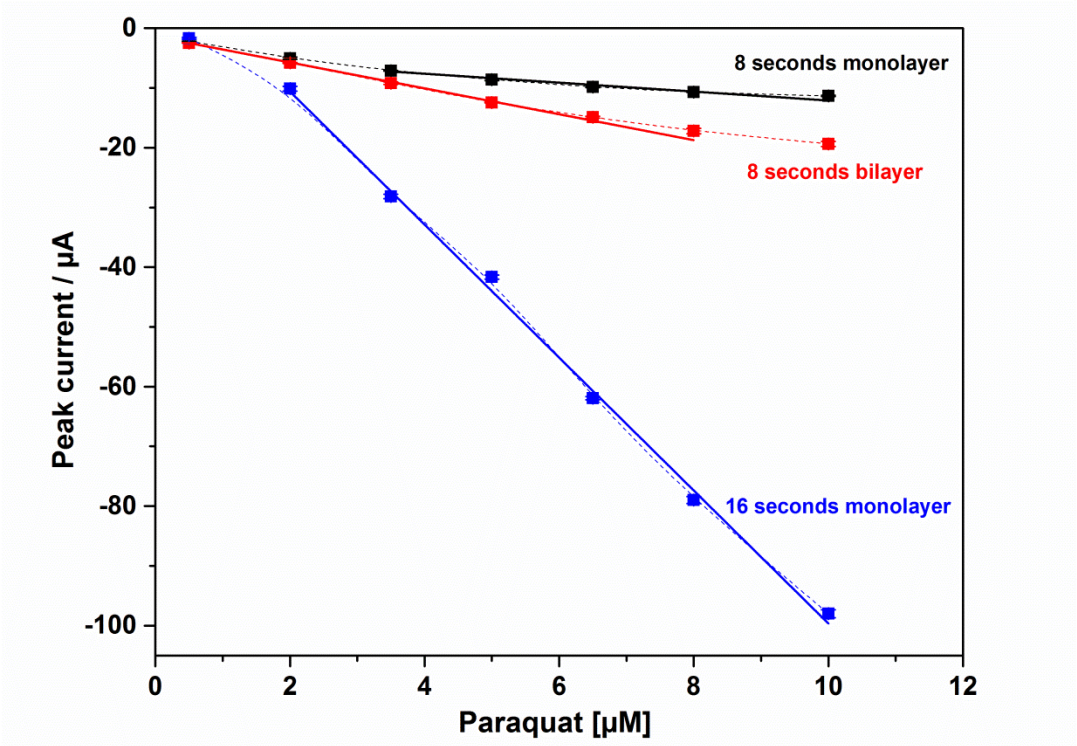

Figure V-12: Calibration curves of 8, 16 seconds monolayer and 8 seconds bilayer film deposition at GCE for 0.5-10 µM paraquat in 70 mM $NaNO_3$.

SWV response of 16 seconds monolayer, bilayer, and trilayer showed linear increase for 0.5-10 µM concentration of paraquat while for trilayer signal intensity decreased and was even lower than 16 seconds monolayer (Figure V-13). The possible explanation for this phenomenon can be limited diffusion of paraquat to electrode surface due to very thick film as we have already seen in CV experiments that trilayer films have highest response but in SWV as the time of analysis is shorter, limited diffusion results in low intensity signal . From these observations it can be said that it is not always true that the thicker film will ultimately give better response, the response by CV was better but by SWV it was decreased so one has to optimise the best suitable film thickness for favorable signal. 16 seconds bilayer response for both CV and SWV was similar to 30 seconds monolayer and as it is obvious that deposition time for 30 seconds monolayer and 16 seconds bilayer is almost equal so it can be concluded that 30 seconds monolayer or 16 seconds bilayer are the best and optimal deposition time for

better response and sensitivity of parquat sensing by square wave voltammetry at silica films modified GCE.

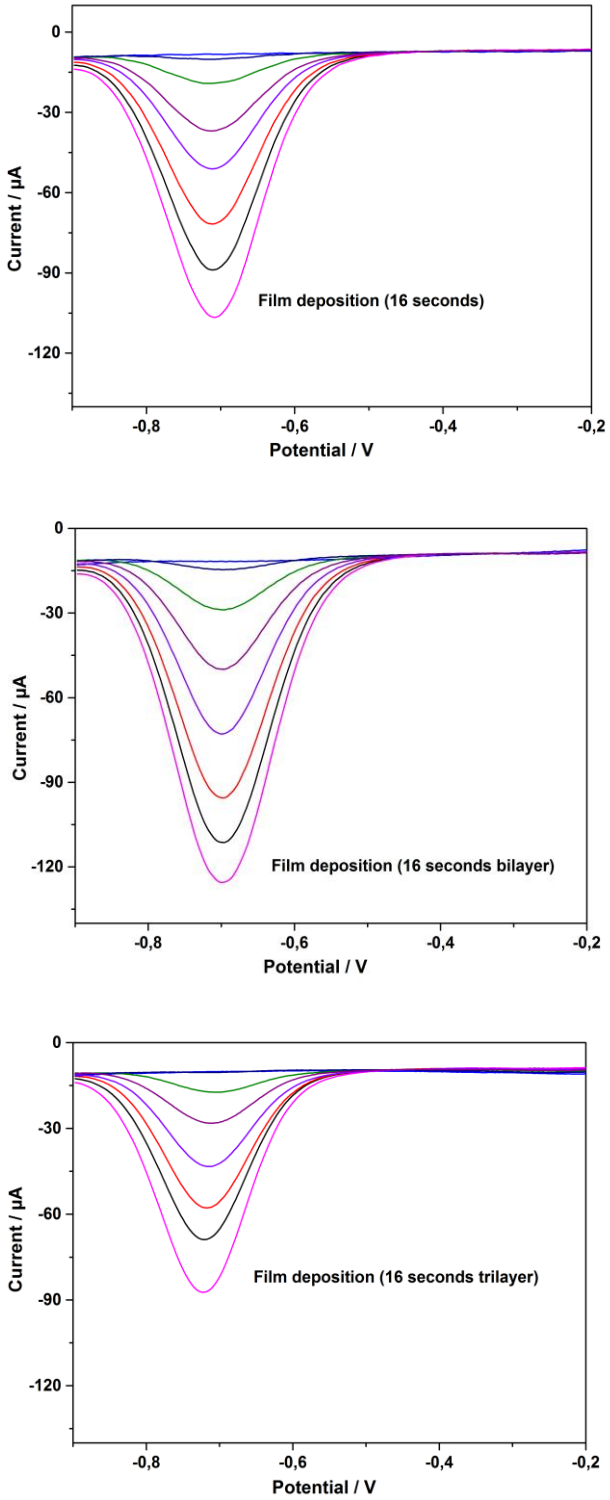

Figure V-13: Square wave voltammograms of 0.5-10 µM of paraquat in 70 mM $NaNO_3$ (pH 6) on 16 seconds monolayer, 16 seconds bilayer and trilayer film deposition.

In case of 8 seconds bilayer and 16 seconds trilayer films SWV response of paraquat was decreased (Figure V-11, 13). The higher cyclic voltammetric and lower square wave voltammetric response of paraquat at trilayer is due to thicker film matrix and time of analysis, as the film thickness and prolonged time of analysis contributes to higher cyclic voltammetric response, diffusion hindrance (due to thick film) and short time of scan can be the reason for decreased response by square wave voltammetry.

Calibration curves for 16 seconds monolayer and trilayer were linear (Figure V-14) with increasing concentration of paraquat between 0.5-10 µM (N = 7) and bilayer film calibration was similar to obtained for 30 seconds monolayer film (R^2 values shown in table V- 2). SWV experiments were repeated in all cases and results obtained were similar. Maximum signal response is observed for 16 seconds bilayer followed by 16 seconds monolayer and then 16 seconds trilayer.

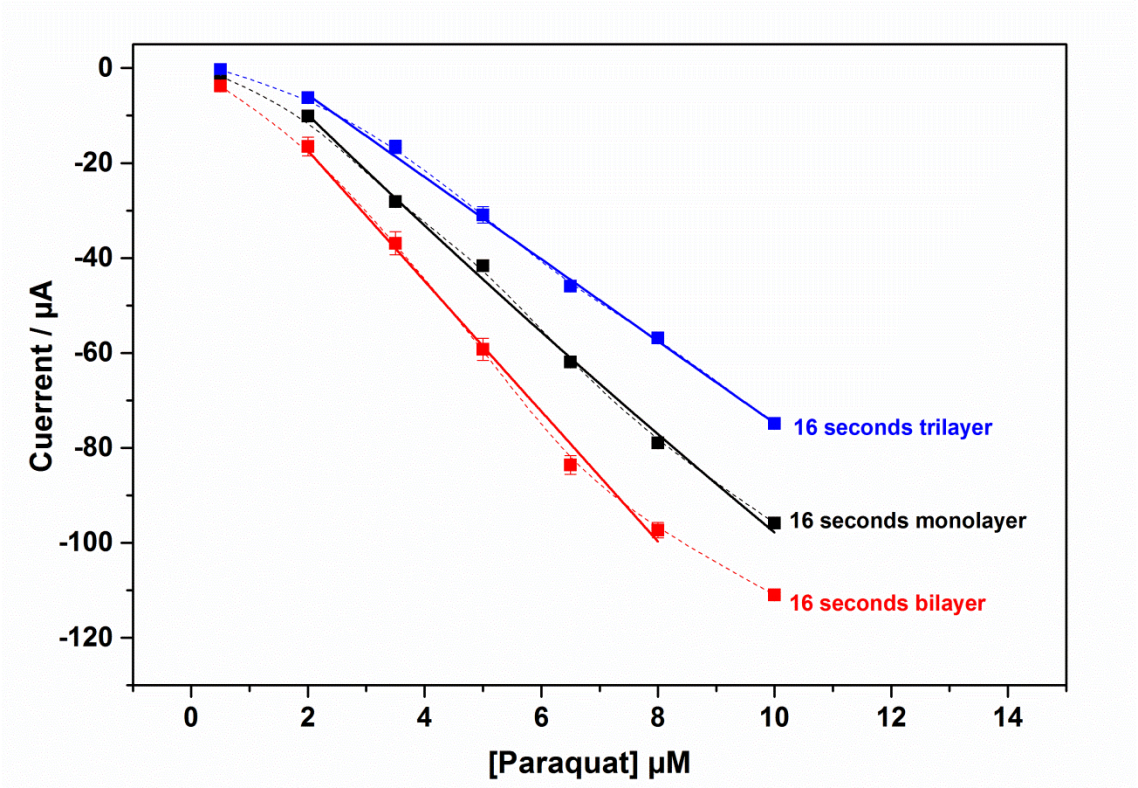

Figure V-14: Calibration curves by square wave voltammetry of 16 seconds monolayer, 16 seconds bilayer and trilayer silica film deposition, where not visible, error bars are smaller than points.

Table V-2: Slope, Intercept and R^2 values for multilayer silica film deposited for different deposition time at GCE

Film deposition time	Slope	Intercept	R^2
8 seconds bilayer	-2,128	-1,424	0,995
16 seconds monolayer	-11.294	12.376	0,996
16 seconds bilayer	-13.727	10.090	0,991
16 seconds trilayer	-8.646	11.654	0,999

5.3.5 Conclusion

Multi-layered deposition technique was used to produce several layers of silica film onto GCE with aim of further improving paraquat sensitivity and limit of detection. However, results obtained for SWV at these multi-layered modified electrodes did not show to improve the sensitivity rather trilayer films showed low response than monolayer and bilayer films. Cyclic voltammetry response recorded at thicker films was considerably high as compared to monolayer films which showed that accumulation was higher in thicker films but it requires long time as was the case in CV experiment. The lower SWV can be due to limited diffusion of analyte in multi-layered films. Further characterization of multi-layered is required by TEM, Grazing Incidence X-Ray Diffraction (GIXD) to verify the films thickness and vertical orientation.

In the next part of this chapter, we will discuss the effect of electrode size and geometry on paraquat detection. Third section of chapter is about fabrication, modification, characterization and ultimately detection of paraquat at these modified microelectrode arrays.

5.4 Microelectrode arrays fabrication and modification with silica thin films

Microelectrodes are electrodes which have at least one dimension smaller than the diffusion layer thickness of analytes.[247] The initial studies regarding microelectrodes and their application started in 1980's.[248] In the last part of this chapter, we fabricated microelectrode arrays modified with silica thin films and used for the detection of paraquat. Microelectrode arrays have recently gained importance in the field of electrochemical and environmental sensing due to favorable properties including steady state signal, lower Ohmic drop of potential, application in static solutions and lower concentration of supporting electrolytes required to carry out electroanalytical analysis.[249]

5.4.1 Microelectrode arrays fabrication

Microelectrode arrays at glassy carbon substrate were prepared by forming a layer of polyimide resist by spin coating and then second layer of photoresist followed by UV lithography to form the pores in approximate diameter of 20 µm. In the next step photoresist was stripped off and electrodes surface rinsed. This procedure was performed in clean room facility. These electrodes were cured for 30 minutes at high temperature (450°C Nabertherm p330) with T ramp of 5 °C for up and down under the flow of nitrogen in the oven for better attachment of polyimide membrane to the electrode surface (Figure V-12). Curing is very crucial step for better adhesion and reproducibility of these microelectrode arrays as in our experiments the uncured microelectrode arrays showed poor electrochemical response and stability. Uncured electrodes were also not able to stand the template extraction step as the polyimide layer withers away in acidic solution.

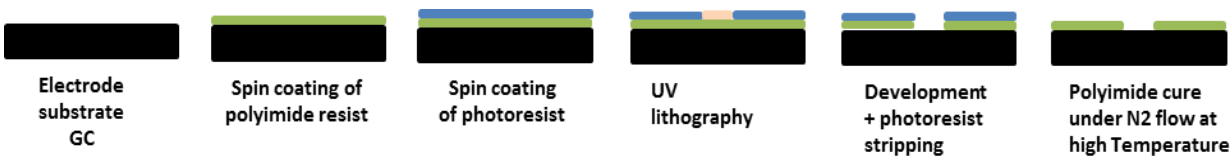

Figure V-15: Schematic representation of microelectrode arrays fabrication at glassy carbon substrate.

To calculate to number of microelectrodes fabricated at glassy carbon electrodes we can calculate the limiting current of individual microelectrode by using following equation:

$$I_{\text{lim}} = 4nFCDr$$

Where I_{lim} is the limiting current in case of µelectrodes, n is number of electrons transferred, C is concentration of redox probe; D is diffusion constant of redox probe and r is radius of single microelectrode. Calculated limiting current of each µelectrode is 2.83 nA, whereas limiting current measured by using cyclic voltammetry for electrochemically active area (which is 0.5 cm in diameter in our study) was found to be 3 µA (Figure V-18). If the total current (3 µA) obtained using electrochemically active area is divided by the current intensity calculated for individual microelectrode we get 1060 µelectrodes under electrochemically active area. Electrochemically active area of glassy carbon macroelectrode was found to be 0.19625 cm^2 calculated by following equation:

$$A = \pi r^2$$

We can also calculate the total number of µelectrodes / cm^2 by dividing the number of microelectrodes under electrochemically active area by value 0.19625. The number of µelectrodes calculated in this method was found to be ~5400 µelectrodes / cm^2 with diameter of 20 µm each.

5.4.2 Electrochemical characterization of microelectrode arrays

The diffusion of electroactive species at macroelectrodes is planar and results in peak shape voltammogram whereas in case of microelectrodes it is radial and diffusion layer is larger than the microelectrode radius hence sigmoidal voltammogram are obtained due to higher flux of electroactive species towards electrode surface.[250] Microelectrodes in contrast to macroelectrodes provide better signal to noise ratio due to efficient flux of analyte molecules towards their surface.[251] Electrochemical characterization of unmodified microelectrode arrays was done with 0.5 mM $Ru(NH_3)_6Cl_3$ in 0.1 M KCl at scan rate ranging from 1mV s^{-1} -1V s^{-1} (Figure V-16). Electrochemical Characterization of microelectrode arrays at different scan rates confirmed the linear behaviour i.e. increased limiting current with higher scan rate.

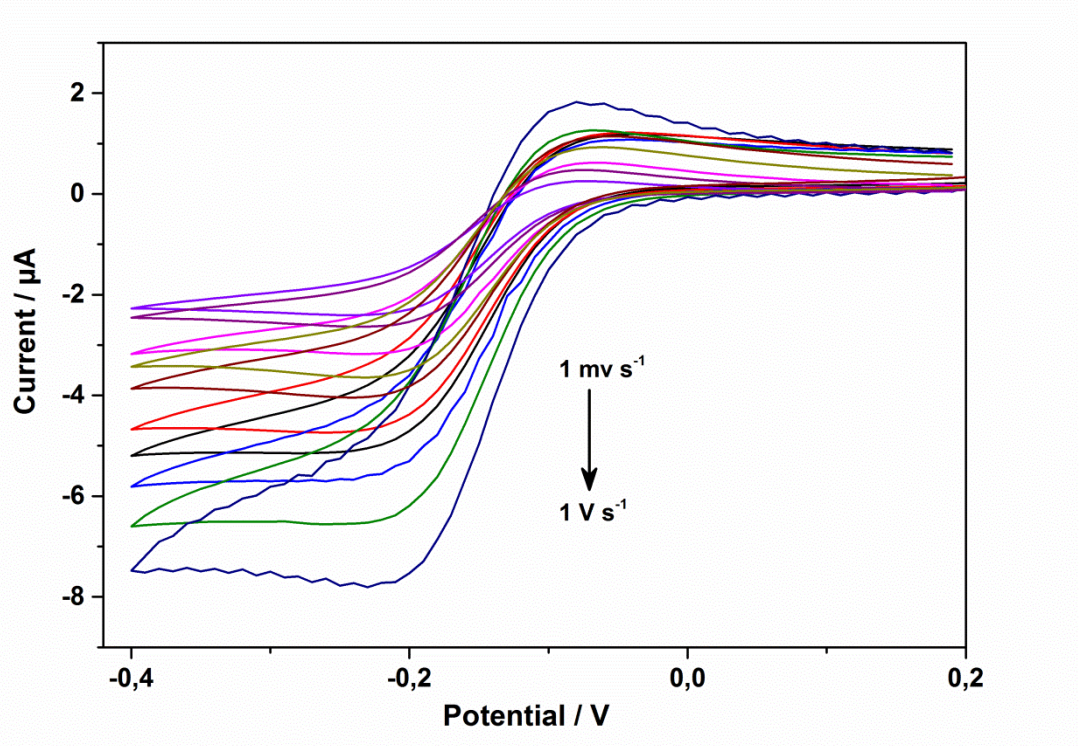

Figure V-16: Cyclic voltammetric characterization of microelectrode arrays by different scan rates (1 mV s^{-1} -1 V s^{-1})

5.4.3 Microelectrode arrays modification by silica thin films

Mesoporous silica thin films can be deposited with the help of EASA method at non-planar electrode electrodes with different size, shapes and composition[252] which is difficult to achieve by using other available methods for sol-gel based silica thin films. Mesoporous silica thin films can be electrochemically deposited by potentiostatic or galvanostatic methods, at carbon based electrodes potentiostatic deposition may result in hydrogen evolution due to water reduction as a result of potential applied (-2.2 V) which results in non-homogenous film deposition. This problem can be solved by depositing silica films with the help of galvanostatic procedure in which controlled current intensity is applied.[252] Microelectrode arrays were modified according to the procedure described in chapter III. 3-aminopropyltriethoxysilane (APTES) was electrografted on high temperature cured microelectrode arrays followed by silica thin film deposition for 20 seconds (optimized between 10-45 seconds) with the help of electro-assisted self-assembly process (Figure V-17). Modified microelectrode arrays were dried at 130 °C for at least 12 hours for better cross linking of silica film. A typical voltammogram and potential vs. deposition time graph

obtained as a result of APTES electrografting and galvanostatic deposition of mesoporous silica thin films at microelectrodes at glassy carbon substrate are shown in Figure V-17.

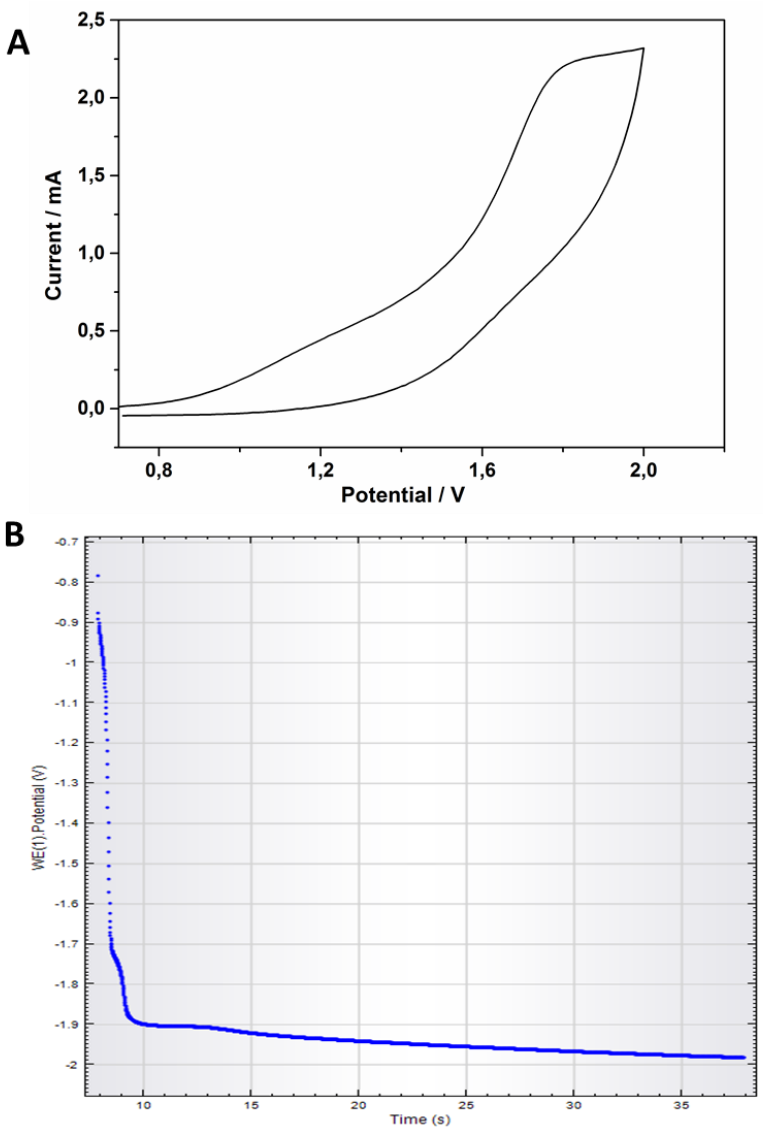

Figure V-17: (A) Cyclic voltammogram of 1 mM APTES dissolved in Acetonitrile and 0.1 M NBu_4BF_4 as electrolyte electrografted at microelectrode arrays on GCE substrate, scan rate = 500 mV s^{-1} (B) Variation of potential with time obtained for electrochemically assisted deposition of silica thin film at microelectrode arrays by galvanostatic method, (Current density = 3.71×10^{-4} A / cm^{-2}).

5.4.4 Electrochemical characterization of microelectrode arrays modification

Electrochemical characterization of bare and modified microelectrode arrays was performed by using 0.5 mM $Ru(NH_3)_6Cl_3$ redox probe, Characterization was performed

before and after each modification (Figure V-18) At bare microelectrode arrays redox signal is higher initially (solid line 1), after APTES electrografting redox signal is decreased (dashed line 2) which confirmed the presence of APTES at microelectrodes surface, after the silica film deposition (dotted line 3) redox activity is almost lost and after template extraction (dotted-dashed line 4) redox signal is back. Template extraction from mesopores was carried out in 0.1 M HCl in ethanol for 1 hour according to previously published procedure.[231] The intensity of electrochemical signal after template is lower than the un-modified microelectrode, similar response is observed in previous studies with modified microelectrodes where the redox signal is lowered at modified electrodes suggesting hindrance in diffusion through mesopores towards electrode surface.[252]

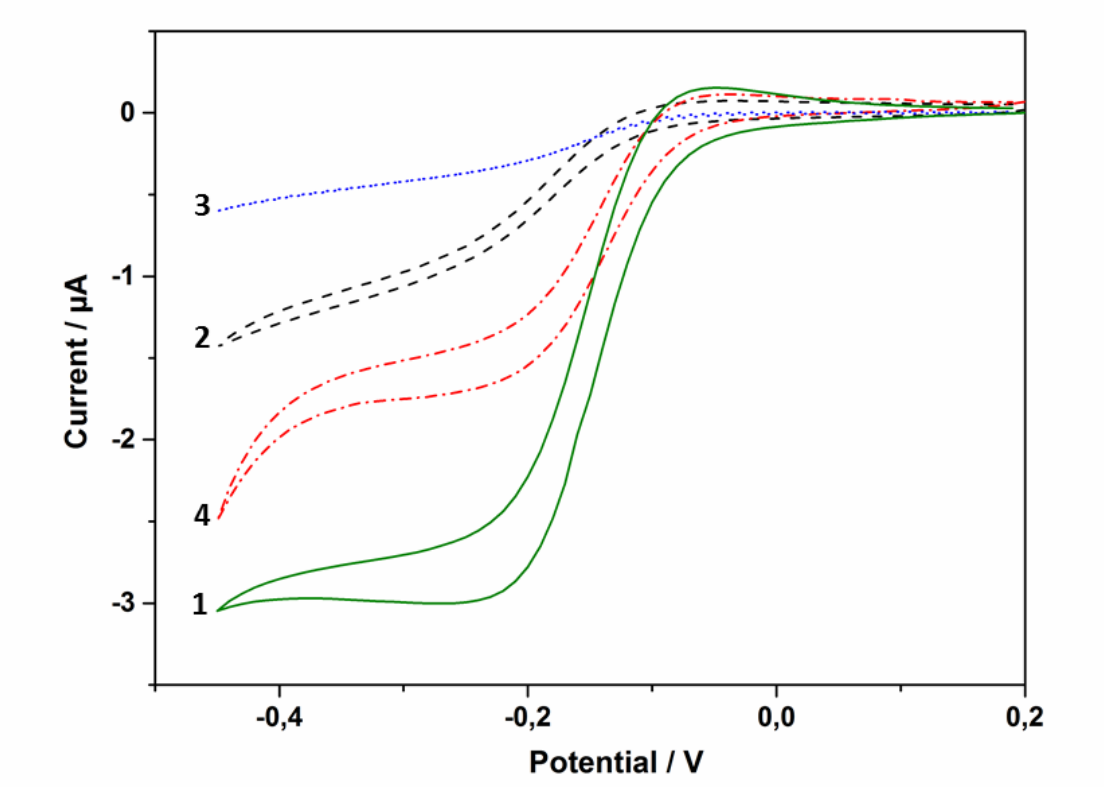

Figure V-18: Cyclic voltammetry of 0.5 mM $Ru(NH_3)_6Cl_3$ in 0.1 M KCl at microelectrode arrays, at (1) Bare, (2) APTES electrografted, (3) Surfactant-templated silica film, (4) After removal of template from mesopores, Scan rate = 5 mV s^{-1}.

5.4.5 Scanning electron microscopic characterization of microelectrode arrays modification

Scanning electron microscopic images obtained after the modification of microelectrode arrays confirmed the modification of individual pores. Clumps of silica beads

are visible at the edges and in the middle of pores. As suggested by previously conducted study when depositing silica thin films at microelectrodes formation of beads is un avoidable though a homogenous silica thin films with mesopores can be deposited underneath the beads which was confirmed by electron microscopy.[252]

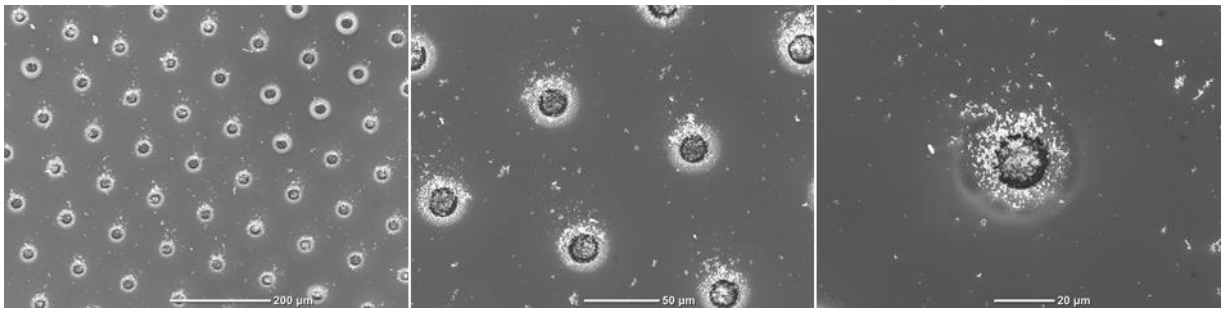

Figure V-19: Scanning electron microscopic images of mesoporous silica thin films modified microelectrode arrays fabricated at glassy carbon substrate at various magnifications.

5.4.6 Paraquat detection at silica thin films modified microelectrode arrays

Paraquat detection at silica film modified microelectrode arrays was carried out with the help of square wave voltammetry by using previously optimised parametrs in chapter IV. Microelectrodes carry the advantage of electroanalysis at lower concentrations of supporting electrolytes and hence can be used successfully electroanalytical applications for on-site and real sample analysis without need of sample pretreatments. 0.5-10 µM concentration of paraquat in 10 mM NaCl (pH 6) was studied at silica modified microelectrode arrays (Figure V-20 A) Square wave voltammetric response was linear with increasing concentration of analyte. The same concentration range of paraquat was also used to study its behaviour with square wave voltammetry at 5mM concentration of $NaNO_3$ (pH 6) as supporting electrolyte (figure V-20 B) because in previous experiments $NaNO_3$ was found to be best suitable electrolyte for sensitive detection of paraquat. Here also paraquat showed higher response in case of 5 mM $NaNO_3$ as compared to 10 mM NaCl so 5 mM concentration of $NaNO_3$ was selected as supporting electrolyte for microelectrode square wave voltammetry experiments.

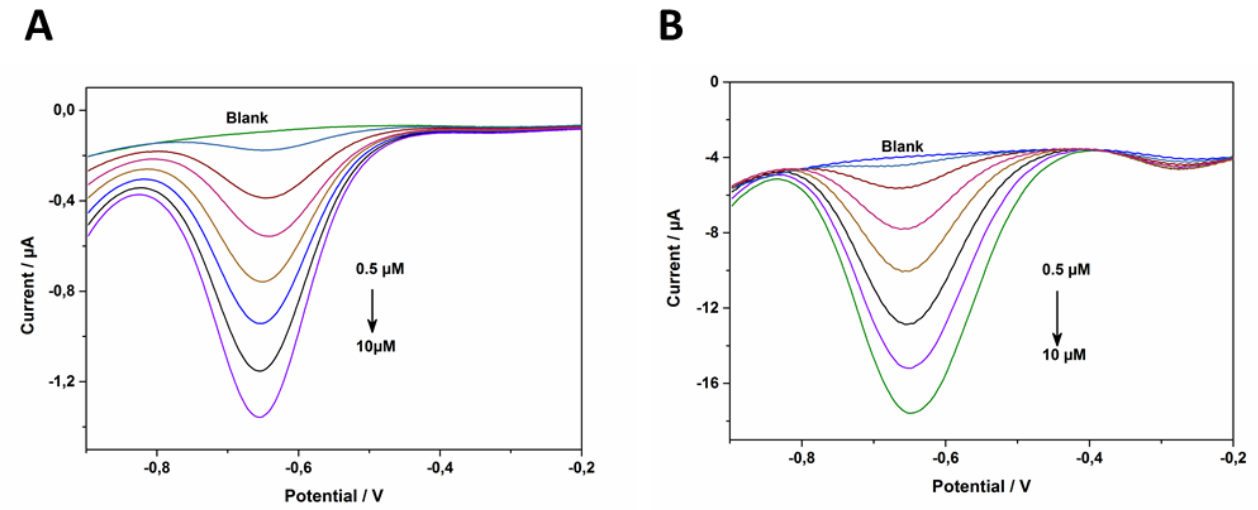

Figure V-20: Square wave voltammograms of 0.5-10 µM paraquat in (A) 10 mM NaCl, (B) 5 mM $NaNO_3$ as electrolyte at silica thin film modified microelectrode arrays.

The plot (figure V-21) shows the current density as a function of paraquat concentration obtained by square wave voltammetry at macroelectrodes and microelectrode arrays modified with silica thin films. It is clearly seen that current density achieved at microelectrode arrays as compared to macroelectrodes for same concentration of paraquat is much higher (1 order of magnitude) which results in improved sensitivity.

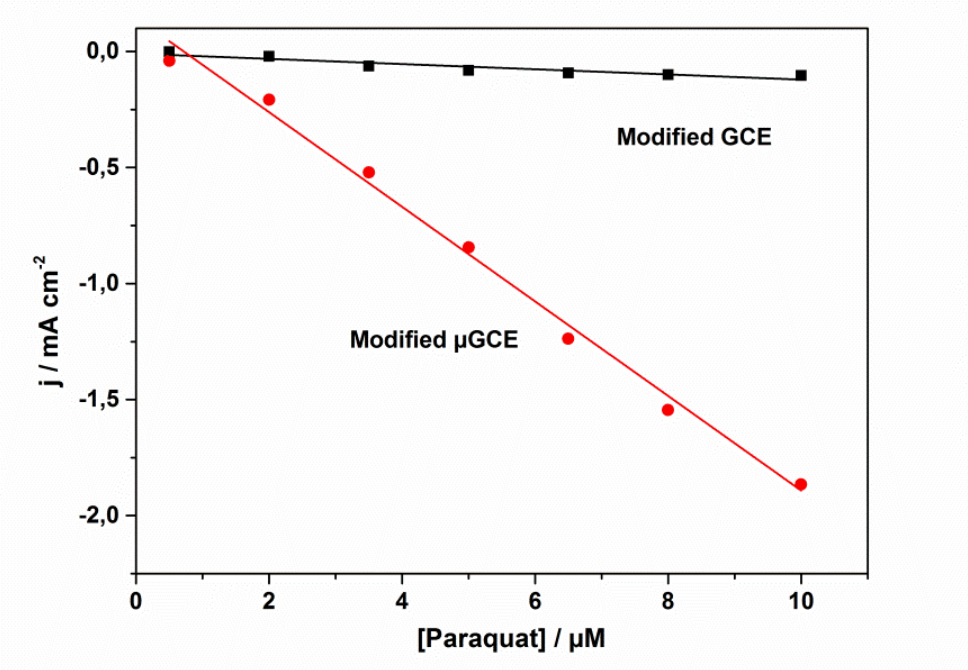

Figure V-21: Current density graph as a function of paraquat concentration (0.5-10 µM in $NaNO_3$) of silica film modified macroelectrode vs. microelectrode arrays.

Low concentration (50-500 nM) analysis of paraquat was performed at modified microelectrode arrays using optimized experimental conditions and supporting electrolyte concentration. These modified microelectrode arrays showed ability to detect and provide electrochemical signal of paraquat even at low concentration (50 nM). The square wave voltammetric response with increasing concentration was linear. Calibration curve was constructed (N = 6) which also showed good linearity and R^2 value of 0.996 (Figure V-22).

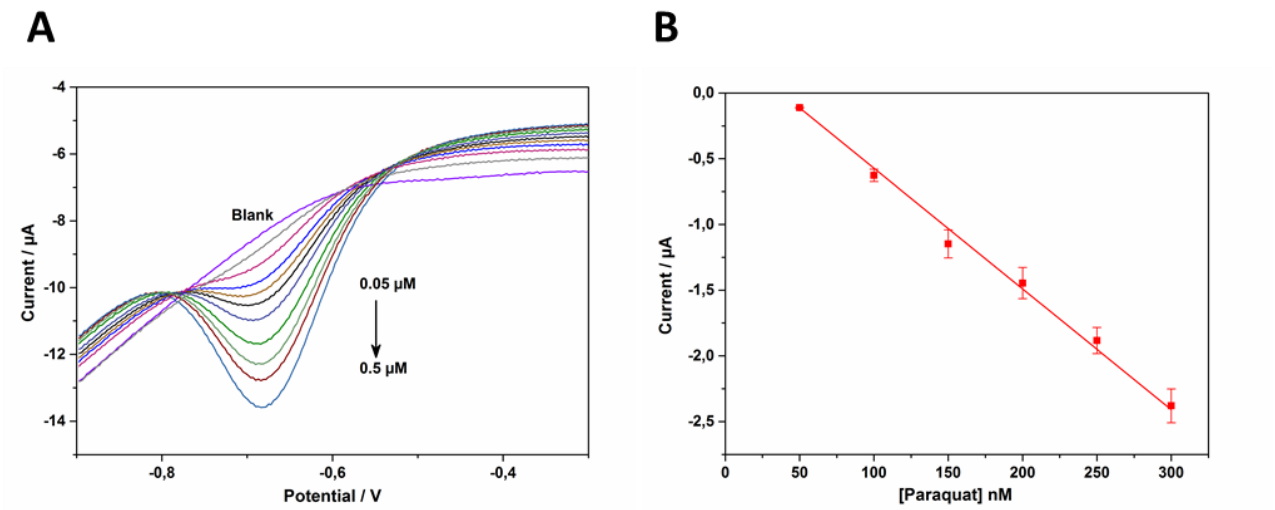

Figure V-22: Square wave voltammograms of (A) 50-500 nM of paraquat in 5 mM NaNO3 (pH 6) at modified microelectrode arrays, (B) Calibration curve of paraquat for 50-300 nM concentration.

From above results related to microelectrode arrays modified with silica thin films we can conclude that it is possible to modify the microelectrode arrays with mesoporous silica films by the help of EASA process. Modified electrodes showed promising results for sensitive detection of paraquat at very low electrolyte concentrations which can be helpful for real sample analysis without pretreatments required.

5.5 Conclusions

Mesoporous silica film thickness and electrode geometry play an important role in the detection of different paraquat, especially on its sensitivity. In the first part of this chapter film thickness was varied by forming monolayer silica films at GCE surfaces for various deposition times ranging from 5-30 seconds. Electrochemical and surface characterization confirmed the homogenous and uniform deposition of films for 16-30 seconds; and the most sensitive detection and accumulation of paraquat was observed at 30 seconds films as pointed out by square wave voltammetry (SWV) and cyclic voltammetry (CV). In a next step, multi-layered silica films were deposited by EASA method with intention of improved paraquat detection and sensitivity. SEM characterization revealed presence of large silica aggregates at surface of trilayer films; similar problem was faced in case of monolayer films deposited for too long time. 16 seconds bilayer and trilayer films were found to be a good compromise whereas the electrochemical response of paraquat with 8 seconds multi-layered deposition was poor. SWV response of paraquat was low on trilayer films even as compared to monolayers and bilayer films. CV response of bilayer and trilayer films with silica aggregates was found to be increased remarkably due to high capacity of these films for paraquat accumulation, but this require long preconcentration time. SWV response for these films was lower due to diffusion limitation as it is performed in limited time. Microelectrode arrays can contribute to sensitive and real time detection of target analytes due to their beneficial properties for electroanalysis. In the last part microelectrode arrays fabricated at GCE substrates were also modified by silica films using EASA method. SEM and electrochemical characterizations confirmed the modification of microelectrode arrays. These modified micro arrays showed promising results by providing high sensitivity for paraquat as compared to macroelectrodes at considerably low electrolyte concentrations.

Further investigations are required for microscopic characterizations of multi-layered films for thickness measurements and confirmation of vertical orientation of these layered films. For microelectrodes arrays, optimization of the best modification and detection conditions, parameters and subsequently use for paraquat detection as well as microscopic characterization (TEM, AFM) of modification is also required.

Chapter VI: Electrochemical Characterization and detection of isoproturon at mesoporous silica modified and unmodified glassy carbon electrodes

In this chapter, we studied in detail the electrochemical response of isoproturon at glassy carbon and indium tin oxide electrodes. Isoproturon is a herbicide commonly used for the control of weeds in different seasonal crops. It is toxic for human health and studies have shown isoproturon and its intermediates to be carcinogenic also. The use of isoproturon in most developing countries is unchecked, although it is banned recently in European Union. It is often detected in ground and surface waters at concentrations higher than permissible limit of 0.1 µg / L^{-1}. Cyclic voltammetry experiments showed formation of intermediate compunds as a result of irreversible oxidation of isoproturon. One among these intermediate compounds exhibited reversible behavior at lower potential value than that of isoproturon oxidation. The reversible peak of intermediate compounds was exploited for the detection of isoproturon by square wave voltammetry at bare and silica film modified glassy carbon electrodes.

6.1 Introduction

Isoproturon (3-(4-isopropylphenyl)-1, 1-dimethylurea) is a broad spectrum herbicide used to control the broad leaf weeds, especially in cereal crops. It is one among the family of phenylurea herbicides and used world-wide. By 2012, isoproturon was the most used herbicide in France for the crops of wheat and barley. It has been banned in European Union since 2016 due to its tendency of disrupt the endocrine system.[117] Isoproturon is water soluble with half-life up to 1 year in groundwater and up to 40 days in surface water. It can be degraded to some extent by photochemical reactions and microbial enzymes into other metabolites.[118,253] Isoproturon and its intermediate compounds can be carcinogenic and can cause health problems to humans and other living organisms.[119,254] It is absorbed very rapidly through oral route causing mild to acute toxicity and classified in class II level of toxicity by World Health Organisation (WHO) with LD_{50} of 1.8 g / kg.[255] It can leach through the soil to reach the aquatic systems. It is often detected in rivers and streams in different countries.[256,257]

Little attention has been paid to the electrochemical detection of isoproturon, there are few reports in literature discussing its detection with systems ranging from voltammetric techniques, molecularly imprinted based luminescent sensing, and at modified electrodes. These studies were based on electrochemical detection of isoproturon by taking into account the irreversible oxidation of the compound which takes place around +1V and using acidic media with pH 1.[162–164,167] Studies have shown that isoproturon undergo electrochemical oxidation and as a result two intermediate compounds are formed namely 4-isopropylaniline and dimethyl amine.[163,258] 4-isopropylaniline being electroactive shows redox activity at potential range much lower (~ +0.4 V at GCE) than isoproturon oxidation. Characterization and electrochemical behavior analysis of electroactive intermediate compound can be helpful for sensitive analytical detection of isoproturon.

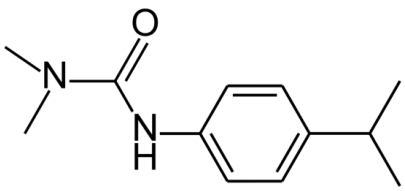

Isoproturon

Scheme VI-1: Structure of isoproturon.

In this chapter, we studied the electrochemical behavior of isoproturon at glassy carbon electrodes (GCE) and indium tin oxide (ITO) electrodes. GCE was selected for futher use due to its stable and more sensitive behavior at wide pH range. Cyclic voltammetric Characterization of isoproturon was performed in detail at different scan rates, solution pH and supporting electrolytes. Finally, isoproturon was determined at unmodified and silica modified GCE with the help of square wave voltammetry.

6.2 Results and discussion

6.2.1 Cyclic voltammetric Characterization of isoproturon

Electrochemical behavior of isoproturon was studied by cyclic voltammetry (CV) at ITO and GCE, ClO_4^- was used as supporting electrolyte anion. CV studies were perfomed at pH range of 0 - 7.0, CV comparison of ITO and GCE showed the latter to be a more promising electrode material for the electrochemical studies of isoproturon. Electrochemical response of isoproturon was observed at ITO electrodes with solution pH 0 and this reponse was lower than at GCE (Figure VI-1 A-C**)**. Cyclic voltammetric response of isoproturon was found to be better at GCE from acidic towards neutral solution, peak intensity was higher for acidic media as compared to neutral. CV scan showed well defined irreversible oxidation reaction for isoproturon at +1 V (pH 0) and +0.93, +0.88 V for pH 4 and 6 respectively at GCE. Whereas at ITO electrodes oxidation potential of isoproturon was at higher potential around +1.46 V (pH 0) and at pH higher than 2 electrochemical activity was not observed. This shows oxidation of isoproturon at GCE and higher pH is easier as compared to ITO electrodes. In addition to oxidation peak I around +1 V, at GCE a less well-defined peak II was also observed around +0.4 V (Figure VI-1). Previous studies have also reported the emergance of peak II as a result of peak I oxidation,[164,258] in those studies researchers usually emphasized on isoproturon detection using peak I solely and did not considered peak II which can be of importance when detecting isoproturon electrochemically. As reversible systems provide more sensitive determination and higher current intensities with the help of square wave voltammetry (SWV). Peak II can be due to the formation of intermediate compounds formed after the oxidation of isoproturon at +1 V which is reported already.[258] We intend to Characterize the peak II and exploit it for the detection of isoproturon using SWV.

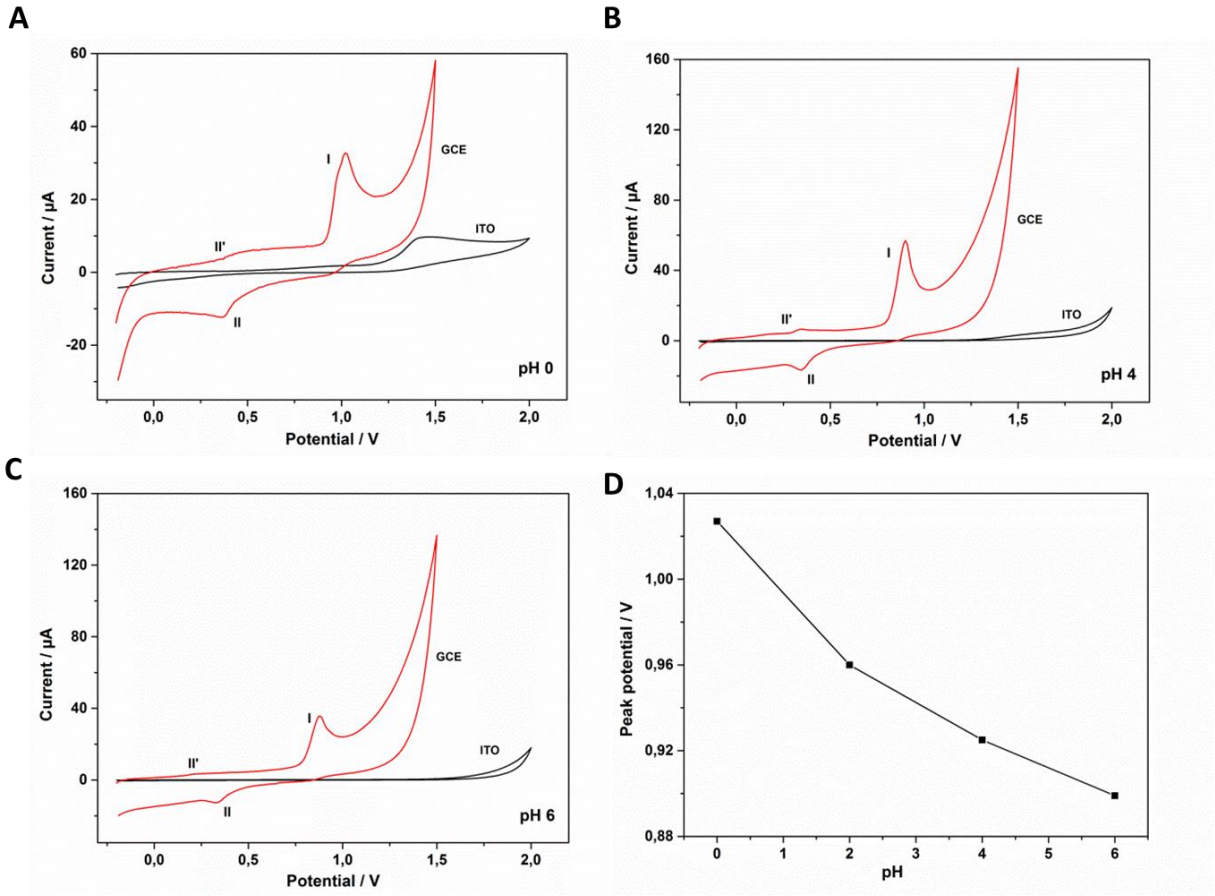

Figure VI-1: Cyclic voltammograms of 100 µM isoproturon at bare GCE and ITO electrodes (A) 1M $HClO_4$ (pH 0), (B and C) 0.1 M $NaClO_4$ (pH 4 and 6), (D) Graph for peak height vs. different pH, scan rate = 50 mV s^{-1}.

To further investigate the peak II formation mechanism, the influence of applied potential was studied. As suggested previously applied potential has critical effect on the formation of intermediate compounds as a result of isoproturon oxidation.[258] CV scans were recorded at potential ranges of -0.2 to +1.2 V and -0.2 to +1.5V. These experiments confirmed that it is important to carefully select the potential window for formation of intermediates due to oxidative cleavage of isoproturon, as in case of black and red curves in figure VI - 2 have the same starting potential value but the end potential is different. Peak II was not observed when the end potential was +1.2 V while at +1.5 V peak II around +0.4 V appeared.

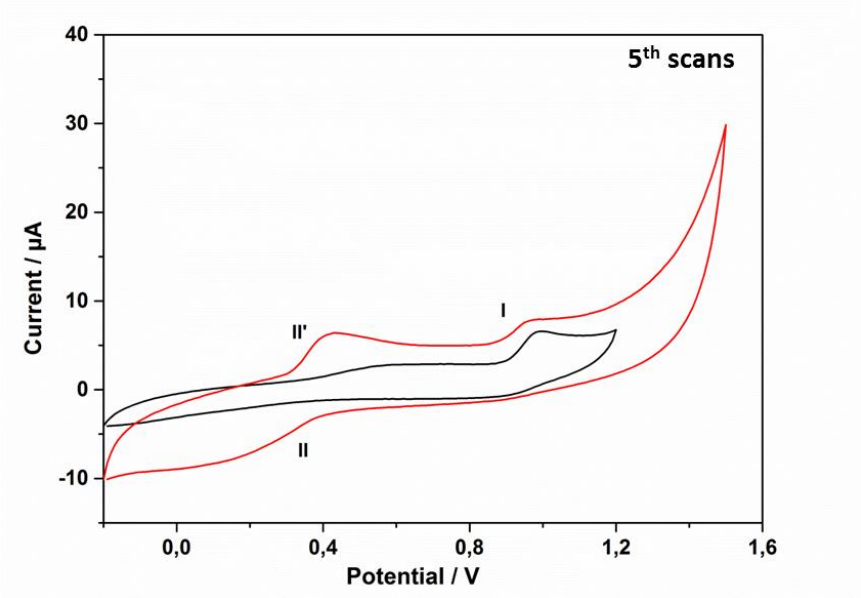

Figure VI-2: Cyclic voltammograms of 100 µM isoproturon in 0.1 M $NaClO_4$ (pH 6) by repetitive cycling (5^{th} scans) scan direction -0.2 to +1.5 V, scan rate = 50 mV s^{-1}.

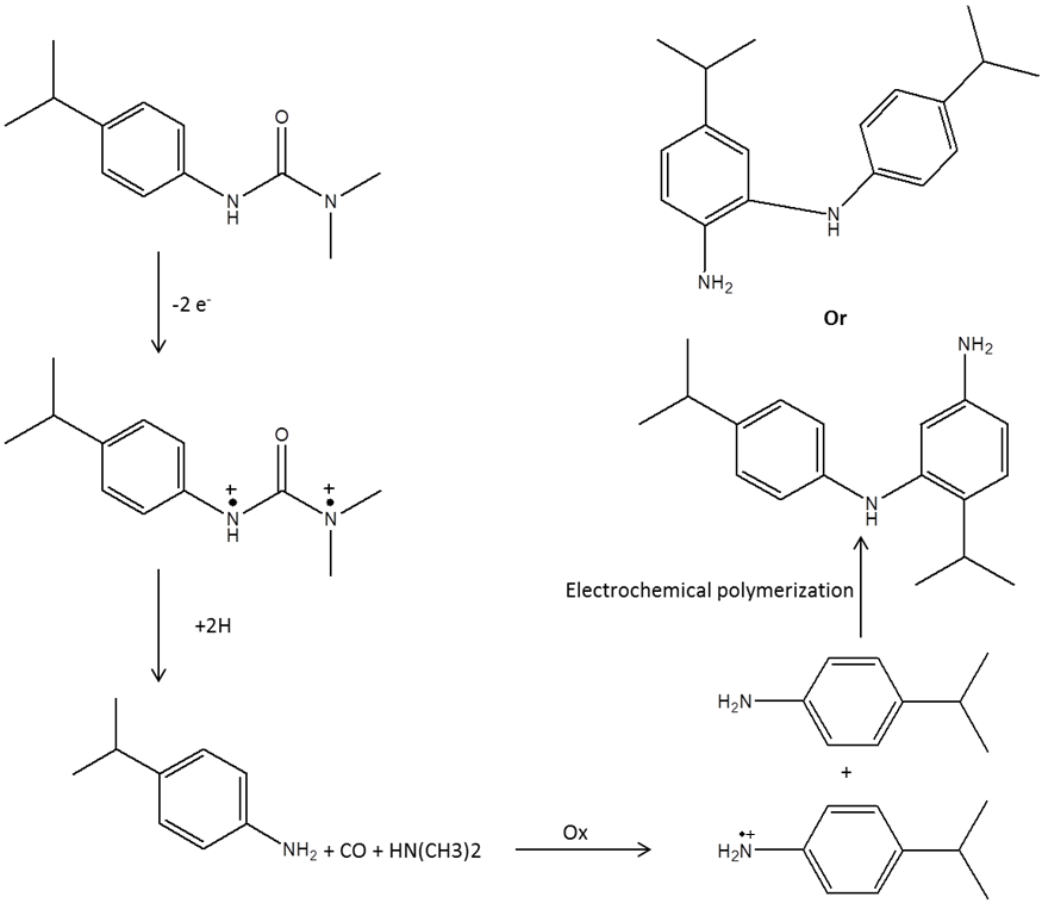

Scheme VI-2: Proposed oxidation mechanism of isoproturon (Adapted from[258]) and electrochemical polymerization of poly (isopropylaniline).

Formation of intermediate compounds as a result of isoproturon oxidation was confirmed by control experiments. Figure VI-3 A shows the multiple CV scans of 0.1 M $NaClO_4$ (pH 6) at bare glassy carbon electrode, no peak is observed in the potential range of -0.2 to +1.5 V as it is obvious in case of presence of isoproturon in the solution which proves that peak II does not arise due to electrolyte ions adsorption. Cyclic voltammetry of 100 µM isoproturon is shown in Figure VI-3 B at potential range of +0 to +0.7 V, as the potential applied is insufficient to oxidize the isoproturon which takes place at +0.88 V (pH 6). Peak II also does not appear which further strengthens the hypothesis of peak II generation as a result of peak I or isoproturon oxidation. In Figure VI-3 C we can see multiple scans conducted as control experiment after oxidizing the isoproturon at electrode surface by applying potential of +1.5 V. The ΔE values for peaks arising as a result of isoproturon oxidation were found to be 57 mV which suggest that it is reversible process and formation of 4-isopropylaniline is a well-defined electrochemical reaction.

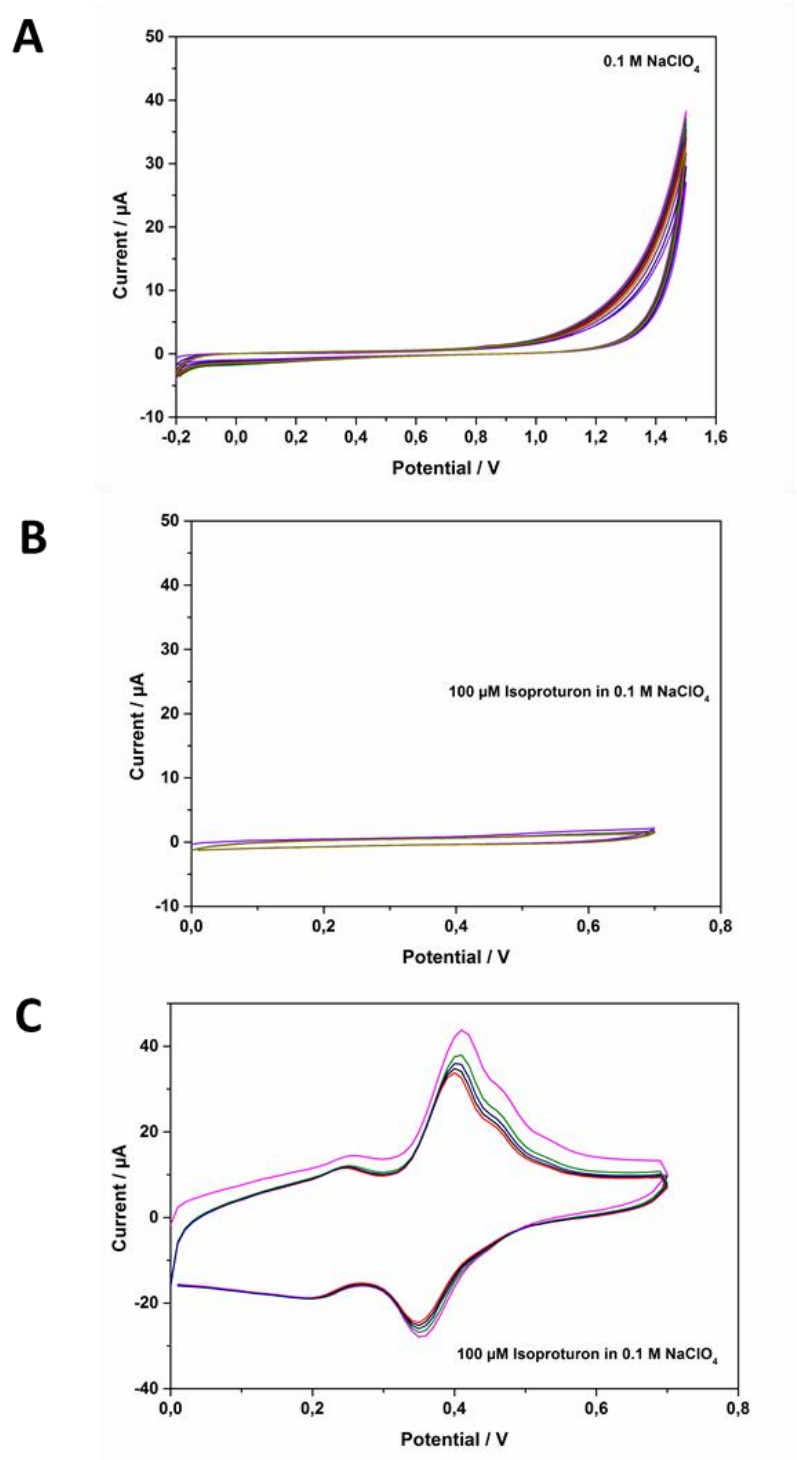

Figure VI-3: Cyclic voltammograms of (A) 0.1 M $NaClO_4$; 100 µM isoproturon in 0.1 M $NaClO_4$, CV multiple scans between 0 and +0.7 V (B) Without applying potential (C) After applying a potential of +1.5V, pH 6, scan rate = 50 mV s^{-1}.

A possible explanation for need of higher potential than isoproturon oxidation can be, that it is required for the electrochemical polymerization of 4-isopropylaniline (formed as a

result of oxidative cleavage of isoproturon) which then forms an electroactive film responsible for redox behavior. Electrochemical polymerization of 2-isopropylaniline showed similar electrochemical behavior as observed here.[259] Different mechanisms for oxidative polymerization of isopropylaniline are possible[260], electrochemical polymerization of aniline is proved to be favorable as it produces polyaniline of high purity and controlled formation of electroactive thin films is possible.[261–263] Electroactive nature of polyaniline is as a result of doping process in which protonic acid or oxidative doping of emeraldine base results in formation of emeraldine salt and subsequently leucoemeraldine base. This process also requires the exchange of anions. Dedoping process is the opposite of doping in which strong alkali or reduction of emeraldine salt to leucoemeraldine is possible. Leucoemeraldine is fully reduced form of polyaniline whereas emeraldine refers to half oxidized form.[264] The reversible peaks at + 0.41 V and +0.36 V seen in Figure VI-3 C corresponds to oxidative doping and dedoping process of poly (isopropylaniline).

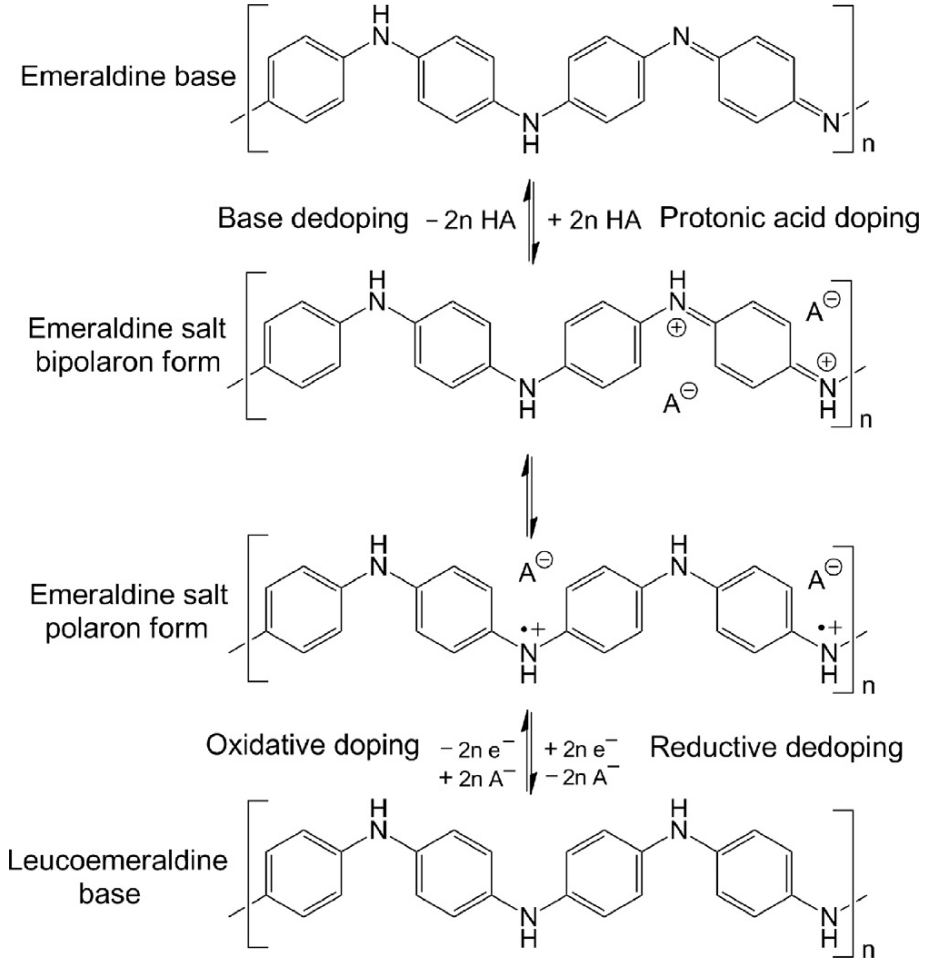

Scheme VI-3: Doping and dedoping of different oxidation states of polyaniline.[263]

6.2.2 Scan rate studies of isoproturon

Cyclic voltammetry characterization of isoproturon was also performed by varying the scan rate from 1 mV s^{-1} - 1 V s^{-1}. Peak I showed diffusion controlled behavior as peak current increased linearly with square root of scan rate. Peak II arose as a result of irreversible oxidation of isoproturon; peak II was not evident in first few scan rates so the reversible response of second peak was recorded from 20 mV s^{-1} - 1 V s^{-1} (Figure VI-4). In this range of scan rate oxidation and reduction reactions of peak II were linear with increasing square root of scan rate which confirmed the diffusion controlled behavior of peak II as well. R2 values for peak I, II and II' were 0.993, 0.996 and 0.999 respectively.

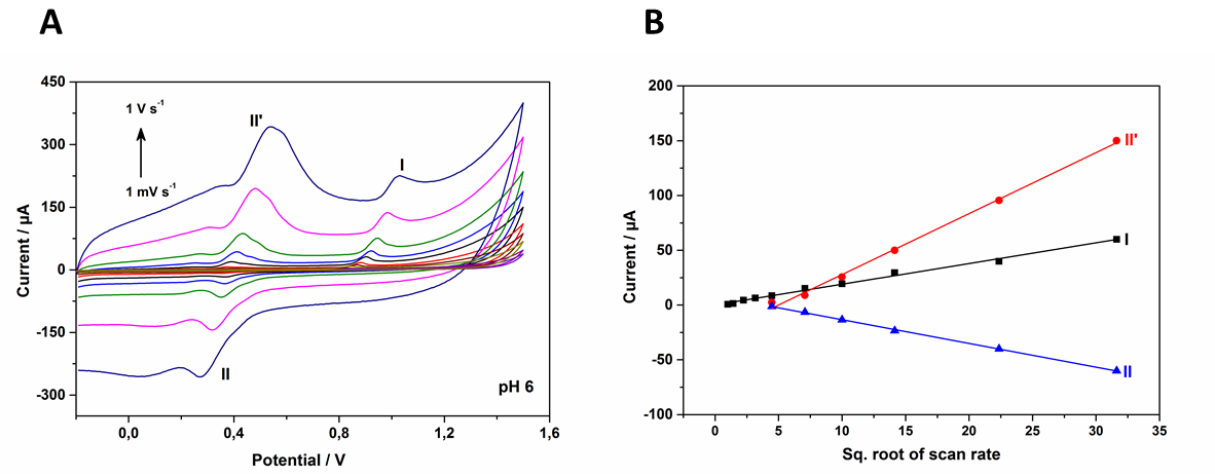

Figure VI-4: Cyclic voltammetry of (A) 100 µM isoproturon in 0.1 M $NaClO_4$, scan rate = 1 mV s^{-1} - 1 V $s^{-1}$and pH 6. (B) Graph of peak height as a function of square root of scan rate for peak I and peak II, II'.

6.2.3 Effect of repetitive scans at peak intensity

Repetitive CV scan were conducted to assess the behavior of both peaks in response to multiple cycling at bare GCE. 100 scans by continuous cyclic voltammetry of 100 µM in 0.1 M $NaClO_4$ were recorded, peak I behavior was not constant, as in first scan intensity was highest and decreased with every scan but after 70 cycles it showed increased intensity, the peak I intensity during repetitive scans was recorded to be highest at 1st scan. On the other hand, constant behavior was observed in case of Peak II where peak intensity of redox reaction increased linearly with increasing number of multiple scans (Figure VI-5).

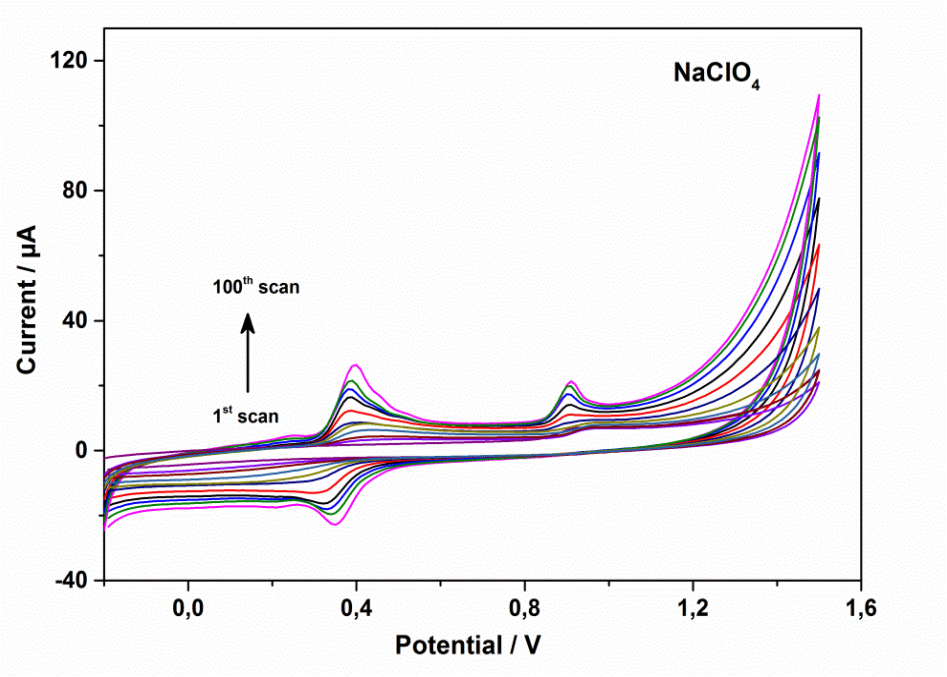

Figure VI-5: Cyclic voltammetry of 100 µM isoproturon in 0.1 M $NaClO_4$ by repetitive cycling (100 scans), scan rate = 100 mV s^{-1} and pH 6.

6.2.4 Effect of supporting electrolyte on electrochemical behavior of isoproturon

The effect of different supporting electrolyte solutions on the peak intensity of isoproturon was studied by repetitive CV scans (100 cycles). 100 µM isoproturon in 0.1 M concentration of NaCl, Na_2SO_4 and $NaNO_3$ was used (Figure VI-6). In the case of NaCl; the response of both peak I and peak II was not well defined, in addition to these peak another reduction peak was observed around +0.85 V which could be some interference from the electrolyte ions as the oxidation of isoproturon is irreversible and the reduction peak at +0.85 V is possibly not associated with isoproturon or intermediates formed due to its oxidation. For Na_2SO_4, the response was similar to $NaClO_4$ whereas the peak I response was more constant i.e. it decreased with each cycle after 1st cycle up to 100 cycles and peak II showed constant behavior. Isoproturon showed better cyclic voltammetric response with $NaNO_3$ among all other supporting electrolytes used. Peak I intensity was high in first cycle and it decreased considerably afterwards whereas peak II intensity was recorded to be highest in case of $NaNO_3$. Oxidation peak II' values of 100 µM isoproturon for 100th cycle for $NaClO_4$, Na_2SO_4 and $NaNO_3$ were found to be 20, 23.6 and 28 µA respectively whereas reduction (peak)

values were -11, -12 and -14 µA in the same order. In addition to peak II a shoulder peak was also observed at +0.26 V also exhibiting reversible nature though smaller in intensity, this shoulder peak is more prominent in case of $NaNO_3$ as compared to Na2SO4 and NaClO4, and it could also be termed as electrochemical polymerization of isopropylaniline in some other form. Based on CV characterization it can be said that the number of intermediate compounds formed as a result of isoproturon oxidation are most probably two as suggested already. $NaNO_3$ was selected as supporting electrolyte for SWV experiments as peak II intensity was recorded to be highest with it.

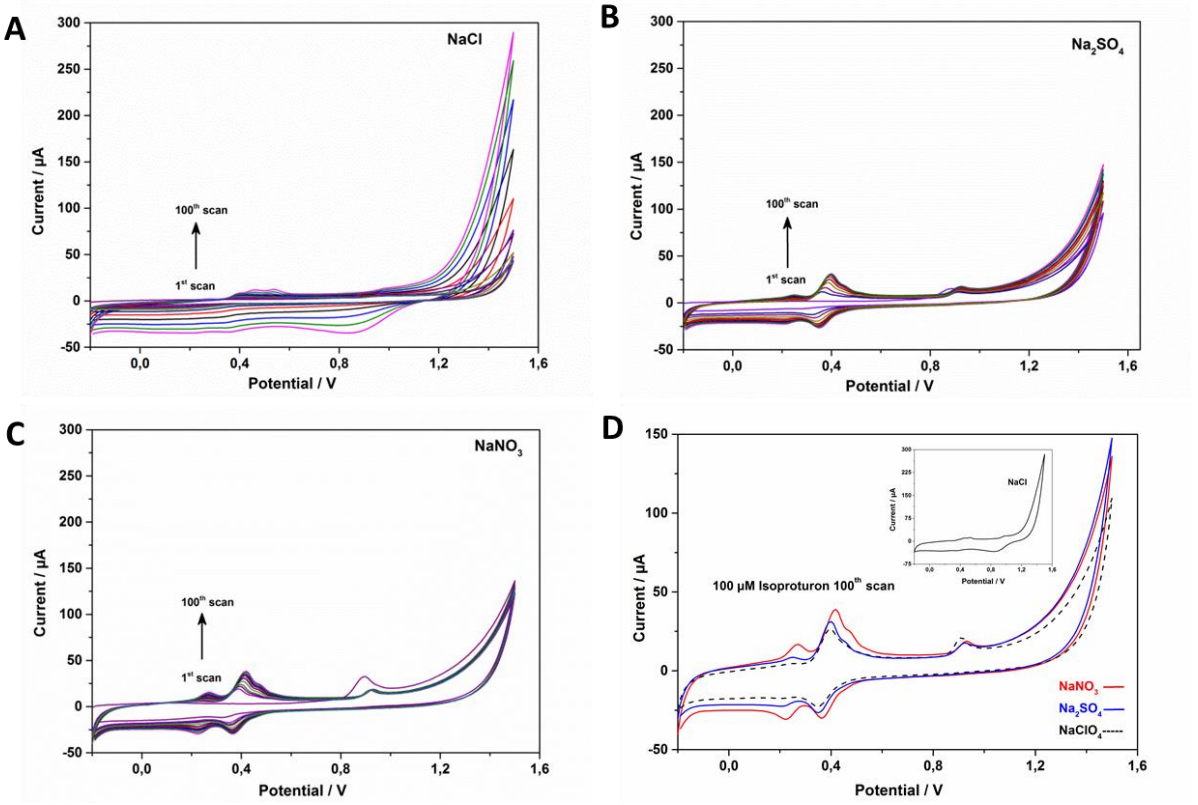

Figure VI-6: Cyclic voltammetry of 100 µM isoproturon in 0.1 M (A) NaCl (B) Na_2SO_4 (C) $NaNO_3$ by repetitive cycling (100 scans), (D) 100th scan of 100 µM isoproturon in different electrolytes (0.1M), scan rate = 100 mV s^{-1} and pH 6.

6.3 Analytical detection of isoproturon

6.3.1 Effect of preconcentration time

Influence of preconcentration time on peak intensity was studied with the help of differential pulse voltammetry (DPV). Preconcentration time was varied from 0–600 seconds

by applying potential of +1.5 V for oxidative cleavage of isoproturon and also electrochemical polymerization of isopropylaniline. Peak intensity increased by increasing preconcentration up to 300 seconds; beyond it i.e. 600 seconds peak intensity decreased (figure VI-7). In similar SWV experiments peak intensity and sharpness was better so SWV was selected for further experiments with the same preconcentration time optimized already.

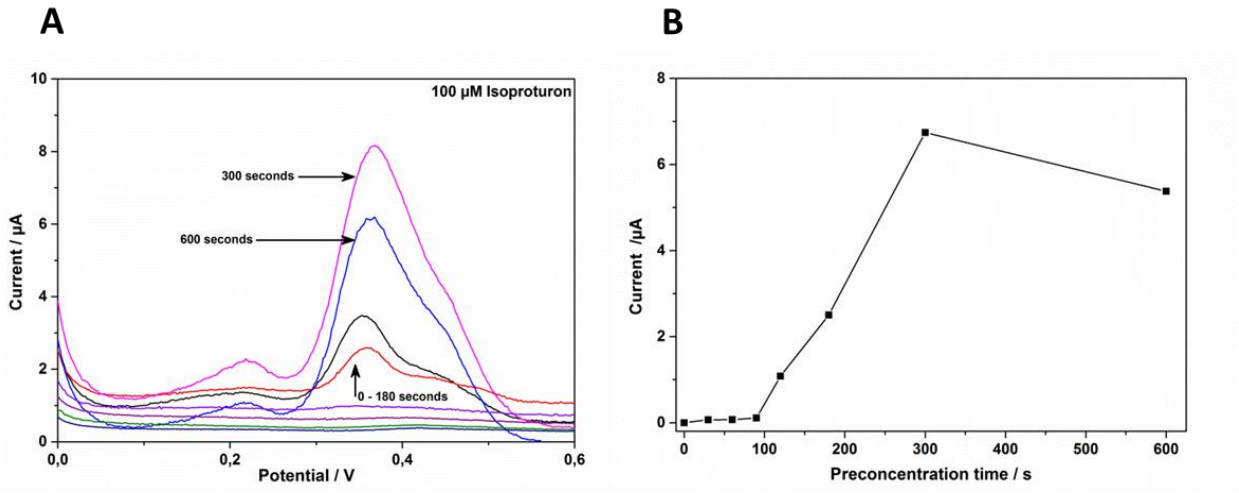

Figure VI-7: (A) Differential pulse voltammetry of 100 µM isoproturon in 0.1 M $NaNO_3$ for preconcentration time of 0-600 seconds (E_{acc}+1.5 V, E_{step} = 2 mV, E_{pulse} = 10 mV, t_{pulse} = 0.1s, scan rate = 5 mV s-1), (B) Graph showing current intensity as a function of preconcentration time.

6.3.2 Quantitative analysis of isoproturon by SWV

Square wave voltammetry was used to detect isoproturon at ordered mesoporous silica modified and unmodified GCE. Glassy carbon electrodes were modified with silica thin films according to procedure explained in chapter III.[216] Modified electrodes were used for SWV after template extraction in acidic ethanol solution. Optimized Parameters for SWV were: E_{step} and amplitude 2 and 5 mV respectively and frequency 10 Hz. Preconcentration was performed at +1.5 V for 5 minutes followed by SWV scan ranging from +1.5 to -0.2 V. 10 - 100 µM isoproturon in 0.1 M NaNO3 showed linear response at both bare and silica modified GCE with increasing concentration at +0.36 V, reversible peak II was recorded at the same potential by cyclic voltammetry. Calibration plots were constructed and were linear with good R^2 value of 0.991, 0.998 for bare and modified GCE respectively. Limit of detection calculated for bare GCE was 11, 8 µM whereas for silica modified electrode it was found to be 2, 9 µM, which is better than bare GCE. One can argue that this system is not very

sensitive as compared to already reported procedures but this is first study to report electrochemical characterization and detection of isoproturon using intermediate (peak II) compounds produced as result of its oxidation with the help of cyclic voltammetry and stripping voltammetry combined square wave voltammetry. Improvements in electrode surface and modifications can provide sensitive detection and low detection limits, furthermore as already reported mesoporous silica thin films can also provide surface protection of the working electrode against fouling agents which can enhance reproducibility and life of sensor.[94,95,265]

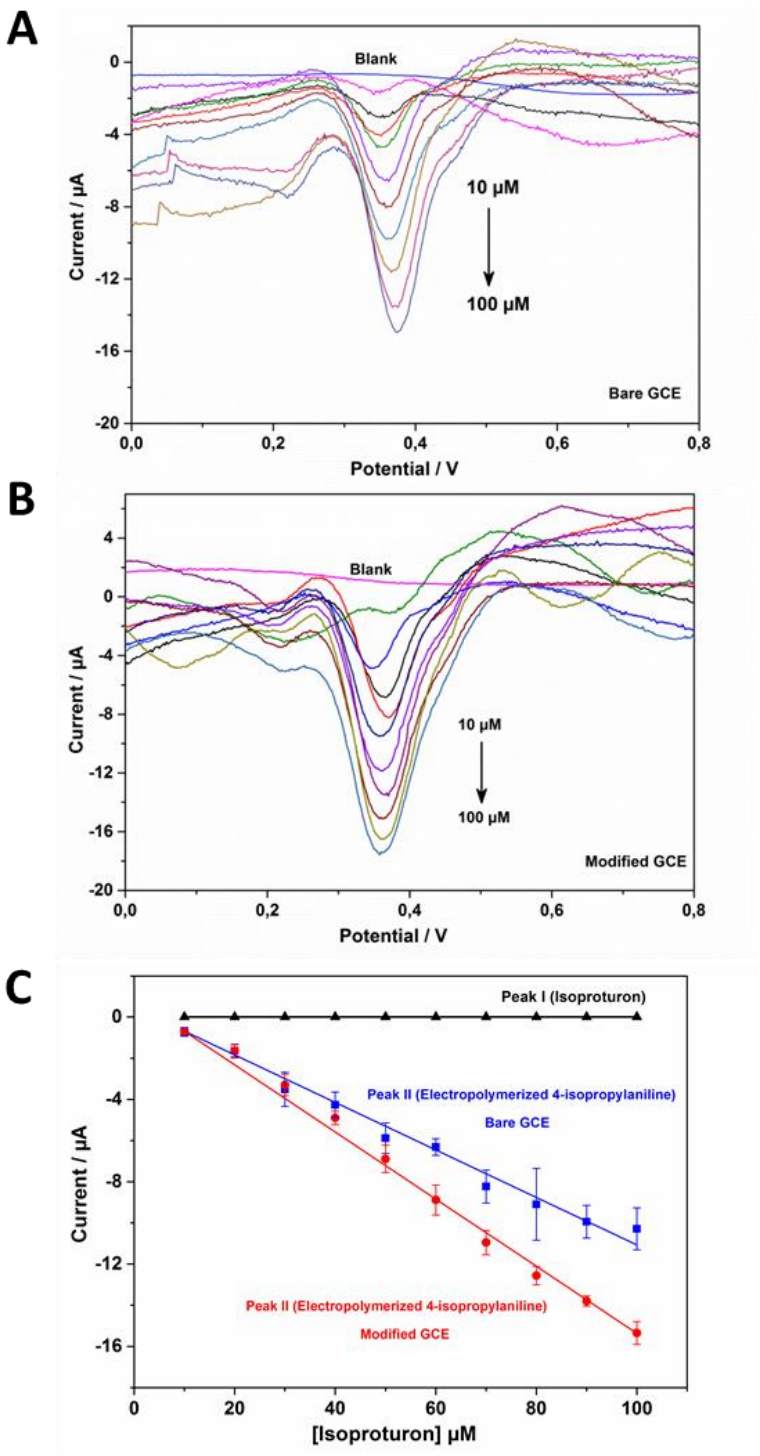

Figure VI-8: Square wave voltammetry of 10-100 µM isoproturon in 0.1 M $NaNO_3$ pH 6 (A) at bare GCE (B) Silica film modified GCE, deposition potential 1.5 V, deposition time 300 seconds, E_{step} 2 mV, amplitude 5 mV, Frequency 10 Hz. (C) calibration curves at unmodified and modified electrodes.

6.4 Conclusions

Glassy carbon electrodes were found to be more suitable than ITO for electrochemical studies of isoproturon as the signal intensity and applicability was better at a wide pH range with GCE. Cyclic voltammetric response isoproturon was found to be similar at bare and silica modified electrode. At high potential (around +1 V at GCE) isoproturon undergoes oxidative cleavage and as result of it 4-isopropylaniline and dimethyl amine are formed as intermediates. If the potential is applied up to +1.5 V, 4-isopropylaniline polymerizes electrochemically to form an electroactive film, this film showed reversible redox reaction. Application of optimum potential was found to be very critical for proper oxidation of isoproturon and as a result of it formation of intermediate compounds. $NaNO_3$ as electrolyte and solution pH 6 was selected as best conditions for electrochemical characterization and detection, whereas preconcentration time of 5 minutes at applied potential of +1.5 V was found to be more suitable for proper oxidation of isoproturon. One among the two intermediate compounds formed showed linear response for 10 - 100 µM concentration range of isoproturon by SWV at bare and silica modified electrodes. Limits of detection for bare and modified GCE was found to be 11, 8 µM and 2, 9 µM respectively which are much higher than permissible limits of isoproturon in (0.5 µM) in drinking water. LOD was calculated with the help of Eq. 4.4 in chapter IV. Although this study does not provide very sensitive determination but it is first report regarding the electrochemical characterization of isoproturon intermediate compounds formation and their use for its electrochemical detection. Electrode surface improvement can result in more sensitive analysis, nature of the electrode material can also play major role in sensitivity hence other carbon based materials can also be exploited for better sensitivity. Electrode modification combined with analyte specific functionalization could also improve the sensitivity and selectivity of the system as well as durability of the sensor due molecular sieving abilities of silica thin films.

Conclusions and perspectives

In the course of this thesis, I worked on modification of glassy carbon electrodes (GCE) by mesoporous silica thin films using electro assisted self-assembly (EASA) method and their application for electrochemical sensing of different herbicides. EASA process is widely used these days for production of ordered mesoporous silica thin films with vertical orientation of pores to underlying electrode surface. Applications of these thin films and advantages of carbon based electrodes in electrochemistry are discussed in detail in **chapter I** of the thesis. General conclusions of this study include:

Stability and proper adhesion of silica films was a major obstacle for the application of carbon based electrodes in the field of sensing and electroanalysis. Silica films stability problem was solved by electrografting 3-aminopropyltriethoxysilane (APTES) to be used as anchor for good adhesion of these films. Electrochemical and surface Characterization by XPS, SEM and TEM confirmed the covalent attachment of APTES to electrode surface and as a result of it much improved adhesion of silica films and homogenous deposition at glassy carbon electrodes. APTES grafting did not affected the porosity and orientation of mesopores. Furthermore, Functionalization of these films was successfully performed with azide organosilane and subsequent click coupling of the azide functions with ferrocene (**Chapter III**). This can open new avenues for the use of modified glassy carbon electrodes in the field electroanalysis and electrochemical applications requiring mechanically stable/Functionalized silica films.

As a practical demonstration of mesoporous silica modified glassy carbon electrodes application in electroanalysis, electrochemical sensing of paraquat at modified electrodes was performed. Paraquat is a commonly used herbicide, which exhibit two reversible peaks in cathodic potential domain each with single electron transfer. Carbon based electrodes are more suited for analysis of analytes which have redox activity at very low or high potential range. Paraquat due to its cationic nature had electrostatic interaction with negatively charged mesoporous silica films, as a result modified electrodes showed almost 30x higher sensitivity as compared to unmodified electrodes. Limit of detection found by this method for laboratory samples and real samples was 4 nM and 12 nM respectively, much lower than permissible limits of 40-60 nM in drinking water. Solution pH, electrolyte strength and nature showed to

have critical effect on the sensitivity of paraquat detection on mesoporous silica modified electrodes (**Chapter IV**).

To further exploit the electrostatic interaction of paraquat and mesoporous silica films for sensitive sensing of the herbicide, we studied the effect of film thickness and its role in accumulation of paraquat inside film matrix. According to hypothesis thicker film should accommodate larger amount of analyte as compared to thinner ones. Film thickness was varied by varying film deposition time and by depositing multi-layered films, the later to produce silica films without having large number of silica beads on film surface, a phenomenon observed in case of longer deposition time. Silica aggregates at film surface can have undesired effects in electroanalysis and reproducibility of the results. Results showed that thicker films can accumulate large amount of paraquat but it is always not helpful in sensitive determination of paraquat, as the analyte molecules face diffusion limitation in case of thicker film resulting in low square wave voltammetric response. The electrochemical response with thick films was high by cyclic voltammetry multiple scans, suggesting these films can accommodate more analyte but this process require longer accumulation time. Microelectrode arrays fabricated at GCE were also modified with silica films and used for electrochemical detection of paraquat, as the microelectrodes can provide very sensitive determination due to their characteristic properties beneficial for electroanalysis. These modified electrodes showed to be promising for sensitive analysis of analytes using low electrolyte concentrations, a very useful property for real sample and on-site analysis (**Chapter V**).

In the final part of the thesis we studied the electrochemical behavior and detection of isoproturon, another herbicide used for weed control in cereal crops. Cyclic voltammetric Characterization of isoproturon was performed at bare GC and ITO electrodes to assess its redox mechanism and intermediates formation. One among intermediate compounds formed due to oxidative cleavage of isoproturon was used for stripping voltammetry combined SWV determination of this herbicide. Optimisation of solution pH, supporting electrolyte and preconcentration parameters was done. Finally, SWV determination of isoproturon based on its electrochemically formed intermediate (4-isoprpylaniline) was carried out at silica modified and unmodified GC electrodes. Calibration curves were linear from 10 - 100 µM with increasing concentrations. Modified electrodes showed better sensitivity with 2, 6 µM limit of detection as compared to 11, 8 µM at unmodified electrodes (**Chapter VI**).

Future perspectives of this study can be categorised into few points which include:

- Further optimisation of microelectrode arrays modification with mesoporous silica and Characterization using microscopic techniques such as AFM and TEM is required. Electrochemical experiments have shown promising results for sensitive detection of paraquat on mesoporous silica modified microelectrode arrays. Microelectrode arrays can greatly enhance the sensitivity of electrochemical system but fabrication and stability can be an issue which needs to be addressed.
- For cationic molecules sensing, can we tune the pore diameter (small pore size) of mesoporous silica thin films? This could improve the sensitivity and selectivity of these films for cationic molecules and would also make it possible to work with low concentrations of electrolytes by taking into account the Debye length with relation to pore size as discussed in chapter IV.
- Silica films which are functionalized to be redox active or can make π-π interactions with neutral molecules such as isoproturon and catechol could improve the sensitivity for electrochemical detection of these molecules.
- Improved sensitivity for detection of neutral molecules could be achieved using mesoporous silica films with template molecules such as CTA^+ inside the pores. These compounds can be accumulated inside the template matrix by solubilisation into liquid crystalline phase and hence sensitivity could be increased as well as protection of electrode surface from fouling.
- At acidic pH mesoporous silica films show cationic behaviour, this can be exploited for the sensing of anionic molecules by using electrostatic interactions similar to paraquat detection in chapter IV.

Conclusions et perspectives

Dans le cadre de cette thèse, j'ai travaillé sur la modification des électrodes en carbone vitreux (GCE) par des films minces de silice mésoporeuse en utilisant la méthode d'auto-assemblage électro-assemblage assisté (EASA) et leur application pour la détection électrochimique de différents herbicides. Le procédé EASA est aujourd'hui largement utilisé pour la production de films minces de silice mésoporeuse ordonnée avec orientation verticale des pores par rapport à la surface de l'électrode sous-jacente. Les applications de ces couches minces et les avantages des électrodes à base de carbone en électrochimie sont discutés en détail dans le chapitre I de la thèse. Les conclusions générales de cette étude comprennent :

La stabilité et la bonne adhésion des films de silice a été un obstacle majeur pour l'application des électrodes à base de carbone dans le domaine de la détection et de l'électroanalyse. Le problème de stabilité des films de silice a été résolu par électrogreffage de 3-aminopropyltriéthoxysilane (APTES) à utiliser comme ancrage pour une bonne adhérence de ces films. La caractérisation électrochimique et de surface par XPS, SEM et TEM a confirmé la fixation covalente de l'APTES à la surface de l'électrode et, grace à cela, l'adhérence des films de silice et le dépôt homogène au niveau des électrodes de carbone vitreux. La greffe APTES n'a pas affecté la porosité et l'orientation des mésopores. De plus, la fonctionnalisation de ces films a été réalisée avec succès avec l'azoture organosilane et le couplage par clic des fonctions azoture avec le ferrocène (chapitre III). Cela peut ouvrir de nouvelles voies pour l'utilisation d'électrodes en carbone vitreux modifié dans les applications d'électroanalyse sur le terrain et les applications électrochimiques nécessitant des films de silice mécaniquement stables ou fonctionnalisés.

Dans le cadre d'une démonstration pratique de l'application des électrodes en carbone vitreux modifié à la silice mésoporeuse dans l'électroanalyse, la détection électrochimique du paraquat aux électrodes modifiées a été réalisée. Le paraquat est un herbicide couramment utilisé, qui présente deux pics réversibles dans le domaine du potentiel cathodique, chacun avec un seul transfert d'électrons. Les électrodes à base de carbone conviennent mieux à l'analyse des analytes qui ont une activité redox à un potentiel très faible ou élevé. En raison de sa nature cationique, le paraquat a eu une interaction électrostatique avec des films de silice mésoporeuse chargés négativement, de sorte que les électrodes modifiées ont montré une sensibilité presque 30 fois plus élevée que les électrodes non modifiées. La limite de

détection trouvée par cette méthode pour les échantillons de laboratoire et les échantillons réels était de 4 nM et 12 nM respectivement, soit beaucoup moins que les limites admissibles de 40 à 60 nM dans l'eau potable. Le pH de la solution, la force de l'électrolyte et la nature ont montré un effet critique sur la sensibilité de la détection du paraquat sur les électrodes modifiées à la silice mésoporeuse (chapitre IV).

Afin d'exploiter davantage l'interaction électrostatique des films de paraquat et de silice mésoporeuse pour la détection sensible de l'herbicide, nous avons étudié l'effet de l'épaisseur du film et son rôle dans l'accumulation du paraquat à l'intérieur de la matrice du film. Selon l'hypothèse, les films plus épais devraient contenir une plus grande quantité d'analyte que les films plus minces. L'épaisseur du film variait en fonction du temps de dépôt du film et en déposant des films multicouches, ce dernier pour produire des films de silice sans avoir un grand nombre de billes de silice à la surface du film, phénomène observé dans le cas d'un temps de dépôt plus long. Les agrégats de silice à la surface du film peuvent avoir des effets indésirables dans l'électroanalyse et la reproductibilité des résultats. Les résultats ont montré que les films plus épais peuvent accumuler de grandes quantités de paraquat, mais ce n'est pas toujours utile dans la détermination sensible du paraquat, car les molécules d'analyte sont confrontées à une limitation de diffusion dans le cas de films plus épais, ce qui entraîne une réponse électrochimiques. La réponse électrochimique des films épais a été élevée par voltampérométrie cyclique, ce qui suggère que ces films peuvent contenir plus d'analyte, mais ce processus nécessite un temps d'accumulation plus long. Les microélectrodes fabriquées à GCE ont également été modifiées avec des films de silice et utilisées pour la détection électrochimique du paraquat, car les microélectrodes peuvent fournir une détermination très sensible en raison de leurs propriétés caractéristiques bénéfiques pour l'électroanalyse. Ces électrodes modifiées se sont révélées prometteuses pour l'analyse sensible des analytes en utilisant de faibles concentrations d'électrolytes, une propriété très utile pour les échantillons réels et l'analyse sur site (chapitre V).

Dans la dernière partie de la thèse, nous avons étudié le comportement électrochimique et la détection de l'isoproturon, un autre herbicide utilisé pour lutter contre les mauvaises herbes dans les cultures céréalières. La caractérisation voltampérométrique cyclique de l'isoproturon a été effectuée aux électrodes GC et ITO nues afin d'évaluer son mécanisme redox et la formation d'intermédiaires. L'un des composés intermédiaires formés en raison du clivage oxydatif de l'isoproturon a été utilisé pour la détermination de la

voltampérométrie de cet herbicide. L'optimisation du pH de la solution, de l'électrolyte de soutien et des paramètres de préconcentration a été effectuée. Enfin, la détermination de la SWV de l'isoproturon à partir de son intermédiaire formé par voie électrochimique (4-isopropylaniline) a été effectuée à la silice modifiée et non modifiée. Les courbes d'étalonnage étaient linéaires de 10 à 100 µM avec des concentrations croissantes. Les électrodes modifiées ont montré une meilleure sensibilité avec une limite de détection de 2,6 µM comparativement à 11,8 µM aux électrodes non modifiées (chapitre VI).

Les perspectives d'avenir de cette étude peuvent être classées en quelques points qui incluent:

- L'optimisation de la modification des réseaux de microélectrodes avec de la silice mésoporeuse et la caractérisation par des techniques microscopiques telles que l'AFM et le TEM est nécessaire. Les expériences électrochimiques ont montré des résultats prometteurs pour la détection sensible du paraquat sur des réseaux de microélectrodes modifiées à la silice mésoporeuse. Les réseaux de microélectrodes peuvent améliorer considérablement la sensibilité des systèmes électrochimiques, mais la fabrication et la stabilité peuvent être une question qui doit être abordée.
- Pour la détection de molécules cationiques, pouvons-nous régler le diamètre des pores (petite taille des pores) des films minces de silice mésoporeuse? Cela pourrait améliorer la sensibilité et la sélectivité de ces films pour les molécules cationiques et permettrait également de travailler avec de faibles concentrations d'électrolytes en tenant compte de la longueur de Debye par rapport à la taille des pores, comme indiqué au chapitre IV.
- Les films de silice qui sont fonctionnalisés pour être actifs redox ou qui peuvent faire des interactions π-π avec des molécules neutres comme l'isoproturon et le catéchol pourraient améliorer la sensibilité pour la détection électrochimique de ces molécules.
- Une meilleure sensibilité pour la détection de molécules neutres pourrait être obtenue en utilisant des films de silice mésoporeuse avec des molécules modèles telles que le CTA^+ à l'intérieur des pores. Ces composés peuvent être accumulés à l'intérieur de la matrice du gabarit par solubilisation en phase cristalline liquide, ce qui permet d'augmenter la sensibilité et de protéger la surface de l'électrode contre l'encrassement.

- A pH acide, les films de silice mésoporeux présentent un comportement cationique, qui peut être exploité pour la détection de molécules anioniques en utilisant des interactions électrostatiques similaires à la détection du paraquat dans le chapitre IV.

References:

(1) Lefrou, C.; Fabry, P.; Poignet, J. C. *Electrochemistry: The Basics, with Examples*; 2012.

(2) Hulanicki, A.; Glab, S.; Ingman, F. Chemical Sensors: Definitions and Classification. *Pure Appl. Chem.* **1991**, *63* (9), 1247–1250.

(3) Faridbod, F.; Gupta, V. K.; Zamani, H. A. Electrochemical Sensors and Biosensors. *Int. J. Electrochem.* **2011**, *2011*, 1–2.

(4) Hu, Z.; Grasso, D. *Chemical Oxygen Demand*; Springer, 2007; Vol. 1.

(5) Thévenot, D. R.; Toth, K.; Durst, R. A.; Wilson, G. S. Electrochemical Biosensors: Recommended Definitions and Classification. *Biosens. Bioelectron.* **2001**, *16* (1–2), 121–131.

(6) Wang, Y.; Xu, H.; Zhang, J.; Li, G. Electrochemical Sensors for Clinic Analysis. *Sensors* **2008**, *8* (4), 2043–2081.

(7) Stradiotto, N. R.; Yamanaka, H.; Zanoni, M. V. B. Electrochemical Sensors: A Powerful Tool in Analytical Chemistry. *J. Braz. Chem. Soc.* **2003**, *14* (2), 159–173.

(8) Bobacka, J.; Ivaska, A.; Lewenstam, A. Potentiometric Ion Sensors. *Chem. Rev.* **2008**, *108* (2), 329–351.

(9) Bakker, E.; Pretsch, E. Nanoscale Potentiometry. *TrAC - Trends Anal. Chem.* **2008**, *27* (7), 612–618.

(10) Rumyantseva, M. N.; Labeau, M. Copper and Nickel Doping Effect on Interaction of SnO2films with H2S. *J. Mater. Chem.* **1997**, *7* (9), 1785–1790.

(11) Fleischer, M.; Meixner, H. Sensitive, Selective and Stable CH4detection Using Semiconducting Ga2O3thin Films. *"Sensors and Actuators, B: Chemical."* 1995, pp 81–84.

(12) de Lacy Costello, B. P. J.; Evans, P.; Ratcliffe, N. M. Preparation of Polypyrrole Composites and the Effect of Volatile Amines on Their Electrical Properties. *Analyst* **1996**, *121* (6), 793.

(13) Smyntyna, V.; Golovanov, V.; Kačiulis, S.; Mattogno, G.; Righini, G. Influence of Chemical Composition on Sensitivity and Signal Reproducibility of CdS Sensors of Oxygen. *Sensors Actuators B. Chem.* **1995**, *25* (1–3), 628–630.

(14) Qu, W.; Meyer, J.-U. Thick-Film Humidity Sensor Based on Porous $MnWO_4$ Material.

Meas. Sci. Technol. **1997**, *8* (6), 593–600.

(15) Wang, J. Stripping Analysis at Bismuth Electrodes: A Review. *Electroanalysis* **2005**, *17* (15–16), 1341–1346.

(16) Zuman, P. Role of Mercury Electrodes in Contemporary Analytical Chemistry. *Electroanalysis* **2000**, *12* (15), 1187–1194.

(17) Wang, J. *Analytical Electrochemistry*; John Wiley & Sons, Inc.: Hoboken, NJ, USA, 2006; Vol. 3.

(18) Uslu, B.; Ozkan, S. Solid Electrodes in Electroanalytical Chemistry: Present Applications and Prospects for High Throughput Screening of Drug Compounds. *Comb. Chem. High Throughput Screen.* **2007**, *10* (7), 495–513.

(19) Tarasevich, M. R.; Efremov, B. N.; Trasatti, S. *Electrodes of Conductive Metal Oxides*; Elsevier Science, 1980; Vol. 5.

(20) Uslu, B.; Ozkan, S. Electroanalytical Application of Carbon Based Electrodes to the Pharmaceuticals. *Anal. Lett.* **2007**, *40* (5), 817–853.

(21) Kissinger, P. T.; Heiniman, W. . *Laboratory Techniques in Electroanalytical Chemistry*; Marcel Dekker, New York., 1984.

(22) Wang, J. *Analytical Electrochemistry*, 2nd ed.; John Wiley & Sons, Inc.: Hoboken, NJ, USA, 2006.

(23) Yamada, S.; Sato, H. Some Physical Properties of Glassy Carbon. *Nature* **1962**, *193* (4812), 261–262.

(24) Van der Linden, W. E.; Dieker, J. W. Glassy Carbon as Electrode Material in Electro-Analytical Chemistry. *Anal. Chim. Acta* **1980**, *119* (1), 1–24.

(25) Jenkins, G. M.; Kawamura, K. Structure of Glassy Carbon. *Nature* **1971**, *231* (5299), 175–176.

(26) R. A. Durst, A. J. Baumer, R. W. Murray, R. P. B. Chemically Modified Electrodes: Recommended Terminology and Definitions. *Int. Union Pure Appl. Chem.* **1997**, *57* (6), 1491–1505.

(27) Durst, R. A. Chemically Modified Electrodes: Recommended Terminology and Definitions (IUPAC Recommendations 1997). *Pure Appl. Chem.* **1997**, *69* (6), 1317–1324.

(28) Bard, A. J. Chemical Modification of Electrodes. *J. Chem. Educ.* **1983**, *60* (4), 302.

(29) Walcarius, A. Electroanalysis with Pure, Chemically Modified, and Sol-Gel-Derived Silica-Based Materials. *Electroanalysis* **2001**, *13* (8–9), 701–718.

(30) Murray, R.A., Ewing, A.G., Durst, R. A. Chemically Modified Electrodes: Molecular Design for Electroanalysis. *EAnalytical Chem.* **1987**, *58* (5), 379–390.

(31) Navrátilová, Z.; Kula, P. Clay Modified Electrodes: Present Applications and Prospects. *Electroanalysis* **2003**, *15* (10), 837–846.

(32) Walcarius, A. Zeolite-Modified Electrodes in Electroanalytical Chemistry. *Anal. Chim. Acta* **1999**, *384* (1), 1–16.

(33) Wang, J. Modified Electrodes for Electrochemical Sensors. *Electroanalysis* **1991**, *3* (4–5), 255–259.

(34) Hench, L. L.; West, J. K. The Sol-Gel Process. *Chem. Rev.* **1990**, *90* (1), 33–72.

(35) Schubert, U. Chemistry and Fundamentals of the Sol-Gel Process. In *The Sol-Gel Handbook*; Wiley-VCH Verlag GmbH & Co. KGaA: Weinheim, Germany, 2015; Vol. 1–3, pp 1–28.

(36) Jiang, H.; Blouin, C. Insertions and the Emergence of Novel Protein Structure: A Structure-Based Phylogenetic Study of Insertions. *BMC Bioinformatics* **2007**, *8* (1), 444.

(37) Etienne, M.; Zhang, L.; Vilà, N.; Walcarius, A. Mesoporous Materials-Based Electrochemical Enzymatic Biosensors. *Electroanalysis* **2015**, *27* (9), 2028–2054.

(38) Rouquerol, J.; Avnir, D.; Everett, D. H.; Fairbridge, C.; Haynes, M.; Pernicone, N.; Ramsay, J. D. F.; Sing, K. S. W.; Unger, K. K. Guidelines for the Characterization of Porous Solids. In *Characterization of Porous Solids Iii*; 1994; Vol. 87, pp 1–9.

(39) Kresge, C. T.; Leonowicz, M. E.; Roth, W. J.; Vartuli, J. C.; Beck, J. S. Ordered Mesoporous Molecular Sieves Synthesized by a Liquid-Crystal Template Mechanism. *Nature* **1992**, *359* (6397), 710–712.

(40) Kresge, C. T.; Roth, W. J. The Discovery of Mesoporous Molecular Sieves from the Twenty Year Perspective. *Chem. Soc. Rev.* **2013**, *42* (9), 3663.

(41) Walcarius, A.; Etienne, M.; Sayen, S.; Lebeau, B. Grafted Silicas in Electroanalysis: Amorphous Versus Ordered Mesoporous Materials. *Electroanalysis* **2003**, *15* (5–6), 414–421.

(42) Wang, H.; Liu, Y.; Li, M.; Huang, H.; Xu, H. M.; Hong, R. J.; Shen, H. Multifunctional TiO2nanowires-Modified Nanoparticles Bilayer Film for 3D Dye-Sensitized Solar Cells. *Optoelectron. Adv. Mater. Rapid Commun.* **2010**, *4* (8), 1166–

1169.

(43) Walcarius, A. Mesoporous Materials-Based Electrochemical Sensors. *Electroanalysis* **2015**, *27*, 1–39.

(44) Walcarius, A. Template-Directed Porous Electrodes in Electroanalysis. *Anal. Bioanal. Chem.* **2010**, *396* (1), 261–272.

(45) Liu, Y.; Goebl, J.; Yin, Y. Templated Synthesis of Nanostructured Materials. *Chem. Soc. Rev.* **2013**, *42* (7), 2610–2653.

(46) Stein, A.; Melde, B. J.; Schroden, R. C. Hybrid Inorganic-Organic Mesoporous Silicates—Nanoscopic Reactors Coming of Age. *Adv. Mater.* **2000**, *12* (19), 1403–1419.

(47) Soler-Illia, G. J. A. A.; Azzaroni, O. Multifunctional Hybrids by Combining Ordered Mesoporous Materials and Macromolecular Building Blocks. *Chem. Soc. Rev.* **2011**, *40* (2), 1107.

(48) Fryxell, G. E.; Mattigod, S. V.; Lin, Y.; Wu, H.; Fiskum, S.; Parker, K.; Zheng, F.; Yantasee, W.; Zemanian, T. S.; Addleman, R. S.; et al. Design and Synthesis of Self-Assembled Monolayers on Mesoporous Supports (SAMMS): The Importance of Ligand Posture in Functional Nanomaterials. *J. Mater. Chem.* **2007**, *17* (28), 2863.

(49) Hoffmann, F.; Cornelius, M.; Morell, J.; Fröba, M. Silica-Based Mesoporous Organic–Inorganic Hybrid Materials. *Angew. Chemie Int. Ed.* **2006**, *45* (20), 3216–3251.

(50) Sanchez, C.; Boissière, C.; Grosso, D.; Laberty, C.; Nicole, L. Design, Synthesis, and Properties of Inorganic and Hybrid Thin Films Having Periodically Organized Nanoporosity. *Chem. Mater.* **2008**, *20* (3), 682–737.

(51) Walcarius, A.; Despas, C.; Bessiere, J. Selective Monitoring of Cu(II) Species Using a Silica Modified Carbon Paste Electrode. *Anal. Chim. Acta* **1999**, *385* (1–3), 79–89.

(52) Yantasee, W.; Deibler, L. A.; Fryxell, G. E.; Timchalk, C.; Lin, Y. Screen-Printed Electrodes Modified with Functionalized Mesoporous Silica for Voltammetric Analysis of Toxic Metal Ions. *Electrochem. commun.* **2005**, *7* (11), 1170–1176.

(53) Tallman, D. E.; Petersen, S. L. Composite Electrodes for Electroanalysis: Principles and Applications. *Electroanalysis* **1990**, *2* (7), 499–510.

(54) Wu, S.; Ju, H. X.; Liu, Y. Conductive Mesocellular Silica–Carbon Nanocomposite Foams for Immobilization, Direct Electrochemistry, and Biosensing of Proteins. *Adv. Funct. Mater.* **2007**, *17* (4), 585–592.

(55) Díaz, I.; García, B.; Alonso, B.; Casado, C. M.; Morán, M.; Losada, J.; Pérez-Pariente,

J. Ferrocenyl Dendrimers Incorporated into Mesoporous Silica: New Hybrid Redox-Active Materials †. *Chem. Mater.* **2003**, *15* (5), 1073–1079.

(56) Zhou, M.; Guo, L.; Lin, F.; Liu, H. Electrochemistry and Electrocatalysis of Polyoxometalate-Ordered Mesoporous Carbon Modified Electrode. *Anal. Chim. Acta* **2007**, *587* (1), 124–131.

(57) Jiang, Y.-X.; Ding, N.; Sun, S.-G. Enhanced IR Absorption of CO Adsorbed on Pd Nanoparticles Embedded in the Mesoporous Molecular Sieve SBA-15. *J. Electroanal. Chem.* **2004**, *563* (1), 15–21.

(58) Dai, Z. H.; Ni, J.; Huang, X. H.; Lu, G. F.; Bao, J. C. Direct Electrochemistry of Glucose Oxidase Immobilized on a Hexagonal Mesoporous Silica-MCM-41 Matrix. *Bioelectrochemistry* **2007**, *70* (2), 250–256.

(59) Slowing, I. I.; Trewyn, B. G.; Giri, S.; Lin, V. S.-Y. Mesoporous Silica Nanoparticles for Drug Delivery and Biosensing Applications. *Adv. Funct. Mater.* **2007**, *17* (8), 1225–1236.

(60) Fang, X.; Zhao, X.; Fang, W.; Chen, C.; Zheng, N. Self-Templating Synthesis of Hollow Mesoporous Silica and Their Applications in Catalysis and Drug Delivery. *Nanoscale* **2013**, *5* (6), 2205.

(61) Wang, Y.; Caruso, F. Mesoporous Silica Spheres as Supports for Enzyme Immobilization and Encapsulation. *Chem. Mater.* **2005**, *17* (5), 953–961.

(62) Sun, Z.; Deng, Y.; Wei, J.; Gu, D.; Tu, B.; Zhao, D. Hierarchically Ordered Macro-/Mesoporous Silica Monolith: Tuning Macropore Entrance Size for Size-Selective Adsorption of Proteins. *Chem. Mater.* **2011**, *23* (8), 2176–2184.

(63) Brinker, C. J.; Lu, Y.; Sellinger, A.; Fan, H. Evaporation-Induced Self-Assembly: Nanostructures Made Easy. *Adv. Mater.* **1999**, *11* (7), 579–585.

(64) Grosso, D.; Cagnol, F.; Soler-Illia, G. J. de A. A.; Crepaldi, E. L.; Amenitsch, H.; Brunet-Bruneau, A.; Bourgeois, A.; Sanchez, C. Fundamentals of Mesostructuring Through Evaporation-Induced Self-Assembly. *Adv. Funct. Mater.* **2004**, *14* (4), 309–322.

(65) Koganti, V. R.; Dunphy, D.; Gowrishankar, V.; McGehee, M. D.; Li, X.; Wang, J.; Rankin, S. E. Generalized Coating Route to Silica and Titania Films with Orthogonally Tilted Cylindrical Nanopore Arrays. *Nano Lett.* **2006**, *6* (11), 2567–2570.

(66) Yamaguchi, A.; Uejo, F.; Yoda, T.; Uchida, T.; Tanamura, Y.; Yamashita, T.; Teramae, N. Self-Assembly of a Silica-Surfactant Nanocomposite in a Porous Alumina Membrane. *Nat. Mater.* **2004**, *3* (5), 337–341.

(67) Fukumoto, H.; Nagano, S.; Kawatsuki, N.; Seki, T. Photo-Alignment Behavior of Mesoporous Silica Thin Films Synthesized on a Photo-Cross-Linkable Polymer Film. *Chem. Mater.* **2006**, *18* (5), 1226–1234.

(68) Hara, M.; Nagano, S.; Seki, T. Π−π Interaction-Induced Vertical Alignment of Silica Mesochannels Templated by a Discotic Lyotropic Liquid Crystal. *J. Am. Chem. Soc.* **2010**, *132* (39), 13654–13656.

(69) Richman, E. K.; Brezesinski, T.; Tolbert, S. H. Vertically Oriented Hexagonal Mesoporousfilms Formed through Nanometre-Scaleepitaxy. *Nat. Mater.* **2008**, *7* (9), 712–717.

(70) Yamauchi, Y.; Sawada, M.; Komatsu, M.; Sugiyama, A.; Osaka, T.; Hirota, N.; Sakka, Y.; Kuroda, K. Magnetically Induced Orientation of Mesochannels in Mesoporous Silica Films at 30 Tesla. *Chem. - An Asian J.* **2007**, *2* (12), 1505–1512.

(71) Kao, K. C.; Lin, C. H.; Chen, T. Y.; Liu, Y. H.; Mou, C. Y. A General Method for Growing Large Area Mesoporous Silica Thin Films on Flat Substrates with Perpendicular Nanochannels. *J. Am. Chem. Soc.* **2015**, *137* (11), 3779–3782.

(72) Walcarius, A.; Sibottier, E.; Etienne, M.; Ghanbaja, J. Electrochemically Assisted Self-Assembly of Mesoporous Silica Thin Films. *Nat. Mater.* **2007**, *6* (8), 602–608.

(73) Teng, Z.; Zheng, G.; Dou, Y.; Li, W.; Mou, C.-Y.; Zhang, X.; Asiri, A. M.; Zhao, D. Highly Ordered Mesoporous Silica Films with Perpendicular Mesochannels by a Simple Stöber-Solution Growth Approach. *Angew. Chemie Int. Ed.* **2012**, *51* (9), 2173–2177.

(74) Xu, F.-F.; Cui, F.-M.; Ruan, M.-L.; Zhang, L.-L.; Shi, J.-L. Structural Characteristics of Oriented Mesostructured Silica Thin Films. *Langmuir* **2010**, *26* (10), 7535–7539.

(75) Del Valle, M. A.; Gacitua, M.; Diaz, F. R.; Armijo, F.; Soto, J. P. Electro-Synthesis and Characterization of Polythiophene Nano-Wires/Platinum Nano-Particles Composite Electrodes. Study of Formic Acid Electro-Catalytic Oxidation. *Electrochim. Acta* **2012**, *71*, 277–282.

(76) Fernández, I.; Sánchez, A.; Díez, P.; Martínez-Ruiz, P.; Di Pierro, P.; Porta, R.; Villalonga, R.; Pingarrón, J. M. Nanochannel-Based Electrochemical Assay for Transglutaminase Activity. *Chem. Commun.* **2014**, *50* (87), 13356–13358.

(77) Cheng, J.; Rathi, S. J.; Stradins, P.; Frey, G. L.; Collins, R. T.; Williams, S. K. R. Free Standing Silica Thin Films with Highly Ordered Perpendicular Nanopores. *RSC Adv.* **2014**, *4* (15), 7627–7633.

(78) Robertson, C.; Beanland, R.; Boden, S. A.; Hector, A. L.; Kashtiban, R. J.; Sloan, J.;

Smith, D. C.; Walcarius, A. Ordered Mesoporous Silica Films with Pores Oriented Perpendicular to a Titanium Nitride Substrate. *Phys. Chem. Chem. Phys.* **2015**, *17* (6), 4763–4770.

(79) Wang, Q.; Yang, Q.; Su, B. Adsorption of Microperoxidase-11 in Vertical Silica Mesochannels and Electrochemical Investigation of Its Electron Transfer Properties. *Electrochim. Acta* **2015**, *161*, 290–296.

(80) Yan, F.; He, Y.; Ding, L.; Su, B. Highly Ordered Binary Assembly of Silica Mesochannels and Surfactant Micelles for Extraction and Electrochemical Analysis of Trace Nitroaromatic Explosives and Pesticides. *Anal. Chem.* **2015**, *87* (8), 4436–4441.

(81) Wu, M.-S.; Sun, X.-T.; Zhu, M.-J.; Chen, H.-Y.; Xu, J.-J. Mesoporous Silica Film-Assisted Amplified Electrochemiluminescence for Cancer Cell Detection. *Chem. Commun.* **2015**, *51* (74), 14072–14075.

(82) Li, J.; Zhu, W.; Ji, J.; Wang, P.; Wang, C.; Yin, X.; Wang, H.; Lan, Y.; Gao, N.; Li, G. Emulsion Droplets as a Dynamic Interface for the Direct and Large-Scale Synthesis of Ultrathin Free-Standing Mesoporous Silica Films as Well as 2D Polymeric and Carbon Nanomaterials. *Nanoscale* **2016**, *8* (5), 3093–3099.

(83) Guo, X.; Zeng, Y.; Wang, Z.; Qu, L.; Shao, Z.; Yuan, Z.; Yi, B. Improvement of PEMFC Performance and Endurance by Employing Continuous Silica Film Incorporated Water Transport Plate. *Electrochim. Acta* **2016**, *191*, 116–123.

(84) Goux, A.; Etienne, M.; Aubert, E.; Lecomte, C.; Ghanbaja, J.; Walcarius, A. Oriented Mesoporous Silica Films Obtained by Electro-Assisted Self-Assembly (EASA). *Chem. Mater.* **2009**, *21* (4), 731–741.

(85) Herzog, G.; Sibottier, E.; Etienne, M.; Walcarius, A. Electrochemically Assisted Self-Assembly of Ordered and Functionalized Mesoporous Silica Films: Impact of the Electrode Geometry and Size on Film Formation and Properties. *Faraday Discuss.* **2013**, *164* (1), 259.

(86) Feng, D.; Wei, J.; Wang, M.; Yue, Q.; Deng, Y.; Asiri, A. M.; Zhao, D. Advances in Mesoporous Thin Films via Self-Assembly Process. *Adv. Porous Mater.* **2013**, *1* (2), 164–186.

(87) Innocenzi, P.; Malfatti, L. Mesoporous Thin Films: Properties and Applications. *Chem. Soc. Rev.* **2013**, *42* (9), 4198.

(88) Carretero-Genevrier, A.; Drisko, G. L.; Grosso, D.; Boissiere, C.; Sanchez, C. Mesoscopically Structured Nanocrystalline Metal Oxide Thin Films. *Nanoscale* **2014**, *6* (23), 14025–14043.

(89) Mahoney, L.; Koodali, R. T. Versatility of Evaporation-Induced Self-Assembly (EISA) Method for Preparation of Mesoporous TiO2 for Energy and Environmental Applications. *Materials (Basel).* **2014**, *7* (4), 2697–2746.

(90) Mousty, C.; Walcarius, A. Electrochemically Assisted Deposition by Local PH Tuning: A Versatile Tool to Generate Ordered Mesoporous Silica Thin Films and Layered Double Hydroxide Materials. *J. Solid State Electrochem.* **2015**, *19* (7), 1905–1931.

(91) Innocenzi, P.; Malfatti, L.; Kidchob, T.; Falcaro, P. Order−Disorder in Self-Assembled Mesostructured Silica Films: A Concepts Review. *Chem. Mater.* **2009**, *21* (13), 2555–2564.

(92) Soler-Illia, G. J. A. A.; Angelomé, P. C.; Fuertes, M. C.; Calvo, A.; Wolosiuk, A.; Zelcer, A.; Bellino, M. G.; Martínez, E. D. Mesoporous Hybrid and Nanocomposite Thin Films. A Sol-Gel Toolbox to Create Nanoconfined Systems with Localized Chemical Properties. *J. Sol-Gel Sci. Technol.* **2011**, *57* (3), 299–312.

(93) Ehlert, N.; Mueller, P. P.; Stieve, M.; Lenarz, T.; Behrens, P. Mesoporous Silica Films as a Novel Biomaterial: Applications in the Middle Ear. *Chem. Soc. Rev.* **2013**, *42* (9), 3847.

(94) Yan, F.; Zheng, W.; Yao, L.; Su, B. Direct Electrochemical Analysis in Complex Samples Using ITO Electrodes Modified with Permselective Membranes Consisting of Vertically Ordered Silica Mesochannels and Micelles. *Chem. Commun.* **2015**, *51* (100), 17736–17739.

(95) Serrano, M. B.; Despas, C.; Herzog, G.; Walcarius, A. Mesoporous Silica Thin Films for Molecular Sieving and Electrode Surface Protection against Biofouling. *Electrochem. commun.* **2015**, *52*, 34–36.

(96) Xu, L.; He, N.; Du, J.; Deng, Y.; Li, Z.; Wang, T. A Detailed Investigation for Determination of Tannic Acid by Anodic Stripping Voltammetry Using Porous Electrochemical Sensor. *Anal. Chim. Acta* **2009**, *634* (1), 49–53.

(97) Etienne, M.; Goux, A.; Sibottier, E.; Walcarius, A. Oriented Mesoporous Organosilica Films on Electrode: A New Class of Nanomaterials for Sensing. *J. Nanosci. Nanotechnol.* **2009**, *9* (4), 2398–2406.

(98) Herzog, G.; Vodolazkaya, N. A.; Walcarius, A. Platinum Ultramicroelectrodes Modified with Electrogenerated Surfactant-Templated Mesoporous Organosilica Films: Effect of Film Formation Conditions on Its Performance in Preconcentration Electroanalysis. *Electroanalysis* **2013**, *25* (12), 2595–2603.

(99) Vilà, N.; Ghanbaja, J.; Aubert, E.; Walcarius, A. Electrochemically Assisted Generation of Highly Ordered Azide-Functionalized Mesoporous Silica for Oriented

Hybrid Films. *Angew. Chemie - Int. Ed.* **2014**, *53* (11), 2945–2950.

(100) Wu, K. C.-W.; Jiang, X.; Yamauchi, Y. New Trend on Mesoporous Films: Precise Controls of One-Dimensional (1D) Mesochannels toward Innovative Applications. *J. Mater. Chem.* **2011**, *21* (25), 8934.

(101) Urbanova, V.; Walcarius, A. Vertically-Aligned Mesoporous Silica Films. *Zeitschrift für Anorg. und Allg. Chemie* **2014**, *640* (3–4), 537–546.

(102) Walcarius, A. Silica-Based Electrochemical Sensors and Biosensors: Recent Trends. *Curr. Opin. Electrochem.* **2018**, 1–10.

(103) Hileman, B. Herbicides in Agriculture. *Environ. Sci. Technol.* **1982**, *16* (12), 645A–650A.

(104) Aktar, W.; Sengupta, D.; Chowdhury, A. Impact of Pesticides Use in Agriculture: Their Benefits and Hazards. *Interdiscip. Toxicol.* **2009**, *2* (1), 1–12.

(105) Gupta, S. K.; Jani, J. P.; Saiyed, H. N.; Kashyap, S. K. Health Hazards in Pesticide Formulators Exposed to a Combination of Pesticides. *Indian J. Med. Res.* **1984**, *79*, 666–672.

(106) Hurley, P. M.; Hill, R. N.; Whiting, R. J. Mode of Carcinogenic Action of Pesticides Inducing Thyroid Follicular Cell Tumors in Rodents. *Environ. Health Perspect.* **1998**, *106* (8), 437–445.

(107) Rupa, D. S.; Reddy, P. P.; Reddi, O. S. Reproductive Performance in Population Exposed to Pesticides in Cotton Fields in India. *Environ. Res.* **1991**, *55* (2), 123–128.

(108) Eliassen, J.-E.; Vahl, O. Seasonal Variations in Biochemical Composition and Energy Content of Liver, Gonad and Muscle of Mature and Immature Cod, Gadus Morhua (L.) from Balsfjorden, Northern Norway. *J. Fish Biol.* **1982**, *20* (6), 707–716.

(109) Muir, D. C. G.; Teixeira, C.; Wania, F. Empirical and Modeling Evidence of Regional Atmospheric Transport of Current-Use Pesticides. *Environ. Toxicol. Chem.* **2004**, *23* (10), 2421–2432.

(110) Andreu, V.; Picó, Y. Determination of Pesticides and Their Degradation Products in Soil: Critical Review and Comparison of Methods. *TrAC - Trends Anal. Chem.* **2004**, *23* (10–11), 772–789.

(111) Wahid, H.; Ahmad, S.; Nor, M. A. M.; Rashid, M. A. Summary for Policymakers. In *Climate Change 2013 - The Physical Science Basis*; Intergovernmental Panel on Climate Change, Ed.; Cambridge University Press: Cambridge, 2017; Vol. 51, pp 1–30.

(112) Pretty, J.; Bharucha, Z. P. Integrated Pest Management for Sustainable Intensification of Agriculture in Asia and Africa. *Insects* **2015**, *6* (1), 152–182.

(113) Harris, R. M. Paraquat and Diquat. In *Molecules of Death*; PUBLISHED BY IMPERIAL COLLEGE PRESS AND DISTRIBUTED BY WORLD SCIENTIFIC PUBLISHING CO., 2007; pp 265–280.

(114) Watts, M. Paraquat Monograph. Pesticide Action Network Asia & the Pacific (PAN AP); 2011.

(115) Saeed, S. A. M.; Wilks, M. F.; Coupe, M. Acute Diquat Poisoning with Intracerebral Bleeding. *Postgrad. Med. J.* **2001**, *77* (907), 329–332.

(116) H.F. LAM, J. TAKEZAWA, B. N. G. and E. W. V. S. A Comparison of the Effects of Paraquat and Diquat. *Toxicology* **1980**, *18*.

(117) Britt E. Erickson. EU Bans Endocrine Disrupting Herbicides. *Chemical & Engineering News*. 2016, p 18.

(118) Kulshrestha, G.; Mukerjee, S. K. The Photochemical Decomposition of the Herbicide Isoproturon. *Pestic. Sci.* **1986**, *17* (5), 489–494.

(119) Behera, B. C.; Bhunya, S. P. Genotoxic Effect of Isoproturon (Herbicide) as Revealed by Three Mammalian in Vivo Mutagenic Bioassays. *Indian J. Exp. Biol.* **1990**, *28* (9), 862–867.

(120) Srivastava , M. K. , and Raizada, R. B. Developmental Toxicity of the Substituted Phenylurea Herbicide Isoproturon in Rats . *Vet. Hum. Toxicol.* **1995**, 220 – 223.

(121) Sarkar, S. N.; Gupta, P. K. Fetotoxic and Teratogenic Potential of Substituted Phenylurea Herbicide Isoproturon, in Rats. *Indian J. Exp. Biol.* **1993**, *31* (3), 280–282.

(122) EPA. *EPA Chemical Summary: 2,4-Dichlorophenoxyacetic Acid*; 2015.

(123) IARC (International Agency for Research on Cancer). IARC Monographs Evaluate DDT, Lindane, and 2,4-D. *Who* **2015**, No. June, 2.

(124) Hakim, D. A Pesticide Banned, or Not, Underscores Trans-Atlantic Trade Sensitivities. *New York Times*. 2015.

(125) Gilliom, R. J.; E., J.; G., C.; Hamilton, P. A.; Martin, J. D.; Nakagaki, N.; Nowell, L. H.; Scott, J. C.; Stackelberg, P. E.; Thelin, G. P.; et al. Pesticides in the Nation's Streams and Ground Water, 1992-2001. *(No. 1291)* **2006**, 172.

(126) Albers, C. N.; Banta, G. T.; Hansen, P. E.; Jacobsen, O. S. The Influence of Organic Matter on Sorption and Fate of Glyphosate in Soil - Comparing Different Soils and

Humic Substances. *Environ. Pollut.* **2009**, *157* (10), 2865–2870.

(127) Gao, S.; You, J.; Zheng, X.; Wang, Y.; Ren, R.; Zhang, R.; Bai, Y.; Zhang, H. Determination of Phenylurea and Triazine Herbicides in Milk by Microwave Assisted Ionic Liquid Microextraction High-Performance Liquid Chromatography. *Talanta* **2010**, *82* (4), 1371–1377.

(128) Raju, K. R.; Akella, S. Spectrophotometric Determination of Isoproturon and Metoxuron Using Ethylacetoacetate and Application to Technical and Formulation Grade Samples. *Talanta* **1996**, *43*, 577–581.

(129) Fung, Y.; Mak, J. L. L. Determination of Pesticides in Drinking Water by Micellar Electrokinetic Capillary Chromatography. **2001**, No. I, 2260–2269.

(130) Posecion, N. C.; Ostrea, E. M.; Bielawski, D. M. Quantitative Determination of Paraquat in Meconium by Sodium Borohydride-Nickel Chloride Chemical Reduction and Gas Chromatography/Mass Spectrometry (GC/MS). *J. Chromatogr. B Anal. Technol. Biomed. Life Sci.* **2008**, *862* (1–2), 93–99.

(131) Braithwaite, R. A. Emergency Analysis of Paraquat in Biological Fluids. *Hum. Exp. Toxicol.* **1987**, *6* (1), 83–86.

(132) Yao, F.; Liu, H.; Wang, G.; Du, L.; Yin, X.; Fu, Y. Determination of Paraquat in Water Samples Using a Sensitive Fluorescent Probe Titration Method. *J. Environ. Sci. (China)* **2013**, *25* (6), 1245–1251.

(133) Rai, M.K.;Joyce vanisha Das, Gupta, V. K. A Sensitive Determination of Paraquat by Spectrophot. *Talanta* **1997**, *45*, 343–348.

(134) Chuntib, P.; Jakmunee, J. Simple Flow Injection Colorimetric System for Determination of Paraquat in Natural Water. *Talanta* **2015**, *144*, 432–438.

(135) Fang, H.; Zhang, X.; Zhang, S. J.; Liu, L.; Zhao, Y. M.; Xu, H. J. Ultrasensitive and Quantitative Detection of Paraquat on Fruits Skins via Surface-Enhanced Raman Spectroscopy. *Sensors Actuators, B Chem.* **2015**, *213*, 452–456.

(136) Thiyagarajan, N.; Chang, J. L.; Senthilkumar, K.; Zen, J. M. Disposable Electrochemical Sensors: A Mini Review. *Electrochem. commun.* **2014**, *38*, 86–90.

(137) Walcarius, A. Electrocatalysis, Sensors and Biosensors in Analytical Chemistry Based on Ordered Mesoporous and Macroporous Carbon-Modified Electrodes. *TrAC - Trends Anal. Chem.* **2012**, *38*, 79–97.

(138) Walcarius, A.; Lamberts, L. Square Wave Voltammetric Determination of Paraquat and Diquat in Aqueous Solution. *J. Electroanal. Chem.* **1996**, *406* (1–2), 59–68.

(139) Selva, T. M. G.; ReisdeAraujo, W.; CesardaPaixão, T. R. L. Non-Invasive Salivary Electrochemical Quantification of Paraquat Poisoning Using Boron Doped Diamond Electrode. *Electroanalysis* **2015**, *27* (7), 1642–1648.

(140) Tyszczuk-Rotko, K.; Bęczkowska, I.; Nosal-Wiercińska, A. Simple, Selective and Sensitive Voltammetric Method for the Determination of Herbicide (Paraquat) Using a Bare Boron-Doped Diamond Electrode. *Diam. Relat. Mater.* **2014**, *50*, 86–90.

(141) De Souza, D.; Machado, S. A. S. Study of the Electrochemical Behavior and Sensitive Detection of Pesticides Using Microelectrodes Allied to Square-Wave Voltammetry. *Electroanalysis* **2006**, *18* (9), 862–872.

(142) De Souza, D.; Codognoto, L.; Machado, S. A. S.; Avaca, L. A. Electroanalytical Determination of the Herbicide Paraquat in Natural Water and Commercial Tea Samples with Gold Electrodes Obtained from Recordable Compact Disc. *Anal. Lett.* **2005**, *38* (2), 331–341.

(143) de Figueiredo-Filho, L. C. S.; Baccarin, M.; Janegitz, B. C.; Fatibello-Filho, O. A Disposable and Inexpensive Bismuth Film Minisensor for a Voltammetric Determination of Diquat and Paraquat Pesticides in Natural Water Samples. *Sensors Actuators, B Chem.* **2017**, *240*, 749–756.

(144) de Figueiredo-Filho, L. C. S.; dos Santos, V. B.; Janegitz, B. C.; Guerreiro, T. B.; Fatibello-Filho, O.; Faria, R. C.; Marcolino-Junior, L. H. Differential Pulse Voltammetric Determination of Paraquat Using a Bismuth-Film Electrode. *Electroanalysis* **2010**, *22* (11), 1260–1266.

(145) Ribeiro, J. A.; Carreira, C. A.; Lee, H. J.; Silva, F.; Martins, A.; Pereira, C. M. Voltammetric Determination of Paraquat at DNA-Gold Nanoparticle Composite Electrodes. *Electrochim. Acta* **2010**, *55* (27), 7892–7896.

(146) Farahi, A.; Achak, M.; El Gaini, L.; El Mhammedi, M. A.; Bakasse, M. Electrochemical Determination of Paraquat in Citric Fruit Based on Electrodeposition of Silver Particles onto Carbon Paste Electrode. *J. Food Drug Anal.* **2015**, *23* (3), 463–471.

(147) Gevaerd, A.; De Oliveira, P. R.; Mangrich, A. S.; Bergamini, M. F.; Marcolino-Junior, L. H. Evaluation of Antimony Microparticles Supported on Biochar for Application in the Voltammetric Determination of Paraquat. *Mater. Sci. Eng. C* **2016**, *62*, 123–129.

(148) Niu, L. M.; Liu, F.; Wang, W.; Lian, K. Q.; Ma, L.; Shi, H. M.; Kang, W. J. Electrochemical Behavior of Paraquat on a Highly Ordered Biosensor Based on an Unmodified DNA-3D Gold Nanoparticle Composite and Its Application. *Electrochim. Acta* **2015**, *153*, 190–199.

(149) Li, J.; Lei, W.; Xu, Y.; Zhang, Y.; Xia, M.; Wang, F. Fabrication of Polypyrrole-Grafted Nitrogen-Doped Graphene and Its Application for Electrochemical Detection of Paraquat. *Electrochim. Acta* **2015**, *174*, 464–471.

(150) Garcia, L. L. C.; Figueiredo-Filho, L. C. S.; Oliveira, G. G.; Fatibello-Filho, O.; Banks, C. E. Square-Wave Voltammetric Determination of Paraquat Using a Glassy Carbon Electrode Modified with Multiwalled Carbon Nanotubes within a Dihexadecylhydrogenphosphate (DHP) Film. *Sensors Actuators, B Chem.* **2013**, *181*, 306–311.

(151) Ye, X.; Gu, Y.; Wang, C. Fabrication of the Cu2O/Polyvinyl Pyrrolidone-Graphene Modified Glassy Carbon-Rotating Disk Electrode and Its Application for Sensitive Detection of Herbicide Paraquat. *Sensors Actuators, B Chem.* **2012**, *173*, 530–539.

(152) Lopes, I. C.; De Souza, D.; MacHado, S. A. S.; Tanaka, A. A. Voltammetric Detection of Paraquat Pesticide on a Phthalocyanine-Based Pyrolitic Graphite Electrode. *Anal. Bioanal. Chem.* **2007**, *388* (8), 1907–1914.

(153) Kalinke, C.; Mangrich, A. S.; Marcolino-Junior, L. H.; Bergamini, M. F. Carbon Paste Electrode Modified with Biochar for Sensitive Electrochemical Determination of Paraquat. *Electroanalysis* **2016**, *28* (4), 764–769.

(154) Lu, T. H.; Sun, I. W. Electrocatalytic Determination of Paraquat Using a Nafion Film Coated Glassy Carbon Electrode. *Talanta* **2000**, *53* (2), 443–451.

(155) Zen, J.-M.; Jeng, S.-H.; Chen, H.-J. Determination of Paraquat by Square-Wave Voltammetry at a Perfluorosulfonated Ionomer/Clay-Modified Electrode. *Anal. Chem.* **1996**, *68* (3), 498–502.

(156) Alvarez, E.; Sevilla, M. T.; Pinilla, J. M.; Hernandez, L. Cathodic Stripping Voltammetry of Paraquat on a Carbon Paste Electrode Modified with Amberlite XAD-2 Resin. *Anal. Chim. Acta* **1992**, *260* (1), 19–23.

(157) El Mhammedi, M. A.; Bakasse, M.; Chtainia, A. Electrochemical Studies and Square Wave Voltammetry of Paraquat at Natural Phosphate Modified Carbon Paste Electrode. *J. Hazard. Mater.* **2007**, *145* (1–2), 1–7.

(158) El Mhammedi, M. A.; Bakasse, M.; Chtaini, A. Square-Wave Voltammetric Determination of Paraquat at Carbon Paste Electrode Modified with Hydroxyapatite. *Electroanalysis* **2007**, *19* (16), 1727–1733.

(159) Sundari, P. A.; Manisankar, P. Development of Nano Poly(3-Methyl Thiophene)/Multiwalled Carbon Nanotubes Sensor for the Efficient Detection of Some Pesticides. *J. Braz. Chem. Soc.* **2011**, *22* (4), 746–755.

(160) Manisankar, P.; Selvanathan, G.; Viswanathan, S.; Gurumallesh Prabu, H. Electrochemical Determination of Some Organic Pollutants Using Wall-Jet Electrode. *Electroanalysis* **2002**, *14* (24), 1722–1727.

(161) Li, S.; Tao, H.; Li, J. Molecularly Imprinted Electrochemical Luminescence Sensor Based on Enzymatic Amplification for Ultratrace Isoproturon Determination. *Electroanalysis* **2012**, *24* (7), 1664–1670.

(162) Noyrod, P.; Chailapakul, O.; Wonsawat, W.; Chuanuwatanakul, S. The Simultaneous Determination of Isoproturon and Carbendazim Pesticides by Single Drop Analysis Using a Graphene-Based Electrochemical Sensor. *J. Electroanal. Chem.* **2014**, *719*, 54–59.

(163) Manisankar, P.; Selvanathan, G.; Vedhi, C. Utilization of Sodium Montmorillonite Clay-Modified Electrode for the Determination of Isoproturon and Carbendazim in Soil and Water Samples. *Appl. Clay Sci.* **2005**, *29* (3–4), 249–257.

(164) Manisankar, P.; Selvanathan, G.; Vedhi, C. Determination of Pesticides Using Heteropolyacid Montmorillonite Clay-Modified Electrode with Surfactant. *Talanta* **2006**, *68* (3), 686–692.

(165) Sundari, P. A.; Manisankar, P. Development of Nano Poly(3-Methyl Thiophene)/Multiwalled Carbon Nanotubes Sensor for the Efficient Detection of Some Pesticides. *J. Braz. Chem. Soc.* **2011**, *22* (4), 746–755.

(166) Manisankar, P.; Selvanathan, G.; Viswanathan, S.; Gurumallesh Prabu, H. Electrochemical Determination of Some Organic Pollutants Using Wall-Jet Electrode. *Electroanalysis* **2002**, *14* (24), 1722–1727.

(167) Li, S.; Tao, H.; Li, J. Molecularly Imprinted Electrochemical Luminescence Sensor Based on Enzymatic Amplification for Ultratrace Isoproturon Determination. *Electroanalysis* **2012**, *24* (7), 1664–1670.

(168) Autolab Application Note EC08. Basic Overview of the Working Principle of a Potentiostat/Galvanostat (PGSTAT) – Electrochemical Cell Setup. *Metrohm Autolab.B.V* **2011**, 1–3.

(169) Scholz, F. *Electroanalytical Methods*, 2nd ed.; Scholz, F., Bond, A. M., Compton, R. G., Fiedler, D. A., Inzelt, G., Kahlert, H., Komorsky-Lovrić, Š., Lohse, H., Lovrić, M., Marken, F., et al., Eds.; Springer Berlin Heidelberg: Berlin, Heidelberg, 2010.

(170) Adenier, A.; Chehimi, M. M.; Gallardo, I.; Pinson, J.; Vilà, N. Electrochemical Oxidation of Aliphatic Amines and Their Attachment to Carbon and Metal Surfaces. *Langmuir* **2004**, *20* (19), 8243–8253.

(171) Compton, R. G.; Banks, C. E. *Understanding Voltammetry*; IMPERIAL COLLEGE PRESS, 2010.

(172) Mirceski, V.; Gulaboski, R.; Lovric, M.; Bogeski, I.; Kappl, R.; Hoth, M. Square-Wave Voltammetry: A Review on the Recent Progress. *Electroanalysis* **2013**, *25* (11), 2411–2422.

(173) Kounaves, S. P. Voltammetric Techniques. In *Inorganic Electrochemistry*; pp 49–136.

(174) Lasia, A. *Electrochemical Impedance Spectroscopy and Its Applications*, *Modern Aspects of Electrochemistry*; 1999; Vol. 32.

(175) Eith, C.; Kolb, M.; Seubert, A.; Viehweger, K. H. (Ed). Practical Ion Chromatography An Introduction Practical Ion Chromatography An Introduction. *Metrohm Monogr.* **2001**, 1–160.

(176) Zhou, W.; Wang, Z. L. Scanning Microscopy for Nanotechnology: Techniques and Applications. In *Scanning Microscopy for Nanotechnology: Techniques and Applications*; Springer, 2007; pp 1–522.

(177) Chen, C. J. *Introduction to Scanning Tunneling Microscopy*; Oxford University Press, 2007; Vol. 29.

(178) Krivanek, O. L.; Zhou, W.; Chisholm, M. F.; Idrobo, J. C.; Lovejoy, T. C.; Ramasse, Q. M.; Dellby, N. *Low Voltage Electron Microscopy*; David C. Bell and Erdman, N., Ed.; Wiley, 2012.

(179) Heide, P. Van der. Introduction. In *X-Ray Photoelectron Spectroscopy*; John Wiley & Sons, Inc.: Hoboken, NJ, USA, 2011; pp 1–12.

(180) Tampere university of Technology. Electron spectroscopy (XPS, AES, UPS) http://www.tut.fi/en/research/research-fields/photonics/surface-science/electron-spectroscopy/index.htm.

(181) Li, W.; Ding, L.; Wang, Q.; Su, B. Differential Pulse Voltammetry Detection of Dopamine and Ascorbic Acid by Permselective Silica Mesochannels Vertically Attached to the Electrode Surface. *Analyst* **2014**, *139* (16), 3926–3931.

(182) Saadaoui, M.; Fernández, I.; Sánchez, A.; Díez, P.; Campuzano, S.; Raouafi, N.; Pingarrón, J. M.; Villalonga, R. Mesoporous Silica Thin Film Mechanized with a DNAzyme-Based Molecular Switch for Electrochemical Biosensing. *Electrochem. commun.* **2015**, *58*, 57–61.

(183) Zhou, Z.; Guo, W.; Xu, L.; Yang, Q.; Su, B. Two Orders-of-Magnitude Enhancement in the Electrochemiluminescence of $Ru(Bpy)_3^{2+}$ by Vertically Ordered Silica

Mesochannels. *Anal. Chim. Acta* **2015**, *886*, 48–55.

(184) Valle, M. A.; Hernández, L. A.; Díaz, F. R.; Ramos, A. Electrosynthesis and Characterization of Poly (3 , 4- Ethylenedioxythiophene) Nanowires. *Int. J. Electrochem. Sci.*, **2015**, *10*, 5152–5163.

(185) Hernández, L. A.; del Valle, M. A.; Díaz, F. R.; Fermin, D. J.; Risbridger, T. A. G. Polymeric Nanowires Directly Electrosynthesized on the Working Electrode. *Electrochim. Acta* **2015**, *166*, 163–167.

(186) Lin, X.; Yang, Q.; Ding, L.; Su, B. Ultrathin Silica Membranes with Highly Ordered and Perpendicular Nanochannels for Precise and Fast Molecular Separation. *ACS Nano* **2015**, *9* (11), 11266–11277.

(187) Herzog, G.; Vodolazkaya, N. A.; Walcarius, A. Platinum Ultramicroelectrodes Modified with Electrogenerated Surfactant-Templated Mesoporous Organosilica Films: Effect of Film Formation Conditions on Its Performance in Preconcentration Electroanalysis. *Electroanalysis* **2013**, *25* (12), 2595–2603.

(188) Rafiee, M.; Karimi, B.; Farrokhzadeh, S.; Vali, H. Hydroquinone Functionalized Oriented MCM-41 Mesochannels at the Electrode Surface. *Electrochim. Acta* **2013**, *94*, 198–205.

(189) Rafiee, M.; Karimi, B.; Arshi, S.; Vali, H. Ethylenediamine-Modified Oriented MCM-41 at the Electrode Surface, Cobalt Adsorption Ability and Electrochemical Performance. *Dalt. Trans.* **2014**, *43* (12), 4901.

(190) Vilà, N.; Ghanbaja, J.; Walcarius, A. Clickable Bifunctional and Vertically Aligned Mesoporous Silica Films. *Adv. Mater. Interfaces* **2016**, *3* (2), 1–11.

(191) Liu, L.; Yellinek, S.; Valdinger, I.; Donval, A.; Mandler, D. Important Implications of the Electrochemical Reduction of ITO. *Electrochim. Acta* **2015**, *176*, 1374–1381.

(192) Sibottier, E.; Sayen, S.; Gaboriaud, F.; Walcarius, A. Factors Affecting the Preparation and Properties of Electrodeposited Silica Thin Films Functionalized with Amine or Thiol Groups. *Langmuir* **2006**, *22* (20), 8366–8373.

(193) Sayen, S.; Walcarius, A. Electro-Assisted Generation of Functionalized Silica Films on Gold. *Electrochem. commun.* **2003**, *5* (4), 341–348.

(194) Possari, R.; Carvalhal, R. F.; Mendes, R. K.; Kubota, L. T. Electrochemical Detection of Cysteine in a Flow System Based on Reductive Desorption of Thiols from Gold. *Anal. Chim. Acta* **2006**, *575* (2), 172–179.

(195) Bélanger, D.; Pinson, J. Electrografting: A Powerful Method for Surface Modification.

Chem. Soc. Rev. **2011**, *40* (7), 3995.

(196) Downard, A. J. Electrochemically Assisted Covalent Modification of Carbon Electrodes. *Electroanalysis* **2000**, *12* (14), 1085–1096.

(197) Randriamahazaka, H.; Ghilane, J. Electrografting and Controlled Surface Functionalization of Carbon Based Surfaces for Electroanalysis. *Electroanalysis* **2016**, *28* (1), 13–26.

(198) Cruickshank, A. C.; Tan, E. S. Q.; Brooksby, P. A.; Downard, A. J. Are Redox Probes a Useful Indicator of Film Stability? An Electrochemical, AFM and XPS Study of Electrografted Amine Films on Carbon. *Electrochem. commun.* **2007**, *9* (7), 1456–1462.

(199) Adenier, A.; Chehimi, M. M.; Gallardo, I.; Pinson, J.; Vilà, N. Electrochemical Oxidation of Aliphatic Amines and Their Attachment to Carbon and Metal Surfaces. *Langmuir* **2004**, *20* (19), 8243–8253.

(200) Barbier, B. Electrochemical Bonding of Amines to Carbon Fiber Surfaces Toward Improved Carbon-Epoxy Composites. *J. Electrochem. Soc.* **1990**, *137* (6), 1757.

(201) Etienne, M.; Quach, A.; Grosso, D.; Nicole, L.; Sanchez, C.; Walcarius, A. Molecular Transport into Mesostructured Silica Thin Films: Electrochemical Monitoring and Comparison between P6m, P63//WWIC, and Pm3n Structures. *Chem. Mater.* **2007**, *19* (4), 844–856.

(202) Valvekens, P.; Jonckheere, D.; De Baerdemaeker, T.; Kubarev, A. V.; Vandichel, M.; Hemelsoet, K.; Waroquier, M.; Van Speybroeck, V.; Smolders, E.; Depla, D.; et al. Base Catalytic Activity of Alkaline Earth MOFs: A (Micro)Spectroscopic Study of Active Site Formation by the Controlled Transformation of Structural Anions. *Chem. Sci.* **2014**, *5* (11), 4517–4524.

(203) Ghanem, M. A.; Chrétien, J.-M.; Pinczewska, A.; Kilburn, J. D.; Bartlett, P. N. Covalent Modification of Glassy Carbon Surface with Organic Redox Probes through Diamine Linkers Using Electrochemical and Solid-Phase Synthesis Methodologies. *J. Mater. Chem.* **2008**, *18* (41), 4917.

(204) Deinhammer, R. S.; Ho, M.; Anderegg, J. W.; Porter, M. D. Electrochemical Oxidation of Amine-Containing Compounds: A Route to the Surface Modification of Glassy Carbon Electrodes. *Langmuir* **1994**, *10* (4), 1306–1313.

(205) Vilà, N.; Walcarius, A. Electrochemical Response of Vertically-Aligned, Ferrocene-Functionalized Mesoporous Silica Films: Effect of the Supporting Electrolyte. *Electrochim. Acta* **2015**, *179*, 304–314.

(206) Etienne, M.; Guillemin, Y.; Grosso, D.; Walcarius, A. Electrochemical Approaches for the Fabrication and/or Characterization of Pure and Hybrid Templated Mesoporous Oxide Thin Films: A Review. *Anal. Bioanal. Chem.* **2013**, *405* (5), 1497–1512.

(207) Yan, F.; Lin, X.; Su, B. Vertically Ordered Silica Mesochannel Films: Electrochemistry and Analytical Applications. *Analyst* **2016**, *141* (12), 3482–3495.

(208) Guillemin, Y.; Etienne, M.; Aubert, E.; Walcarius, A. Electrogeneration of Highly Methylated Mesoporous Silica Thin Films with Vertically-Aligned Mesochannels and Electrochemical Monitoring of Mass Transport Issues. *J. Mater. Chem.* **2010**, *20* (32), 6799.

(209) Vilà, N.; Ghanbaja, J.; Aubert, E.; Walcarius, A. Electrochemically Assisted Generation of Highly Ordered Azide-Functionalized Mesoporous Silica for Oriented Hybrid Films. *Angew. Chemie - Int. Ed.* **2014**, *53* (11), 2945–2950.

(210) Sagar, G. R. Uses and Usefulness of Paraquat. *Hum. Exp. Toxicol.* **1987**, *6* (1), 7–11.

(211) Gao, R.; Choi, N.; Chang, S. I.; Kang, S. H.; Song, J. M.; Cho, S. I.; Lim, D. W.; Choo, J. Highly Sensitive Trace Analysis of Paraquat Using a Surface-Enhanced Raman Scattering Microdroplet Sensor. *Anal. Chim. Acta* **2010**, *681* (1–2), 87–91.

(212) Tanner, C. M.; Kame, F.; Ross, G. W.; Hoppin, J. A.; Goldman, S. M.; Korell, M.; Marras, C.; Bhudhikanok, G. S.; Kasten, M.; Chade, A. R.; et al. Rotenone, Paraquat, and Parkinson's Disease. *Environ. Health Perspect.* **2011**, *119* (6), 866–872.

(213) Hamilton, D. J.; Ambrus, Á.; Dieterle, R. M.; Felsot, A. S.; Harris, C. A.; Holland, P. T.; Katayama, A.; Kurihara, N.; Linders, J.; Unsworth, J.; et al. Regulatory Limits for Pesticide Residues in Water (IUPAC Technical Report). *Pure Appl. Chem.* **2003**, *75* (8), 1123–1155.

(214) Bird, C. L.; Kuhn, A. T. Electrochemistry of the Viologens. *Chem. Soc. Rev.* **1981**, *10* (1), 49.

(215) Walcarius, A.; Sibottier, E.; Etienne, M.; Ghanbaja, J. Electrochemically Assisted Self-Assembly of Mesoporous Silica Thin Films. *Nat. Mater.* **2007**, *6* (8), 602–608.

(216) Nasir, T.; Zhang, L.; Vilà, N.; Herzog, G.; Walcarius, A. Electrografting of 3-Aminopropyltriethoxysilane on a Glassy Carbon Electrode for the Improved Adhesion of Vertically Oriented Mesoporous Silica Thin Films. *Langmuir* **2016**, *32* (17), 4323–4332.

(217) Despas, C.; Vodolazkaya, N. A.; Ghanbaja, J.; Walcarius, A. Preparation of Ordered and Oriented Mesoporous Silica Thin Films Bearing Octyl or Hexadecyl Groups by Electrochemically Assisted Self-Assembly and Evaluation of Their Transport

Properties. *J. Solid State Electrochem.* **2015**, *19* (7), 2075–2085.

(218) Zheng, W.; Yan, F.; Su, B. Electrochemical Determination of Chloramphenicol in Milk and Honey Using Vertically Ordered Silica Mesochannels and Surfactant Micelles as the Extraction and Anti-Fouling Element. *J. Electroanal. Chem.* **2016**, *781*, 383–388.

(219) Kistenmacher, T. J.; Marsh, R. E. Crystal and Molecular Structure of an Antiinflammatory Agent, Indomethacin, 1-(p-Chlorobenzoyl)-5-Methoxy-2-Methylindole-3-Acetic Acid. *J. Am. Chem. Soc.* **1972**, *94* (4), 1340–1345.

(220) Williams, M. L. CRC Handbook of Chemistry and Physics, 76th Edition. *Occup. Environ. Med.* **1996**, *53* (7), 504–504.

(221) Marcus, Y. Thermodynamics of Solvation of Ions. Part 5.—Gibbs Free Energy of Hydration at 298.15 K. *J. Chem. Soc., Faraday Trans.* **1991**, *87* (18), 2995–2999.

(222) Karman, C.; Vilà, N.; Walcarius, A. Amplified Charge Transfer for Anionic Redox Probes through Oriented Mesoporous Silica Thin Films. *ChemElectroChem* **2016**, *3* (12), 2130–2137.

(223) Behrens, S. H.; Grier, D. G. The Charge of Glass and Silica Surfaces. *J. Chem. Phys.* **2001**, *115* (14), 6716–6721.

(224) Wang, M.; Revil, A. Electrochemical Charge of Silica Surfaces at High Ionic Strength in Narrow Channels. *J. Colloid Interface Sci.* **2010**, *343* (1), 381–386.

(225) Schoch, R. B.; Han, J.; Renaud, P. Transport Phenomena in Nanofluidics. *Rev. Mod. Phys.* **2008**, *80* (3), 839–883.

(226) Plecis, A.; Schoch, R. B.; Renaud, P. Ion Transport in Nanochannels: Experimental and Theoretical Study of the Exclusion-Enrichment Effect on a Chip. *Nano Lett.* **2005**, *5*, 1147–1155.

(227) Kirby, B. J.; Hasselbrink, E. F. Zeta Potential of Microfluidic Substrates: 1. Theory, Experimental Techniques, and Effects on Separations. *Electrophoresis* **2004**, *25* (2), 187–202.

(228) Lev, O.; Sampath, S. Sol-Gel Electrochemistry. In *Electroanalytical Chemistry, A Series of Advances, Vol. 23*; Bard, A. J., Zoski, C. G., Eds.; CRC Press: Boca Raton, 2010; pp 211–304.

(229) Hamilton, D. J.; Ambrus, Á.; Dieterle, R. M.; Felsot, A. S.; Harris, C. A.; Holland, P. T.; Katayama, A.; Kurihara, N.; Linders, J.; Unsworth, J.; et al. Regulatory Limits for Pesticide Residues in Water (IUPAC Technical Report). *Pure Appl. Chem.* **2003**, *75* (8), 1123–1155.

(230) Brett, C. M. A. Electrochemical Sensors for Environmental Monitoring. Strategy and Examples. *Pure Appl. Chem.* **2001**, *73* (12).

(231) Walcarius, A.; Sibottier, E.; Etienne, M.; Ghanbaja, J. Electrochemically Assisted Self-Assembly of Mesoporous Silica Thin Films. *Nat. Mater.* **2007**, *6* (8), 602–608.

(232) Giordano, G.; Durante, C.; Gennaro, A.; Guglielmi, M. Multilayer Deposition of Silica Sol−Gel Films by Electrochemical Assisted Techniques. *J. Phys. Chem. C* **2016**, *120* (50), 28820–28824.

(233) Tomcik, P.; Bustin, D. Voltammetric Determination of Iodide by Use of an Interdigitated Microelectrode Array. *Anal. Bioanal. Chem.* **2001**, *371* (4), 562–564.

(234) Dawson, K.; Baudequin, M.; Sassiat, N.; Quinn, A. J.; O'Riordan, A. Electroanalysis at Discrete Arrays of Gold Nanowire Electrodes. *Electrochim. Acta* **2013**, *101*, 169–176.

(235) Kilchenmann, S. C.; Rollo, E.; Bianchi, E.; Guiducci, C. Metal-Coated Silicon Micropillars for Freestanding 3D-Electrode Arrays in Microchannels. *Sensors Actuators, B Chem.* **2013**, *185*, 713–719.

(236) Davis, F.; Higson, S. P. J. Arrays of Microelectrodes: Technologies for Environmental Investigations. *Environ. Sci. Process. Impacts* **2013**, *15* (8), 1477.

(237) Oliveira, T. M. B. F.; Becker, H.; Longhinotti, E.; De Souza, D.; de Lima-Neto, P.; Correia, A. N. Carbon-Fibre Microelectrodes Coupled with Square-Wave Voltammetry for the Direct Analysis of Dimethomorph Fungicide in Natural Waters. *Microchem. J.* **2013**, *109*, 84–92.

(238) Suzuki, I.; Fukuda, M.; Shirakawa, K.; Jiko, H.; Gotoh, M. Carbon Nanotube Multi-Electrode Array Chips for Noninvasive Real-Time Measurement of Dopamine, Action Potentials, and Postsynaptic Potentials. *Biosens. Bioelectron.* **2013**, *49*, 1–6.

(239) Tsigara, A.; Benkhial, A.; Warren, S.; Akkari, F.; Wright, J.; Frehill, F.; Dempsey, E. Metal Microelectrode Nanostructuring Using Nanosphere Lithography and Photolithography with Optimization of the Fabrication Process. *Thin Solid Films* **2013**, *537*, 269–274.

(240) Tomčík, P. Microelectrode Arrays with Overlapped Diffusion Layers as Electroanalytical Detectors: Theory and Basic Applications. *Sensors (Switzerland)* **2013**, *13* (10), 13659–13684.

(241) Liu, L.; Walcarius, A. Kinetics of the Electrochemically-Assisted Deposition of Sol–gel Films. *Phys. Chem. Chem. Phys.* **2017**, *19* (23), 14972–14983.

(242) Piegari, A.; Masetti, E. Thin Film Thickness Measurement: A Comparison of Various

Techniques. *Thin Solid Films* **1985**, *124* (3–4), 249–257.

(243) Nasir, T.; Herzog, G.; Hébrant, M.; Despas, C.; Liu, L.; Walcarius, A. Mesoporous Silica Thin Films for Improved Electrochemical Detection of Paraquat. *ACS Sensors* **2018**, *3* (2), 484–493.

(244) Giordano, G.; Durante, C.; Gennaro, A.; Guglielmi, M. Multilayer Deposition of Silica Sol−Gel Films by Electrochemical Assisted Techniques. *J. Phys. Chem. C* **2016**, *120* (50), 28820–28824.

(245) Walcarius, A.; Lamberts, L. Square Wave Voltammetric Determination of Paraquat and Diquat in Aqeous Solution. *J. Electroanal. Chem.* **1996**, *406*, 59–68.

(246) Farahi, A.; Achak, M.; El Gaini, L.; El Mhammedi, M. A.; Bakasse, M. Electrochemical Determination of Paraquat in Tomato at Ag/NP-Modified Graphite Electrode Using Square Wave Voltammetry. *Food Anal. Methods* **2016**, *9* (1), 139–147.

(247) Lord, H. L.; Zhan, W.; Pawliszyn, J. Fundamentals and Applications of Needle Trap Devices. *Anal. Chim. Acta* **2010**, *677* (1), 3–18.

(248) Wightman, R. M. Microvoltammetric Electrodes. *Anal. Chem.* **1981**, *53* (9), 1125A–1134A.

(249) Chen, R.; Li, Y.; Huo, K.; Chu, P. K. Microelectrode Arrays Based on Carbon Nanomaterials: Emerging Electrochemical Sensors for Biological and Environmental Applications. *RSC Adv.* **2013**, *3* (41), 18698.

(250) Wittkampf, M.; Cammann, K.; Amrei, M.; Reichelt, R. Characterization of Microelectrode Arrays by Means of Electrochemical and Surface Analysis Methods. *Sensors Actuators B* **1997**, *40*, 79–84.

(251) M. Wightman and D. O. Wipf. "Voltammetry at Microelectrodes,." In *Electroanalytical Chemistry*; Marcel Decker, New York, 1898; p 267.

(252) Herzog, G.; Sibottier, E.; Etienne, M.; Walcarius, A. Electrochemically Assisted Self-Assembly of Ordered and Functionalized Mesoporous Silica Films: Impact of the Electrode Geometry and Size on Film Formation and Properties. *Faraday Discuss.* **2013**, *164*, 259.

(253) Sørensen, S. R.; Bending, G. D.; Jacobsen, C. S.; Walker, A.; Aamand, J. Microbial Degradation of Isoproturon and Related Phenylurea Herbicides in and below Agricultural Fields. *FEMS Microbiol. Ecol.* **2003**, *45* (1), 1–11.

(254) Pérès, F.; Coste, M.; Ribeyre, F.; Ricard, M.; Boudou, A. Effects of Methylmercury

and Inorganic Mercury on Periphytic Diatom Communities in Freshwater Indoor Microcosms. *J. Appl. Phycol.* **1997**, *9* (3), 215–227.

(255) Serrano-Cinca, C.; Fuertes-Callén, Y.; Mar-Molinero, C. Measuring DEA Efficiency in Internet Companies. *Decis. Support Syst.* **2005**, *38* (4), 557–573.

(256) World Health Organization. Isoproturon in Drinking-Water Background Document for Development of WHO Guidelines for Drinking-Water Quality. *America (NY).* **1996**, *2*, 4.

(257) Nitschke, L.; Schüssler, W. Surface Water Pollution by Herbicides from Effluents of Waste Water Treatment Plants. *Chemosphere* **1998**, *36* (1), 35–41.

(258) Manisankar, P.; Vedhi, C.; Selvanathan, G. Electrochemical Studies of Isoproturon. **2007**, No. July, 211–214.

(259) Bhandari, H.; Choudhary, V.; Dhawan, S. K. Synergistic Effect of Copolymers Composition on the Electrochemical, Thermal, and Electrical Behavior of 5-Lithiosulphoisophthalic Acid Doped Poly(Aniline-Co-2-Isopropylaniline): Synthesis, Characterization, and Applications. *Polym. Adv. Technol.* **2009**, *20* (12), 1024–1034.

(260) Sapurina, I.; Tenkovtsev, A. V.; Stejskal, J. Conjugated Polyaniline as a Result of the Benzidine Rearrangement. *Polym. Int.* **2015**, *64* (4), 453–465.

(261) Nguyen, D. N.; Yoon, H. Recent Advances in Nanostructured Conducting Polymers: From Synthesis to Practical Applications. *Polymers (Basel).* **2016**, *8* (4), 118.

(262) Gospodinova, N.; Terlemezyan, L. Conducting Polymers Prepared by Oxidative Polymerization: Polyaniline. *Prog. Polym. Sci.* **1998**, *23* (8), 1443–1484.

(263) Ćirić-Marjanović, G. Recent Advances in Polyaniline Research: Polymerization Mechanisms, Structural Aspects, Properties and Applications. *Synth. Met.* **2013**, *177* (3), 1–47.

(264) Wang, Y.; Tran, H. D.; Liao, L.; Duan, X.; Kaner, R. B. Nanoscale Morphology, Dimensional Control, and Electrical Properties of Oligoanilines. *J. Am. Chem. Soc.* **2010**, *132* (30), 10365–10373.

(265) Vilà, N.; André, E.; Ciganda, R.; Ruiz, J.; Astruc, D.; Walcarius, A. Molecular Sieving with Vertically Aligned Mesoporous Silica Films and Electronic Wiring through Isolating Nanochannels. *Chem. Mater.* **2016**, *28* (8), 2511–2514.

Electrochemical sensors of environmental pollutants based on carbon electrodes modified by ordered mesoporous silica

In this thesis, we present the electrochemical detection of herbicides i.e. paraquat and isoproturon in aqueous samples. These herbicides are used worldwide extensively for weed control in different crops. Their intensive use is a source of environmental contamination and their toxicity is a threat to Human health. Electrochemical sensing is a promising and advantageous technique as compared to conventional detection methods due to its properties such as rapid analysis, ease of operation, cost effectiveness and high sensitivity as a result of working electrode modification. Here, we modified electrodes modified with mesoporous silica thin films to act as herbicide sensors. These electrodes were modified by electrochemically assisted self-assembly process, a well-established process for electrode modification by our group. In the first part adhesion of mesoporous silica film at carbon electrodes was improved with the help of a primary amine which acted as molecular glue for better attachment of these films at electrodes surface. In the next part these modified electrodes were used for electrochemical detection of above stated herbicides. Modified electrodes showed enhanced sensitivity and low limit of detection as compared to unmodified ones. Effect of different solution parameters as well as film thickness and electrode geometry was also studied and found to have critical impact on sensitivity of the system.

Keywords: Mesoporous silica films, Glassy carbon electrodes, APTES electrografting Electrochemical sensing, Paraquat, Isoproturon.

Dans cette thèse, nous présentons la détection électrochimique des herbicides, c'est-à-dire le paraquat et l'isoproturon dans des échantillons aqueux. Leur utilisation intensive est une source de contamination de l'environnement et leur toxicité constitue une menace pour la santé. La détection électrochimique est une technique prometteuse et avantageuse par rapport aux méthodes de détection conventionnelles en raison de ses propriétés telles que l'analyse rapide, la facilité d'utilisation, la rentabilité et la sensibilité élevée résultant de la modification de l'électrode de travail. Ici, nous avons modifié les électrodes modifiées avec des films minces de silice mésoporeuse pour agir comme capteurs d'herbicide. Ces électrodes ont été modifiées par un processus d'auto-assemblage assisté par électrochimie, un processus bien établi pour la modification des électrodes par notre groupe. Dans la première partie, l'adhérence du film de silice mésoporeux aux électrodes de carbone a été améliorée à l'aide d'une amine primaire qui a agi comme colle moléculaire pour une meilleure fixation de ces films à la surface des électrodes. Dans la partie suivante, ces électrodes modifiées ont été utilisées pour la détection électrochimique des herbicides susmentionnés. Les électrodes modifiées ont montré une sensibilité accrue et une limite de détection basse par rapport aux électrodes non modifiées. L'effet des différents paramètres de la solution ainsi que l'épaisseur du film et la géométrie de l'électrode ont également été étudiés et ont un impact critique sur la sensibilité du système.

Mots-clés: Films de silice mésoporeuse, électrodes de carbone vitreux, électrogreffage APTES, détection électrochimique, Paraquat, Isoproturon.